

PROGRESS REPORT

PLACER COUNTY ROSEVILLE RAILYARD AIR TOXICS MONITORING PROJECT

Prepared by

**Placer County Air Pollution Control District
3091 County Center Drive, Suite 240
Auburn, CA 95603**

Prepared for

**Ms. Angela Latigue
EPA Region IX
75 Hawthorne Street
SAN FRANCISCO, CA 94105**

Project Assistance ID #
XA-96962901-0

November 2007

1. INTRODUCTION

This progress report to EPA Region IX summarizes the findings of several research efforts funded by a grant from EPA Region IX to augment the Roseville Railyard Air Monitoring Project (RRAMP). RRAMP is an air monitoring study designed to characterize the magnitude of diesel particulate matter (DPM) emissions emanating from the Union Pacific Rail Road (UPRR) facility located in Placer County, CA. RRAMP was conceived as a follow-up research study to provide real world DPM concentrations to assess the accuracy of the findings of the Roseville rail yard health risk assessment (HRA) conducted by the California Air Resources Board (CARB). CARB's HRA evaluated the potential public health risks resulting from the UPRR facility located in Roseville, CA based on estimates of DPM emissions emanating from the rail yard and meteorological data collected at a site several miles from the railyard. The purpose of RRAMP is to use the latest monitoring techniques to obtain actual ambient DPM concentrations emanating from the Roseville rail yard facility and on-site meteorological data during three successive intensive summer air monitoring periods (mid-June through mid-October) for three years (2005 through 2007). The EPA Region IX awarded a grant to the Placer County APCD (District) in April 2006 to cover the following three components: a portion of the summer 2006 base program, as well as augmentation of the base program consisting of measurements by CARB of VOC and carbonyl compounds at one pair of upwind/downwind sites in the summer of 2006 and analyses by UC Davies of archived ambient particulate samples collected by UC Davies from one pair of upwind/downwind sites during the summer of 2005.

1.1 Background of RRAMP

In 2000, community concerns about the UPRR facility in Roseville led the District to seek the assistance from CARB to conduct a HRA for diesel emissions emanating from the rail yard. This was a major undertaking, and after almost three years, CARB released their findings in October 2004. CARB concluded that:

- *DPM emissions from railyard operations are estimated to be about 25 tons per year;*
- *Excess cancer risk levels between 100 and 500 in a million, based on California-derived diesel toxicity, affect an area in which 14,000 to 26,000 people live; and*
- *Excess cancer risk levels between 10 and 100 in a million affect an area in which about 140,000 to 155,000 people live.*

Based on these findings and other community concerns regarding the rail yard, the District decided that a follow-up air monitoring study was imperative and the District Board of Directors approved the Roseville Railyard Air Monitoring Project (RRAMP) at their October 2004 meeting. The objectives of RRAMP are as follows: (1) to determine, through ambient air monitoring, localized air pollutant/toxic impacts from emissions emanating from the UPRR facility; (2) to verify the effectiveness of mitigation measures to be implemented by the UPRR; (3) to provide feedback to the public regarding air quality conditions relevant to objectives 1 and 2; and (4) to improve the accuracy of future HRAs.

In August 2005 the District submitted an application under EPA's "Local-Scale Air Toxic Ambient Monitoring" grant solicitation to request funding for year two of RRAMP. The District's grant proposal requested funds to cover a portion of the summer 2006 base program costs as well as augment the RRAMP measurements by including measurements of VOC and carbonyl compounds

at one pair of upwind/downwind monitoring sites during the summer of 2006, and analyzing archived samples collected by UC Davis at one pair of upwind/downwind sites in the summer of 2005 for a large suite of analytes including elements and organic species. EPA Region IX awarded the District the requested funding in the amount of \$218,101 on April 18, 2006.

1.2 Study Area

UPRR's Roseville rail yard is located within a one-quarter mile wide by four-mile long area primarily in the community of Roseville, CA, northeast of Sacramento. Approximately two-thirds of the facility is located within Placer County, and one-third within Sacramento County. The rail yard operates around the clock, 365 days a year, and is considered one of the largest such facilities in the western United States. On an annual basis, approximately 31,000 locomotives stop at the facility each year, and 98% of Union Pacific's Northern California traffic moves through the facility.

The facility service area, including staging tracks, wash racks, service tracks, maintenance shop, and ready tracks, is situated near the eastern part of the rail yard, while the hump and trim, rockpile yard, and main receiving yard are situated more toward the central-western part of the facility. According to CARB's estimates, approximately 50% of the DPM emissions are from locomotives moving throughout the rail yard, about 45% are from idling emissions, and 5% from the testing of locomotives. The greatest emissions tend to be produced within the facility service area (estimated to be about 8 tons per year). Within this area, almost three-fourths of the emissions are from idling locomotives. The area with the second greatest amount of emissions (estimated to be about 7.5 tons per year) is the hump and trim area.

As can be seen from Figures 1 and 2, some residential communities abut the rail yard. Therefore, emissions from the rail yard can have a direct and substantial air quality impact on individuals residing in these areas, as was determined from CARB's HRA. CARB concluded that emissions from the railyard have very little temporal variation both during a 24-hour period or from month to month.



Figure 1. Aerial Photo of Roseville Railyard



Figure 2. Operational Layout of Railyard

1.3 Ambient Air Monitoring Network

Recognizing the limitations for directly measuring DPM in ambient air, and recognizing that it would be virtually impossible to try to distinguish between DPM from rail yard locomotives versus nearby diesel truck traffic on Interstate-80 (about 1 mile southeast of the railyard), a unique

monitoring approach was conceived. The meteorological data indicate that the prevailing wind direction, primarily at night, during the summer months is from the southeast (see Figure 3). Therefore, two pairs of upwind/downwind monitoring sites are being utilized (see Figure 4), arranged optimally to coincide with the predominant wind direction for the summer sampling periods. The two downwind sites are located within the maximum impact areas, namely the rail yard service area and maintenance yard. Each pair of upwind/downwind monitoring sites is situated such that the only source of emissions between the downwind and upwind sites is the rail yard facility.

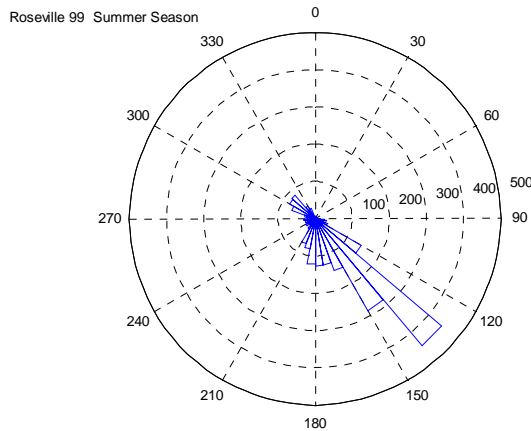


Figure 3. Summer Windrose

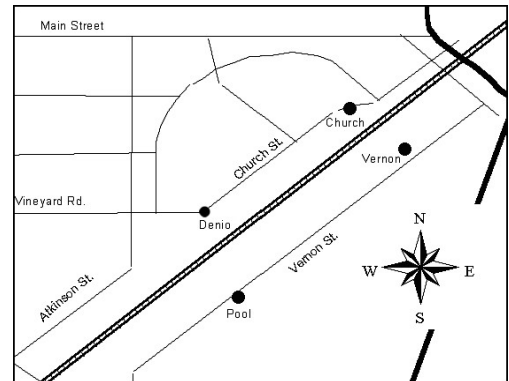


Figure 4. Location of Upwind/Downwind Sites

The overall monitoring concept is to utilize co-located samplers at each site consisting of continuous Aethalometer measurements of black carbon (BC), continuous PM2.5 Beta Attenuation Mass (BAM) monitors to measure PM2.5 mass, continuous NOx analyzers, and a pair of PM2.5 federal reference method (FRM) filter-based samplers to measure PM2.5 mass collected on Teflon filters and PM2.5 elemental carbon collected on quartz filters. The use of a continuous NOx analyzer and Aethalometer at each site helps with diesel plume detection since simultaneous peaks in both NOx and BC indicate the presence of a diesel emissions plume. The FRM units were operated during a seven-hour nighttime period (2200 PST to 0500 PST) when the wind direction is predominantly from the southeast. The FRM results of mass and elemental carbon provide a cross reference for the continuous mass and black carbon measurements obtained with the co-located BAM units and Aethalometers, respectively. The upwind sites measure ambient concentrations in the background air due to emissions from regional pollution sources, whereas the downwind sites measure both the background concentrations plus the additional emissions from the rail yard.

2. PROJECT TASKS

This project includes the following six tasks: (1) equipment procurement and installation; (2) network operations and data processing; (3) laboratory analyses; (4) quality assurance; (5) data validation and data analysis; and (6) management and reporting. These six tasks are described below.

Task 1. Equipment Procurement and Installation. The equipment and instruments identified in the EPA grant proposal were installed on site in the summer of 2005. All on-site instrument testing, calibration, repairs and/or replacement activities have been completely documented. All continuous monitors were connected with on-site data loggers to allow for daily data downloading. Arrangements for technical support from other regulatory agencies were made to ensure continuous sampling throughout the entire monitoring period.

Task 2. Network Operations and Data Processing. Routine on-site operations and external QA audits were conducted. On-site operations include: (1) inspection of instruments; (2) periodic performance tests; (3) FRM filter receipt, deployment, retrieval, storage, and shipment to the South Coast AQMD (SCAQMD) laboratory; (4) documentation of instrument, station, and meteorological conditions; (5) preventive maintenance; (6) corrective maintenance; and (7) transmission of data, and documentation. Other on-site operations include: (1) periodic download and examination of field data; (2) review of site documentation; (3) replenishment of consumables and supplies; (4) calibration, repair, and maintenance; and (5) coordination with auditors. Two site audits were conducted by CARB during the 2006 summer study period in July and October.

Task 3. Laboratory Analyses. Analyses of FRM filters for PM_{2.5} mass, organic carbon, and elemental carbon were conducted by the SCAQMD; CARB analyzed ambient samples collected in canisters for VOC compounds and on cartridges for carbonyls; and UC Davies analyzed archived impactor samples collected in summer 2005 for elements and organic species including PAHs.

Task 4. Quality Assurance. The Quality Assurance Project Plan (QAPP) was developed and submitted to EPA Region IX for approval in July 2005. The Quality Management Plan (QMP) was prepared and submitted to EPA Region IX for approval in June 2006. Both documents have been approved by EPA Region IX.

Task 5. Data Validation and Analysis. A preliminary data screening procedure for the raw data was developed to guide District staff in flagging suspect data based on specific data validation criteria. The SCAQMD's laboratory results for PM_{2.5} mass, organic carbon and elemental carbon undergo similar data review by SCAQMD staff and are then incorporated into the RRAMP database. The Desert Research Institute (DRI), the contractor selected by the District through a competitive procurement process, performs additional data reviews and appropriate data analyses to meet the study objectives.

Task 6. Management and Reporting. The efforts of different project participants are coordinated by District staff. A summary of the project participant's results/findings for those efforts funded by the EPA Region IX grant are presented below and reports prepared by these project participants are attached to this progress report (see Section 3 for details).

3. SUMMARY OF RESULTS

3.1 Base Monitoring Program for Summer 2006

DRI performed a detailed data review, data analysis, and interpretation of results to support the first of two general study objectives, namely: (1) to determine the impacts from the UPRR facility as measured by the differences between upwind and downwind monitoring site pairs; and

(2) to determine any discernible trends in reduced impacts over a three-year period as a result of emissions mitigations implemented by UPRR. The second study objective will be addressed following the third year of monitoring. DRI's data analysis report for the 2006 summer monitoring period (the second year annual report prepared for the District) was reviewed and approved by the RRAMP Technical Advisory Committee (TAC). This report is attached to this progress report as Attachment 1. A summary of DRI's data analysis report for the 2006 summer monitoring period is presented below.

Data Capture

According to the findings presented in DRI's data analysis report for the 2005 summer monitoring period, the TAC reviewed the wind data collected during the 2005 sampling period and decided to modify the sampling period for the FRM filter-based samplers from a 12-hour and 24-hour basis to a 7-hour nighttime basis (10:00 PM to 5:00 AM) during which time winds generally blow from the upwind monitoring sites to the downwind monitoring sites. Using this modified monitoring strategy, the differences between the upwind and downwind measurements should represent the maximum impact from the rail yard without impacts from other sources.

Consistent with the 2005 summer monitoring period, the following instruments were deployed at each RRAMP monitoring site in the summer of 2006: continuous monitors for PM2.5, black carbon (indicative of diesel particulates), and NOx; filter-based FRM samplers for PM2.5 mass, organic carbon, and elemental carbon; and meteorological equipment primarily for wind speed and wind direction. Continuous monitors provide hourly average concentration measurements that can be analyzed with respect to specific wind conditions.

The second-year monitoring period of RRAMP began on June 15, 2006 and was scheduled to end September 30, 2006. Two weeks were added to the project due to the air quality impact from the Ralston fire such that the actual end date was October 15, 2006. The same pairs of upwind/downwind sites (Pool/Denio and Vernon/Church) were used as the previous year. Both pairs of upwind/downwind sites functioned during the entire second-year monitoring period unlike the first-year monitoring period when the Vernon/Church pair only became operational late in the summer of 2005. The data collected during the two-week period impacted by the Ralston fire incident were excluded in DRI's data analysis to ensure that the ambient measurements would reflect the impacts from the rail yard alone. A summary of the data capture for continuous data collected during the 2006 summer study period is shown in Table 1. As can be seen from this table, we successfully captured a very high percentage of possible data. This reflects a successful field program.

Table 1. Data Capture for Continuous Measurements During Summer 2006.

Site	Wind Speed	Wind Direction	NO	NOx	BC	PM2.5
Denio	99.9%	99.9%	96.6%	96.6%	92.2%	99.2%
Pool	99.9%	99.9%	98.4%	98.4%	96.7%	89%
Church	100%	100%	97.8%	97.8%	95.8%	99.3%
Vernon	100%	100%	99.1%	99.1%	94.8%	99.2%

Results

DRI's data analysis report for the summer 2006 monitoring period describes a number of detailed statistical analyses; some of the key results are summarized here. Three screening criteria were established to determine the conditions for which upwind versus downwind analyses are appropriate: (1) winds need to be from a semi-circular arc between 45 degrees (i.e., northeasterly) through 225 degrees (i.e., southwesterly); (2) only winds speeds from 0.5 to 4 m/s were used to avoid calm or windy conditions; and (3) only overnight hours from 10 PM to 5 AM PST were used. This is the time frame when the winds blow most consistently across the rail yard directly from the upwind to the downwind sites, and therefore the emissions from the rail facility can most readily be detected. Once the subset of appropriate data was finalized, DRI evaluated the differences between upwind and downwind site concentrations of black carbon (BC), PM_{2.5}, NO, and NO_x. The results are shown in Figures 5 through 8. The data collected during the Ralston fire period were excluded from the data analyses.

Figure 5 shows the 7-hour average nighttime concentrations of BC for the 2006 summer monitoring period. This bar chart shows the average concentrations for which data are available from all four monitoring sites. The concentrations at both downwind sites (Denio and Church) are significantly higher than at their corresponding upwind sites (Pool and Vernon). The red bars depict the uncertainty of the values depicted, and as can be seen, these are small in comparison to the observed concentrations. From a statistical standpoint, we have greater than a 99.9% confidence that these findings are real and not due to chance alone. Also shown in Figure 1 are the differences between the upwind and downwind pairs to show the presumed impact from the rail yard facilities. In the 2006 intensive sampling period, the difference in BC concentrations between the Denio/Pool pair is over 2 $\mu\text{g}/\text{m}^3$. A comparisons of both upwind sites and both downwind sites are shown as the two rightmost bars. The difference between the two upwind sites is relatively small indicating that the upwind sites consistently reflect the same background conditions.

Figure 5. Nighttime 7-hour Average Black Carbon Concentrations

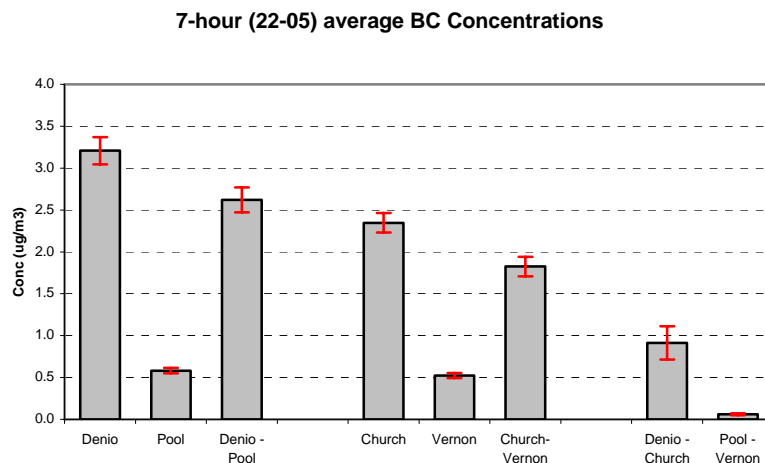


Figure 6 shows the 7-hour average nighttime concentrations of PM_{2.5} mass for the 2006 summer monitoring period. While the downwind sites have levels that are statistically higher than the upwind sites, these differences are not as pronounced as for BC. This is because PM_{2.5} mass is

a regional pollutant impacted by multiple sources that is measured by both upwind and downwind sites. Nevertheless, the differences in PM_{2.5} mass concentrations between the upwind and downwind sites are 6 to 8 $\mu\text{g}/\text{m}^3$.

Figure 6. Nighttime 7-hour Average PM_{2.5} Concentrations

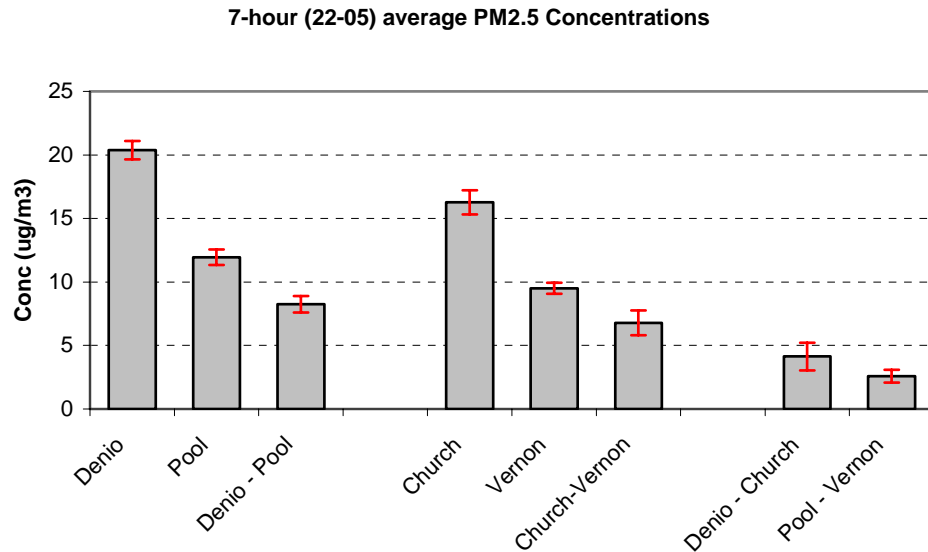


Figure 7 shows the 7-hour average nighttime NO concentrations for the 2006 summer monitoring period. NO is a good indicator of fresh NO_x emissions, since ultimately with time, NO converts to NO₂. This chart may be the most indicative of all charts indicating that the downwind sites are picking up the emissions from the rail yard facility. While downwind sites show NO concentrations of about 100 ppb, the upwind sites show NO concentrations that are less than 10 ppb.

Figure 7. Nighttime 7-hour Average NO Concentrations

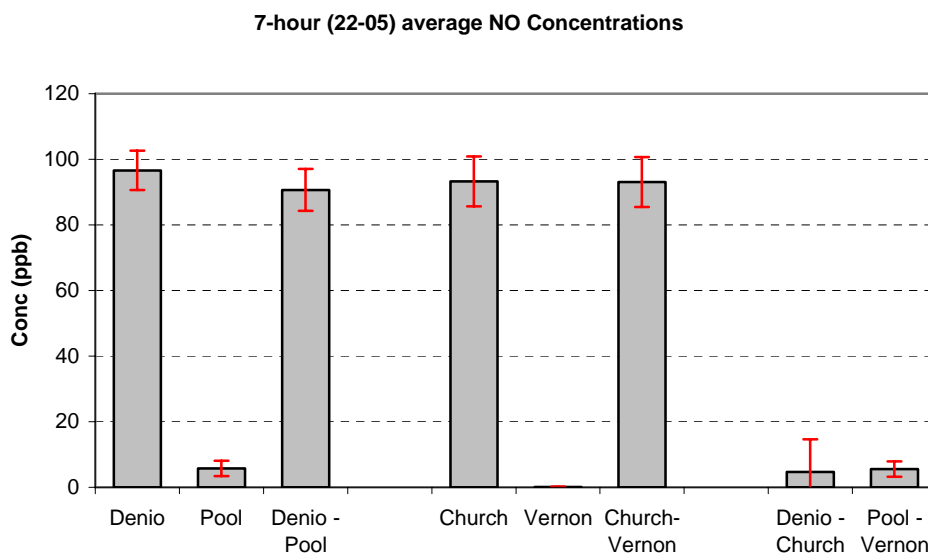
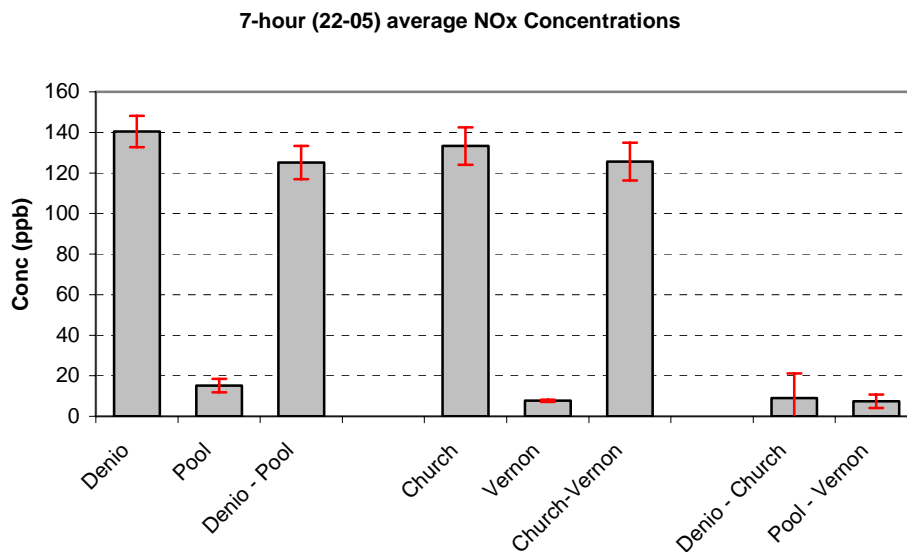


Figure 8 shows the 7-hour average nighttime NOx concentrations for the 2006 summer monitoring period. While the results presented in Figures 7 and 8 are very similar, there are some interesting differences. The downwind sites show a very high percentage of NOx as NO, meaning that these sites are dominated by fresh emissions. Conversely, the upwind sites have a low percentage of NOx as NO, meaning that the upwind areas are affected to a much greater degree from aged NOx emissions, perhaps attributable to earlier mobile source emissions in the local or greater Sacramento area. In any case, the differences between upwind and downwind NOx concentrations are dramatic.

Figure 8. Nighttime 7-hour Average NOx Concentrations



The most important finding is that all the results are consistent with each other, and show that the downwind monitors are capturing the effects of the rail yard emissions.

Conclusions

DRI's data analysis report for the summer 2006 monitoring period showed generally good agreement with no significant biases between paired instruments. The revised FRM sampling schedule adopted in the second year greatly improved the data quality. The differences in mean concentrations between the two pairs of downwind and upwind sites (Denio-Pool and Church-Vernon) are all significant at above the 99% confidence level.

Downwind sites show statistically significant impacts of BC, NO, NOx, and PM2.5. The high NO/NOx ratio at the downwind sites indicates that downwind sites are dominated by fresh NO emissions while upwind sites are more indicative of aged NO emissions. This strongly suggests that the downwind sites are indeed picking up the emissions from the rail yard facility.

Overall, the summer 2006 results were very similar to the summer 2005 results with substantially higher NO, NOx, and BC concentrations at the downwind sites relative to the upwind sites. The multiple year trend analysis will be conducted after the end of the third year of sampling.

3.2 Elemental and Organic Analysis of Archived Summer 2005 Samples

During the summer of 2005 (i.e., the first year of RRAMP), Dr. Thomas Cahill of U.C. Davis, deployed his eight-stage DRUM impactor samplers at one pair of RRAMP upwind and downwind sites as UC Davis' in-kind support for RRAMP. UC Davis also analyzed the impactor samples for mass as part of their in-kind support. As part of the EPA Region IX grant funding, UC Davis analyzed the archived DRUM impactor samples as well as Lundgren impactor samples collected in the summer and fall of 2005 for elements and organic species including air toxics and potential markers for locomotive diesel exhaust.

Dr. Cahill's report containing the results of these analyses and his findings is included as Attachment 2 to this progress report. This report has been reviewed by the RRAMP's TAC who concluded that: (1) further research is needed to identify the sources of zinc in the samples, and (2) the data doesn't support the author's conclusion that diesel exhaust from locomotives is more hazardous than diesel exhaust from trucks. Dr. Cahill's report states that zinc could serve as a tracer for lubricating oil from locomotives exhaust. However, the UPRR representative on the TAC is not convinced that zinc is a component of locomotive lubricating oils. Thus, a detailed analysis of locomotive lubricating oil is needed. Regarding Dr. Cahill's assertion that diesel exhaust from locomotives is more hazardous than diesel exhaust from trucks, the TAC's position is that the usual measure of cancer risk from diesel exhaust is not due to the risk from individual PAHs but rather due to exposure to a mixture of compounds in diesel exhaust as measured by a long term epidemiological study of railway workers. Because of these concerns, neither the District nor the TAC endorses the views and opinions expressed in Dr. Cahill's report.

Dr. Cahill's concludes that:

- The rail yard diesel exhaust mass (and sulfur) peaks in size at about 0.3 μm , which is about 3 times larger in size than that for a diesel truck under load. On the other hand, the PAHs are almost entirely less than 0.1 μm in diameter, implying that most of the PAHs come from the lubricating oil rather than the diesel fuel.
- The coarse soils of the Roseville rail yard and its vicinity contain anthropogenic metals (e.g., zinc and copper) at levels much higher than that of standard soils.
- The data for *n*-alkanes reveals that the soil is highly contaminated by heavy petroleum products. In addition, the coarse sulfur values also indicate a primary diesel source for *n*-alkanes in the yard.
- About half of the identified $\text{PM}_{2.5}$ organic mass is associated with biogenic sugars and fatty acids while the other half consists mainly of petroleum based *n*-alkanes. PAHs represented only a few percent of the identified organic mass.
- Diesel exhaust from the Roseville rail yard is about three times richer in the most toxic components (e.g., benzo{a}pyrene) than exhaust from diesel trucks.
- There was about six times more benzo{a}pyrene associated with the rail yard emissions compared to diesel trucks per unit of very fine plus ultra fine mass as well as per unit of black carbon.

3.3 VOCs and Carbonyls

Another component of work sponsored by the EPA Region IX grant funding involved an augmentation of the base program for the summer 2006 monitoring period by adding monitoring for VOC and carbonyl compounds at the rail yard. Ambient samples were collected by District staff and

analyzed by CARB. A pair of Xon Tech 910A gas-phase samplers with polished Summa stainless steel canisters to collect VOCs and PQ100 cartridges to collect carbonyls was deployed at the Denio (downwind) and Pool (upwind) sites every sixth day between June 21 and October 13, 2006. Samples were collected on the same seven-hour nighttime schedule as the FRM filter based measurements. After sampling, the canisters and cartridges were sent back to CARB for analysis. The VOC and carbonyl compounds that were analyzed included: 1,1,1-trichloroethane, 1,3-butadiene, acetaldehyde, acetone, acetonitrile, acrolein, acrylonitrile, benzene, bromomethane, carbon tetrachloride, chloroform, dichloromethane, cis/trans-1-3 dichloropropene, formaldehyde, methyl ethyl ketone, m,p,o-xylenes, and o,p-dichlorobenzene. Although many of these compounds are not associated with rail yard emissions, any VOC or carbonyl compound originating from operations within the rail yard should show up as upwind/downwind differences.

CARB's laboratory results indicated that many VOC and carbonyl measurements were below the instrument detection limit at both the downwind and upwind sites. CARB staff presented the results for seven gaseous organic species (acrolein, acrylonitrile, acetaldehyde, benzene, chloroform, formaldehyde, and toluene) from the Denio and Pool sites at a TAC meeting in late 2006. These results are included as Attachment 3 to this progress report. In general, the concentrations of acrolein, acetaldehyde and formaldehyde were higher at Denio than Pool. The reverse was generally true for acrylonitrile, chloroform and toluene. Benzene concentrations were similar at both sites indicating a regional source. Because the Pool monitoring site is located next to the Roseville municipal swimming pool, the VOC and carbonyl concentrations measured at the Pool site may be influenced by materials used for pool cleaning and sanitation. After reviewing CARB's laboratory results, the TAC unanimously concluded that these results are not very useful in quantifying the impact of rail yard emissions on ambient air quality.

4. BENEFITS TO THE PUBLIC

Emissions from railroad operations are a significant source of ozone and PM precursors, directly emitted PM, and toxic air pollutants. Because emissions reductions from railroads are primarily under EPA authority, very little information is available to local agencies. CARB's health risk assessment of the Roseville rail yard released in October 2004 estimated cancer risks in excess of 500 in a million just from this one facility alone. This is much greater than the risks caused by the vast majority of individual stationary sources subject to local regulations. It should be pointed out that CARB's health risk assessment did not have any measured data to work with; instead they estimated DPM emissions, and used meteorological data from monitors some distance from the rail yard facility, and computer models to estimate health risks. Thus, the Roseville rail yard monitoring project supported by EPA Region IX grant funding will provide actual measurements of pollutants associated with diesel emissions emanating from the Roseville rail yard operations. This information will allow CARB to conduct a more robust assessment of the health risks to the public due to UPRR operations in Roseville. Further, since UPRR has committed, under a letter of agreement with the District to implement innovative emissions reducing technologies and practices, reduced levels of air toxics are expected to occur. This monitoring study will serve as both a baseline for pre-implementation conditions and provide the basis of being able to demonstrate in subsequent years the measurable improvement and associated lower cancer risk to the public from implementation of these control measures. The multi-year trends analysis, which will be conducted

after the 2007 summer data has been analyzed, should provide a measure of the effectiveness of UPRR's mitigation measures.

District staff provide information on the monitoring project and the status of UPRR's mitigation measures to the public and City staff in the following ways: (1) participation at quarterly meetings of the City Railyard Committee; (2) submittal of an annual report plus a presentation to the District's Governing Board every December; (3) presentations at several city and neighborhood association meetings; and (4) hosting tours of the RRAMP monitoring sites for community organizations. The District has received very positive feedback from the attendees of these meetings and tours. District staff will continue updating the public as new information becomes available.

5. MEASURING PROJECT SUCCESS

The success of this monitoring project is measured in several ways. First, the proposed monitoring objectives have been achieved including: (1) meeting the scheduled sampling period of June through October; (2) meeting the data completeness targets; (3) meeting the measurement objectives for the monitoring equipment; and (4) being able to qualify the data collected. DRI's data analysis report demonstrates that a sufficient number of high quality data, that meet the project's QA objectives, have been obtained to determine upwind/downwind differences and provide a good foundation for a three-year trends analysis after the 2007 summer field monitoring program has been completed and the data analyzed.

Another measure of judging the success of a project is determining the effectiveness of the integration/coordination of information between all project team members. District staff has had the responsibility of coordinating the efforts of project team members, as well as maintaining communications between all project team members for RRAMP. RRAMP can be considered a very successful project based on the excellent cooperation and support that the District continues to receive from all project team members.

Finally, the third element for success is the timeliness of the project, data analyses, and release of information to the public. Field sampling occurs during the summer; laboratory analyses and data base compilation occurs in the fall; data analyses occur in early winter, and results and reports are released each April following the year of the field sampling. With contingency plans in place, and with proper oversight and management by the District, schedule slippages are minimized, and overall project timelines met as closely as possible to the target dates.

Attachment 1

DRI's Second Annual RRAMP Data Analysis Report



Roseville Rail Yard Air Monitoring Project (RRAMP)

Second Annual Report Review and Summary of Year 2 (2006) Data

Prepared for

Placer County Air Pollution Control District
3091 County Center Drive, Suite 240
Auburn, CA 95603

Prepared by

David E. Campbell and Eric M Fujita
Desert Research Institute
Division of Atmospheric Sciences
2215 Raggio Parkway
Reno, NV 89512

April 16, 2007

TABLE OF CONTENTS

1. INTRODUCTION	1-1
1.1 Background.....	1-1
1.2 Objectives of RRAMP Data Analysis	1-2
2. EVALUATION AND VALIDATION OF RRAMP DATA.....	2-1
2.1 Aethalometer Black Carbon Data.....	2-1
2.2 Application of Time and Wind Criteria.....	2-2
2.3 Hourly Pollutant Data Distributions.....	2-3
2.4 Hourly Pollutant Time Series	2-4
2.5 Related Pollutant Ratios	2-4
2.6 Collocation Data.....	2-5
2.6.1 Collocated Aethalometer Black Carbon Data.....	2-5
2.6.2 Collocated BAM PM _{2.5} Mass Concentration Data	2-6
2.7 Filter versus Continuous Data	2-7
2.7.1 Filter Gravimetric Mass Versus Continuous BAM Mass Concentrations.....	2-7
2.7.2 Filter Elemental Carbon Versus Aethalometer BC Concentrations	2-8
3. RESULTS	3-1
3.1 Upwind/Downwind Differences.....	3-1
3.2 FRM filter results	3-2
4. CONCLUSIONS AND RECCOMENDATIONS	4-1
4.1 Data Evaluation and Validation.....	4-1
4.2 Data Analysis.....	4-1
5. REFERENCES	5-1
APPENDIX A: Measurement Methods.....	A1
APPENDIX B: Time-Series Plots of Hourly Data.....	B1

LIST OF TABLES

Table 1–1. Summary of RRAMP Measurements During Summer 2006. Filter samples were collected every third day for 7 hours (or alternating 7 and 24 hour samples at Church and Vernon).....	1-3
Table 2–1. Number of 5 minute aethalometer BC data points eliminated or flagged during the QA process. The full data set is composed of over 35,000 data points.	2-10
Table 2–2. Precision analysis of collocated Aethalometer data. Linear regressions use data from the sampler used at the upwind site as the independent (x) variable.	2-10
Table 2–3. Precision analysis of collocated BAM data. Linear regressions use data from the sampler used at the upwind site as the independent (x) variable.	2-11
Table 2–4. Comparison of filter results and continuous sampler data. Linear regressions use FRM filter data as the independent (x) variable. Adjustments that were applied to data are highlighted in bold.	2-12
Table 3–1. Means, standard deviations, and standard errors of the means for 7-hour (2200 to 0500 PST) and 24-hour (midnight to midnight PST) BC, PM _{2.5} , NO and NO _x concentrations at the four RRAMP sites. The differences in mean concentrations between the two pairs of downwind and upwind sites (Denio-Pool and Church-Vernon) during the overnight period and pooled standard error of the differences are also shown.....	3-3
Table 3–2. Means and statistics for hourly (2200 to 0500 PST) NO/NO _x , BC/PM _{2.5} , and BC(1)/BC(2) ratios at the four RRAMP sites. The standard deviation and 2-sigma standard errors of the means are included to indicate the significance of the differences.....	3-4
Table 3–3. Means and 2-sigma standard errors for TOR analysis results of the 7-hour overnight FRM filter samples.....	3-4
Table 3–4. Elemental to total carbon ratios and total carbon to PM _{2.5} ratios for 7-hour overnight FRM filter samples. All values are calculated from the differences in concentration between downwind and upwind sites, without blank correction. The group mean and 2-sigma standard errors of the means are included to indicate the significance of the differences.....	3-5

LIST OF FIGURES

Figure 1-1. Map showing locations of the two upwind (Pool and Vernon) and two downwind (Denio and Church) sampling locations. The bearing between the Vernon/Church and Pool/Denio pairs is 137 and 162 degrees, respectively.....	1-4
Figure 2-1. Comparison of hourly mean wind speeds (m/s) from 22:00-5:00 at site pairs.	2-13
Figure 2-2. Hourly average wind speed (meters per second) from instruments collocated after the main study period. E2237 was used at Denio, E2238 at Pool, and 4515 at Vernon.	2-14
Figure 2-3. Distribution of hourly mean wind speeds (m/s) from 22:00-5:00 at Denio site.	2-15
Figure 2-4. Frequency of hourly average wind directions at the four sites during overnight hours (22:00 to 05:00 PST). Wind directions have been rounded to the nearest 45 degrees. Only hours where winds were between 45° and 225° were used to determine downwind-upwind differences.....	2-15
Figure 2-5. Differences in mean hourly wind direction between site pairs.....	2-16
Figure 2-6. Hourly average wind direction (degrees) from instruments collocated after the main study period. BAM 4514 is believed to be accurate due to its excellent agreement with BAM 4515 during the collocation tests. The dashed lines representing a 1:1 relationship are included for comparison.....	2-17
Figure 2-7. Histograms showing the frequency distribution of hourly averaged NO data at the four sites.....	2-18
Figure 2-8. Histograms showing the frequency distribution of hourly averaged NOx data at the four sites.....	2-19
Figure 2-9. Histograms showing the frequency distribution of hourly averaged Aethalometer BC(1) data at the four sites.....	2-20
Figure 2-10. Histograms showing the frequency distribution of hourly averaged BAM PM2.5 data at the four sites.....	2-21
Figure 2-11. Correlation of hourly BC(1) (ug/m3) averaged data from collocated Aethalometers 02/23/06-05/01/06. Instrument 626 was later used at the Denio site, and 624 at Pool.	2-22
Figure 2-12. Correlation of hourly averaged BC(1) (ug/m3) data from collocated Aethalometers 10/17/06-11/06/06.....	2-22
Figure 2-13. Relative difference between collocated Aethalometers used at Denio and Pool sites. Data are from hourly averages of channel 1 BC. Table gives distribution of absolute values of relative differences, with approximate 95 th percentile in bold.	2-23
Figure 2-14. Correlation of hourly averaged BC data (ug/m3) from collocated Aethalometers 02/23/06-05/01/06. 623 was later used at Church and A479 at Vernon.....	2-24

Figure 2-15. Correlation of hourly averaged BC data (ug/m3) data from collocated Aethalometers 10/17/06-11/06/06.....	2-24
Figure 2-16. Relative difference between collocated Aethalometers used at Church and Vernon sites. Data are from hourly averages of channel 1 BC. Table gives distribution of absolute values of relative differences, with approximate 95 th percentile in bold....	2-25
Figure 2-17. Correlation of hourly PM2.5 (ug/m3) averaged data from collocated EBAMS 02/23/06-05/01/06. Instrument E2237 was later used at the Denio site, and E2238 at Pool.	2-26
Figure 2-18. Correlation of hourly averaged PM2.5 (ug/m3) data from collocated EBAMS 10/17/06-11/06/06.....	2-26
Figure 2-19. Difference between collocated EBAMS used at Denio and Pool sites. Data represented are hourly averages. Table gives distribution of absolute values of differences, with approximate 95 th percentile in bold.....	2-27
Figure 2-20. Correlation of hourly averaged data from collocated BAMS 02/23/06-05/01/06. 4514 was later used at Church and 4515 at Vernon.....	2-28
Figure 2-21. Correlation of hourly averaged data from collocated BAMS 10/17/06-11/06/06.	2-28
Figure 2-22. Difference between collocated BAMS used at Church and Vernon sites. Data represented are hourly averages. Table gives distribution of absolute values of differences, with approximate 95 th percentile in bold.....	2-29
Figure 2-23. Correlation plots comparing average BAM PM2.5 to gravimetric mass from FRM filters for 24hr samples at 2 sites.	2-30
Figure 2-24. Correlation plots comparing average BAM PM2.5 to gravimetric mass from FRM filters for 7hr samples at 4 sites.	2-31
Figure 2-25. Correlation plots comparing average aethalometer BC(1) to elemental carbon from FRM filters for 24hr samples at Church and Vernon.....	2-32
Figure 2-26. Correlation plots comparing average aethalometer BC(1) to elemental carbon from FRM filters for 7hr samples at 4 sites.....	2-33
Figure 2-27. Correlation plot comparing difference in elemental carbon (EC) concentration from FRM filters between downwind and upwind sites to difference in average Aethalometer black carbon (BC) for 7hr samples at 2 site pairs.	2-34
Figure 3-1. Mean BC, PM _{2.5} , NO and NO _x concentrations at the four RRAMP monitoring sites and differences of the two pairs of downwind and upwind sites (Denio-Pool and Church-Vernon). Differences between the two downwind and two upwind sites are also shown for comparison. Error bars are the standard errors of the means.	3-6

1. INTRODUCTION

The Roseville Rail Yard Air Monitoring Project (RRAMP) is being undertaken under the auspices of the Placer County APCD (PCAPCD), in cooperation with the Union Pacific Railroad (UPRR), Sacramento Metro AQMD, and USEPA Region IX. The purpose of the project is to monitor for diesel locomotive emissions from the UPRR's J.R. Davis Rail Yard, located in Roseville, CA. The monitoring segment of the study consists of intensive monitoring by PCAPCD in each of the summers in 2005-2007 (mid-July to mid-October). Laboratory support for the study is provided by the California Air Resources Board and the South Coast Air Quality Management District. This second interim report summarizes the results of an independent review conducted by the Desert Research Institute of the internal, spatial, temporal, and physical consistency of each data set obtained during the second year of the monitoring program. This report also provides an initial summary and analysis of the data. It is preceded by a similar report for the first year of the monitoring program (Campbell and Fujita, 2006).

1.1 Background

The characterization of a community's exposure to air pollutants is essential in assessing cumulative impacts to public health. An important part of such assessments is the identification and quantification of disproportionate impacts that may be experienced by certain communities due to their proximity to sources of hazardous air pollutants. At the request of the Placer County Air Pollution Control District (PCAPCD), the California Air Resources Board (ARB) initiated a risk assessment study in 2000 of diesel emissions from the Union Pacific Railroad's J.R. Davis Rail Yard, located in Roseville, CA. The results of this assessment study, released in October 2004 (ARB, 2004), concluded excess cancer risk levels between 100 and 500 in a million in the neighborhood immediately downwind of the rail yard and risk levels between 10 and 100 in a million for up to 155,000 people that reside in a larger urbanized area downwind of the facility. Based upon these findings and community concerns, the PCAPCD initiated the Roseville Rail Yard Air Monitoring Project (RRAMP) in 2005. The purpose of this three-year monitoring study is to measure the air quality impacts of emissions, primarily diesel, from the rail yard facility and effects of mitigation measures that are implemented at the facility during this three-year period.

The main objectives of the RRAMP measurement program is to determine the localized air pollutant impacts from the emissions at the UPRR facility and to determine if any trends can be detected as a result of emissions mitigations which UPRR has agreed to implement over the three-year period of RRAMP. The air quality monitoring segment of the study commenced in summer 2005 and consists of intensive monitoring in each of the summers in 2005-2007 (mid-July to end of September). Monitoring for the RRAMP consists of two upwind/downwind pairs of monitoring sites aligned as optimally as possible to wind direction which most persistently is perpendicular to the rail yard tracks. The field measurements that were made during summer 2006 are summarized in Table 1-1. The prevailing winds during the late night through early morning hours in the summer months coincide with the conditions that are most favorable for achieving the monitoring objectives for the study. The map in Figure 1-1 shows the locations of the two upwind (Pool and Vernon) and two downwind (Denio and Church) sampling sites. The upwind/downwind wind directions between the Vernon/Church and Pool/Denio pairs are 137

and 162 degrees, respectively. Meteorologic data was also collected at the Roseville AQMD monitoring station which is located East of the area shown in the figure at 151 N Sunrise Bl.

Meeting RRAMP objectives depend upon factors that may contribute to the variations and overall uncertainty in downwind/upwind differences in pollutant concentrations over a three year period. These factors include precision and accuracy of measurements (the main focus of this interim report), diurnal, daily, seasonal, and annual variations in meteorological conditions that affect transport and dispersions of emissions, spatial and temporal variations in activity patterns that can affect the concentrations measured at downwind locations under the same meteorological conditions, and the expected changes in emission levels due to the mitigation measures that will be implemented by UPRR during the 3-year study relative to overall measurement uncertainty.

1.2 Objectives of RRAMP Data Analysis

This report is the second of three annual reports that provide analyses of the RRAMP data. Data analysis effort for the first two annual reports consists of the following six tasks.

1. Provide additional review of the RRAMP monitoring data to identify possible outliers and other data inconsistencies.
2. Provide general descriptive statistics for each measured parameter.
3. Compare the RRAMP black carbon (aethalometer) and PM_{2.5} (BAM) measurements with Federal Reference Method (FRM) particulate data and determine degree of correlation among methods.
4. Examine the temporal variations in specific ratios of pollutants and characterize variations in contributions of aged versus fresh emissions and elemental carbon versus total carbonaceous particulate matter.
5. Perform statistical analyses to determine upwind/downwind differences in concentrations of black carbon and PM_{2.5}.

The final report at the end of the three-year monitoring program will include the following additional task.

6. Using BC and/or EC as surrogates to estimate the mass concentrations and associated uncertainties of diesel particulate matter (DPM) levels at the downwind monitoring sites.
7. Examine trends in black carbon and PM_{2.5} concentrations over the three-year duration of the RRAMP and determine their statistical significance.

Table 1–1. Summary of RRAMP Measurements During Summer 2006. Filter samples were collected every third day for 7 hours (or alternating 7 and 24 hour samples at Church and Vernon).

	Denio Site					
	Wind Spd & Dir (hourly)	NO/NOx (hourly)	Aethalometer BC (5 minute)	EBAM PM _{2.5} (hourly)	Teflon Filter for PM _{2.5}	Quartz Filter for TOR
monitoring period	6/15~10/15	6/15~10/15	6/15~10/15	6/15~10/15	6/16~10/14	6/16~10/14
total observations	2965	2952	35584	2965	41	41
valid observations	2963	2853	32820	2942	41	40
% valid	99.9%	96.6%	92.2%	99.2%	100%	98%

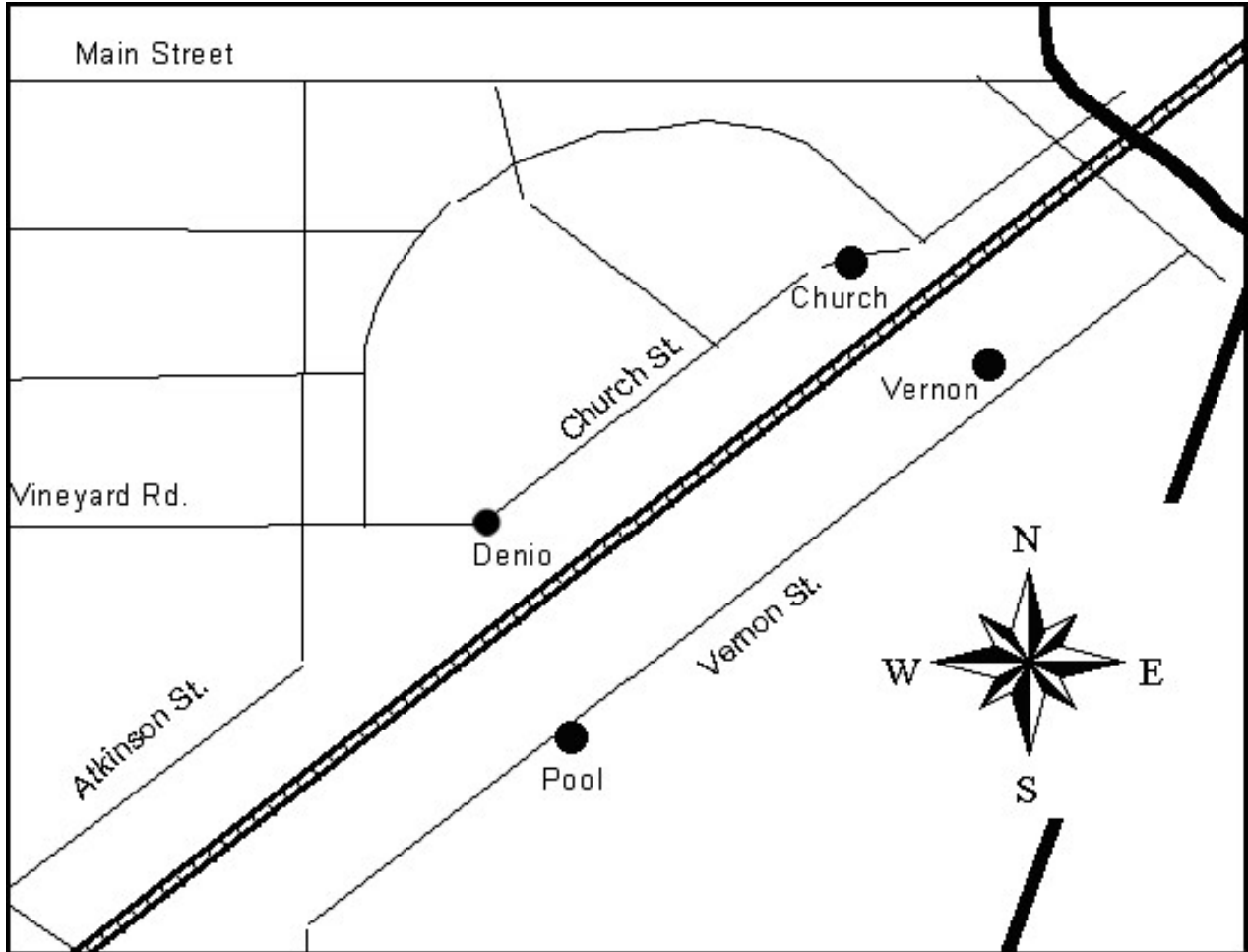
	Pool Site					
	Wind Spd & Dir (hourly)	NO/NOx (hourly)	Aethalometer BC (5 minute)	EBAM PM _{2.5} (hourly)	Teflon Filter for PM _{2.5}	Quartz Filter for TOR
monitoring period	6/15~10/15	6/15~10/15	6/15~10/15	6/15~10/15	6/16~10/14	6/16~10/14
total observations	2965	2952	35584	2965	41	41
valid observations	2963	2906	34424	2638	41	41
% valid	99.9%	98.4%	96.7%	89.0%	100%	100%

	Church St. Site					
	Wind Spd & Dir (hourly)	NO/NOx (hourly)	Aethalometer BC (5 minute)	BAM PM _{2.5} (hourly)	Teflon Filter for PM _{2.5}	Quartz Filter for TOR
monitoring period	6/15~10/15	6/15~10/15	6/15~10/15	6/15~10/15	6/16~10/14	6/16~10/14
total observations	2965	2952	35584	2965	42	42
valid observations	2965	2888	34106	2944	40	41
% valid	100.0%	97.8%	95.8%	99.3%	95%	98%

	Vernon St. Site					
	Wind Spd & Dir (hourly)	NO/NOx (hourly)	Aethalometer BC (5 minute)	BAM PM _{2.5} (hourly)	Teflon Filter for PM _{2.5}	Quartz Filter for TOR
monitoring period	6/15~10/15	6/15~10/15	6/15~10/15	6/15~10/15	6/16~10/14	6/16~10/14
total observations	2965	2952	35584	2965	42	42
valid observations	2965	2926	33738	2941	40	41
% valid	100.0%	99.1%	94.8%	99.2%	95%	98%

	Roseville Met Tower						
	Wind Spd (m/s)	Std Dev. Of Wind Dir	Temp. @ 2m (F°)	Delta of Temp. (F°)	RH (%)	SR (W/m ²)	Pressure (in/Hg)
monitoring period	6/15~10/15	6/15~10/15	6/15~10/15	6/15~10/15	6/15~10/15	6/15~10/15	7/15~10/15
total observations	2953	2953	2953	2953	2953	2953	2953
valid observations	2953	2953	2953	2953	2953	2953	2953
% valid	100.0%	100.0%	100.0%	100.0%	100%	100%	100%

Figure 1-1. Map showing locations of the two upwind (Pool and Vernon) and two downwind (Denio and Church) sampling locations. The bearing between the Vernon/Church and Pool/Denio pairs is 137 and 162 degrees, respectively.



2. EVALUATION AND VALIDATION OF RRAMP DATA

The determination of differences in measured parameters between the upwind and downwind sites requires a quantitative assessment of the relative precision between the paired samplers and measurement biases. Relative precision and bias were evaluated by examining the collocated sampler data collected before and after the summer sampling period, and accuracy was assessed by comparing time-averaged continuous sampler data with results from time-integrated filter methods. We also describe exceptional events and characteristics of the data that may affect the observed differences between paired measurements. The specific procedures described below were used to validate and analyze the continuous pollutant data and time-averaged filter-based FRM data. PCAPCD staff provided an initial review of the data by flagging suspect data due to sampler malfunctions or flow rates that were out of range. The validation checks performed by DRI checked the consistency of the data between sites and between pollutants at the same site. For consistency, these procedures will be applied to the data for all three years in the project final report. Appendix A describes the methods that were used during the summer 2006 measurement program and estimates of measurement precision and bias.

2.1 Aethalometer Black Carbon Data

The Aethalometer data is known to be strongly affected by electronic noise spikes which create exaggerated increases or decreases in individual measurements of light attenuation. Since the instruments estimate black carbon concentrations based on the slope of the change in attenuation, a single spike will produce two periods of inaccurate measurement. However, time-averaging those two periods together will negate the effect of the spike and give the correct value. Problems can occur when the time-averaged values do not contain a sufficient number of individual measurements to effectively cancel out the noise (this issue is discussed in the 2005 version of the aethalometer documentation provided by Magee Scientific). In this 2006 study the instruments were operated with the default 5-minute time constant, so each hourly average contains a maximum of 12 discrete measurements. Therefore, the probability of the two halves of a noise-related “bounce” in the signal being split between two hourly averages is 1:6.

Another issue is the periodic advancing of the filter tape to keep the optical attenuation in range of the detectors. When the tape changes there is a 15 minute gap in data collection and baseline shifting may occur. The instruments were operated with a preset tape advance schedule to minimize data loss per recommendation made in the first annual interim data review and analysis report. Overall, tape advance times varied slightly but were generally consistent starting at 5:25, 13:25, 21:25 and rarely occurred during the critical overnight hours except at Denio, where there were apparent tape advances at 1:35 from 7/29-8/7, and at Pool where an apparent tape advance occurred at 23:15 on 6/26.

The Aethalometers used in this study were dual wavelength instruments that simultaneously made measurements of the transmittance of the filter tape at 880 nm (Channel 1) and 370 nm (Channel 2) and converted them to black carbon concentrations using fixed mass absorption efficiency factors for each wavelength. All analysis of data presented in this report is for the data from channel 1, unless stated otherwise, since the longer wavelength is known to be absorbed more specifically by elemental carbon soot. The channel 2 data was used only for quality assurance purposes.

We calculated the incremental change in BC between successive 5-minute aethalometer measurements and prepared a histogram of the changes, then flagged pairs of data points that result in incremental changes that are clearly inconsistent with the overall distribution. Based on this analysis, we set criteria for flagging unrealistic spikes in data for further investigation. Basically this step involves making two passes through the data. The first pass involves an “eyeball” check to flag data that are inconsistent. Then a second pass through the data set is used to identify and flag potentially invalid data based on specific quantitative criteria developed to identify invalid data.

An algorithm was applied to the 5 minute averaged data to identify all ‘bounces’ (negative/positive pairs) and confirm that they did not overlap two different hourly averaging periods. In addition, we identified all values < -1 ug/m³ not associated with ‘bounce’. These were eliminated from the data set along with unreasonably large spikes (> 80 ug/m³) and excessively negative values (< -10 ug/m³). Data periods affected by this screening were: Vernon - 7/21-7/22 (all hours) and 7/23 (3 and 4 AM); Church - 7/22 (2, 3, and 4 AM).

We also examined all spikes (absolute change between successive 5 min values > 10 ug/m³) not associated with ‘bounce’ to see if they were consistent with surrounding data and data from the other sites. Inconsistent spikes were flagged as questionable data (QD) and isolated spikes as local events (E). Finally, we removed all out-of-range flow, QD, and local Events from dataset before averaging by day or overnight period. A relatively small number of the more than 10,000 possible 5 minute data points for each site were flagged by this process, as shown in Table 2–1. After removing all invalid or suspect data points, we averaged the 5-minute BC data by hour, eliminating hours with less than nine (9) valid 5-minute observations (i.e., $\geq 75\%$ data capture).

2.2 Application of Time and Wind Criteria

Based on prior data and analysis, it was decided that the evaluation of downwind-upwind differences in pollutant concentrations would be done on a restricted set of data adhering to the following criteria:

- Time period from 10PM to 5AM PST, when vertical mixing is limited.
- Wind speeds between 0.5 and 4 m/s (the maximum wind speed was increased from earlier criteria based on analysis of current wind data).
- Wind direction at downwind sites between 45 and 225 degrees (from general direction of rail yards).

After filtering out data for all measured parameters associated with hours that do not meet criteria for the time period of interest (2200 - 0500 PST) we compared wind data from all four sites. Scatter plots of hourly wind vector speeds comparing upwind/downwind pairs, upwind pair, and downwind pair are shown in Figure 2-1. Scatter plots indicate generally higher wind speeds at downwind sites, which is expected due to greater fetch. There were some exceptions, especially for the Vernon site where several of the highest hourly wind speeds were recorded. However the correlation between the two upwind sites Vernon and Pool is good, so no bias was indicated. Comparison of downwind and upwind pairs is generally about 1:1, except for wind speeds > 2.5 m/s at Denio which exceed those measured at Church by as much as 1.5 m/s. A 20 to 25% bias in wind speeds measured by the two EBAMs used at Denio and Pool was apparent in

the pre and post-study period collocation data. To determine which instrument was responsible for the error we compared to the data from the pair of BAMs during the post-study collocation period, which showed excellent agreement for wind speed. Unfortunately, all 4 instruments were never operated at the same location so there is substantial scatter in the data shown in Figure 2-2, but it seems clear that the bias was due to a combination of the Denio instrument reading high while the Pool instrument read low. Since the mean wind speeds during the study period were 1.5 ± 0.03 m/s at both downwind sites it seems safe to assume this bias did not have a significant impact on the data selection.

The next step was to filter out data that do not meet criteria for wind speed (<1 m/s or >4 m/s at either downwind site). This is a wider range than the 1-5 mph (approximately 0.5 to 2.2 m/s) previously suggested for Year 1 data. Preliminary analysis of the wind data from 2006 indicated that a 5 mph (2.2 m/s) upper limit would exclude about 30% of the available data, as shown in Figure 2-3. As mentioned previously, data from year one will be reanalyzed based on a consistent set of criteria for the final report. Comparison of hourly wind direction at the four sites indicates that flow is still generally consistent across the rail yard at speeds up to 4 m/s (see Figure 2-4).

Next, hourly differences in wind direction for upwind/downwind pairs, upwind pair, and downwind pair were examined for evidence of bias. Based on comparison of wind directions measured at the four sites, there is an apparent bias in the wind direction data from Denio site, as shown in Figure 2-5 where the differences between the wind direction at Denio and the other sites converge towards a delta of about 35 degrees at higher wind speeds, rather than converging to 0-10 degrees as for the Church/Vernon and Pool/Vernon site pairs. Examining the wind data from the pre and post study collocation periods (the met data for each site was collected by the BAM and EBAM PM monitors) indicates that the instrument that had been located at the Denio site (EBAM 2237) was reading about 20 degrees high relative to the instrument used at the Pool site during the post study collocation period (see Figure 2-6). Bias during the pre-study periods and for the other pair of instruments was less significant (5 to 10 degrees).

Fortunately, these biases have little impact on the selection of data for upwind/downwind site comparison since the winds were consistently well within the range of interest during the overnight hours, as shown in Figure 2-4. Applying the wind direction and speed criteria described above to the overnight hourly wind data from the Church site resulted in elimination of 18% of the data from further analysis. All of the hours in this subset also meet the same criteria at the Denio site, regardless of whether or not we adjusted for the apparent biases in winds speed and direction at Denio. An additional 6 to 7 % of the overnight hours met the wind criteria at Denio, but failed on the basis of wind directions outside the specified range at Church.

2.3 Hourly Pollutant Data Distributions

Data distribution plots (histograms) were prepared for each parameter to look for data points that are clearly inconsistent with the overall distribution and flag as outliers.

NO and NO_x. Histograms in Figure 2-7 and Figure 2-8 show no outliers after removing two significantly negative data points from NO record at Pool (>-40 and >-100 ppb). NO at Pool was slightly below zero (-1 ppb) 34% of recorded hours. Similar values for NO_x were recorded 3% of hours. Since no zero values were recorded at the downwind sites, it is not possible to say whether these periods of baseline shift also occurred there. As such, an uncertainty of 1 ppb will be assumed for the hourly measurements.

BC (Channel 1). Histograms in Figure 2-9 show no outliers (data was already screened at 5 min level).

BAM. Histograms in Figure 2-10 show no outliers, except a large spike ($PM_{2.5} = 343 \mu\text{g}/\text{m}^3$) at Church Sept 15, 23:00. This spike falls within the period of the Ralston fire (9/5 to 9/17), so it was not used in our analysis.

2.4 Hourly Pollutant Time Series

Appendix B contains separate time-series plots of hourly data (filtered as per previous steps) for NO, NO_x, PM_{2.5}, BC (channel 1), and wind speed for all four sites. Additionally, NO, NO_x, and BC were plotted together since both NO and BC are expected to be largely due to local diesel emissions at the downwind sites. NO and BC generally track each other well. We examined these plots by month to look for inconsistencies in temporal patterns or inter-parameter relationships and flag questionable data, and used these plots to determine validity of outliers identified by the distribution analysis. If outliers were not consistent with data from related instruments or sites, or if other parameters indicate the occurrence of an exceptional event, they were flagged as invalid. The following data were either flagged as suspect or deleted.

- A period of unusually elevated NO was recorded at Pool from July 25 to 30. Further examination revealed that the data for this period were identical to that reported for the Denio site. In addition, temperature data from Pool NO_x instrument indicate that the air conditioning/heating was not working. Data for Pool were deleted for this period.
- There was a period of continuously high NO at Church from Jul 27-29 that was not observed at any of the other sites. BC was not proportionately high during this period, but NO/NO_x ratios were normal. These NO data were marked as suspect.
- At Denio on Sept. 7 and Sept. 26 large peaks in BC occurred (the one on Sept. 7 was the largest recorded – 11.8 ug/m³) without corresponding increases in NO, PM, or BC at other sites. The BC(1)/BC(2) ratios during these periods were unexceptional. Flagged as suspect.
- A large spike of PM_{2.5} (161 ug/m³) was recorded at Denio on 9/29 22:00, with no corresponding increase in BC or at other sites. It was flagged as suspect.
- At Pool on Aug 3, 0:00, there was a large spike of PM_{2.5} during one hour with no corresponding increase in BC or at other sites. Data were flagged as suspect.
- At Church, reported BAM PM_{2.5} concentrations all equal 1.0 ug/m³ from July 12 – 16. This data was assumed to be due to a malfunction and deleted.

2.5 Related Pollutant Ratios

Additional QA procedures were applied by calculating hourly ratios of BC(1)/BC(2) (measurements using two different wavelengths from the same instrument), PM/BC(1), and NO/NO_x for each site. Appendix B contains separate time-series plots of hourly data NO/NO_x, PM/BC(1) and BC(1)/BC(2) ratio for all four sites.

NO/NO_x ratios were consistent between sites, with similar averages at downwind sites and much lower averages at upwind sites. The maximum ratio is about 0.85 at all sites. No values greater than mean +2 σ of all data existed (no values >0.88). BC/PM ratios were consistent between sites, with similar averages at downwind sites and much lower averages at upwind sites. Several unusually high hourly averages (BC > 50% of PM) were observed at the downwind sites, but all corresponded to period of low PM concentration (<20 ug/m³) and may be attributed to poor accuracy of BAM data at these levels where the measurement precision error is approximately 40% of the reported concentration. BC(1)/BC(2) ratios were higher at downwind sites ($\pm 2\sigma = 0.9$ to 1.6) than typically observed for ambient data (0.8 to 1.2). BC(1)/BC(2) ratios at the Pool site were lower than elsewhere with many values between 0.4 and 0.8, possibly due to a greater influence of PM sources rich in high MW organic carbon such as on-road diesel vehicles or badly maintained cars to which channel 2 is more sensitive.

2.6 Collocation Data

Correlation plots of data from collocated samplers for pre- and post-study periods and regression statistics were used to estimate precision and identify the magnitude of possible biases between samplers. This analysis was used to estimate the uncertainty of the calculated upwind/downwind differences.

2.6.1 Collocated Aethalometer Black Carbon Data

Good agreement was observed between the Aethalometers used at Denio and Pool sites during pre-study collocation tests, as shown in Figure 2-11. The dashed lines show the range of residuals relative to the regression line, $\pm 20\%$. Results were somewhat better for this pair of instruments during the post-study collocation, as shown in Figure 2-12, where the range of residuals is only about $\pm 10\%$. It was demonstrated in the previous year's analysis that the errors are proportional to the measured concentration, rather than a consistent absolute variability. In order to quantify the range of errors, the relative differences between the two collocated instruments (relative error = difference in measured concentration between the two instruments divided by the average of the two measurements).

Although the statistically significant slopes of the regression lines suggest some small bias between the instrument pairs, averaging the biases from the pre- and post-study periods essentially eliminates the bias. In addition, the distribution of errors is always centered within 5% of zero. For these reasons we have chosen not to make any bias correction and allow small changes in the relative response of the instrument pairs to be accounted for by the precision uncertainty.

Figure 2-13 shows the distribution of relative errors during the pre- and post-study periods for the two Aethalometers used at the Denio and Pool sites. The histograms show that the relative errors assume a fairly steep normal distribution with the 95th percentile occurring at <20% relative difference. There was substantially higher relative error during the pre-study collocations, so these larger values of the 95th percentile error are used as the estimates of precision for the aethalometer data. As shown by the dashed lines in the regression plots, this may be somewhat overly conservative for very high BC concentrations, but accounts for the variance well throughout most of the range.

Agreement between the pair of instruments used at the Church/Vernon pair of sites was also good during the pre-study collocation, as shown in Figure 2-14 and Figure 2-15. Figure 2-16 shows that 95% of the relative errors are within 15%. The propagated errors for 7-hour and 24-hour averages shown in Table 2-2 are intended only to represent an estimate of the uncertainty of the aethalometer data in the time averages used for the subsequent downwind-upwind differential analysis. This estimate assumes that the measured concentrations during an averaging period are relatively constant. In practice, the propagated errors for each daily average will be calculated as:

$$\bar{\sigma} = \frac{\sigma \sqrt{\sum_1^n C_i^2}}{\sum_1^n C_i}$$

Where σ is the relative error, C is the measured concentration, and n is the number of measurements averaged.

2.6.2 Collocated BAM PM_{2.5} Mass Concentration Data

Regression analysis revealed a small but significant bias of about 15% for each pair of BAM instruments which was consistent for both the pre- and post-study data periods. The data from the downwind sites was adjusted to account for this bias (Denio*0.82+0.37 and Church*0.88+1.98) using the average of the pre- and post-study regression slopes and intercepts shown in Table 2-3. The average coefficient of variance (CV) is also presented, along with the regression statistics, in Table 2-3 as a gauge of how precision varied between instrument pairs and collocation periods, but it is not useful as an estimate of precision in calculating the uncertainty of the downwind-upwind differences since it may be biased high due to the larger relative differences that occur at very low concentrations. The regression approach avoids this by weighting the higher concentrations more.

The distribution of differences in measured concentration between the collocated pairs of samplers after correcting for bias (Figure 2-19 and Figure 2-22) indicates that the error is random in nature and assumes an approximately normal distribution. This differs from the aethalometer where the error is proportional to measured concentration. From the error distribution we can estimate the precision for each pair at the 95% confidence level as a fixed quantity (11.5 ug/m³ for Denio/Pool and 9.5 ug/m³ for Church/Vernon (i.e., 95% of the observed differences between the collocated pair of instruments are less than the specified precision). The dashed lines on the regression plots (Figure 2-17, Figure 2-18, Figure 2-20, and Figure 2-21) show that the majority of the scatter in the data set is accounted for by the precision error derived from the distribution analysis. Table 2-3 shows the resulting errors 7-hour and 24-hour averages propagated as the root mean square of the hourly precision error:

$$\bar{\sigma} = \frac{\sqrt{\sum_1^n \sigma_i^2}}{n}$$

where n is the number of measurements used in the average and σ is the relative precision error.

2.7 Filter versus Continuous Data

The results of laboratory analysis of the 24-hour (midnight to midnight PST) and 7-hour (2200 to 0500 PST) filter samples collected at the four sites were compared to the averages of corresponding data from the continuous PM and BC instruments. All hourly data collected during the study period was averaged by 24-hr day and overnight period (7 hours), eliminating days with less than 18 valid hours, or nights with less than 5 hours of valid data for any parameter (i.e., $\geq 75\%$ data capture). The date on which the overnight period began was used to designate that average. Correlation plots of FRM PM versus BAM PM (Figure 2-23 and Figure 2-24) and of FRM EC versus aethalometer BC(1) (Figure 2-25 and Figure 2-26) were prepared. We used regression statistics to identify the magnitude of possible biases. The regression statistics are summarized in Table 2–4. The BAM PM results were adjusted to match the FRM PM measurement results, by applying the best-fit regression coefficients for the aggregate data from all sites (shown in the Table in bold face type) to the BAM data.

2.7.1 Filter Gravimetric Mass Versus Continuous BAM Mass Concentrations

For the 24 hour filters there is no statistically significant difference between the site specific means of the averaged continuous and filter data, and regression analysis shows that the slope and intercept of the gravimetric vs. BAM least-squares linear fit are not significantly different from 1.0 and 0.

For the 7 hour filters collected during nighttime hours there is again no statistically significant difference in the site specific means.. Regression analysis shows slopes significantly greater than 1 for Church and Pool sites. Owing to the weak correlation between the FRM and BAM PM_{2.5} concentrations at Denio and Vernon (the correlation for Vernon is not statistically significant at the 95% level), it is not advisable to apply site-specific corrections to the BAM data. The weak correlations can be attributed to the relatively low concentrations experienced and the short sample time for the FRM filters. Good agreement between BAMs and FRM gravimetric mass has been observed in other studies where a larger range of concentrations were sampled (Chow, et al., 2006). Combining all data yields a regression slope of 1.13 ± 0.16 (not significantly greater than 1 at the 95% level) and an intercept of -2.16 ± 4.85 . This regression equation was used to adjust the BAM data before performing the calculation of downwind-upwind differences. Forcing the intercept through zero for the combined data yields a slope of 1.00, but it reduces the goodness of fit and conflicts with the apparent non-zero intercepts for the individual site data in Figure 2-24. In practice, applying the combination of a slope slightly greater than 1 and a small negative intercept results in little change from the measured values with the range of data observed in this study (PM_{2.5} = 1 to 40 ug/m³ for the overnight averages at all sites).

Two outliers were removed from the data for this analysis; both were extreme values of gravimetric mass for the site (20.4 ug/m³ at Vernon on July 1 and 30.6 ug/m³ at Denio on Oct. 5) and the difference between filter and BAM was well outside the range of other data. Data collected during the Ralston fire was excluded from this analysis, as well as the sample days when 24 hour filters were being collected at Church and Vernon in order to avoid biasing the combined regression towards the sites with more 7 hour samples.

The difference in the comparison results between the 24 hour and 7 hour sample groups may be due to the higher fraction of PM that is organic carbon (70% for 24 hour vs. 90% for 7

hour, based on mean ratio of uncorrected OC to gravimetric mass). Since the BAM can overestimate mass for aerosols with high organic content due to the increased fraction of hydrogen atoms in the material¹, the higher slopes observed for the 7-hour overnight samples could result.

2.7.2 Filter Elemental Carbon Versus Aethalometer BC Concentrations

Although there is no statistically significant difference between the mean EC and BC for either the 24-hour or 7-hour data from the individual or combined sites, the regression analysis does indicate some biases (see Figure 2-25, Figure 2-26, and Table 2-4). For the 24-hour samples collected at Church and Vernon there is a consistent slope indicating that the BC/EC ratio was about 0.7. The y-intercepts were not significantly different from zero. For the 7-hour samples the regression results were not significantly different, except at Church where the correlation was again very robust ($r^2 = 0.86$) and the slope was somewhat lower (0.53 ± 0.11 BC/EC).

The primary purpose of relating the Aethalometer BC measurements to filter EC, which is also an operationally defined parameter rather than a distinct physical material, is for the purpose of estimating the concentrations of diesel particulate matter (DPM) that are being contributed by the railyard to the area downwind. This estimation will involve several steps:

1. Determination of the characteristic ratio(s) of PM to EC in relevant diesel source emissions.
2. Characterization of the relationship between BC and EC for DPM in diesel dominated ambient air.
3. Estimation of the concentration of excess BC contributed by the source to the target area (downwind sites).
4. Conversion of BC concentrations to DPM using relationships derived in steps 1 and 2.
5. Validation of estimated DPM impact by comparison with information on local emissions patterns and activity.

In this process we assume that any increase in BC observed at the downwind sites relative to the upwind sites is due to fresh DPM emissions from the railyard area, therefore we may apply PM/EC ratios measured during locomotive load testing in step 1 above. This would not be appropriate for BC measured at the upwind sites, which is presumably from other sources and potentially modified during longer-range transport.

As such, it is only relevant to this process to try to convert the excess BC measured at the downwind sites to EC-equivalent concentrations so that we may use it to estimate DPM. Figure 2-27 shows the correlation between the difference in average overnight 7-hr BC between the upwind and downwind site pairs and difference in corresponding EC from the FRM filters (in other words, we compared the increase in BC and EC measured at the downwind sites relative to the upwind sites. The correlations are quite good, but there seems to be some difference between the 2 site pairs. This could be due to some variation in the response of the Aethalometers (we

¹ The beta-gauge method responds to the density of protons in the filter deposit and assumes a proportional number of neutrons to estimate mass concentration.

only compared the instruments to their upwind/downwind counterparts in analyzing the collocation data).

Table 2–1. Number of 5 minute aethalometer BC data points eliminated or flagged during the QA process. The full data set is composed of over 35,000 data points.

flag	Denio	Pool	Church	Vernon
Local Events	0	0	8	28
Negative	0	0	4	9
Outliers	0	0	3	7
Spikes	13	1	6	0

Table 2–2. Precision analysis of collocated Aethalometer data. Linear regressions use data from the sampler used at the upwind site as the independent (x) variable.

site pair Instrument IDs	Denio/Pool 626/624		Church/Vernon 623/A479	
Test Period	02/23/06-05/01/06	10/17/06-11/06/06	02/23/06-05/01/06	10/17/06-11/02/06
averaging period	1 hour	1 hour	1 hour	1 hour
mean BC (ug/m3)	1.92	2.41	1.62	1.98
<u>regression</u>				
r2	0.97	1.00	0.98	0.99
slope	0.957 ± 0.009	1.027 ± 0.003	0.980 ± 0.007	1.124 ± 0.004
intercept	0.05 ± 0.03	0.01 ± 0.01	0.02 ± 0.02	0.00 ± 0.01
<u>relative difference</u>				
mean	-1.2%	3.2%	0.5%	11.9%
2*stdev	23%	10%	28%	11%
skew	4.57	-1.71	9.06	-0.13
<u>95% error estimates</u>				
1 hr average	20%	10%	15%	17%
7 hr average	8%	4%	6%	6%
24 hr average	4%	2%	3%	3%

Table 2-3. Precision analysis of collocated BAM data. Linear regressions use data from the sampler used at the upwind site as the independent (x) variable.

site pair Instrument IDs	Denio/Pool E2237/E2238		Church/Vernon 4514/4515	
Test Period	05/01/06-05/24/06	10/16/06-10/31/06	05/25/06-06/12/06	10/17/06-11/06/06
averaging period	1 hour	1 hour	1 hour	1 hour
mean PM (ug/m3)	17.9	15.5	10.3	17.1
<hr/>				
<u>regression</u>				
r2	0.72	0.67	0.75	0.86
slope	0.833 ± 0.045	0.805 ± 0.029	0.855 ± 0.047	0.911 ± 0.017
intercept	0.74 ± 1.97	0.00 ± 0.59	1.74 ± 1.26	2.22 ± 0.37
CV	32%	41%	43%	30%
<u>average bias</u>	E2237		4514	
multiply by	0.82		0.88	
add	0.37		1.98	
<hr/>				
<u>absolute difference</u>	E2237 - E2238		4514 - 4515	
mean	4.94	5.55	3.29	4.00
stdev	3.90	4.43	2.97	3.33
skew	1.29	1.33	1.30	1.20
<u>95% error estimates</u>				
1 hr average	11.5	12.0	9.0	10.0
7 hr average	4.3	4.5	3.4	3.8
24 hr average	2.3	2.4	1.8	2.0

Table 2–4. Comparison of filter results and continuous sampler data. Linear regressions use FRM filter data as the independent (x) variable. Adjustments that were applied to data are highlighted in bold.

	number of samples	mean ± 2*stderr	mean ± 2*stderr	r ²	slope ± 2*stderr	y-intercept ± 2*stderr
24hr PM2.5		Gravimetric				
		BAM				
Church	19	12.4 ± 1.9	13.1 ± 2.3	0.70	1.00 ± 0.33	0.73 ± 8.62
Vernon	19	9.7 ± 2.2	11.9 ± 2.7	0.89	1.15 ± 0.20	0.50 ± 4.40
Both	38	11.1 ± 1.5	12.5 ± 1.8	0.79	1.04 ± 0.18	0.88 ± 4.38
24hr EC/BC		EC				
		BC				
Church	18	1.8 ± 0.4	1.5 ± 0.3	0.75	0.67 ± 0.31	0.36 ± 1.26
Vernon	18	1.1 ± 0.3	1.0 ± 0.2	0.73	0.66 ± 0.25	0.25 ± 0.65
Both	36	1.4 ± 0.2	1.3 ± 0.2	0.79	0.70 ± 0.15	0.26 ± 0.51
7hr PM2.5*		Gravimetric				
		BAM				
Denio	16	16.6 ± 2.6	16.1 ± 2.5	0.41	0.61 ± 0.40	5.92 ± 13.75
Pool	17	12.6 ± 3.2	12.4 ± 5.3	0.87	1.52 ± 0.31	-6.82 ± 8.50
Church	17	15.4 ± 2.7	16.1 ± 3.7	0.95	1.38 ± 0.16	-5.76 ± 5.23
Vernon	15	10.4 ± 3.0	8.4 ± 2.0	0.20	0.49 ± 0.33	3.91 ± 7.70
All	65	13.8 ± 1.5	13.4 ± 1.8	0.74	1.11 ± 0.16	-1.82 ± 4.80
7hr EC/BC*		EC				
		BC				
Denio	16	3.1 ± 0.8	3.3 ± 0.8	0.74	0.83 ± 0.30	0.65 ± 2.14
Pool	17	0.6 ± 1.5	0.8 ± 1.4	0.72	0.80 ± 0.26	0.32 ± 0.44
Church	17	2.8 ± 0.8	2.2 ± 0.5	0.86	0.53 ± 0.11	0.72 ± 0.70
Vernon	17	0.8 ± 0.3	0.7 ± 0.2	0.67	0.49 ± 0.18	0.34 ± 0.37
downwind - upwind difference (7hr) *		EC				
		BC				
ΔDenio-Pool	33	2.5 ± 0.6	2.5 ± 0.6	0.80	0.92 ± 0.17	0.13 ± 0.71
ΔChurch-Vernon	30	2.0 ± 0.6	1.5 ± 0.6	0.90	0.55 ± 0.08	0.34 ± 0.29

*Only data for nights when 7-hr samples were collected at all sites were used to calculate statistics shown.

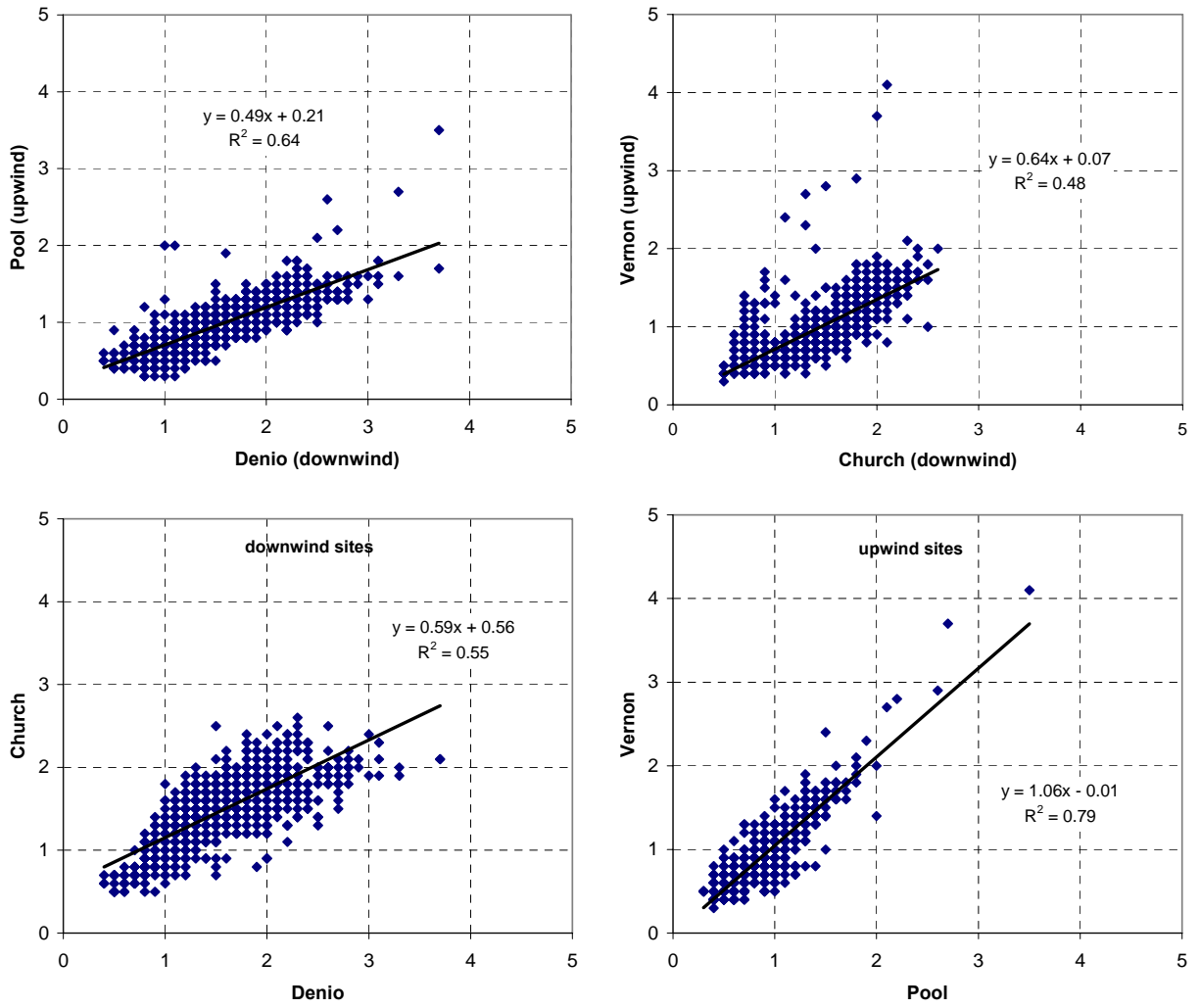


Figure 2-1. Comparison of hourly mean wind speeds (m/s) from 22:00-5:00 at site pairs.

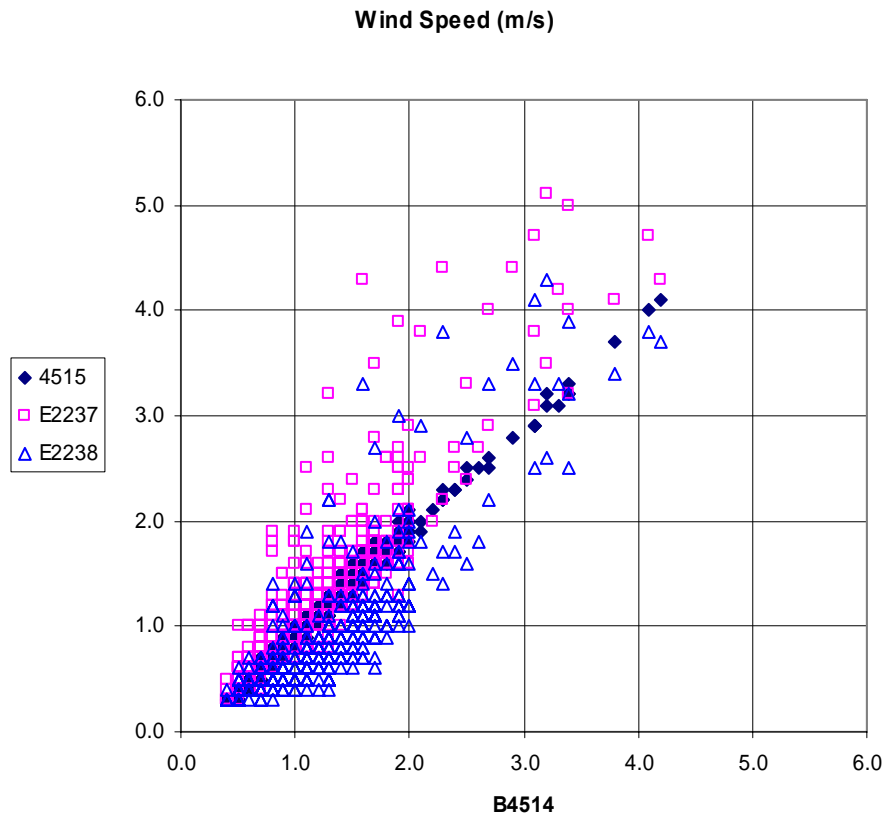


Figure 2-2. Hourly average wind speed (meters per second) from instruments collocated after the main study period. E2237 was used at Denio, E2238 at Pool, and 4515 at Vernon.

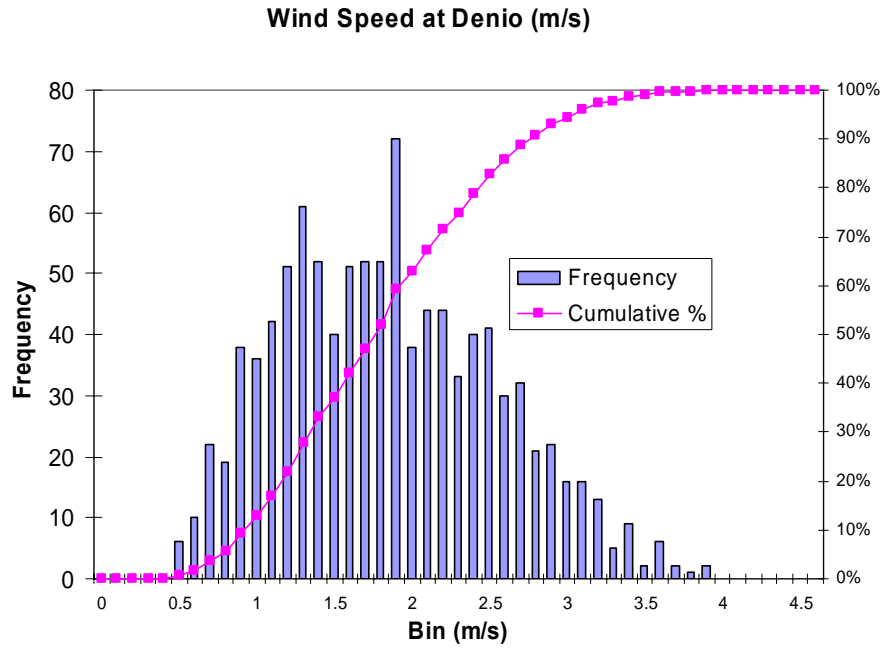


Figure 2-3. Distribution of hourly mean wind speeds (m/s) from 22:00-5:00 at Denio site.

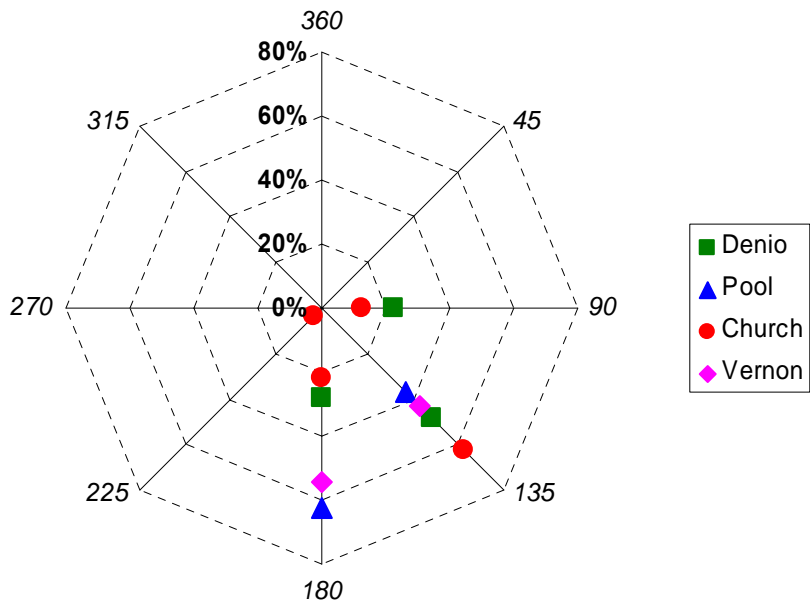


Figure 2-4. Frequency of hourly average wind directions at the four sites during overnight hours (22:00 to 05:00 PST). Wind directions have been rounded to the nearest 45 degrees. Only hours where winds were between 45° and 225° were used to determine downwind-upwind differences.

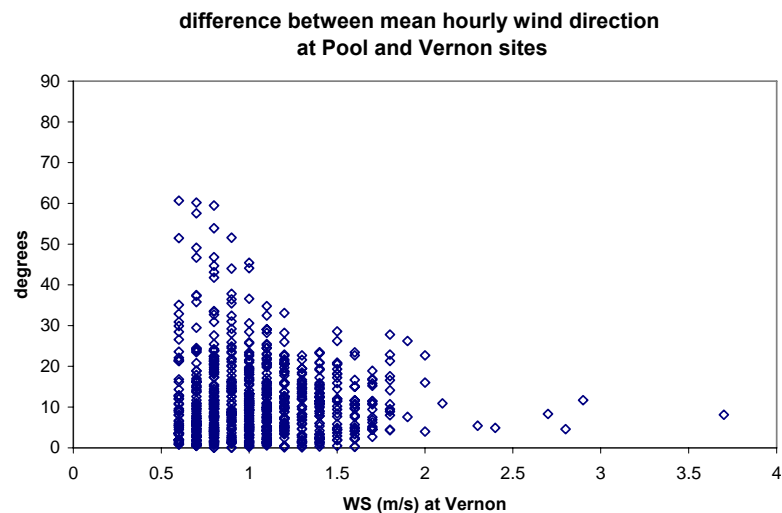
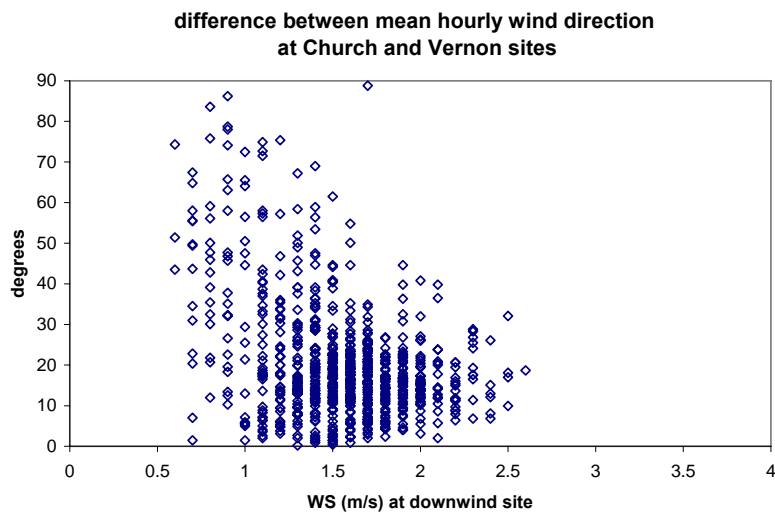
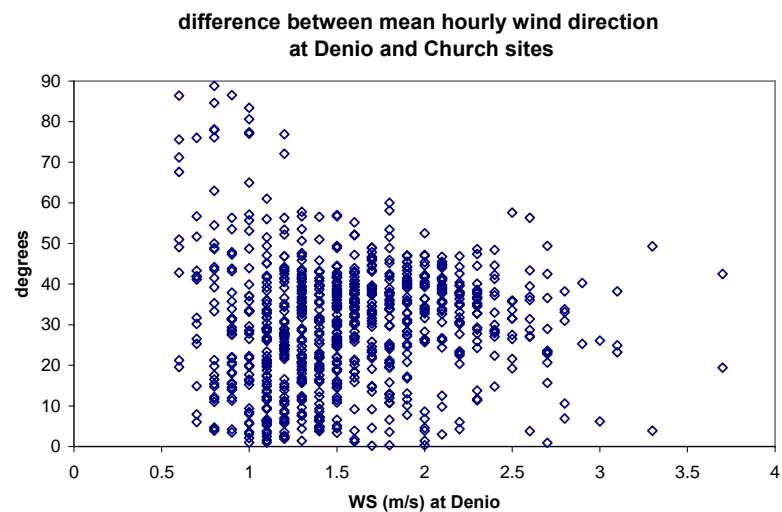
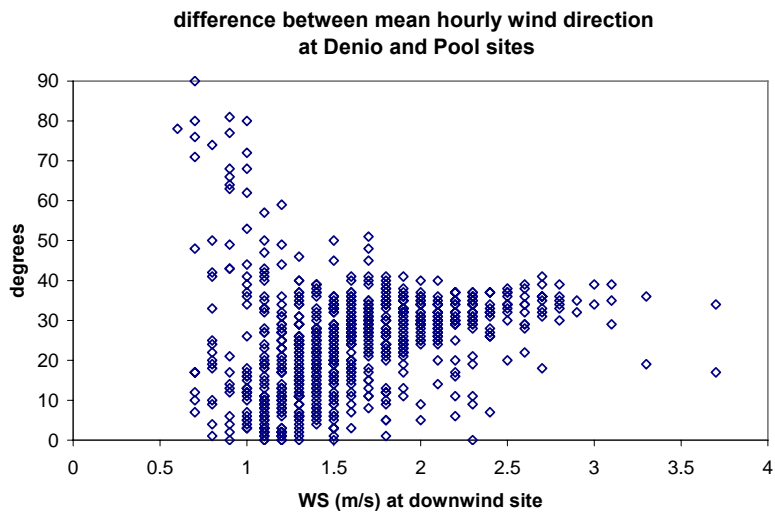


Figure 2-5. Differences in mean hourly wind direction between site pairs.

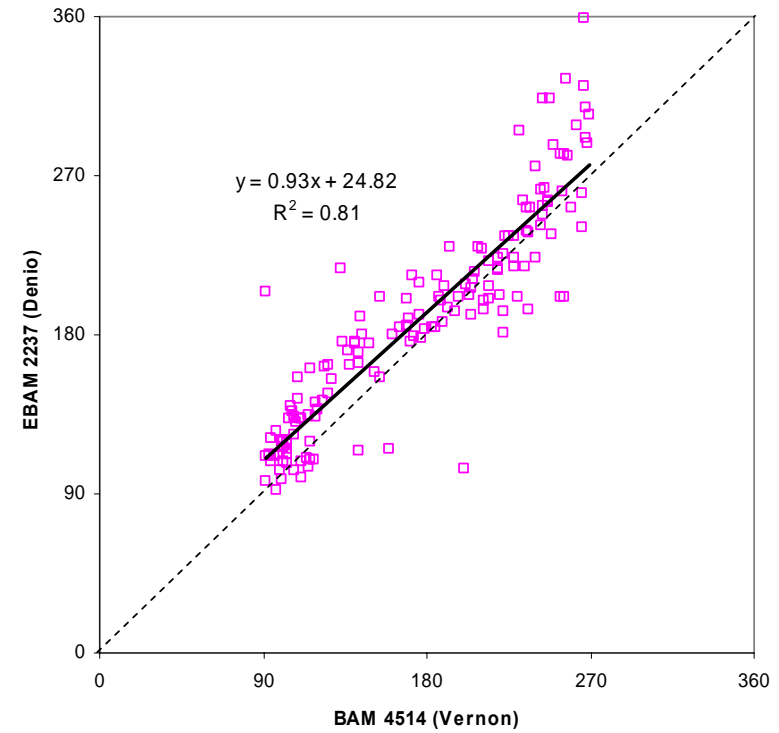
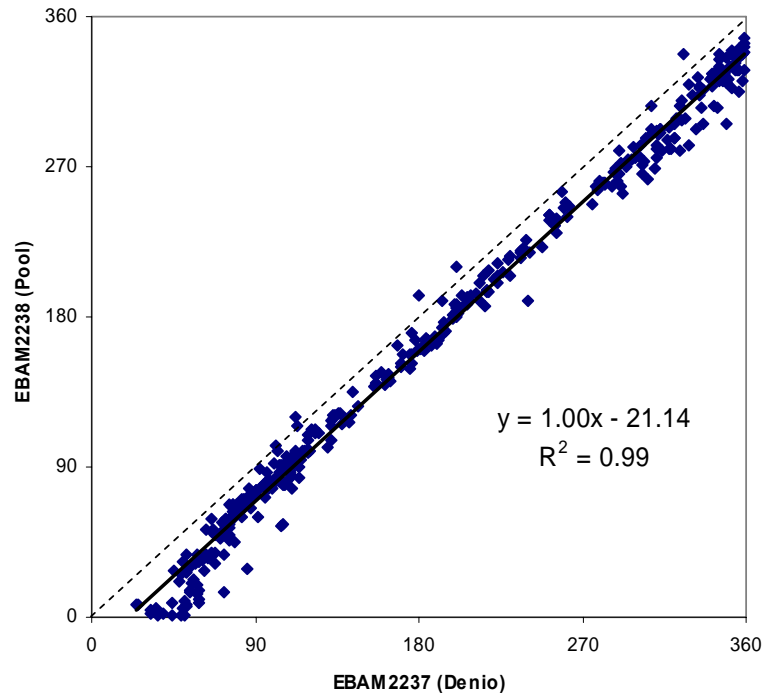
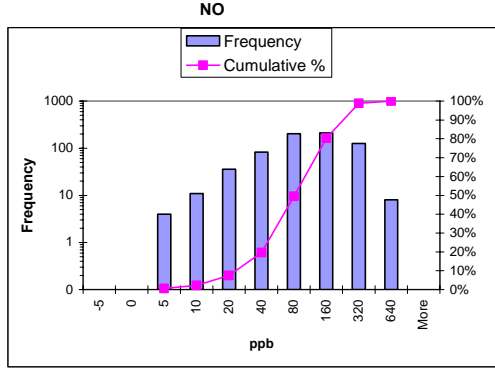


Figure 2-6. Hourly average wind direction (degrees) from instruments collocated after the main study period. BAM 4514 is believed to be accurate due to its excellent agreement with BAM 4515 during the collocation tests. The dashed lines representing a 1:1 relationship are included for comparison.

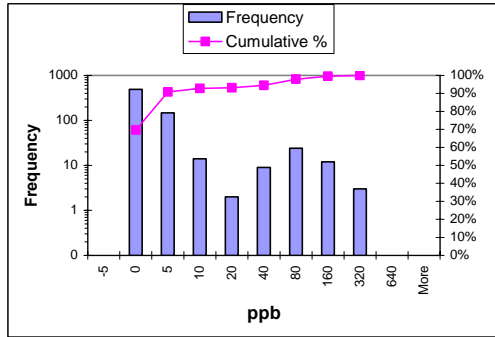
DENIO

Bin (< or =)	Frequency	Cumulative %
-5		
0		
5	4	0.59%
10	11	2.20%
20	36	7.49%
40	83	19.68%
80	203	49.49%
160	210	80.32%
320	126	98.83%
640	8	100.00%
More		



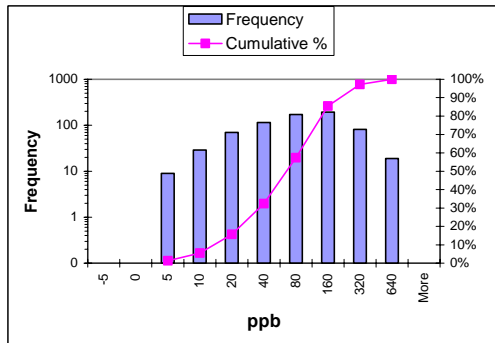
POOL

Bin (< or =)	Frequency	Cumulative %
-5		
0	488	69.71%
5	148	90.86%
10	14	92.86%
20	2	93.14%
40	9	94.43%
80	24	97.86%
160	12	99.57%
320	3	100.00%
640		
More		



CHURCH

Bin (< or =)	Frequency	Cumulative %
-5		
0		
5	9	1.31%
10	29	5.52%
20	70	15.70%
40	115	32.41%
80	172	57.41%
160	193	85.47%
320	81	97.24%
640	19	100.00%
More		



VERNON

Bin (< or =)	Frequency	Cumulative %
-5		
0	648	92.57%
5	39	98.14%
10	4	98.71%
20	3	99.14%
40	4	99.71%
80	1	99.86%
160	1	100.00%
320		
640		
More		

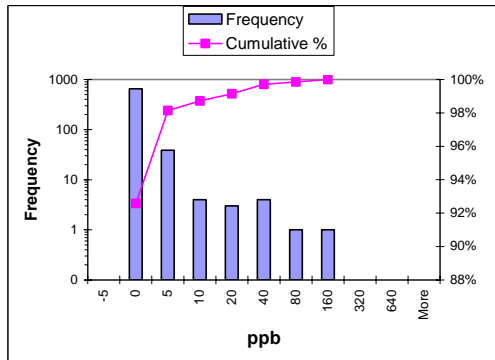
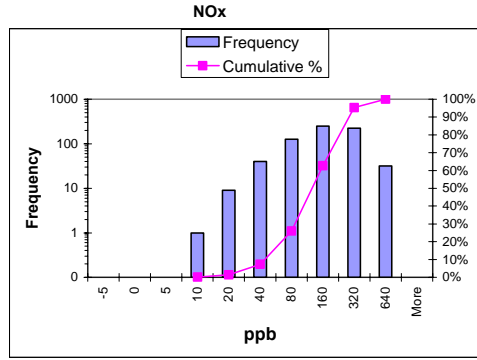


Figure 2-7. Histograms showing the frequency distribution of hourly averaged NO data at the four sites.

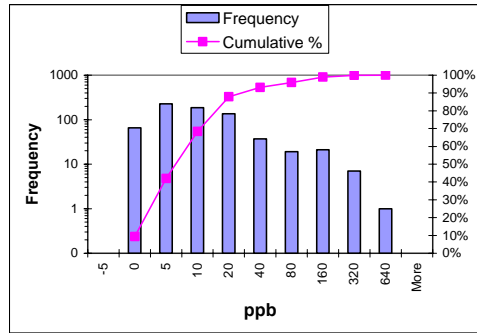
DENIO

Bin (< or =)	Frequency	Cumulative %
-5		
0		
5		
10	1	0.15%
20	9	1.47%
40	40	7.34%
80	127	25.99%
160	250	62.70%
320	222	95.30%
640	32	100.00%
More		



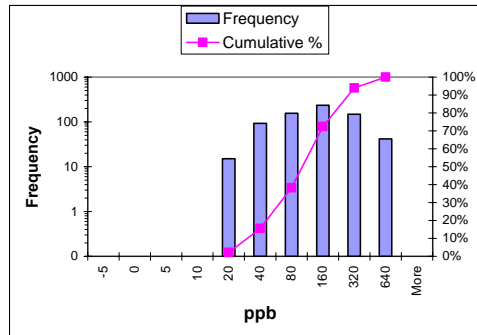
POOL

Bin (< or =)	Frequency	Cumulative %
-5		
0	66	9.43%
5	228	42.00%
10	185	68.43%
20	136	87.86%
40	37	93.14%
80	19	95.86%
160	21	98.86%
320	7	99.86%
640	1	100.00%
More		



CHURCH

Bin (< or =)	Frequency	Cumulative %
-5		
0		
5		
10		
20	15	2.18%
40	92	15.55%
80	156	38.23%
160	235	72.38%
320	148	93.90%
640	42	100.00%
More		



VERNON

Bin (< or =)	Frequency	Cumulative %
-5		
0	17	2.43%
5	247	37.71%
10	245	72.71%
20	149	94.00%
40	34	98.86%
80	6	99.71%
160	2	100.00%
320		
640		
More		

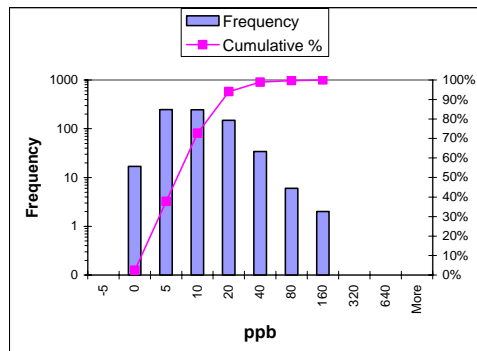
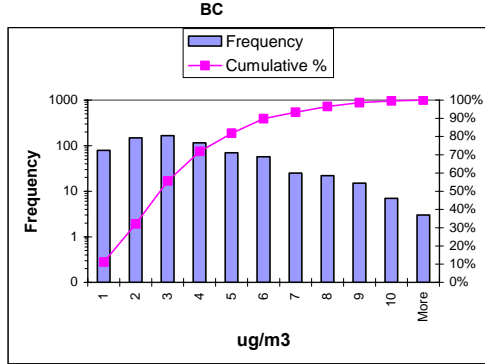


Figure 2-8. Histograms showing the frequency distribution of hourly averaged NOx data at the four sites.

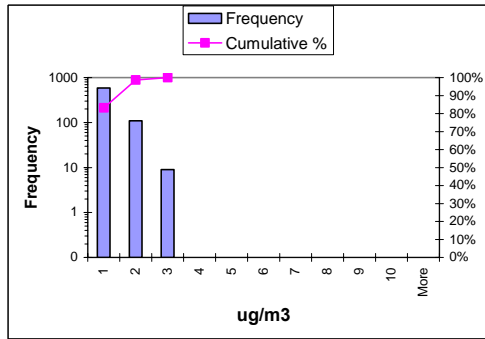
DENIO

Bin (< or =)	Frequency	umulative %
1	79	11.17%
2	148	32.11%
3	166	55.59%
4	115	71.85%
5	70	81.75%
6	57	89.82%
7	25	93.35%
8	22	96.46%
9	15	98.59%
10	7	99.58%
More	3	100.00%



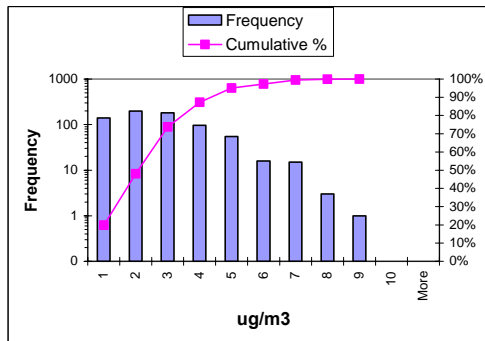
POOL

Bin (< or =)	Frequency	umulative %
1	588	83.17%
2	110	98.73%
3	9	100.00%
4		
5		
6		
7		
8		
9		
10		
More		



CHURCH

Bin (< or =)	Frequency	umulative %
1	140	19.80%
2	199	47.95%
3	182	73.69%
4	96	87.27%
5	55	95.05%
6	16	97.31%
7	15	99.43%
8	3	99.86%
9	1	100.00%
10		
More		



VERNON

Bin (< or =)	Frequency	umulative %
1	616	87.13%
2	80	98.44%
3	11	100.00%
4		
5		
6		
7		
8		
9		
10		
More		

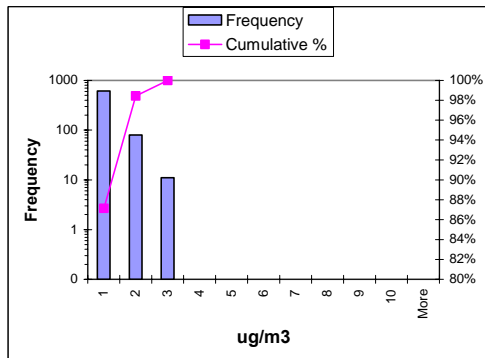
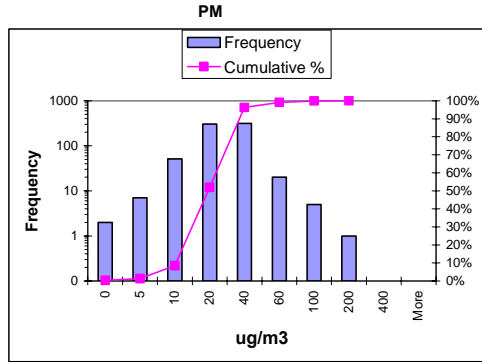


Figure 2-9. Histograms showing the frequency distribution of hourly averaged Aethalometer BC(1) data at the four sites.

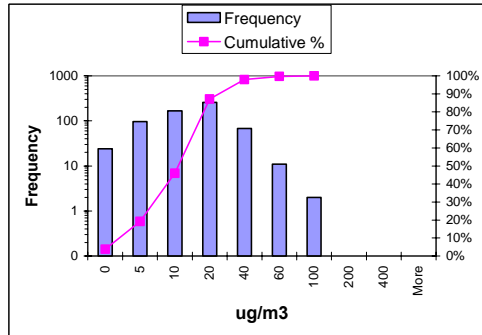
DENIO

Bin (< or =)	Frequency	umulative %
0	2	0.28%
5	7	1.27%
10	51	8.49%
20	307	51.91%
40	314	96.32%
60	20	99.15%
100	5	99.86%
200	1	100.00%
400		
More		



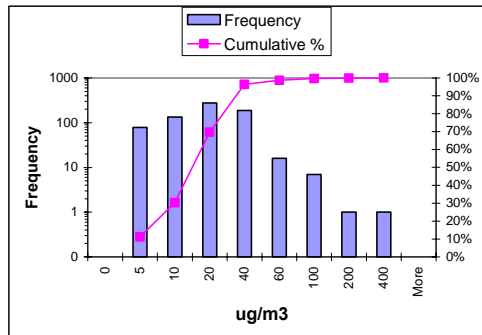
POOL

Bin (< or =)	Frequency	umulative %
0	24	3.83%
5	96	19.14%
10	168	45.93%
20	258	87.08%
40	68	97.93%
60	11	99.68%
100	2	100.00%
200		
400		
More		



CHURCH

Bin (< or =)	Frequency	umulative %
0		
5	78	11.14%
10	134	30.29%
20	276	69.71%
40	187	96.43%
60	16	98.71%
100	7	99.71%
200	1	99.86%
400	1	100.00%
More		



VERNON

Bin (< or =)	Frequency	umulative %
0		
5	161	22.90%
10	226	55.05%
20	268	93.17%
40	43	99.29%
60	5	100.00%
100		
200		
400		
More		

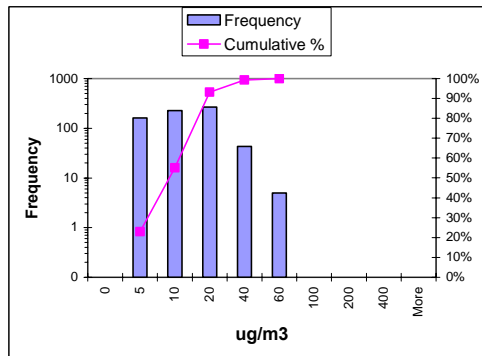


Figure 2-10. Histograms showing the frequency distribution of hourly averaged BAM PM2.5 data at the four sites.

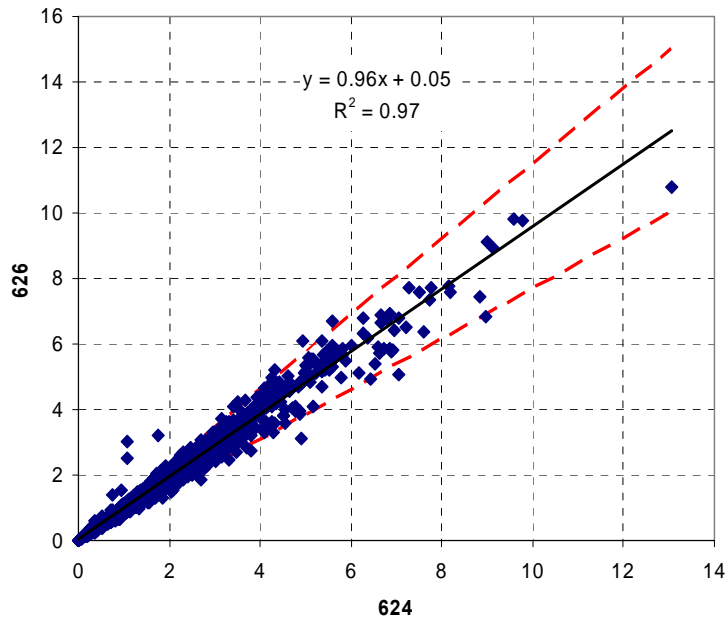


Figure 2-11. Correlation of hourly BC(1) (ug/m³) averaged data from collocated Aethalometers 02/23/06-05/01/06. Instrument 626 was later used at the Denio site, and 624 at Pool.

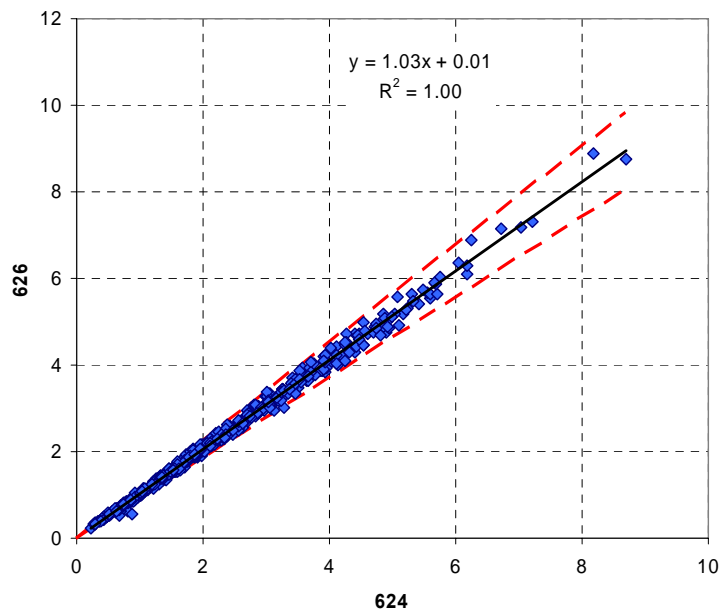
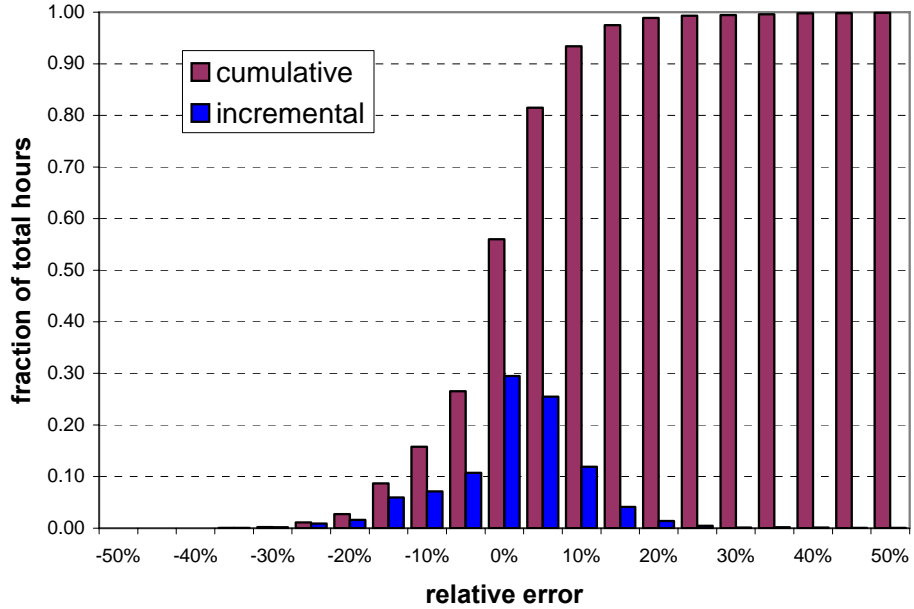


Figure 2-12. Correlation of hourly averaged BC(1) (ug/m³) data from collocated Aethalometers 10/17/06-11/06/06.

02/23/06-05/01/06

relative error	cumulative fraction
<5%	0.55
<10%	0.78
<15%	0.89
<20%	0.96
<25%	0.98
<30%	0.99
<35%	1.00
<40%	1.00
<45%	1.00
<50%	1.00
>50%	0.00



10/17/06-11/06/06

relative error	cumulative fraction
<5%	0.67
<10%	0.94
<15%	0.99
<20%	0.99
<25%	1.00
<30%	1.00
<35%	1.00
<40%	1.00
<45%	1.00
<50%	1.00
>50%	0.00

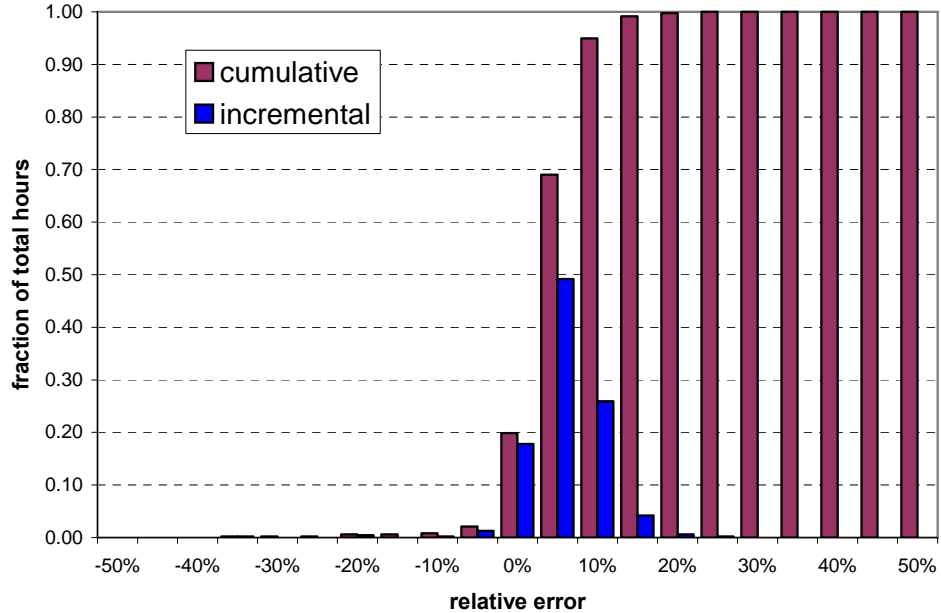


Figure 2-13. Relative difference between collocated Aethalometers used at Denio and Pool sites. Data are from hourly averages of channel 1 BC. Table gives distribution of absolute values of relative differences, with approximate 95th percentile in bold.

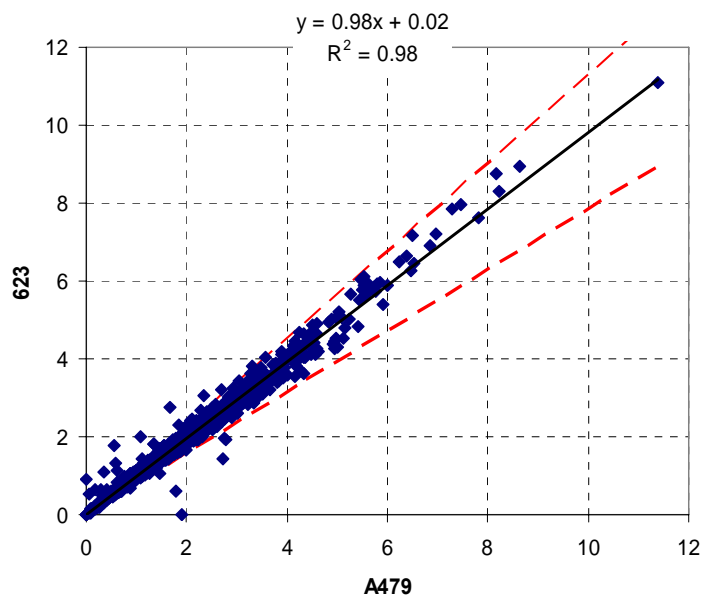


Figure 2-14. Correlation of hourly averaged BC data (ug/m3) from collocated Aethalometers 02/23/06-05/01/06. 623 was later used at Church and A479 at Vernon.

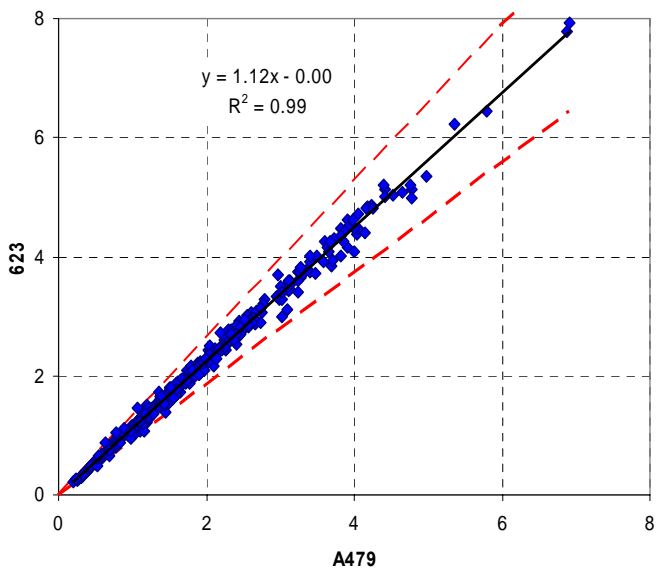
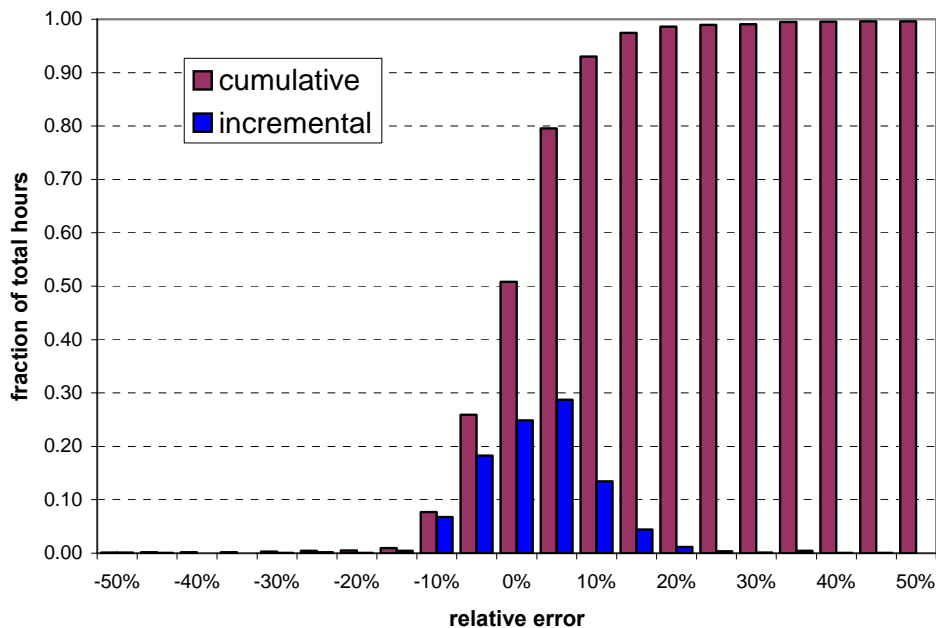


Figure 2-15. Correlation of hourly averaged BC data (ug/m3) data from collocated Aethalometers 10/17/06-11/06/06.

02/23/06-05/01/06

relative error	cumulative fraction
<0%	0.00
<5%	0.54
<10%	0.85
<15%	0.97
<20%	0.98
<25%	0.99
<30%	0.99
<35%	0.99
<40%	0.99
<45%	0.99
>45%	1.00



10/17/06-11/02/06

relative error	cumulative fraction
<0%	0.00
<5%	0.11
<10%	0.30
<15%	0.73
<20%	0.97
<25%	0.98
<30%	0.99
<35%	0.99
<40%	1.00
<45%	1.00
>45%	1.00

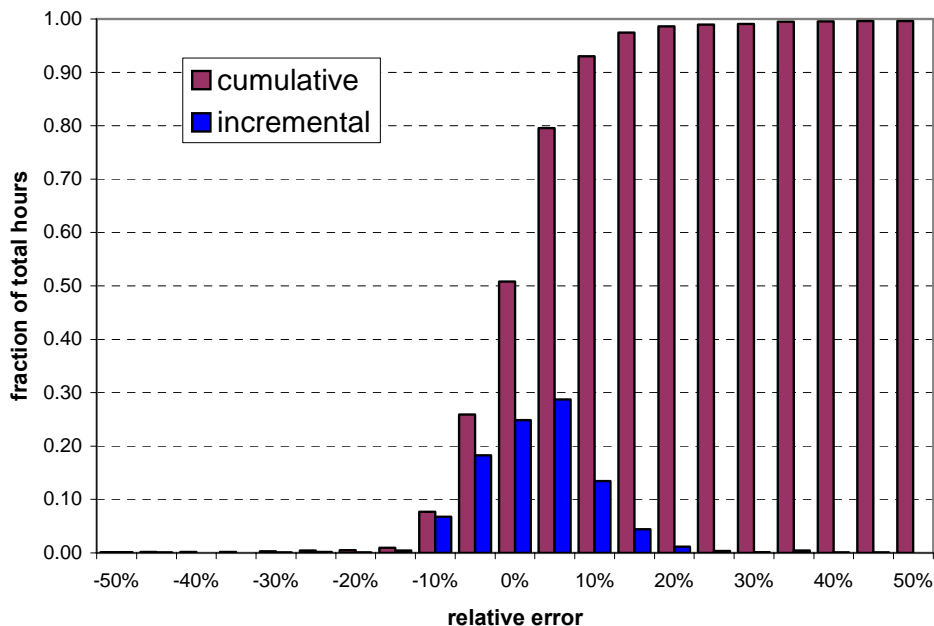


Figure 2-16. Relative difference between collocated Aethalometers used at Church and Vernon sites. Data are from hourly averages of channel 1 BC. Table gives distribution of absolute values of relative differences, with approximate 95th percentile in bold..

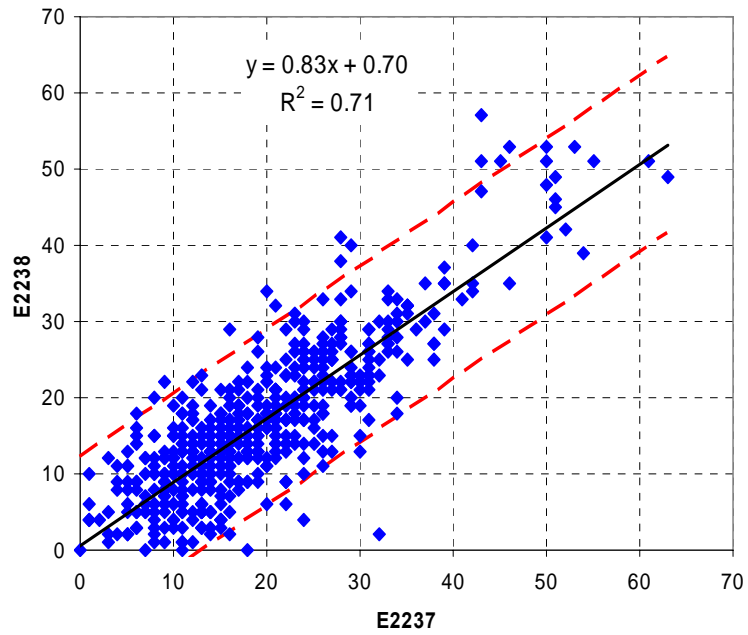


Figure 2-17. Correlation of hourly PM_{2.5} (ug/m³) averaged data from collocated EBAMs 02/23/06-05/01/06. Instrument E2237 was later used at the Denio site, and E2238 at Pool.

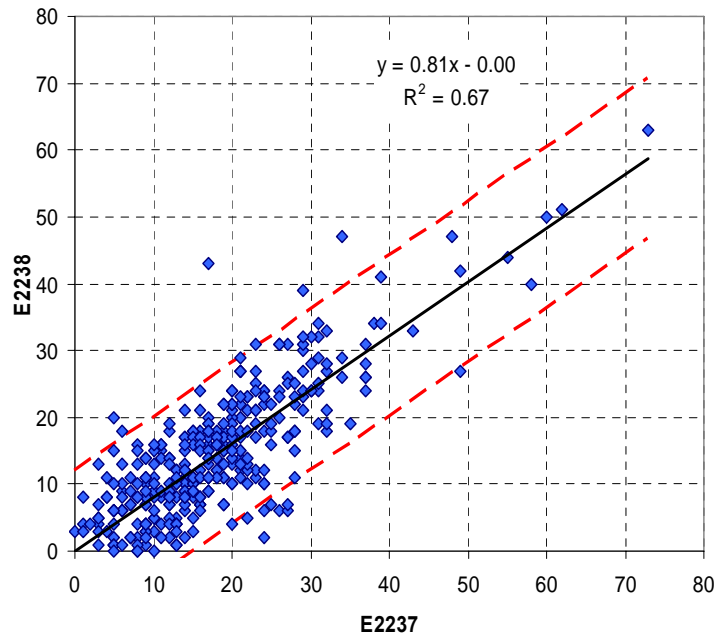
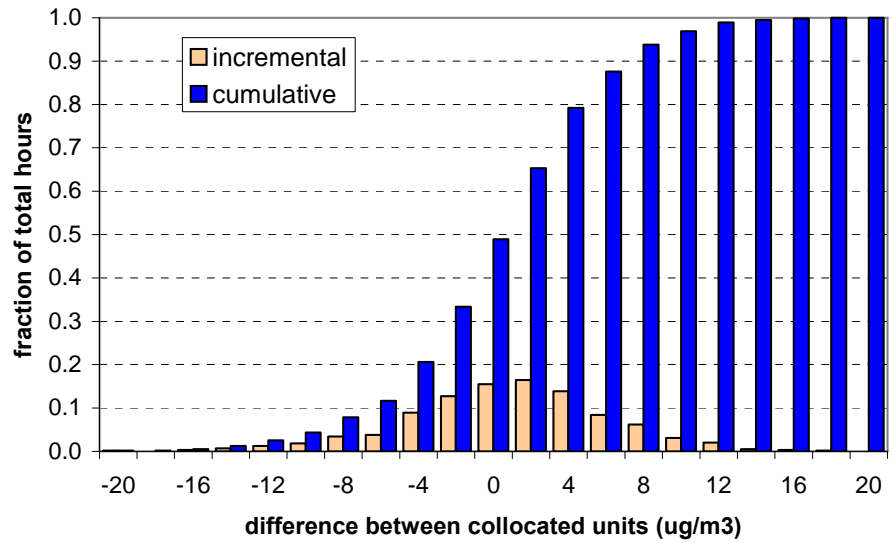


Figure 2-18. Correlation of hourly averaged PM_{2.5} (ug/m³) data from collocated EBAMs 10/17/06-11/06/06.

02/23/06-05/01/06

absolute error (ug/m3)	cumulative fraction
<2	0.32
<4	0.59
<6	0.76
<8	0.86
<10	0.93
<12	0.96
<14	0.98
<16	0.99
<18	1.00
<20	1.00
>20	0.00



10/17/06-11/06/06

absolute error (ug/m3)	cumulative fraction
<2	0.26
<4	0.51
<6	0.73
<8	0.85
<10	0.92
<12	0.95
<14	0.98
<16	0.99
<18	0.99
<20	1.00
>20	0.00

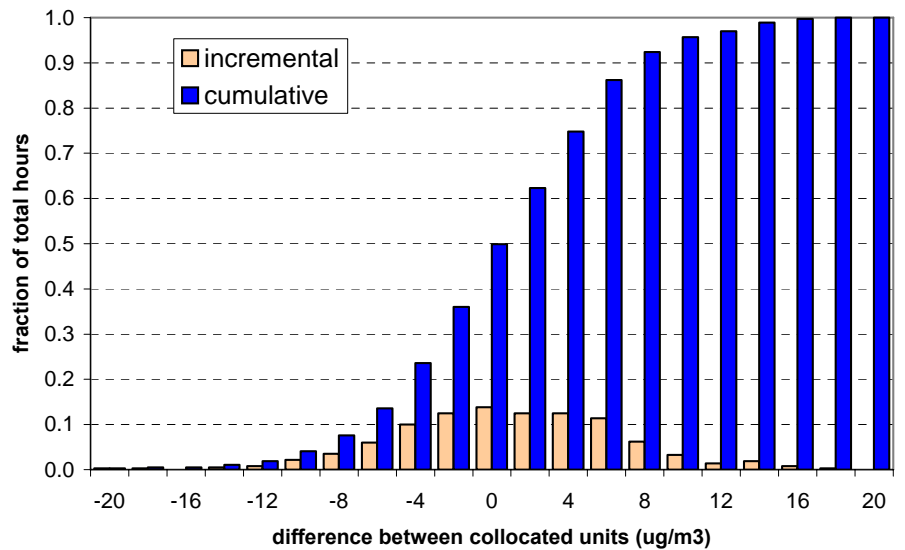


Figure 2-19. Difference between collocated EBAMS used at Denio and Pool sites. Data represented are hourly averages. Table gives distribution of absolute values of differences, with approximate 95th percentile in bold.

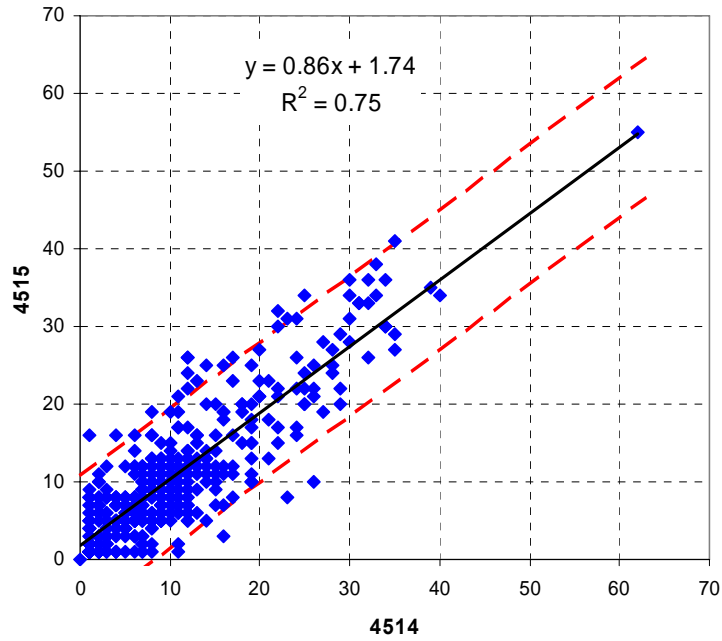


Figure 2-20. Correlation of hourly averaged data from collocated BAMs 02/23/06-05/01/06. 4514 was later used at Church and 4515 at Vernon.

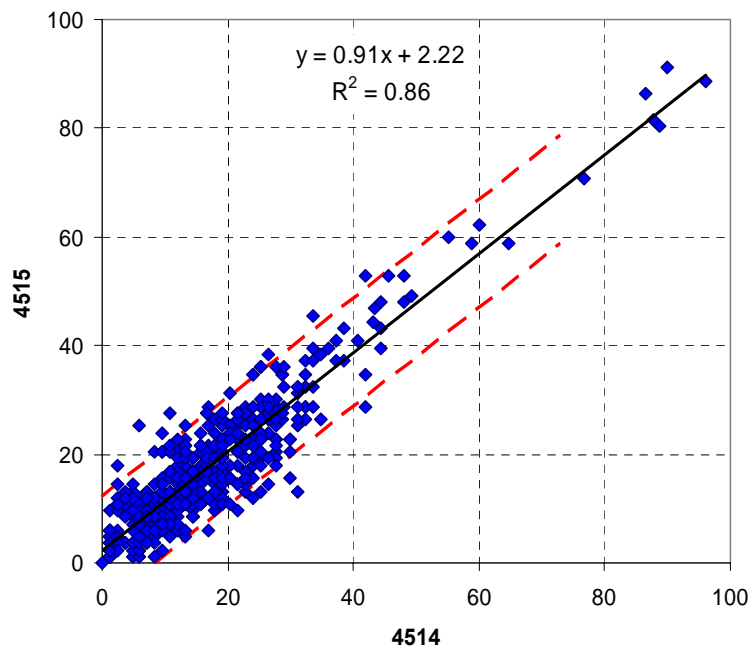
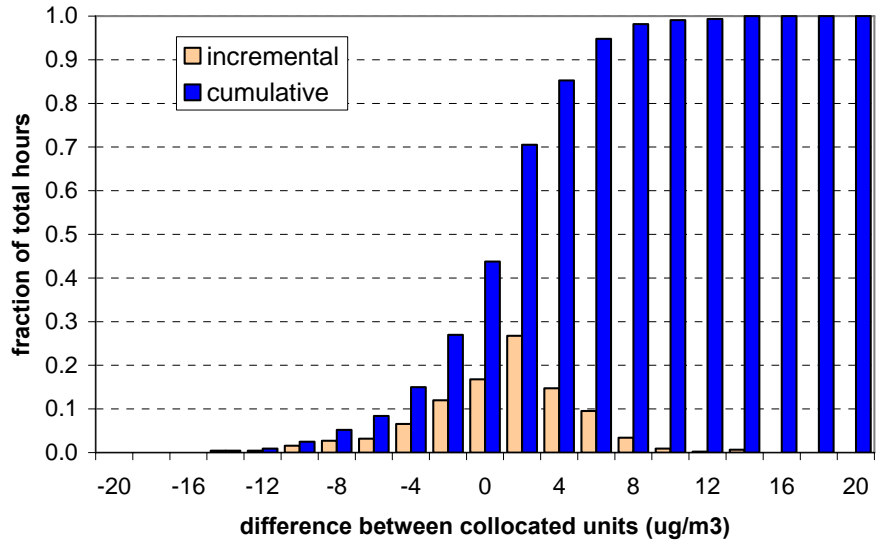


Figure 2-21. Correlation of hourly averaged data from collocated BAMs 10/17/06-11/06/06.

02/23/06-05/01/06

absolute error (ug/m3)	cumulative fraction
<2	0.44
<4	0.70
<6	0.86
<8	0.93
<10	0.97
<12	0.98
<14	1.00
<16	1.00
<18	1.00
<20	1.00
>20	1.00



10/17/06-11/02/06

absolute error (ug/m3)	cumulative fraction
<2	0.31
<4	0.59
<6	0.79
<8	0.90
<10	0.95
<12	0.98
<14	1.00
<16	1.00
<18	1.00
<20	1.00
>20	1.00

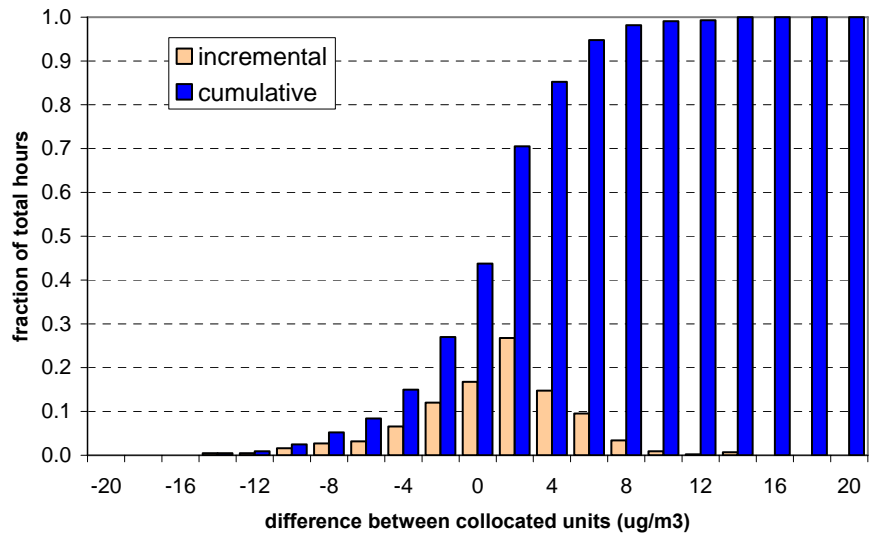


Figure 2-22. Difference between collocated BAMS used at Church and Vernon sites. Data represented are hourly averages. Table gives distribution of absolute values of differences, with approximate 95th percentile in bold.

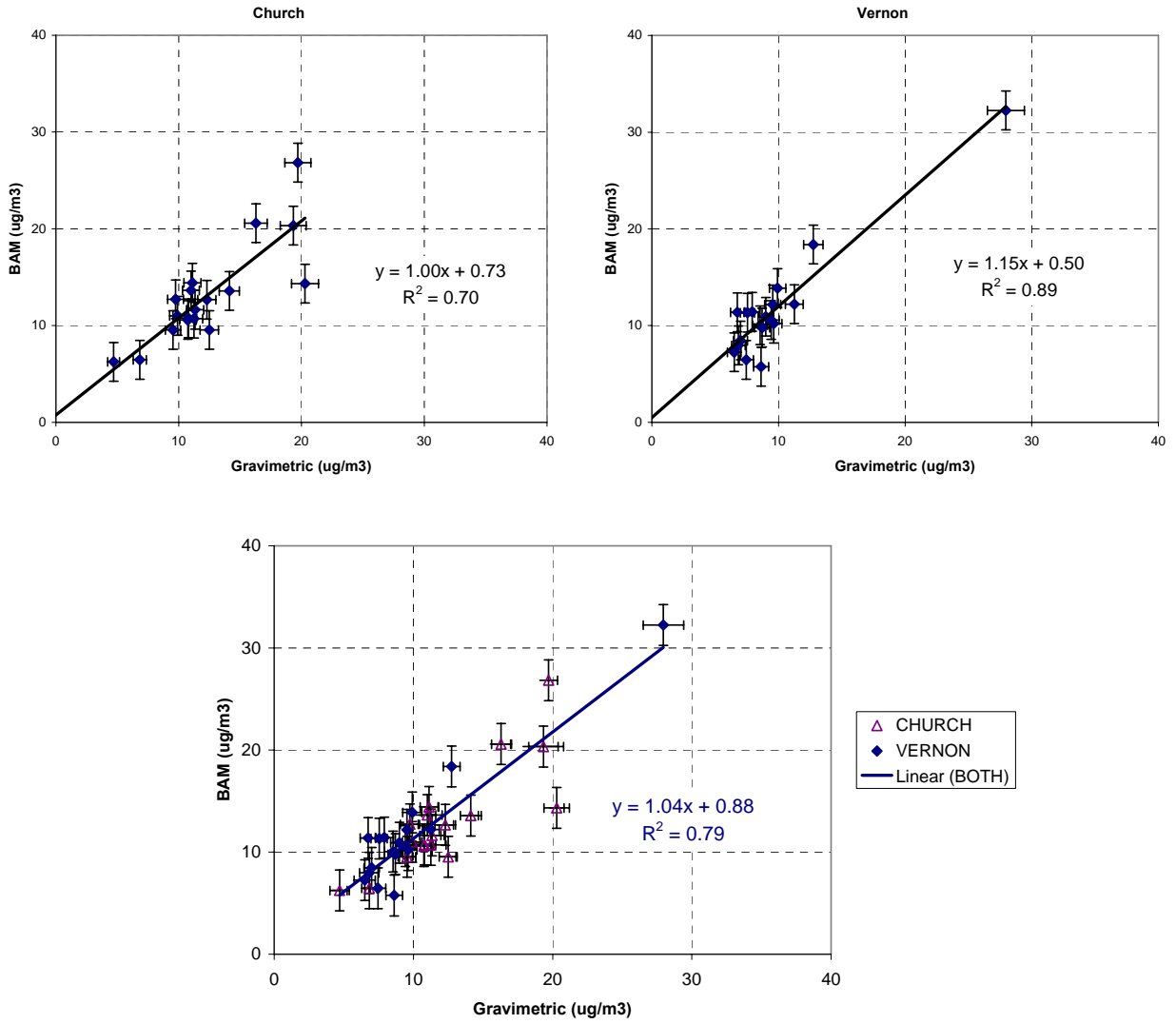


Figure 2-23. Correlation plots comparing average BAM PM2.5 to gravimetric mass from FRM filters for 24hr samples at 2 sites.

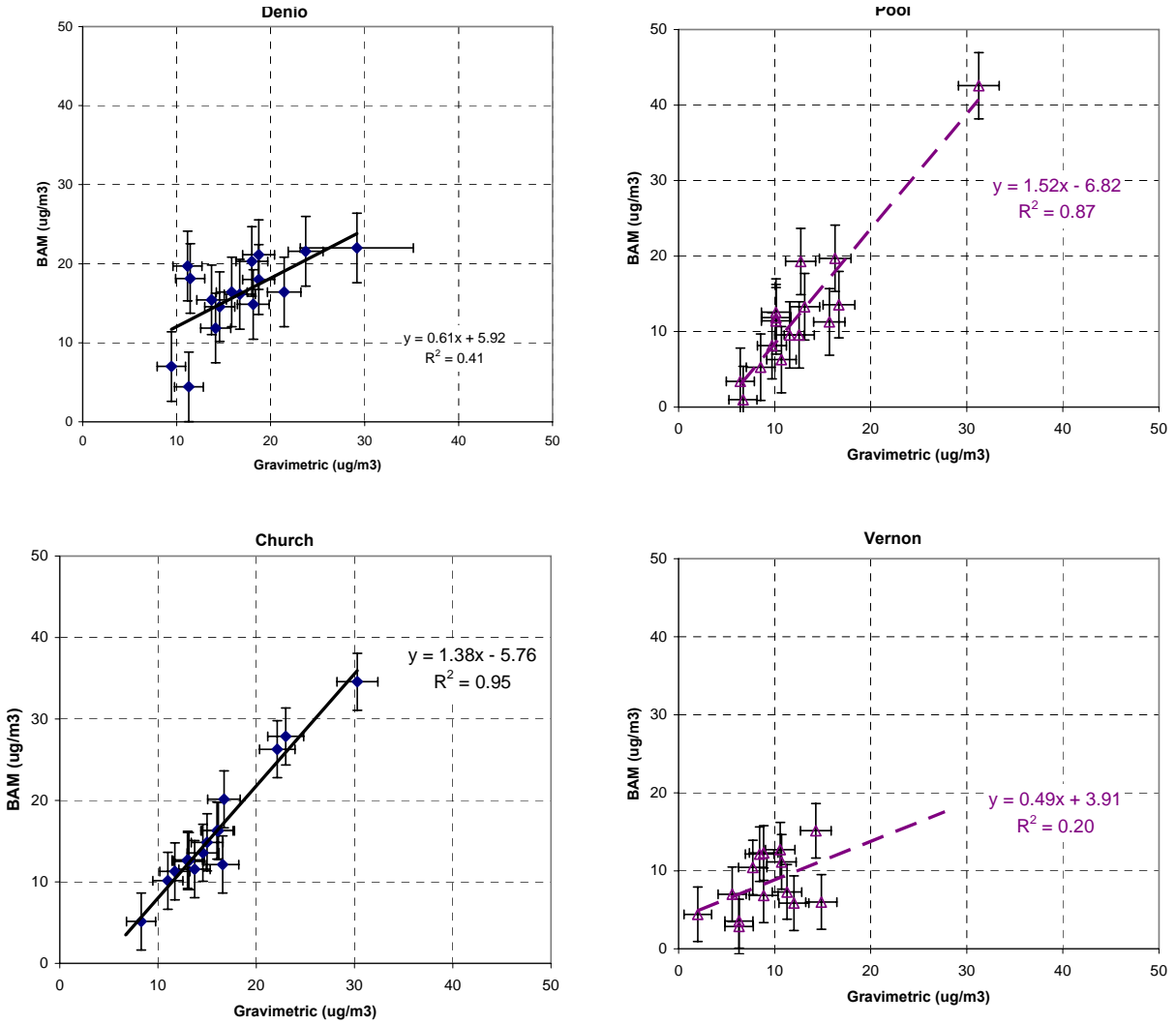


Figure 2-24. Correlation plots comparing average BAM PM2.5 to gravimetric mass from FRM filters for 7hr samples at 4 sites.

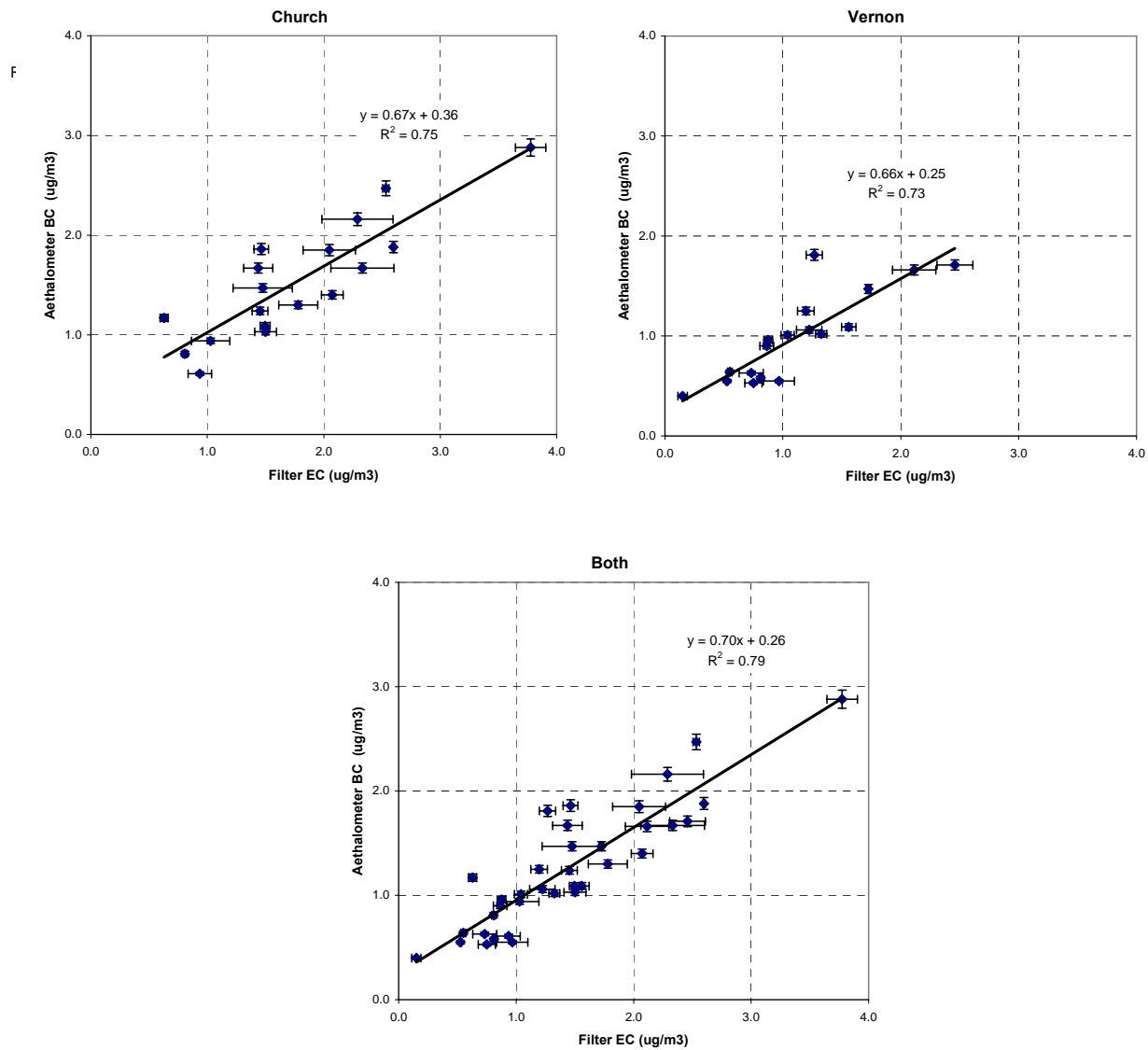


Figure 2-25. Correlation plots comparing average aethalometer BC(1) to elemental carbon from FRM filters for 24hr samples at Church and Vernon.

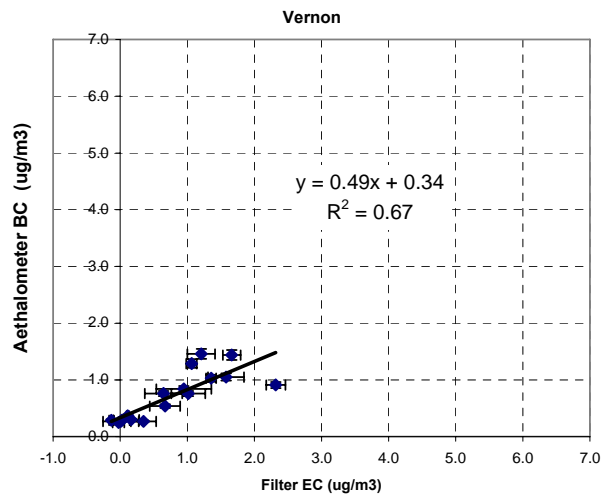
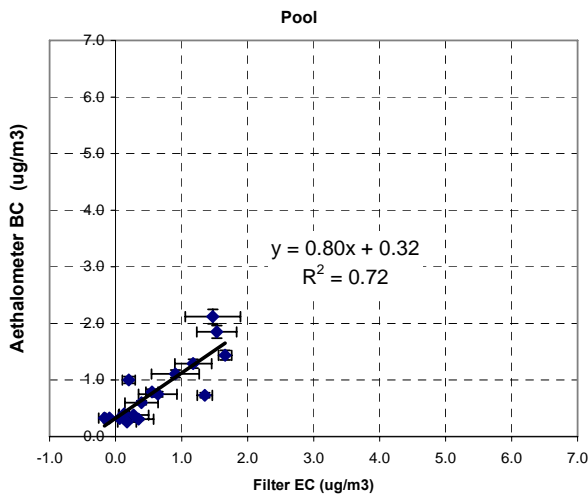
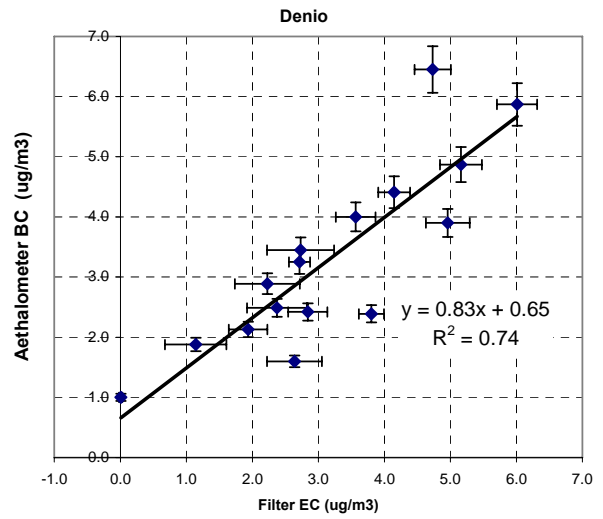
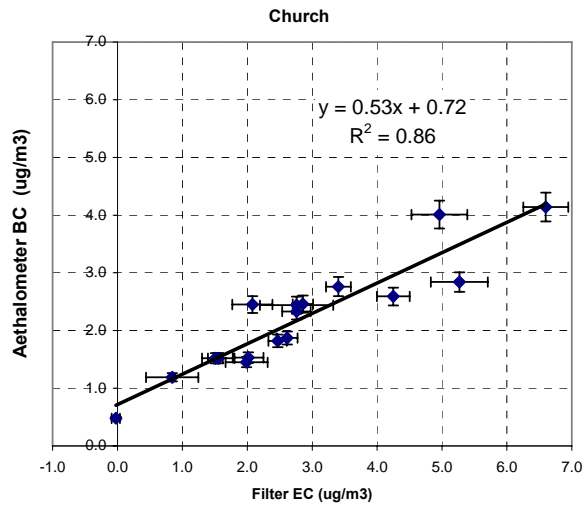


Figure 2-26. Correlation plots comparing average aethalometer BC(1) to elemental carbon from FRM filters for 7hr samples at 4 sites.

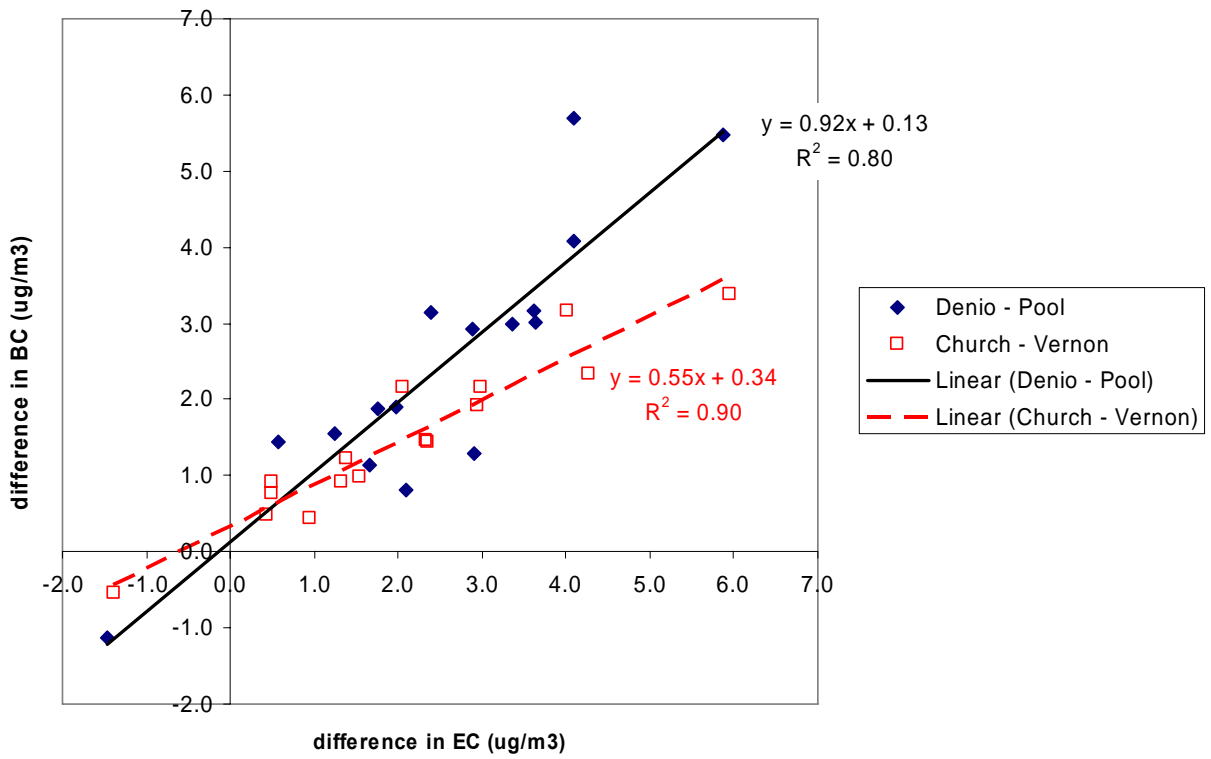


Figure 2-27. Correlation plot comparing difference in elemental carbon (EC) concentration from FRM filters between downwind and upwind sites to to difference in average Aethalometer black carbon (BC) for 7hr samples at 2 site pairs.

3. RESULTS

This section summarizes results of the analysis of RRAMP data to quantify the localized air pollutant impacts from the emissions at the UPRR facility. First we compared the mean diurnal variations in pollutant concentrations at the downwind and upwind monitoring sites. The purpose of these comparisons is to determine whether differences in diurnal patterns of rail yard emissions are detectable in the data. The mean pollutant concentrations were then determined for each monitoring site using the selection criteria for the downwind/upwind analysis. Differences in pollutant concentrations for the pairs of downwind and upwind sites were compared to the standard errors in the mean and propagated measurement uncertainties to address the hypothesis that differences in downwind and upwind pollutant concentrations are statistically significant.

3.1 Upwind/Downwind Differences

We examined the downwind minus upwind concentrations of NO, BC and PM_{2.5} for the two pairs of upwind/downwind sampling locations in order to develop a basis for selecting appropriate subsets of the data that would be used to establish the impact of emissions from the rail yard on downwind pollutant levels. The locations of the two upwind (Pool and Vernon) and two downwind (Denio and Church) sampling sites are shown in Figure 1-1.

We calculated nightly downwind-upwind differences in PM, BC, NO, and NO_x concentrations for each site pair. Uncertainties of differences were calculated as the square root of the sum of the squares of the measurement error, using PM and BC measurement errors determined from the precision and accuracy analysis of the collocation data. NO and NO_x measurement errors are assumed to be consistent with the EPA reference method specifications. All statistics for these calculations are based on the filtered nightly average values.

Table 3-1 shows the means, standard deviations, and standard errors of the means for 7-hour average BC, PM_{2.5}, NO and NO_x concentrations collected between 2200 to 0500 PST at the four RRAMP sites. Mean downwind minus upwind differences in PM, BC, NO and NO_x concentrations were calculated for each site pair for the entire study period excluding the time period of the Ralston fire. Significance of differences was determined from the standard errors of the means, pooled standard error of the differences, root mean squares of the measurement errors, and student's T-test. Using a 2-sample unequal variance (heteroscedastic) Student's t-test, these differences are all significant at above the 99% confidence level. The 2-sigma standard errors for the slope and intercept of linear regressions shown in Table 2-4 were included in the calculation of propagated analytical errors of the seasonal mean PM_{2.5} values in Table 3-1. Descriptive statistics for the 24-hour daily average concentrations are also included in the table. Since the data used for the daily averages were not subjected to the same restrictions on wind speed and wind direction as the overnight (7-hour) averages there are a larger number of valid days included. Data from the period of the Ralston Fire (Sept. 5-17) were excluded from all seasonal averages.

The graphical displays of the downwind-upwind differences are shown in Figure 3-1. Note that the ratios of pollutant concentrations at the upwind relative to downwind sites are lowest for NO and are larger in increasing order for NO_x, BC and PM. [Ratios are not shown in Figure 3-1; they are addressed in Table 3-2. Suggest you include a Aethalometer showing the ratios.] The increasing ratios from NO to PM are consistent with larger contributions of urban

background to the measured PM and BC concentrations. Figure 3-1 also shows the differences between the two downwind and two upwind sites. These differences are small in comparison.

Table 3–2 lists the statistics for several key ratios that indicate the relative contribution of fresh emissions to the measured pollutant mix. Note that all of these ratios are higher at the downwind sites, particularly NO/NO_x which is directly tied to proximity to fuel combustion sources. The higher BC/PM ratios are particularly indicative of diesel vehicle influence. Although the BC(1)/BC(2) ratios vary extensively at each site, the mean values are clearly higher at the downwind sites which is consistent with the greater specificity of the longer BC(1) wavelength to diesel soot. It is also instructive to note that these mean ratios are generally quite consistent for the two downwind sites, supporting the conclusion that both sites are subject to the same types of local influence.

3.2 FRM filter results

As discussed in Section 2.8, the analysis results from the FRM sampler filters collected every third day at each site may ultimately be used to relate the Aethalometer BC and continuous PM data to estimated diesel particulate matter concentrations. They may also prove useful for characterizing differences in the composition of the PM at the upwind and downwind sites by comparing the relative amounts of carbon constituents from the TOR analysis to each other and to the total PM measured by gravimetric analysis of the Teflon filters. Unfortunately, the quartz filters were not pre-fired prior to sampling to reduce the organic carbon artifact that results from absorption of volatile organic species by the filter material. Field blanks collected after the study period confirmed the significance of this artifact, as shown in Table 3–3. Note that there is a clear and consistent difference in composition between the two upwind sites and the two downwind sites.

Since only 4 field blanks were collected and they were not concurrent with the actual samples it is difficult to make a quantitative correction to the organic carbon data with any confidence, however, we may presume that the calculation of downwind – upwind differences in concentration for the paired sites will not be strongly affected by the high artifact levels since both samples should have similar blank levels. This seems supported by the comparison of the blank corrected EC/TC values in Table 3–3 to those in Table 3–4, which lists the elemental to total carbon (EC/TC) ratios and TC/PM ratios calculated using the differences in carbon and gravimetric mass measurements for the two site pairs. EC/TC ratios without blank correction are consistent for sites on the same side of the railyard and higher at the downwind sites, but still much lower than we would expect for an aerosol with a strong diesel exhaust component (source testing from diesel engines typically yields EC/TC ratios $\geq 50\%$). Subtracting the average field blank from the reported values increases the EC/TC ratios but they also become much more variable and the difference between the downwind and upwind sites is no longer clear. In contrast, EC/TC ratios for the downwind-upwind differences (Table 3–4, without blank correction) are quite consistent and high enough to be indicative of strong diesel influence. However, the TC/PM ratios are very inconsistent suggesting some disconnect between the two types of filter samples. The addition of more frequent field blank collection and some collocation testing of the FRM samplers next year may help explain the poor agreement between the gravimetric and TOR results and allow better characterization of the EC/TC ratios at the upwind sites.

Table 3–1. Means, standard deviations, and standard errors of the means for 7-hour (2200 to 0500 PST) and 24-hour (midnight to midnight PST) BC, PM_{2.5}, NO and NO_x concentrations at the four RRAMP sites. The differences in mean concentrations between the two pairs of downwind and upwind sites (Denio-Pool and Church-Vernon) during the overnight period and pooled standard error of the differences are also shown.

Statistics	BC (ug/m ³)				PM _{2.5} (ug/m ³)				NO (ppb)				NO _x (ppb)			
	Denio	Pool	Church	Vernon	Denio	Pool	Church	Vernon	Denio	Pool	Church	Vernon	Denio	Pool	Church	Vernon
<u>2200-0500 averages</u>																
average	3.24	0.59	2.36	0.54	16.9	12.1	16.9	10.2	98	0	93	0	143	8	133	8
stdev	1.48	0.29	1.08	0.30	4.4	4.8	6.5	3.6	55	2	69	1	71	5	84	5
n observations	84	88	88	87	88	83	83	87	84	81	85	87	84	81	85	87
sterr_mean	0.16	0.03	0.12	0.03	0.5	0.5	0.7	0.4	6	0	8	0	8	1	9	1
<u>Downwind-Upwind</u>																
avg delta	2.65		1.81		4.7		6.5		99		93		136		125	
sterr_delta	0.15		0.12		0.5		0.7		6		8		8		9	
T-test	0.00		0.00		0.00		0.00		0.00		0.00		0.00		0.00	
propagated error	1.06		1.04		1.0		1.1		1.1		1.0		1.1		0.8	
<u>Downwind and Upwind pairs</u>																
avg delta	0.91		0.05		0.1		2.1		6		0		11		-1	
ster_delta	0.20		0.01		0.8		0.5		10		0.2		12		0.4	
propagated error	1.29		1.27		1.3		1.3		1.3		1.3		1.3		1.1	
<u>24 hr averages</u>																
average	2.29	0.94	1.69	0.94	13.2	9.6	12.4	10.0	55	8	51	9	87	21	81	24
stdev	0.64	0.42	0.52	0.44	3.5	3.5	3.7	3.8	24	14	34	12	31	21	43	18
n observations	98	104	104	102	104	95	97	102	101	98	102	104	101	98	102	104
sterr_mean	0.06	0.04	0.05	0.04	0.3	0.4	0.4	0.4	2	1	3	1	3	2	4	2

*Data collected during the Ralston Fire (9/5 -9/17) are excluded. Data used to calculate overnight averages are limited to periods of typical wind flow.

Table 3–2. Means and statistics for hourly (2200 to 0500 PST) NO/NO_x, BC/PM_{2.5}, and BC(1)/BC(2) ratios at the four RRAMP sites. The standard deviation and 2-sigma standard errors of the means are included to indicate the significance of the differences.

	Denio NO/NO _x	Pool NO/NO _x	Church NO/NO _x	Vernon NO/NO _x	Denio BC/PM	Pool BC/PM	Church BC/PM	Vernon BC/PM	Denio BC1/BC2	Pool BC1/BC2	Church BC1/BC2	Vernon BC1/BC2
avg	0.65	0.13	0.63	0.05	0.17	0.05	0.15	0.06	1.24	0.85	1.21	1.03
min	0.15	-0.09	0.06	0.00	0.01	0.01	0.02	0.00	0.38	0.40	0.73	0.45
max	0.86	0.83	0.88	0.88	0.72	0.20	0.64	0.22	1.95	1.27	1.74	1.48
stdev	0.10	0.16	0.14	0.13	0.10	0.04	0.08	0.04	0.16	0.19	0.15	0.12
2*stderr	0.01	0.02	0.01	0.02	0.01	0.00	0.01	0.00	0.01	0.02	0.01	0.01

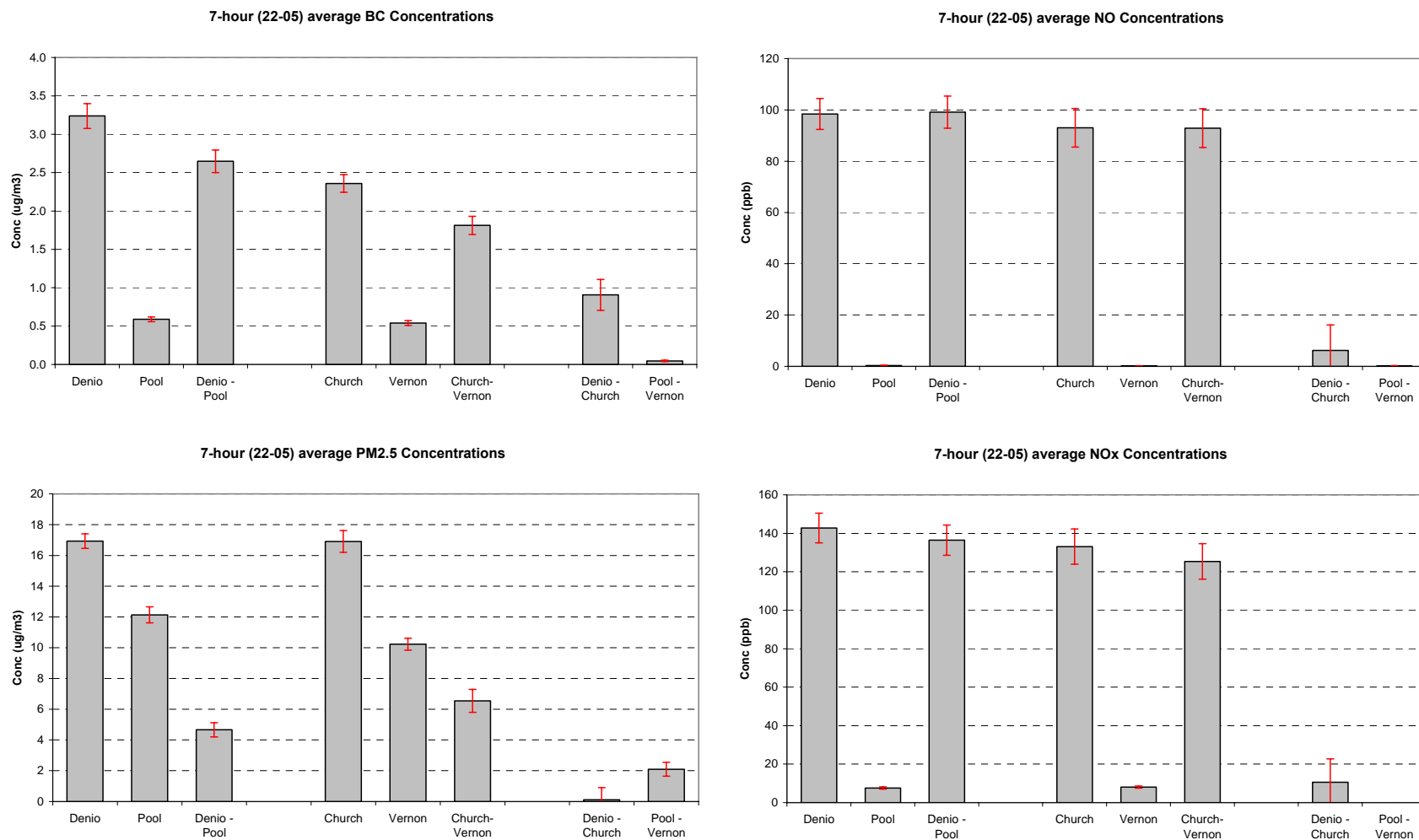
Table 3–3. Means and 2-sigma standard errors for TOR analysis results of the 7-hour overnight FRM filter samples.

	<i>no blank subtraction</i>			<i>blank subtracted</i>
	OC (µg/m ³)	EC (µg/m ³)	EC/TC	EC/TC
DENIO	12.6 ± 1.3	2.9 ± 0.4	0.18 ± 0.11	0.34 ± 0.36
POOL	9.3 ± 1.3	0.9 ± 0.3	0.08 ± 0.09	0.21 ± 0.27
CHURCH	11.1 ± 2.2	2.7 ± 0.7	0.19 ± 0.12	0.36 ± 0.27
VERNON	8.8 ± 2.2	0.9 ± 0.4	0.10 ± 0.12	0.40 ± 0.73
blanks	6.7 ± 0.8	0.3 ± 0.2		

Table 3–4. Elemental to total carbon ratios and total carbon to PM2.5 ratios for 7-hour overnight FRM filter samples. All values are calculated from the differences in concentration between downwind and upwind sites, without blank correction. The group mean and 2-sigma standard errors of the means are included to indicate the significance of the differences.

Date	EC/TC RATIO		TC/PM RATIO	
	DENIO-POOL	CHURCH-VERNON	DENIO-POOL	CHURCH-VERNON
06/19/06	0.34	0.63	0.75	0.61
06/25/06	0.35	0.23	0.91	0.15
07/01/06	0.31	0.44	-1.77	-1.17
07/07/06	0.36	0.39	0.90	1.22
07/13/06	0.34	0.50	1.22	-0.99
07/19/06	0.57	0.37		
07/25/06	0.33	0.24	1.11	
07/31/06	0.37	0.00	1.21	
08/06/06	0.27	0.25	1.64	
08/12/06	1.09	0.58	-0.82	0.53
08/18/06	0.34	0.36	-3.11	1.32
08/24/06	0.24	0.58	1.21	0.77
08/30/06	0.27	0.43	1.44	0.72
09/23/06	0.21	0.48	-4.42	-1.07
09/29/06	0.41	-0.05	2.87	-5.36
10/05/06	0.18	0.17	-4.85	2.11
10/11/06	0.28	0.13	1.36	-11.82
MEAN	0.37	0.34	-0.02	-1.00
2STDERR	0.10	0.10	1.15	2.08

Figure 3-1. Mean BC, PM_{2.5}, NO and NO_x concentrations at the four RRAMP monitoring sites and differences of the two pairs of downwind and upwind sites (Denio-Pool and Church-Vernon). Differences between the two downwind and two upwind sites are also shown for comparison. Error bars are the standard errors of the means.



4. CONCLUSIONS AND RECCOMENDATIONS

This section summarizes the findings and conclusions from the evaluation and validation of the RRAMP data and analysis of the data. Several modifications to the field measurement protocol is suggested for consideration by the RRAMP Technical Advisory Committee.

4.1 Data Evaluation and Validation

- Collocated Aethalometers showed generally good agreement with no significant bias between instruments, but substantial variation (10-20%) on an hourly basis. Improved operating procedures adopted in the second year greatly improved data quality.
- The random error in 1-hour PM_{2.5} BAM is still too large ($\pm 10 \text{ ug/m}^3$) to make comparisons of the hourly data feasible at the measured concentrations. BAM data contained frequent negative values indicating baseline drift. Collocated BAMs showed good agreement in measured PM_{2.5} concentrations after averaging over periods of 6-hours or more.
- NO/NO_x data contained some negative values which were removed. Numerous instances of slightly negative NO data were retained to avoid biasing the averages.
- BC/PM and NO/NO_x ratios are consistently higher at the downwind sites, which is consistent with presence of fresh emissions.
- Averaged PM_{2.5} data from the BAMs is not always well correlated with the corresponding filter gravimetric mass data, and shows some evidence of a slight positive bias at higher concentrations. Adjustments to the BAM data were made to account for this. The correlations are weakest for 7-hr overnight samples at Denio and Vernon where the range of concentrations measured was smallest.
- 24-hour averaged BC data from the Aethalometers is well correlated with the corresponding EC from filter samples. The BC/EC ratio is about 0.7, which is consistent with prior data.
- TOR and gravimetric mass results from the FRM samples are not always consistent. At this point we are unable to determine whether this is due to the presence of inorganic aerosol of local origin or the large organic carbon artifacts from the quartz filters. A more thorough QC process for the FRM samples should be implemented next year.

4.2 Data Analysis

- Overall, there is evidence of substantial impact on the downwind sites. There was a substantial increase in NO, NO_x, and BC at the downwind sites relative to the upwind sites, with the largest differential for NO. The magnitude of the mean concentrations and downwind-upwind site deltas are somewhat different than those observed during the first

year of monitoring but the comparison may not be valid unless differences in sampling period and schedule are accounted for.

- The differences in mean concentrations between the two pairs of downwind and upwind sites (Denio-Pool and Church-Vernon) are all significant at above the 99% confidence level.
- Ratios of pollutant concentrations at the upwind relative to downwind sites are lowest for NO and are larger in increasing order for NO₂, BC and PM. The increasing ratios from NO to PM are consistent with larger contributions of urban background to the measured PM and BC concentrations.
- EC/TC ratios from the FRM filter samples are consistent with initial expectations and show a clear difference in aerosol composition between the upwind and downwind sites.

5. REFERENCES

- Arnott, W. P., H. Moosmüller, et al. (1999). "Photoacoustic spectrometer for measuring light absorption by aerosols: Instrument description." *Atmospheric Environment* 33: 2845-2852.
- Arnott, W. P., K. Hamasha, H. Moosmüller, P.J. Sheridan and J.A. Ogren (2005). "Towards Aerosol Light Absorption Measurements with a 7-Wavelength Aethalometer: Evaluation with a Photoacoustic Instrument and 3-Wavelength Nephelometer." *Aerosol Sci. and Technol.* 39:17-29.
- Campbell, D.E. and E.M. Fujita (2005). Deployment of DRI Mobile Van in Support of the Roseville Rail Yard Air Monitoring Project. Final report submitted to Placer County Air Pollution Control District, Auburn, CA, May 6, 2005.
- Campbell, D.E. and E.M. Fujita (2006). Data Analysis on the Roseville Rail Yard Air Monitoring Project. Final report submitted to the Placer County Air Pollution Control District, Auburn, CA, March 15, 2006.
- Chow, J.C., Watson, J.G., Lowenthal, D.H., Chen, L.W.A., Tropp, R.J., Park, K., Magliano, K.L., 2006. PM_{2.5} and PM₁₀ mass measurements in California's San Joaquin Valley. *Aerosol Science & Technology* 40 (10), 796-810.

APPENDIX A

Measurement Methods

APPENDIX A – MEASUREMENT METHODS

Measurements at each of the four RRAMP sites during summer 2006 consisted of continuous (hourly average) wind speed and wind direction, Aethalometer for black carbon, Beta Attenuation Monitors (BAM) for PM_{2.5} mass, chemiluminescent NO/NO_x analyzers. The four Aethalometers and four BAMs were co-located to assess measurement precision during a 2 week period prior to and after each intensive period. FRM PM_{2.5} filter sampling was conducted every third day during the 2006 intensive monitoring period using a pair of samplers at each site, one loaded with Teflon filters for gravimetric mass analysis and the second unit loaded with quartz filters for carbon analysis. The FRM samplers were operated for 7-hour nighttime periods at Denio and Pool and for alternating 7-hour and 24-hour periods at Church and Vernon. Table 1–1 provides an inventory of the data collected during summer 2006. The data sets were compiled and quality assured by PCAPCD staff.

Aethalometer

The Aethalometer instrument continuously passes ambient air through a quartz-fiber filter tape. Light absorbing particles such as black carbon (BC) cause attenuation of a light beam incident on the tape. By assuming that all light-absorbing material is black carbon, and that the absorption coefficient of the black carbon is known and constant, the net attenuation signals can be converted into black carbon mass concentrations. The time resolution of the Aethalometer is on the order of a fraction of a minute depending on ambient black carbon concentration. Detection limit for the Aethalometer is $\sim 0.1 \mu\text{g}/\text{m}^3$ black carbon for a one minute average.

Two models manufactured by Magee Scientific were used in this study. The rack-mounted AE-20 model at Denio and Pool sites, and the ‘portable’ model AE-42 at Church and Vernon. Both models measure attenuation at two wavelengths (880 nm and 370 nm) and have identical sample collection, detection, and software systems. Flow rates were set to 5 lpm for all units, and data was recorded at the default 5-minute time intervals. Data were collected at both wavelengths, but all black carbon data in the analyses are from the 880nm wavelength of the Aethalometer (channel 1) unless otherwise specified.

There are several operational features of the Aethalometer that can affect comparability of data from multiple instruments. Baseline measurements are made after each tape advance resulting in a 15 minute gap in the data. These tape advances can be set at fixed intervals or initiated automatically at set threshold opacity. The instruments were operated during RRAMP in the fixed interval mode resulting in 15-minute gaps that occur at predetermined times each day. Aethalometer data is also known to be strongly affected by electronic noise spikes which create exaggerated increases or decreases in individual measurements of light attenuation. Another factor that contributes measurement uncertainty is the effect of filter loading on light absorption measurements. The Aethalometer has been shown to overpredict BC concentrations on a fresh filter and underpredict BC concentrations on a loaded filter (Arnott et al., 2005). Arnott et al. found that the Aethalometer BC measurements correlate well with photoacoustic BC and thermal optical elemental carbon if the data are averaged over the full range of filter loading. All of the effects mentioned above can be minimized by averaging the data over longer intervals. This issue was addressed in detail in the Year 1 Annual Report.

Beta Attenuation Monitors

Beta rays (electrons with energies in the 0.01 to 0.1 MeV range) are attenuated according to an approximate exponential (Beer's Law) function of particulate mass, when they pass through deposits on a filter tape. Automated Beta Attenuation Monitor (BAM) samplers utilize a continuous filter tape, first measuring the attenuation through the unexposed segment of tape to correct for blank attenuation. The tape is then exposed to ambient sample flow, accumulating a deposit. The beta attenuation measurement is repeated. The blank-corrected attenuation readings are converted to mass concentrations, with averaging times as short as 30 minutes. Detection limit is $\sim 5 \mu\text{g}/\text{m}^3$ for a one-hour average.

Met One E-BAMs were used at the Denio and Pool sites. Manufacturer's specifications cite an accuracy of 2.5 ug for a 24 hour average, and a $\pm 3\%$ accuracy in the volumetric flow rate. The BAM 1020 model, which has a specified accuracy of $\pm 8\%$ for 1-hour measurements and $\pm 2\%$ for 24-hour averages, was used at Church and Vernon. Cyclones with a 2.5um cut point were used on all units.

Nitric oxide (NO) and nitrogen oxides (NOx)

NO is continuously measured by the chemiluminescence nitric oxide-ozone method (OCM). This method is based on the gas-phase chemical reaction of NO with ozone. In this method ambient air is mixed with a high concentration of ozone so that any NO in the air sample will react and thereby produce light. The light intensity is measured with a photomultiplier and converted into an electronic signal that is proportional to the NO concentration. To measure NOx concentrations, the sum of NO and NO₂ (nitrogen dioxide), the air sample is first reduced to NO by a heated catalyst (molybdenum or gold in the presence of CO) adding to the NO already present in the sample, then passes into the reaction chamber for measurement as described above. The NO₂ concentration is derived by subtracting the NO concentration measurement from the NOx concentration measurements. Four Horiba NOx instruments were used in the study. This instrument has a zero stability of 10 ppb in 24 hours and span drift of less than 1 percent.

Thermal Optical Carbon Measurements

Elemental carbon (EC) and organic carbon (OC) were measured by thermal optical reflectance (TOR) method using the IMPROVE (Interagency Monitoring of Protected Visual Environments) temperature/oxygen cycle (IMPROVE TOR). Samples were collected on quartz filters using Federal Reference Method (FRM) PM_{2.5} samplers. A section of the filter sample is placed in the carbon analyzer oven such that the optical reflectance or transmittance of He-Ne laser light (632.8 nm) can be monitored during the analysis process. The filter is first heated under oxygen-free helium purge gas. The volatilized or pyrolyzed carbonaceous gases are carried by the purge gas to the oxidizer catalyst where all carbon compounds are converted to carbon dioxide. The CO₂ is then reduced to methane, which is quantified by a flame ionization detector (FID). The carbon evolved during the oxygen-free heating stage is defined as "organic carbon". The sample is then heated in the presence of helium gas containing 2 percent of oxygen and the carbon evolved during this stage is defined as "elemental carbon". Some organic compounds pyrolyze when heated during the oxygen-free stage of the analysis and produce additional EC,

which is defined as pyrolyzed carbon (PC). The formation of PC is monitored during the analysis by the sample reflectance or transmittance. EC and OC are thus distinguished based upon the refractory properties of EC using a thermal evolution carbon analyzer with optical (reflectance or transmittance) correction to compensate for the pyrolysis (charring) of OC. Carbon fractions in the IMPROVE method correspond to temperature steps of 120°C (OC1), 250°C (OC2), 450°C (OC3), and 550°C (OC4) in a nonoxidizing helium atmosphere, and at 550°C (EC1), 700°C (EC2), and 850°C (EC3) in an oxidizing atmosphere. The IMPROVE method uses variable hold times of 150-580 seconds so that carbon responses return to baseline values.

Because EC and OC are operationally defined by the method, the specific instrument used, details of its operation, and choice of thermal evolution protocol can influence the split between EC and OC (34). Visual examination of filter darkening at different temperature stages have shown that substantial charring takes place within the filter, possibly due to adsorbed organic gases or diffusion of vaporized particles. The filter transmittance is more influenced by within-filter charring, whereas the filter reflectance is dominated by charring of the near-surface deposit. TOR and TOT corrections converge in the case of only a shallow surface deposit of EC or only a uniformly distributed pyrolyzed organic carbon (POC) through the filter and diverge when EC and POC exist concurrently at the surface and are distributed throughout the filter, respectively, especially when the surface EC evolves prior to the POC. The difference between TOR and TOT partly depends on the POC/EC ratio in the sample (31). Thus, highly loaded source samples would yield similar EC values for TOR and TOT corrections, while lightly loaded source and ambient samples would typically yield different EC values. While EC values for TOR may tend toward higher EC due to underestimation of the POC correction, higher absorption efficiency of POC within the filter may tend toward lower EC values for TOT.

APPENDIX B

Time series plots of hourly data by month

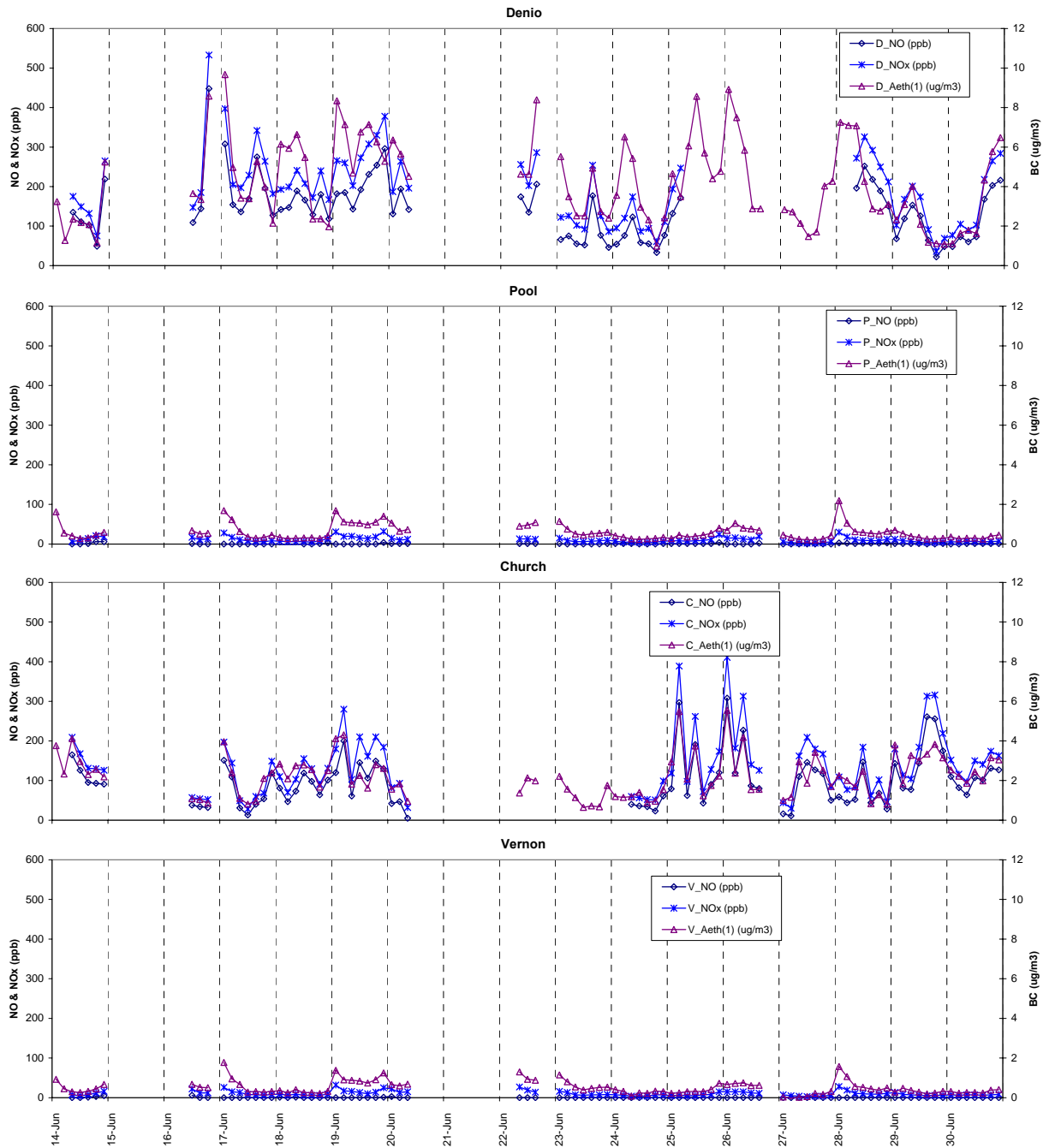


Figure 2. Hourly NO, NOx, and BC for June 2006

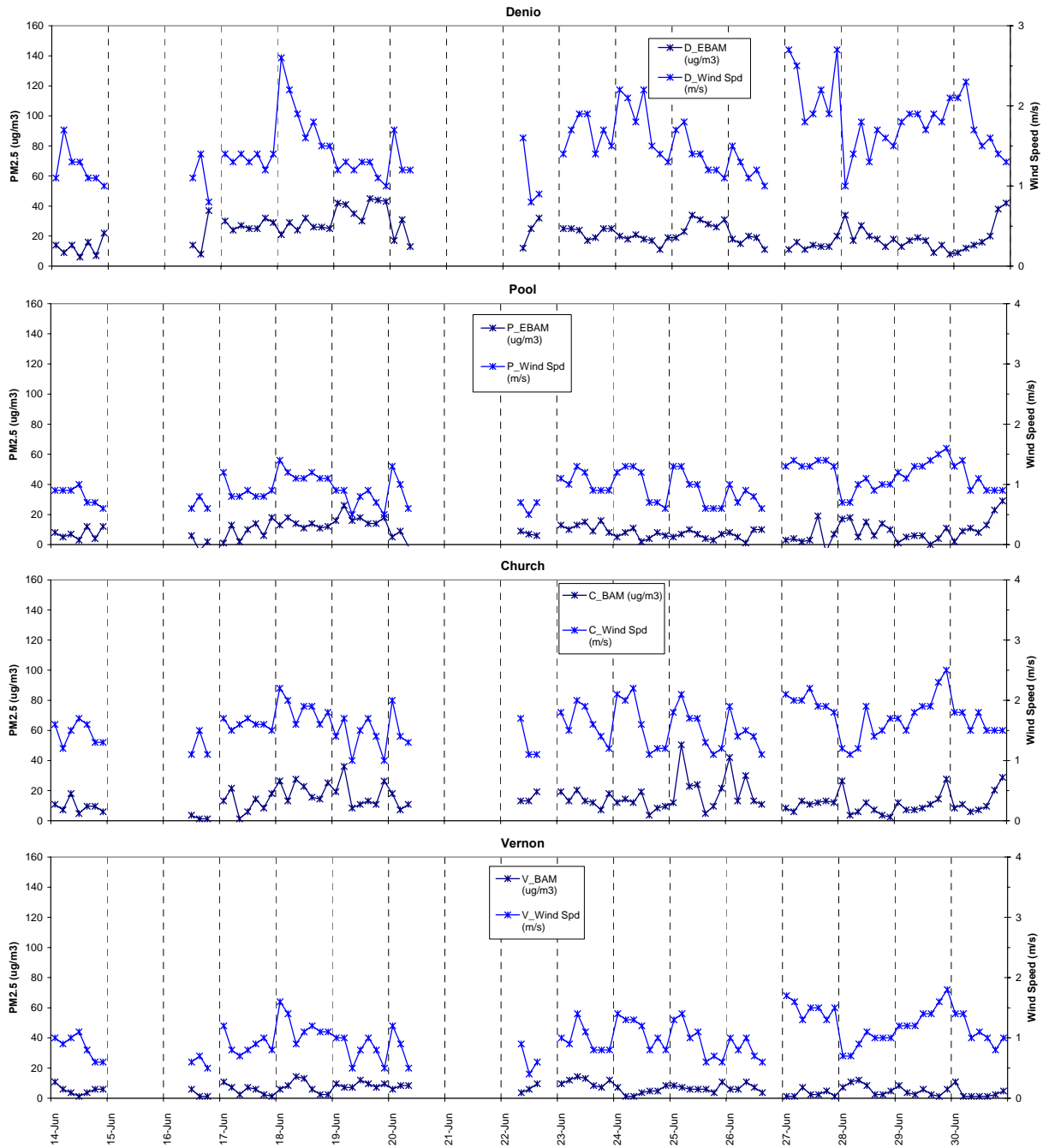


Figure 3. Hourly PM2.5 mass concentration and wind speed for June 2006.

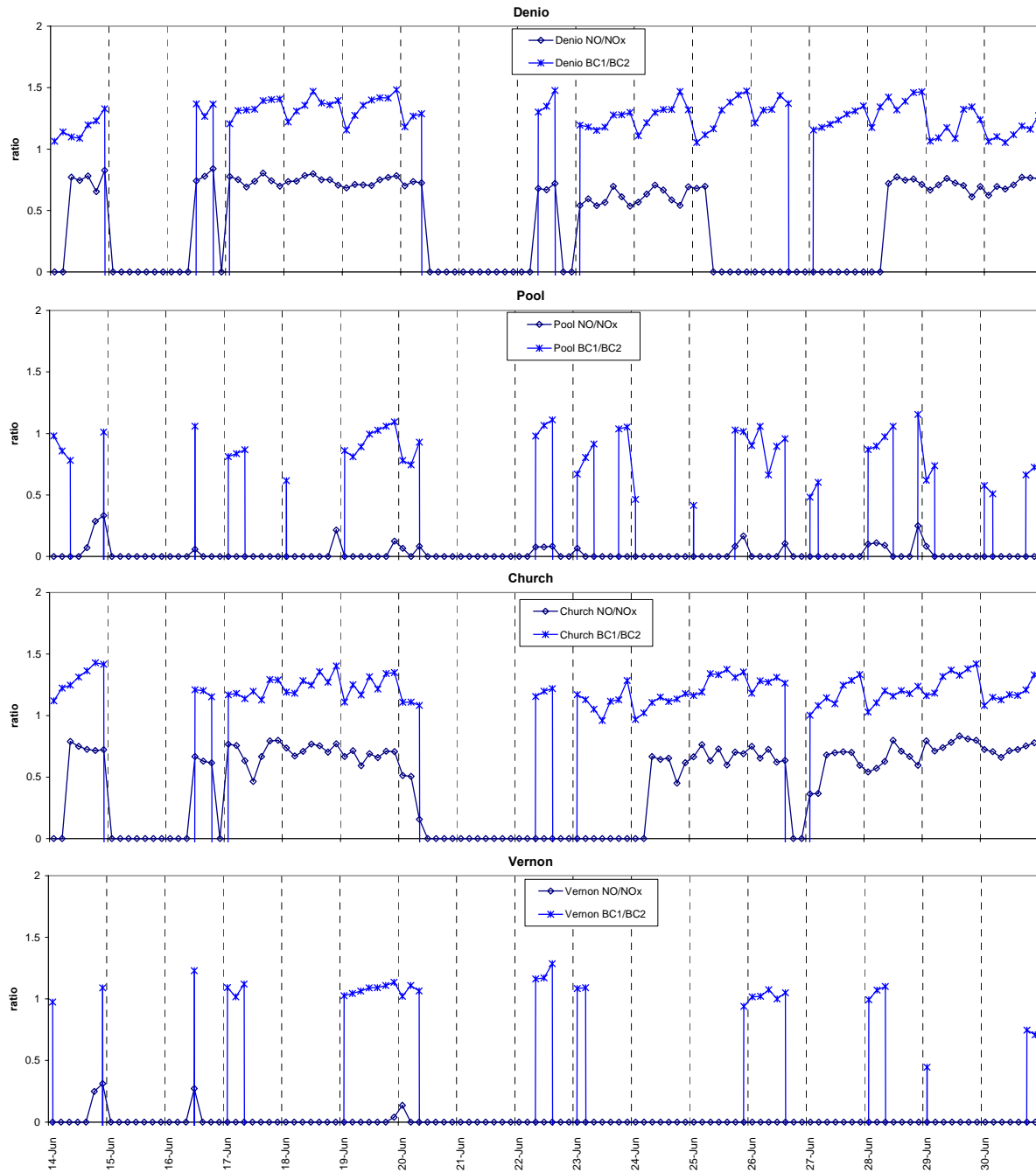


Figure 4. Hourly NO/NO_x ratio and BC(1)/BC(2) ratio for June 2006.

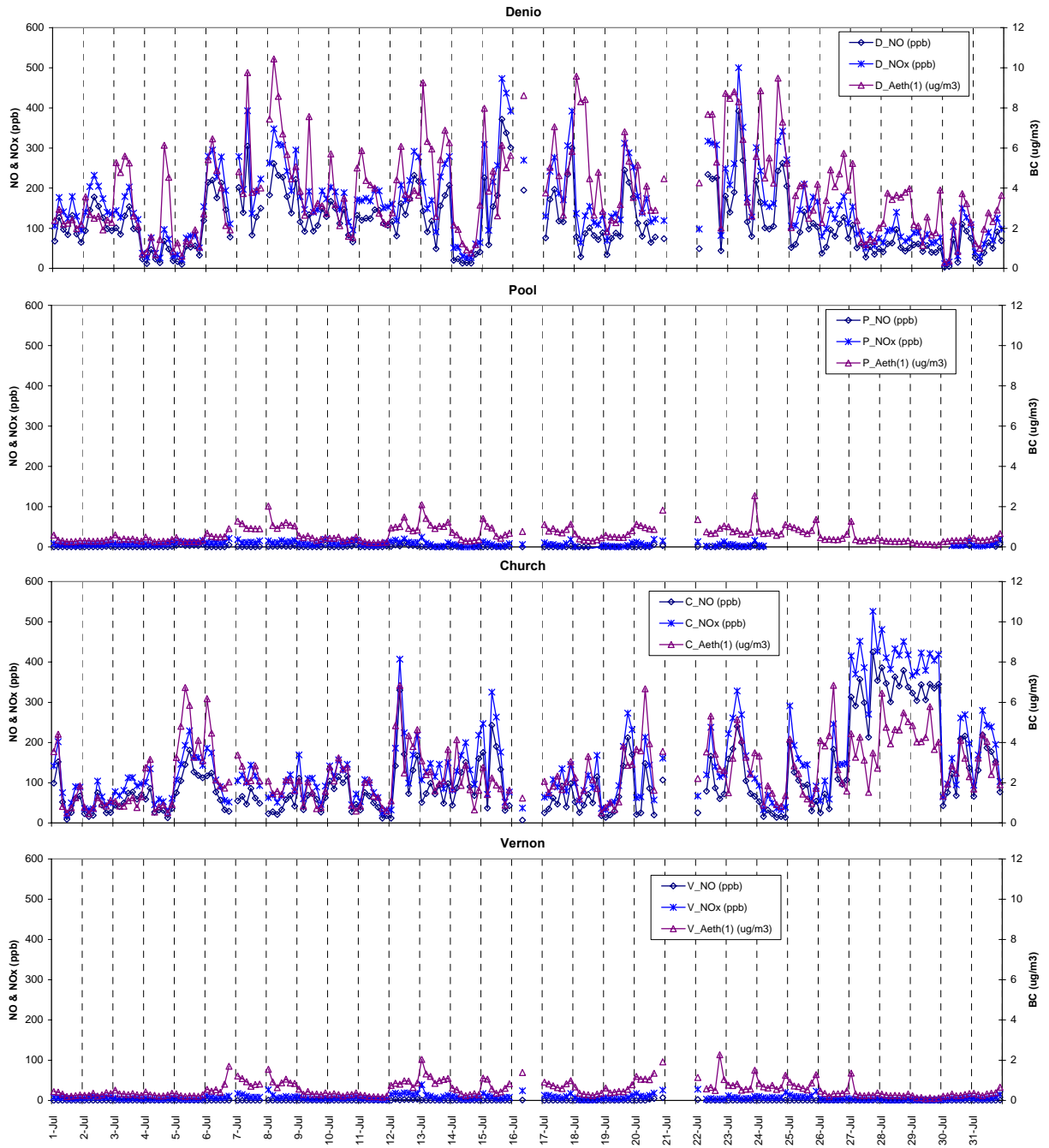


Figure 5. Hourly NO, NOx, and BC for July 2006

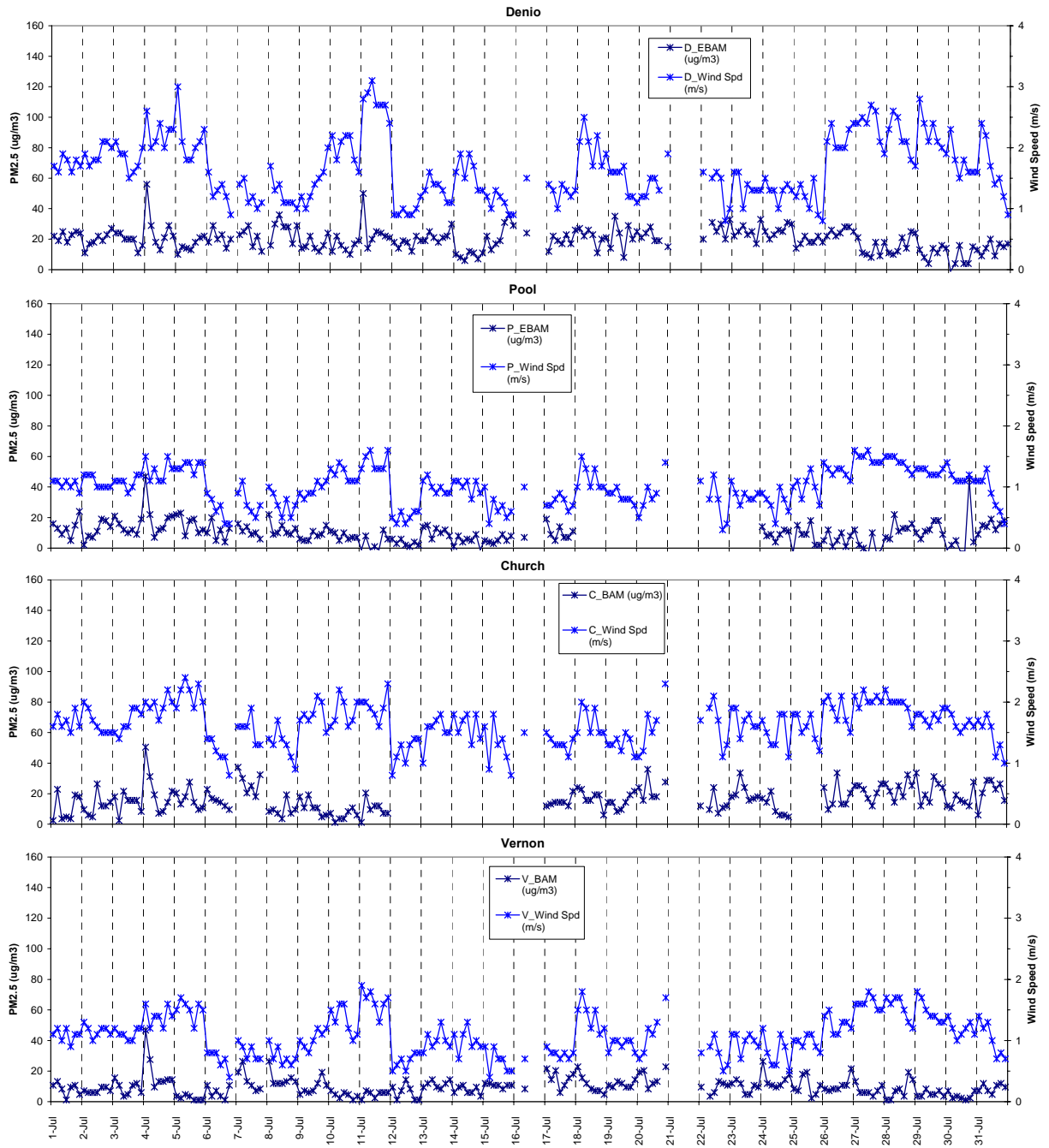


Figure 6. Hourly PM2.5 mass concentration and wind speed for July 2006.

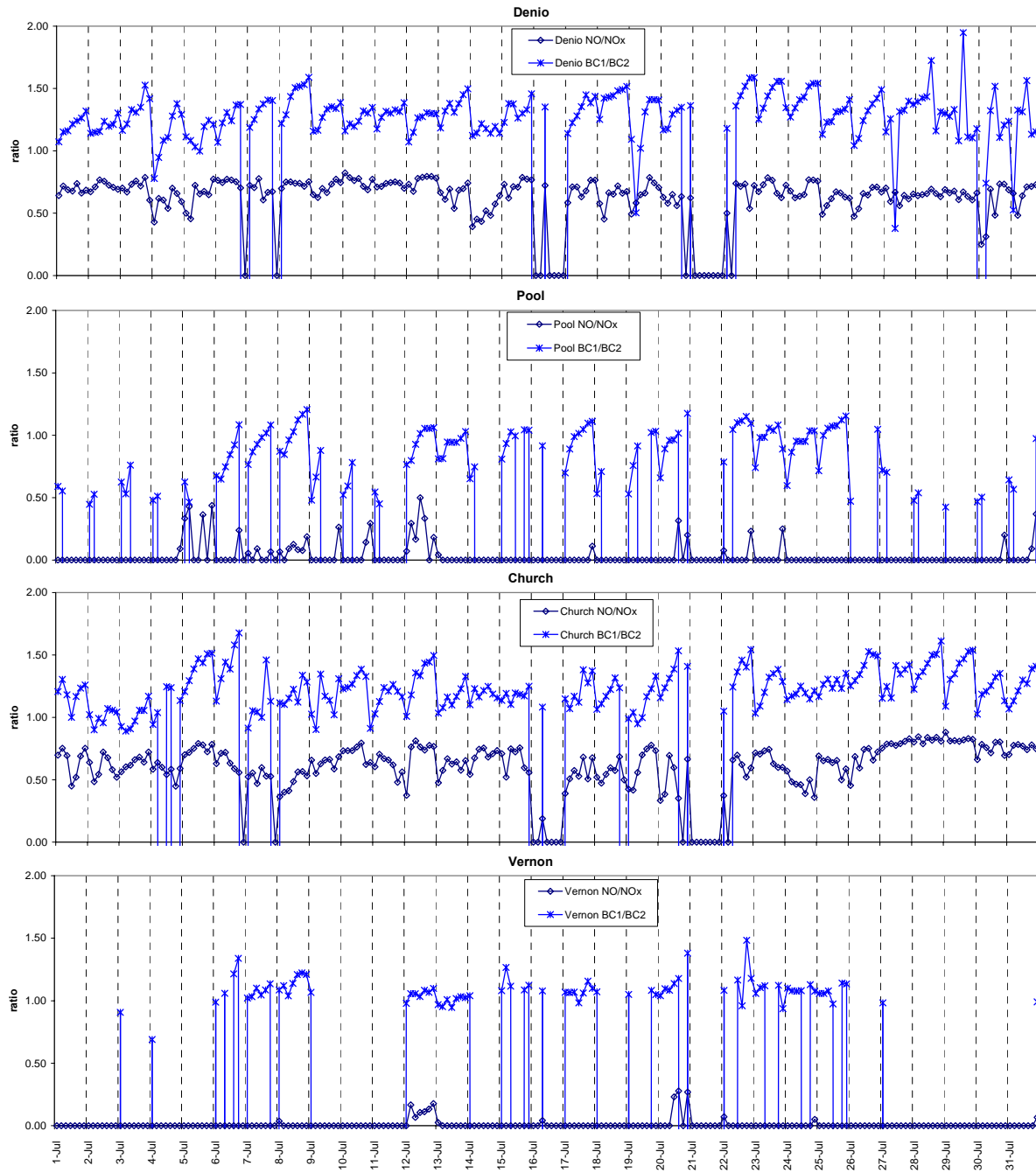


Figure 7. Hourly NO/NOx ratio and BC(1)/BC(2) ratio for July 2006.

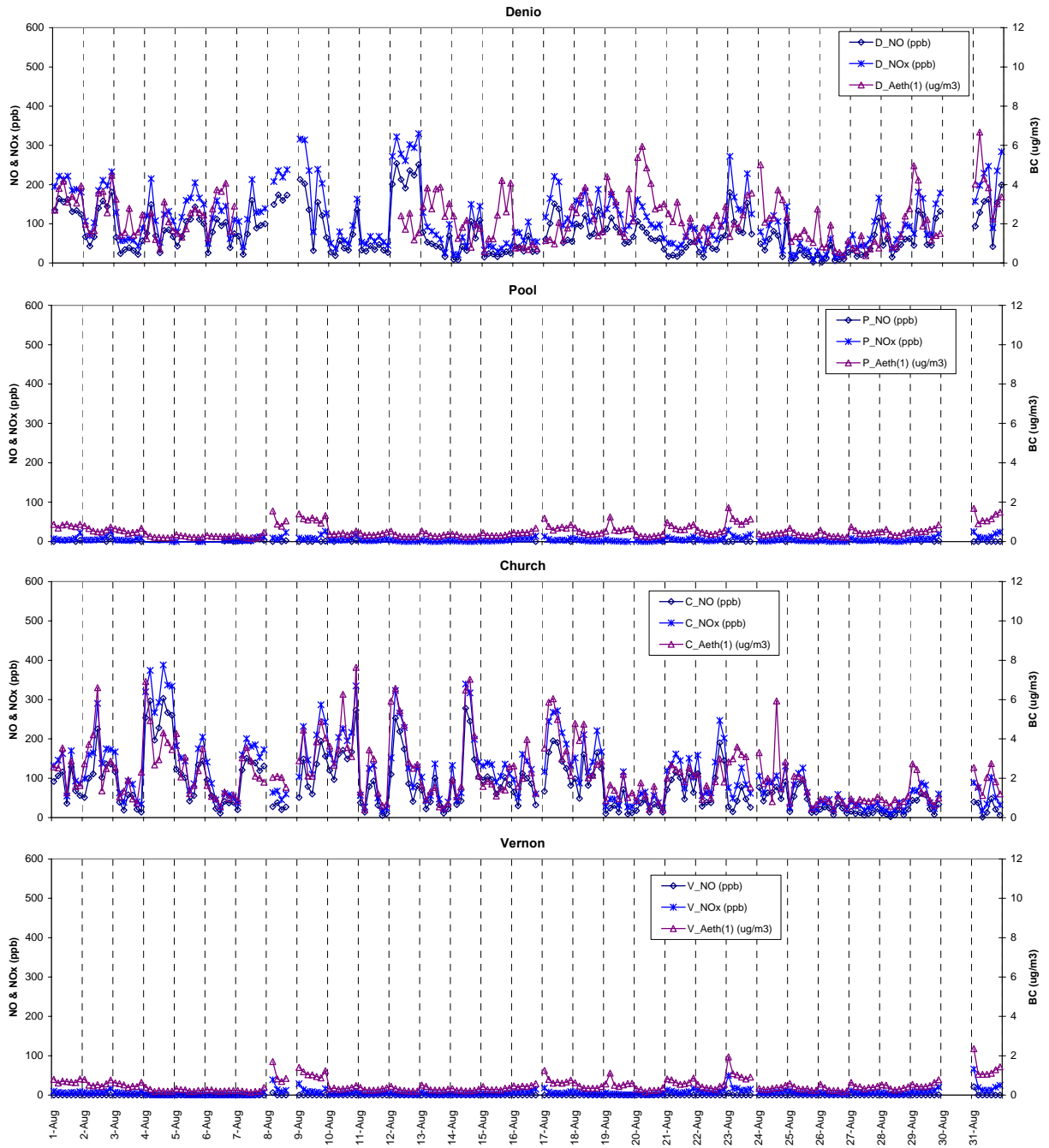


Figure 8. Hourly NO, NOx, and BC for August 2006

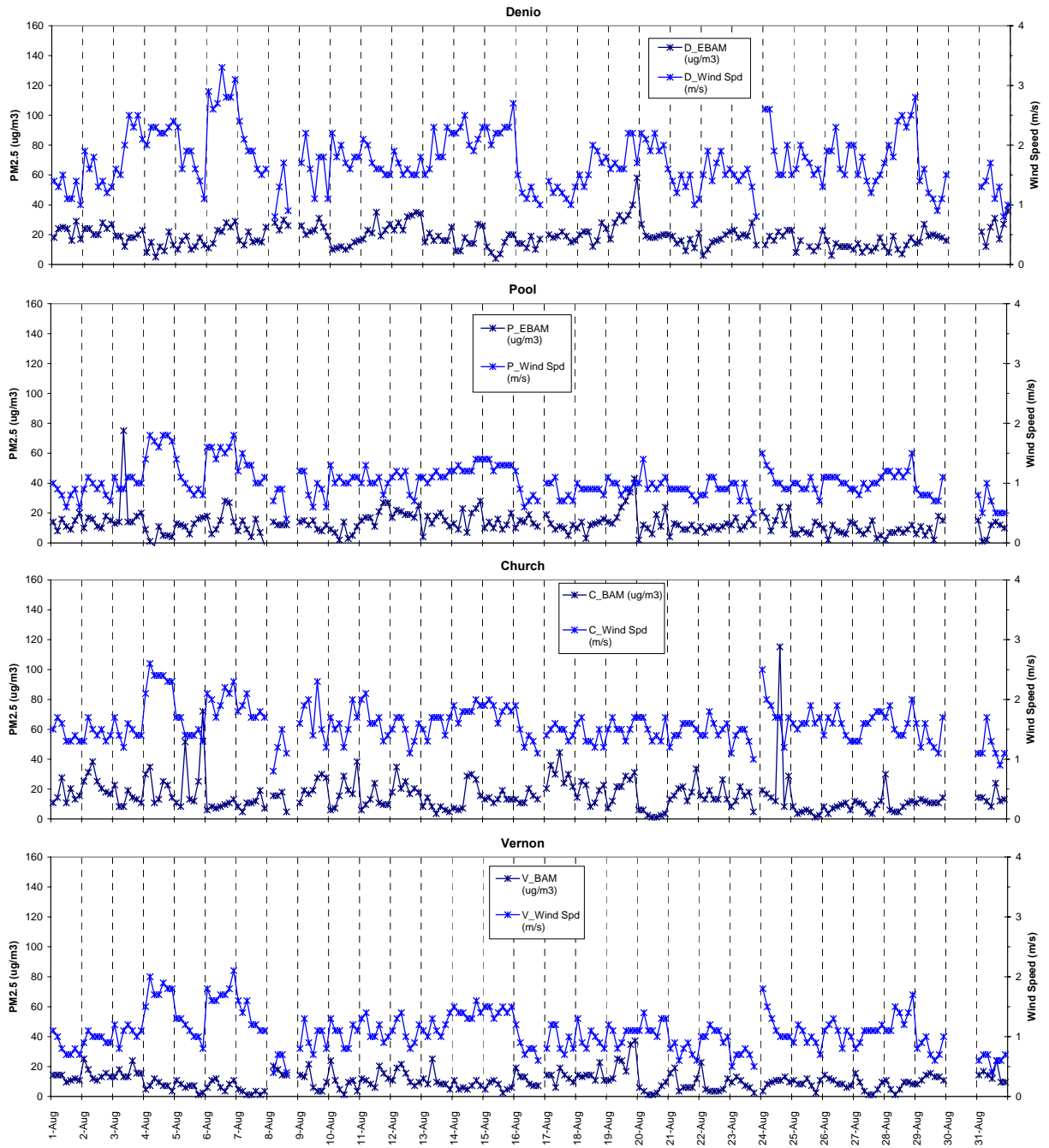


Figure 9. Hourly PM2.5 mass concentration and wind speed for August 2006.

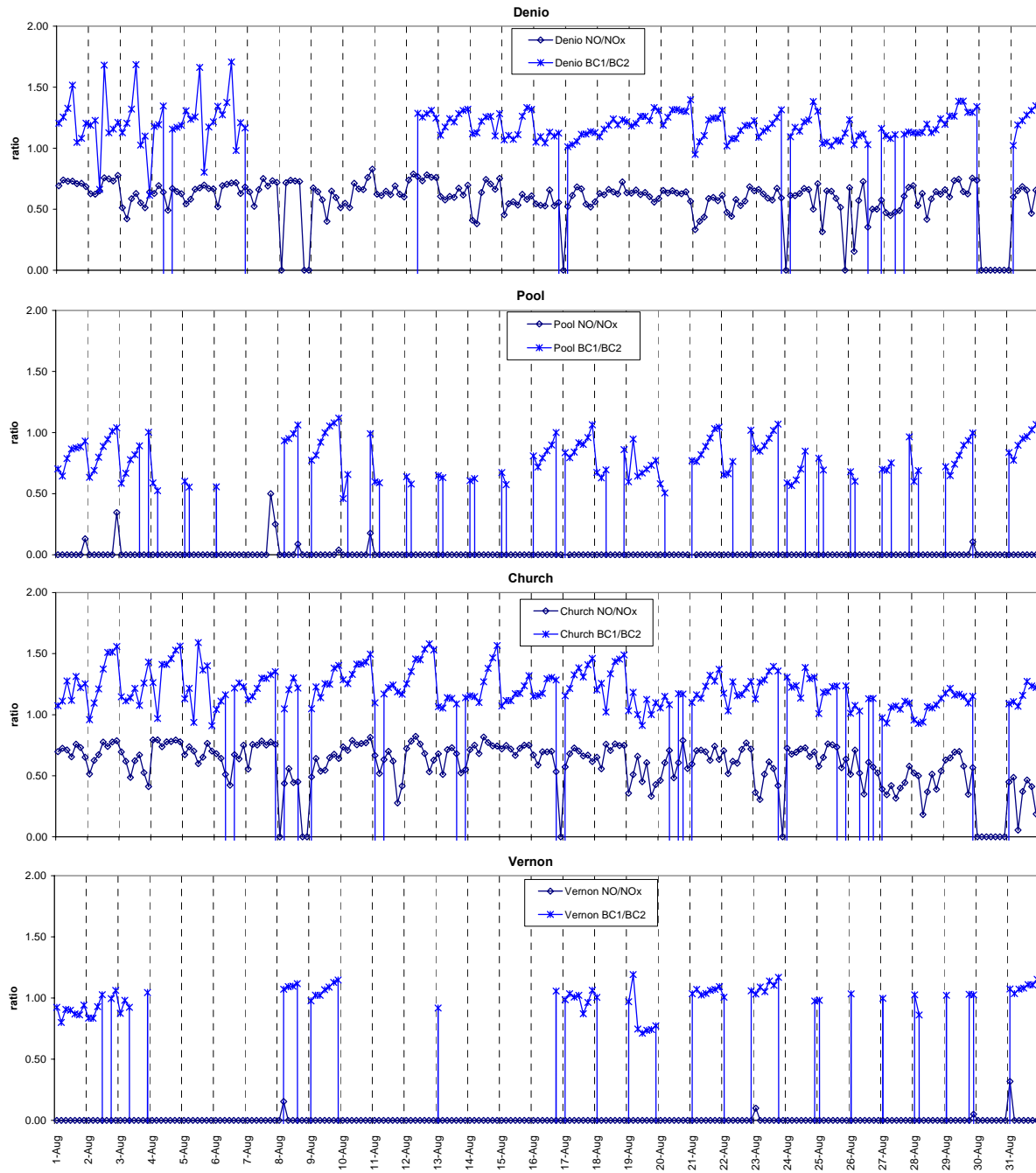


Figure 10. Hourly NO/NO_x ratio and BC(1)/BC(2) ratio for August 2006.

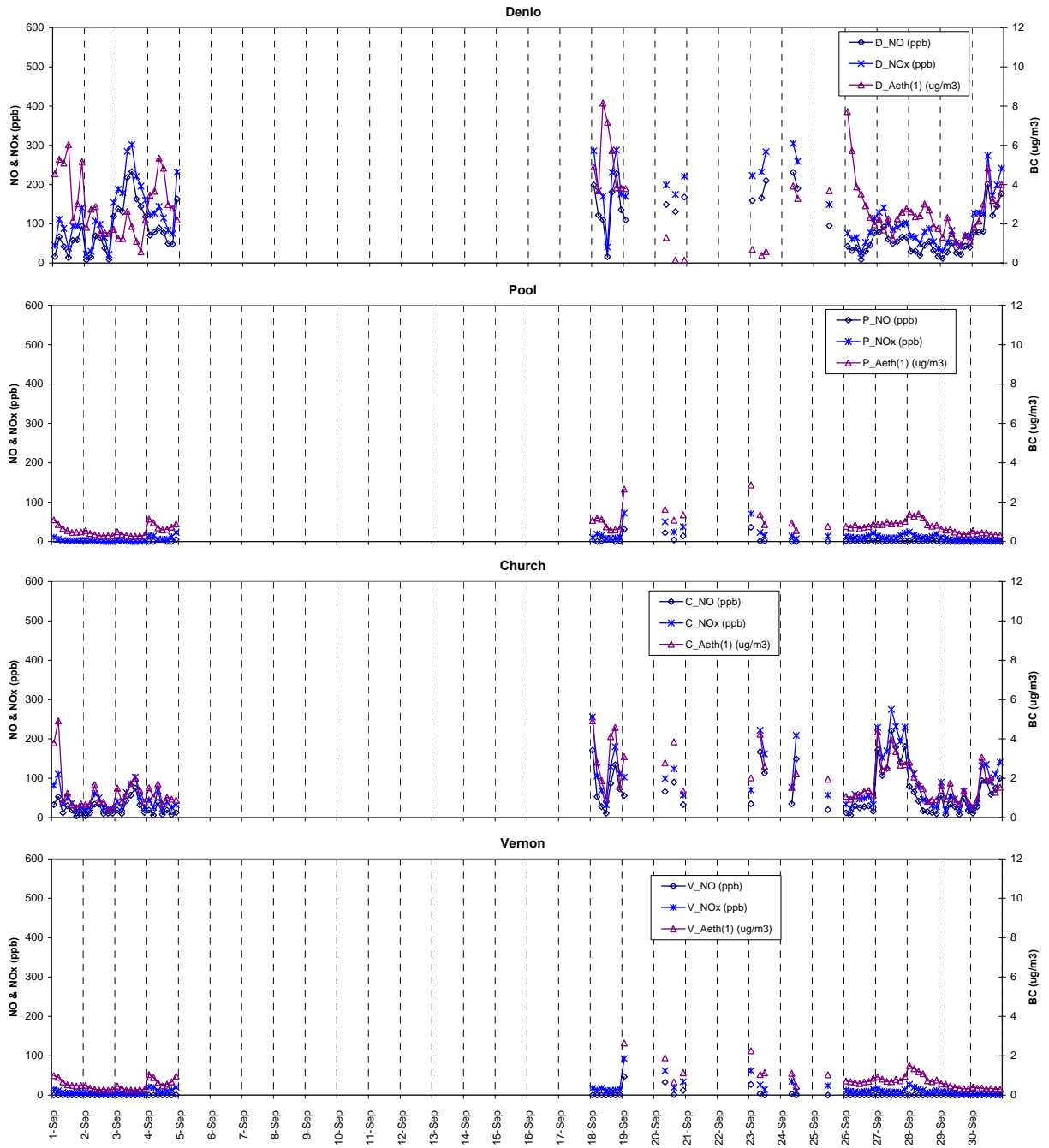


Figure 11. Hourly NO, NOx, and BC for September 2006

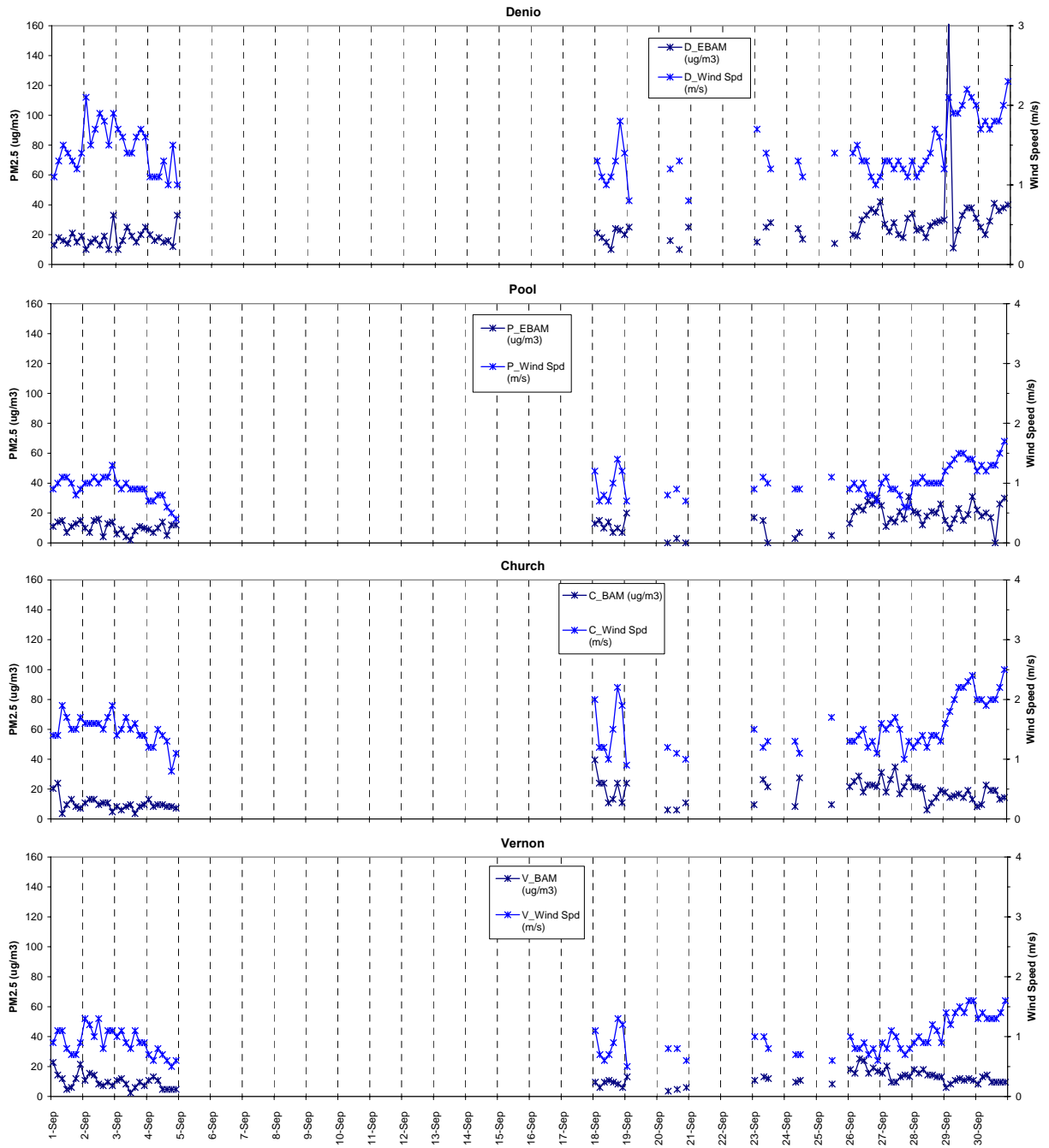


Figure 12. Hourly PM2.5 mass concentration and wind speed for September 2006.

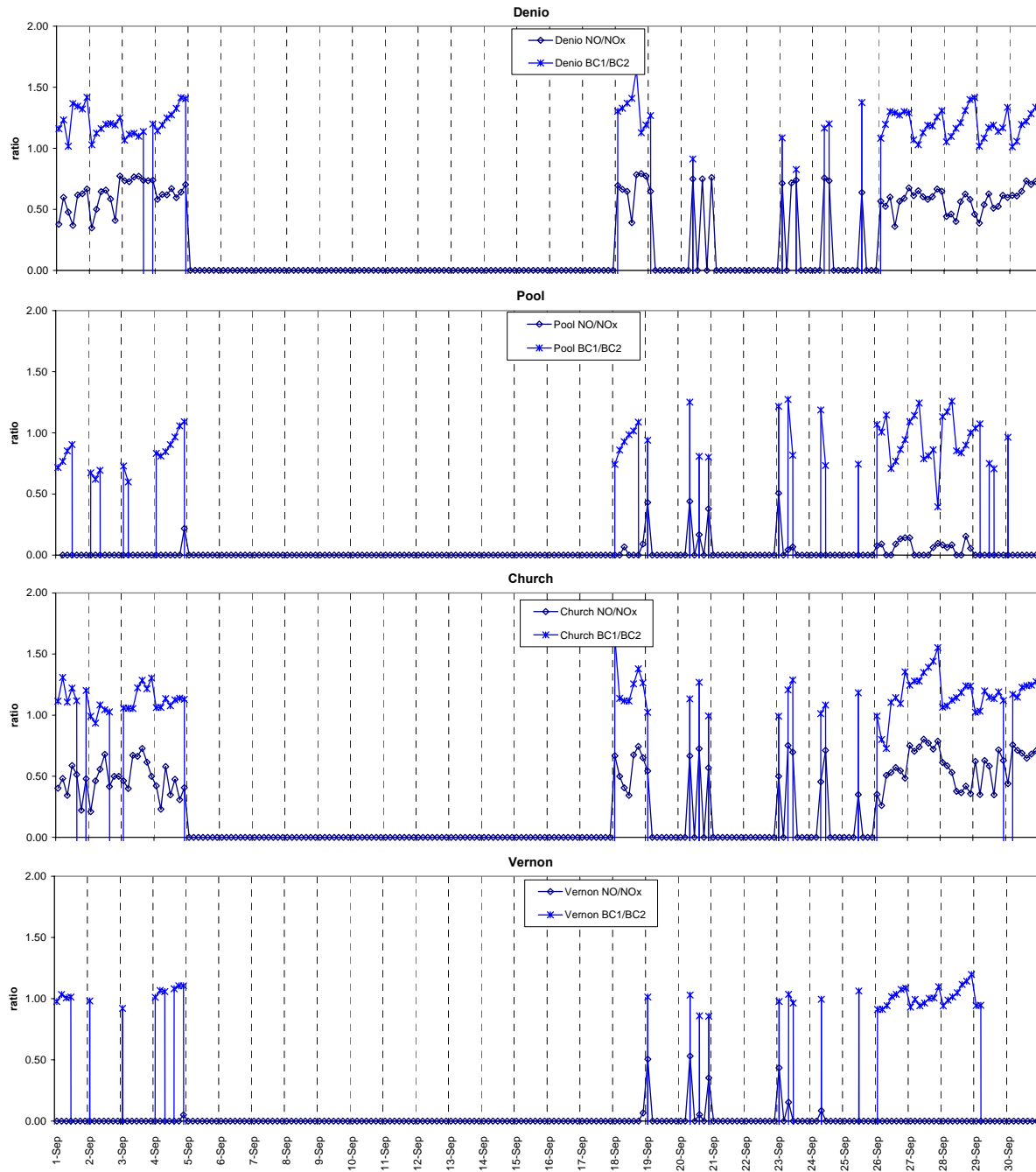


Figure 13. Hourly NO/NO_x ratio and BC(1)/BC(2) ratio for September 2006.

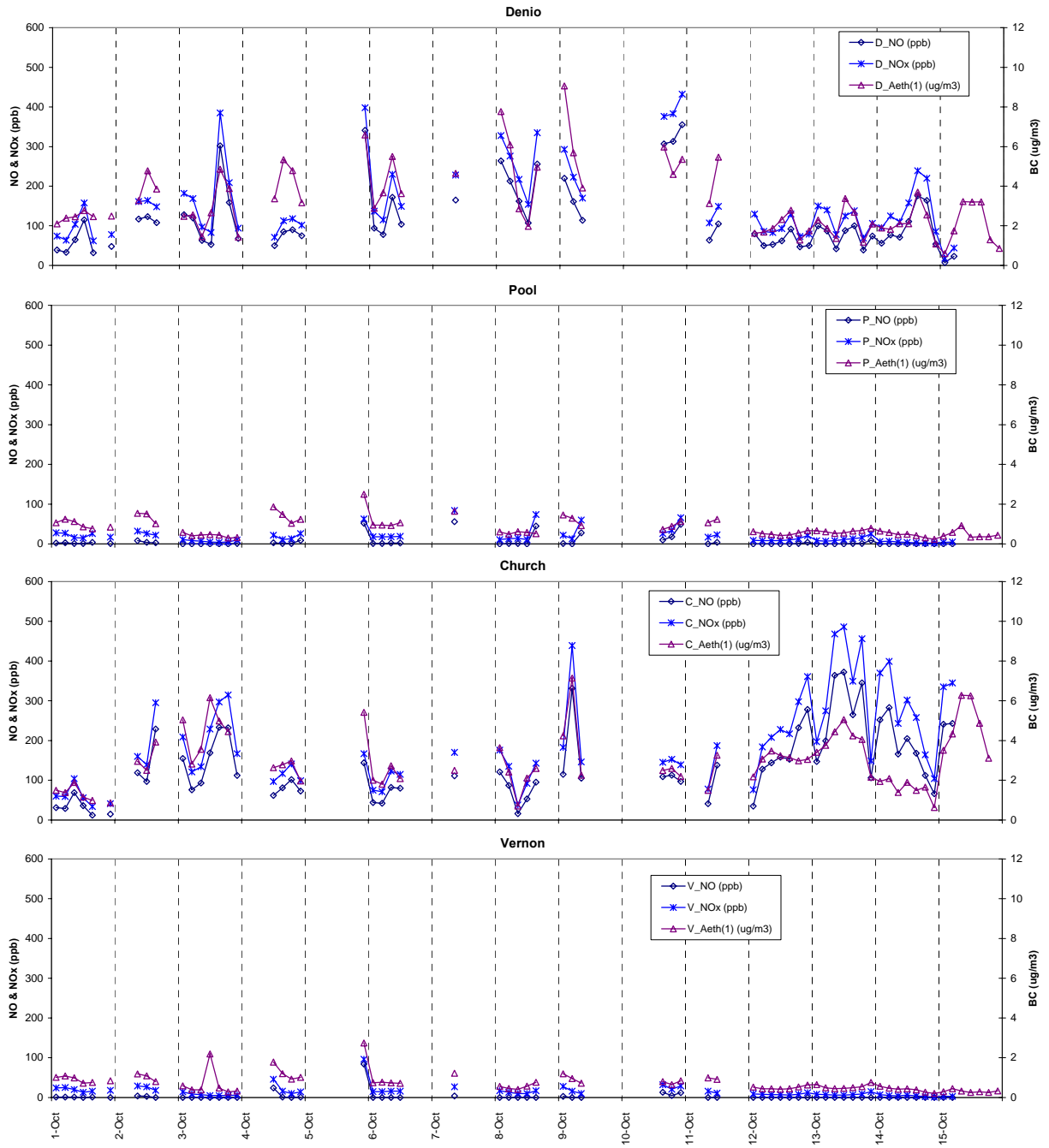


Figure 14. Hourly NO, NOx, and BC for October 2006

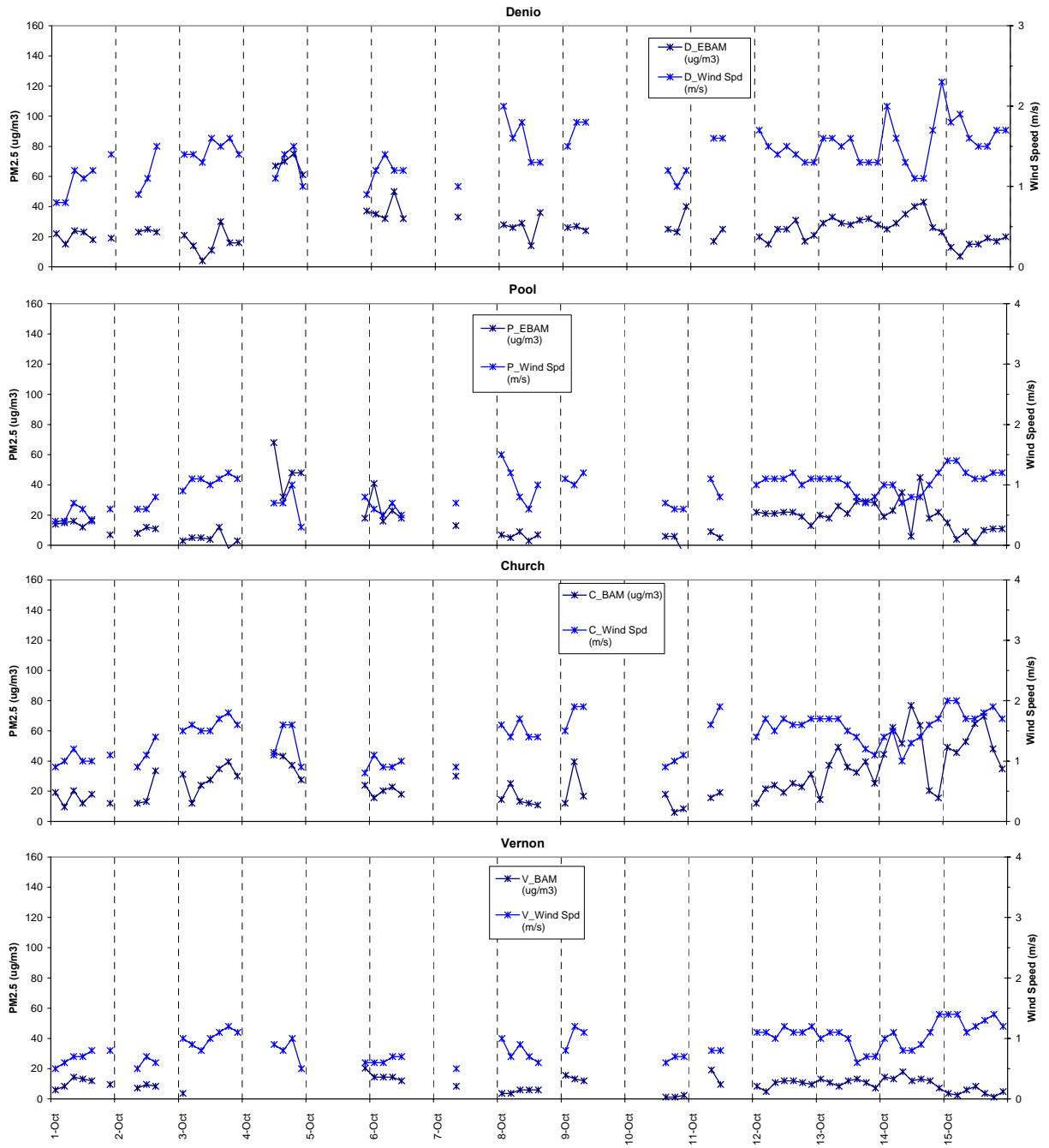


Figure 15. Hourly PM2.5 mass concentration and wind speed for October 2006.

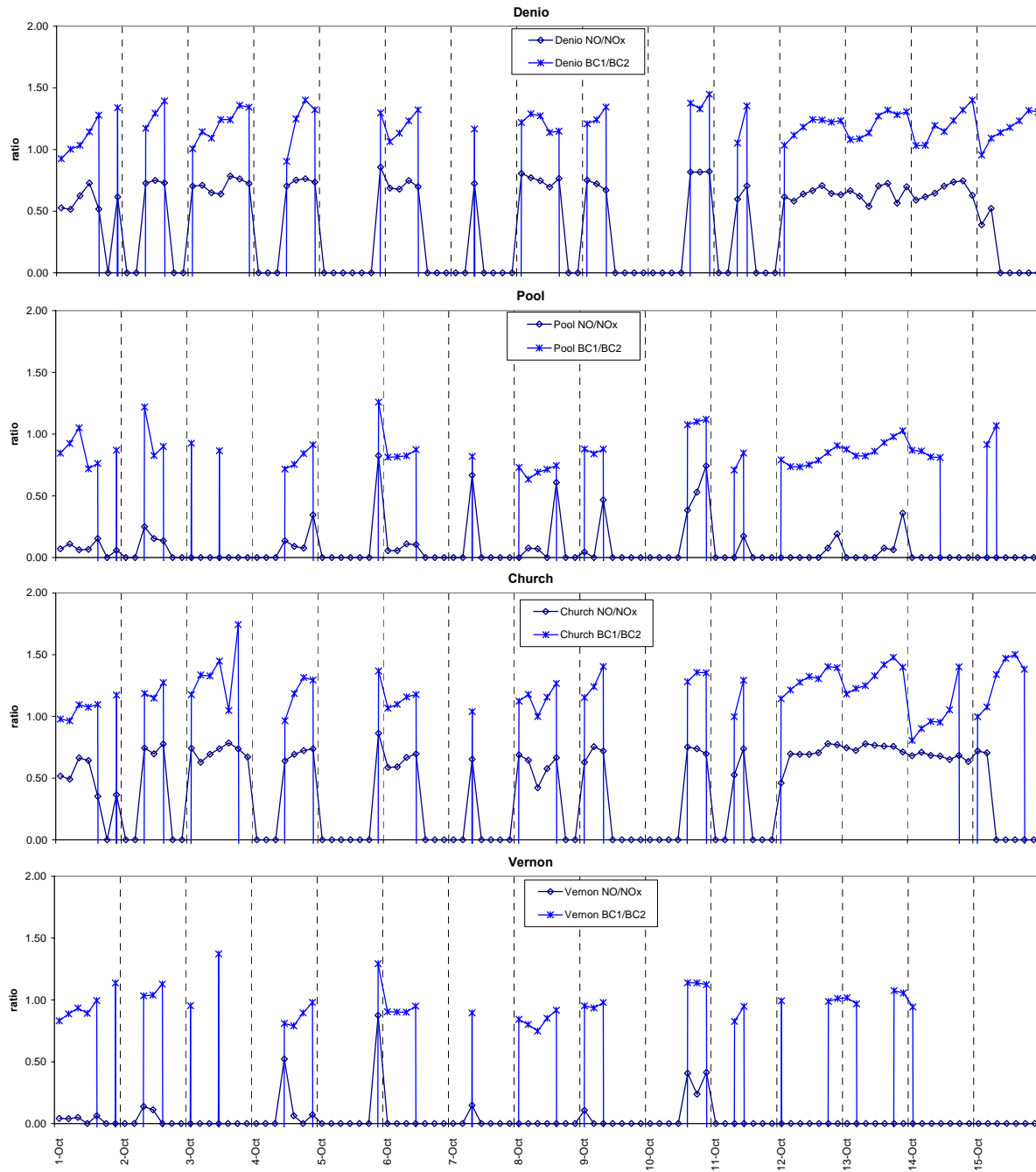


Figure 16. Hourly NO/NO_x ratio and BC(1)/BC(2) ratio for October 2006.

Attachment 2

**Elemental and Organic Composition of Ambient Aerosols
Collected at the Roseville Rail Yard in Summer 2005**

Final Report

Mass, elemental, and organic aerosols by size, time, and composition for the Roseville Railyard Aerosol Monitoring Project (RRAMP)

Prof. Thomas M. Cahill, P.I.^{1,2}, and Prof. Thomas A. Cahill^{3,4}, co-P.I.s, Nicholas J. Spada³,
Project Manager, Drs. David E. Barnes³, Steven S. Cliff³, and Prof. Kevin D. Perry^{3,5},
Staff Scientists, and Erin Fujii³, Student Research Assistant

¹Department of Integrated Natural Sciences, Arizona State University, Glendale, AZ,

²Department of Ecotoxicology, University of California, Davis, CA

³DELTA* Group, Depts. of Physics, Chemical Engineering/Materials Science, and
Applied Science, University of California, Davis, CA

⁴Breathe California of Sacramento/Emigrant Trails (EC/SET), Sacramento, CA, and

⁵Department of Meteorology, University of Utah, Salt Lake City, UT

- DELTA – Detection and Evaluation in Long-range Transport of Aerosols



October 1, 2007

Disclaimer

This report was prepared as an element of work sponsored by the United States Environmental Protection Agency (U.S. EPA) via grant funding managed by the Placer County Air Pollution Control District (District). Neither the U.S. EPA nor the District thereof, nor any of their employees, make any warranty, expressed or implied, as to the accuracy, reliability or completeness of the data presented in this report that was collected independently of the District's Roseville Rail Yard Air Monitoring Project (RRAMP). The views and opinions expressed in the report are solely those of the authors and do not represent an endorsement by the District, members of the RRAMP Technical Advisory Committee, the United States Government, or any agency thereof.

Table of Contents:

	<u>Page</u>	
List of Tables	3	
List of Figures	4	
Abstract	6	
Executive Summary	7	
A. Introduction and RRAMP monitoring data	10	
B. Mass and Elemental analysis of aerosols at the Denio and Pool sites	17	
1. Sampling		
a. Sampling equipment		
b. Sample duration and sites		
c. Quality assurance (see also Appendices)		
2. Results		
C. Organic sampling and analysis of aerosols at the Denio site	48	
1. Methods		
2. Sample Analysis		
3. Results for Organic Constituents		
a. PAHs	52	
b. Alkanes	56	
c. Organic acids	60	
d. Sugars and other polyols	62	
D. Comparison of Rail Yard Data to On-Road vehicles		
1. Diesel trucks	68	
2. Automobile dominated secondary streets	72	
E. Conclusions	82	
References	83	
Acknowledgements	84	
Appendix QA	Quality Assurance Summary	85
Appendix B	Delta Group DRUM Publications	91
Full DRUM Quality Assurance Protocols ver 1/05 (2005)	(Separately Appended)	

List of Tables:

		<u>page</u>
Table 1	Regional meteorology during the study	11
Table 2	Placer County pollutant emissions for the 8 largest contributors to NO _x	16
Table 3	Sampling schedule and mean RRAMP monitoring data for the four time periods utilized	17
Table 4a, 4b	Denio site versus Pool site comparisons in parallel with DELTA Group sampling periods.	18
Table 5	S-XRF comparison, all blind tests since 1999	22
Table 6	Average recovery (%) of isotopically labeled compounds to all the samples and blanks	52
Table 7	Concentrations (pg/m ³) of particulate PAHs observed at the Roseville Rail Yard in the Summer of 2005	53
Table 8	Concentrations (ng/m ³) of particulate <i>n</i> -alkanes observed at the Roseville Rail Yard in the summer of 2005.	56
Table 9	Concentrations (ng/m ³) of particulate <i>n</i> -alkanes observed at the Roseville Rail Yard in the summer of 2005.	61
Table 10	Concentrations (ng/m ³) of particulate sugars observed at the Roseville Rail Yard in the summer of 2005.	63
Table 11	Comparison of RRAMP benzo{a}pyrene results to literature values for diesel trucks	70

List of Figures:		page
Figure 1	The Davis Union Pacific Rail Road Roseville Railyard.	10
Figure 2 a, b, and c	Data on nitric oxide (NO), July – October, 2005	13
Figure 3 a, b, and c	Data on “black carbon” (BC) for July - October, 2005	14
Figure 4 a, b, and c	Data on PM _{2.5} mass, July – October, 2005	15
Figure 5	Nick Spada and David Barnes at the Denio site, Sept. 27, 2005.	20
Figure 6	Precision test for mass	21
Figure 7	Mass from 10.0 to 0.75 µm	23
Figure 8	Mass from 0.75 to 0.09 µm	23
Figure 9	Three components of fine mass versus time	24
Figure 10	Comparison of the Pool and Denio sites for very fine mass	24
Figure 11	Nighttime (9 PM – 6 AM) mass size profiles for early August at the Denio site.	25
Figure 12	Size mode of aerosol mass, July 15, versus other recent diesel studies	26
Figure 13	Typical elemental signatures of diesel, Denio site very fine mode	27
Figure 14	Zielenska et al 2004 diesel characterization results	27
Figure 15	Transition mode elements nickel, copper, and zinc in the Denio site very fine mode.	28
Figure 16	Crustal elements in the very fine mode, Denio site	28
Figure 17	Mass versus typically diesel signature elements, Denio site	29
Figure 18	Comparison of very fine sulfur, Denio Site vs Pool Site	30
Figure 19	Comparison of very fine phosphorus, Denio Site vs Pool Site	31
Figure 20	Comparison of very fine zinc, Denio Site vs Pool Site	31
Figure 21	Comparison of very fine calcium, Denio Site vs Pool Site	32
Figure 22	Comparison of very fine copper, Denio Site vs Pool Site	33
Figure 23	Comparison of very fine nickel, Denio Site vs Pool Site	33
Figure 24	Comparison of very fine potassium, Denio Site vs Pool Site	34
Figure 25	Comparison of very fine vanadium, Denio Site vs Pool Site	34
Figure 26	Comparison of very fine chromium, Denio Site vs Pool Site	35
Figure 27	Sea salt signature in coarse particle fluorine.	36
Figure 28	HYSPLIT trajectory showing Bay Area transport, July 22, 2005	37
Figure 29	Sub-micron Fine sulfur at the Denio site	38
Figure 30	Components of fine sulfur at the Denio site	38
Figure 31	Sub-micron sulfur versus fine iron at the Denio site	39
Figure 32	Size distribution of sulfur and soils, daytime, July 18, 2006	39
Figure 33	Time plots of coarse and fine silicon, Denio site	40
Figure 34	Size distribution of sulfur and soils, nighttime, July 18, 2006	41
Figure 35	Time plots of coarse and fine potassium, Denio site	42
Figure 36	2.5 to 1.15 µm vanadium and chromium, summer, 2005	43
Figure 37	Time plots of sub-microns zinc, summer, 2005	43
Figure 38	HYSPLIT Wind trajectories at the beginning of the zinc episode, on the morning of July 27. The typical night time cross-rail yard winds were weak and of short duration. during this episode.	44
Figure 39	Comparison of very fine copper and zinc at the Pool and Denio sites. Most of the largest metal spikes occur at the Denio site.	45
Figure 40	Size Distribution of elements on July 18, 2006, during night time cross rail yard winds	46

Figure 41	Size Distribution of elements on July 18, 2006, during day time winds from the southwest roughly parallel to the rail yard.	47
Figure 42	Coronene and pyrene concentrations (pg/m^3) in the different size fractions of the 8-stage DRUM sampler and the afterfilter.	53
Figure 43	Profiles of PAHs as a function of molecular mass from the Roseville rail yard and the literature.	55
Figure 44	A selected ion chromatogram of m/z 57 showing the undifferentiated hydrocarbon “envelope”. The n -alkanes are labeled by their carbon number.	58
Figure 45	Concentrations of undifferentiated hydrocarbons in different size fractions of the 8-stage DRUM sampler.	59
Figure 46	The fraction of n -alkanes collected on the after filter of the 8-stage DRUM.	60
Figure 47	Concentration of octadecanoic, hexadecanoic and 9-octadecenoic (oleic) acid as a function of particle size.	62
Figure 48	Sucrose and glucose concentrations (ng/m^3) as a function of aerosol size.	64
Figure 49	Fraction of the identified organic mass belonging to the four different classes of chemicals identified.	65
Figure 50	Mass of aerosols as determined by beta gauge and by the sum of The elements and oxides as determined by S-XRF.	66
Figure 51	Composition of aerosol mass as determined by beta-gauge.	67
Figure 52	Meteorology during the winter sampling, 2006	72
Figure 53	Photograph of winter drum strips, Watt Ave at Florin versus Denio site	73
Figure 54	Coarse and fine mass at Watt and Arden versus the Denio site, winter, 2006	74
Figure 55	Photographs of winter DRUM strips, Watt/Arden, 2004, vs Watt/Arden and Denio, 2006	75
Figure 56	Chlorine aerosols (sea salt) at Watt/Arden and Denio, winter, 2006	76
Figure 57	Iron aerosols (soil) at Watt/Arden vs Denio, winter, 2006	76
Figure 58	Sulfur aerosols (soil) at Watt/Arden vs Denio, winter, 2006	77
Figure 59	Vanadium aerosols (heavy fuel oil) at Watt/Arden vs Denio, winter, 2006	78
Figure 60	Coarse potassium aerosols (soil) at Watt/Arden vs Denio, winter, 2006	78
Figure 61 a,b	Accumulation mode potassium aerosols (wood smoke) and very fine potassium aerosols (vehicular) at Watt/Arden vs Denio, winter 2006	79
Figure 62	Very fine mode phosphorus and zinc aerosols (vehicular, Lubricating oil) at Watt/Arden vs Denio, winter 2006	80
Figure 63	Very fine mode Ni, Cu, and Zn zinc aerosols at Watt/Arden vs Denio 2006	81

Abstract:

Particulate samples were collected on both sides of the Roseville Rail Yard to assess the particulate emissions from the site. The particulate results, combined with the gaseous data collected by RRAMP, show different sources of particulate matter. The first source of aerosols are the emissions from diesel locomotives that give very fine aerosols that are rich in sulfur and polycyclic aromatic hydrocarbons (PAHs).

The second source of particulate matter is the relatively coarse re-suspended dust with relatively high concentrations of certain metals, such as copper and zinc, and heavy hydrocarbons typical of greases and tars.

The last major source of aerosols contains sugars, and sucrose in particular, typically biogenic aerosols but some of which we believe originated from the local farmer's market.

The most significant result from this study was that the rail yard diesel aerosols had higher relative concentrations of the heavier, and more toxic/carcinogenic PAHs such as benzo{a}pyrene, than diesel truck emissions, and a higher fraction of PAHs per unit mass or black carbon, than diesel truck emissions. The relative amount of benzo{a}pyrene in these aerosols was calculated using 11 separate comparisons to literature values on both a very fine/ultra fine mass and a black carbon (BC) basis. Weighting the results by errors yields a value 5.5 ± 0.7 , Denio site benzo{a}pyrene versus diesel truck data.

Executive Summary:

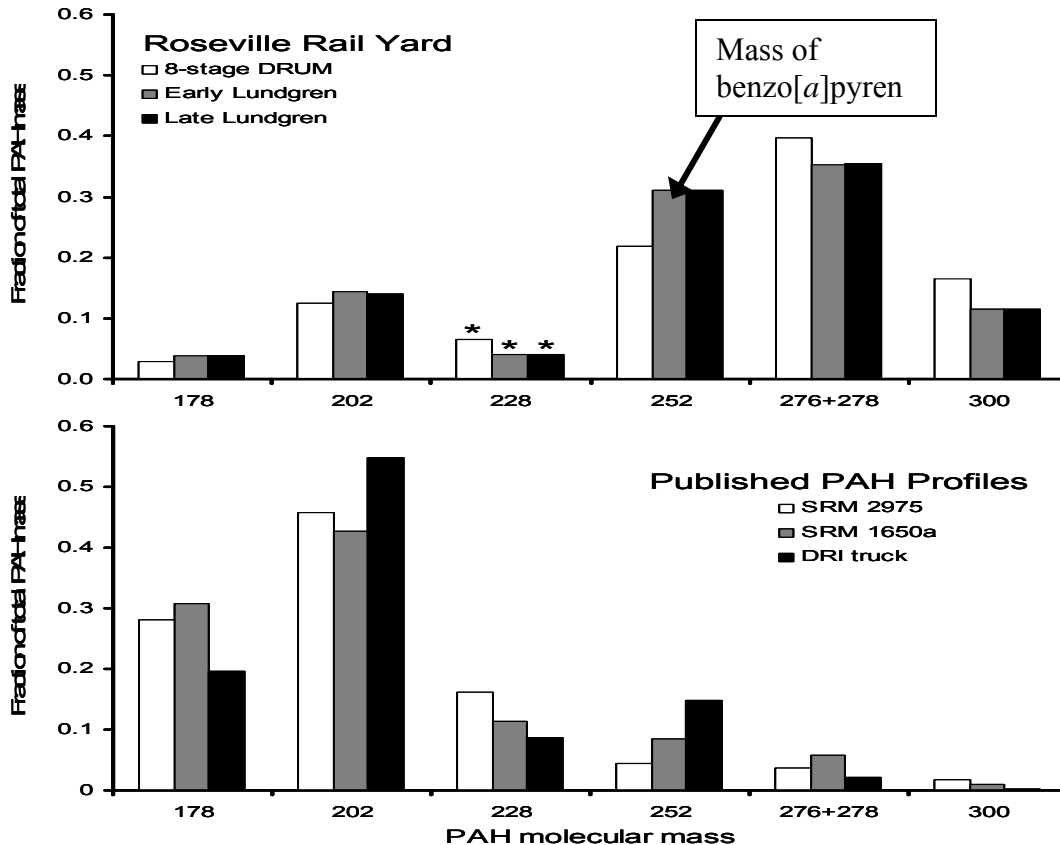
The research programs based at the Union Pacific Rail Road's Davis Roseville rail yard from 2005 through 2007 include the formal multi-agency Roseville Railyard Aerosol Monitoring Program (RRAMP) as well as additional studies, including a contribution from Breathe California of Sacramento-Emigrant Trails (BC/SET) and the Placer County based EPA Region IX enhancement for aerosol elemental and organic components. This report addresses only the latter study, but fuller appreciation and context must include all relevant studies as well as prior and current meteorological and air monitoring data in the region as well as the ARB's impact analysis of 2004.

The UC Davis DELTA Group and Breathe California of Sacramento-Emigrant Trails (BC/SET) collaborated with the RRAMP project to assist BC/SET ongoing studies of aerosol sources and transport in general and diesel exhaust in particular. The RRAMP program was ideal for this purpose, with an upwind-downwind measurement protocol across the Roseville rail yard and numerous pollutant measurements. The DELTA Group contributions included mass by soft beta rays every 3 hours for 5 weeks (8 size modes Denio site, the very fine mode, $0.26 > D_p > 0.09 \mu\text{m}$, Pool Site) and very fine elemental concentrations by synchrotron-induced x-ray fluorescence (S-XRF) every 3 hours (Denio and Pool site) for the period July 12 through August 17. Samples were also taken suitable for later organic analysis at the Denio site from August 5 through October 17, and archived in a freezer. Finally, there was a short winter study in February, 2006.

The results of this early effort lead to a proposal and funding to analyze the remainder of the DRUM stages for the coarser elements, 10.0 to $0.26 \mu\text{m}$. July 12 through August 17, and analyze the organic samples for PAHs, *n*-alkanes, sugars, and fatty acids by GC/MS (Gas Chromatography/Mass Spectrometry). Data from the prior BC/SET studies are included only in so far as to complete the data sets, particularly the very fine elemental data from the Pool and Denio sites.

The key findings are:

1. The key assumptions behind the RRAMP project are sound, with several characteristic diesel species having large rail yard versus background ratios; NO at 22.1-fold background, NO₂ at 7.2-fold, very fine mass and very fine sulfur at 4-fold, black carbon at 2.3-fold, and a number of anthropogenic metals ranging from 1.6 to 2.8-fold.
2. The size of the diesel exhaust peaks in mass (and sulfur, below) at about $0.3 \mu\text{m}$, is roughly 3 times that of a diesel truck under load but similar to size distributions of idling diesel engines. However, the PAHs (pyrene to coronene) peak below $0.1 \mu\text{m}$.



6. PAH (benzo{a}pyrene) emissions were estimated via ratios, rail yard versus diesel trucks, using either very fine/ultra fine mass (vf/uf) mass or elemental or black carbon (BC), Denio and Pool site, for the DELTA 8 DRUM in summer, and two Lundgren impactors in fall. This generated 15 different ratios based on the method used. There was about 7.5 ± 4.0 times more benzo{a}pyrene from the railyard aerosols than from diesel truck aerosols, per unit very fine/ultra fine mass, comparing the DRI laboratory (Zielenska et al, 2004) data to three different estimates of the rail yard vf/uf mass data. The ratio was also be formed versus unit elemental carbon, by comparing our PAH data with literature emission rates of benzo-a-pyrene derived from both laboratory studies (Zielenska et al, 2004) and on-roadway tunnel studies (Gertler et al, 2002); 6.5 ± 2.0 . However, we conclude that the Denio – Pool difference in EC is not a good match to the Denio-only PAHs. Removing these data, and weighting the remaining averages by errors, we derive a ratio, benzo{a}pyrene rail yard/literature diesel truck, of 5.5 ± 0.7 .

7. About half of the identified $PM_{2.5}$ organic mass was in largely biogenic sugars and fatty acids while the other half mainly consisted of petroleum based *n*-alkanes. PAHs represented only a few percent of the identified organic mass.

8. The winter very fine particle mass at the Denio site, $6.6 \mu\text{g}/\text{m}^3$, $0.34 > D_p > 0.09 \mu\text{m}$, was about three times higher than the summer mass at the Denio site, $2.25 \mu\text{g}/\text{m}^3$. This gives a slightly higher summer-fall ratio, 2.0, than we derived from the BC ratio, 1.5, which was used for the summer-fall scaling, making the summer DRUM/fall Lundgren comparisons even closer.

A. Introduction and RRAMP monitoring data

The Davis Railyard of Union Pacific Railroad (UPRR) in Roseville, California, hosts typically 31,000 trains/years for maintenance, repair, and testing, and re-routing, while an additional 16,000 trains/year pass through the yard without stopping. The pollutants emitted by the rail yard are significant components of the gas and aerosol inventory for the region. Through a joint agreement between UPRR and the California Air Resources Board (ARB), Placer and Sacramento Counties APCDs, and the US EPA, Region IX, a multi-year plan is in place for reduction of pollutants and measuring the improvement through the Roseville Railyard Aerosol Monitoring Project (RRAMP).

The RRAMP program is based upon a robust air monitoring program upwind and downwind of the rail yard during summer periods when the winds are especially regular and predictable. This program also includes collaborative programs of Breathe California of Sacramento-Emigrant Trails and specific purpose grants, including the present one from EPA Region IX that funded additional aerosol elemental and organic measurements.



Figure 1 The Davis Union Pacific Rail Road Roseville Railyard.

The sites used for the present program are marked, the “Pool Site”, upwind in summer nights, and the “Denio Site”, downwind in summer nights (Figure 1). Two other sites also are being used in the program. The stability of the metrology during the period was typical of summer conditions near Sacramento.

Table 1 Regional meteorology during the study.

July	2005	Mather AFB weather														Direction		
		Temp		F		RH		%		Press		Visibility		Wind	mph		Precip	160 night
		Max	Avg	Min	Max	Avg	Min	Avg	Max	Avg	Min	Max	Avg					
8	Friday	87	72	57	83	59	35	29.92	10	10	10	14	8	-	0.00	SSW		
9	Saturday	84	73	62	88	65	35	29.91	10	10	10	15	10	18	0.00	SSW		
10	Sunday	80	68	57	94	76	37	29.93	10	10	10	9	7	-	0.00	SSE		
11		96	78	60	94	60	23	29.91	10	10	10	12	1	-	0.00	WSW		
12		102	82	62	83	48	18	29.89	10	10	10	9	4	-	0.00	WSW		
13		104	86	68	78	40	20	29.85	10	10	10	12	5	-	0.00	SW		
14		105	87	69	64	42	20	29.82	10	10	10	10	7	-	0.00	SSW		
15	Friday	105	87	69	69	40	18	29.77	10	10	10	10	6	-	0.00	SW		
16	Saturday	107	88	68	60	38	12	29.77	10	10	10	12	6	-	0.00	S		
17	Sunday	105	86	66	68	40	20	29.77	10	10	10	10	3	-	0.00	SSW		
18		98	82	66	68	46	27	29.76	10	10	10	12	5	-	0.00	SSW		
19		98	80	62	82	53	25	29.76	10	10	10	9	8	-	0.00	SSW		
20		102	81	60	77	42	15	29.8	10	10	10	9	7	-	0.00	SW		
21		87	78	64	73	44	21	29.84	10	10	10	17	9	21	0.00	SSW		
22	Friday	95	77	59	82	50	14	29.9	10	10	10	13	8	16	0.00	SSW		
23	Saturday	104	80	57	94	43	7	29.89	10	10	10	10	4	-	0.00	SSW		
24	Sunday	102	83	64	64	38	15	29.86	10	10	10	15	1	-	0.00	S		
25		100	80	59	82	43	11	29.85	10	10	10	12	6	-	0.00	SSW		
26		102	83	64	73	43	17	29.83	10	10	10	12	3	-	0.00	S		
27		100	81	62	72	43	14	29.86	10	10	10	12	7	-	0.00	SSW		
28		98	78	59	77	47	13	29.84	10	10	10	12	6	-	0.00	SSW		
29	Friday	96	79	62	68	43	22	29.87	10	10	10	12	7	-	0.00	SSW		
30	Saturday	100	81	62	72	47	21	29.94	10	10	10	13	6	-	0.00	SSW		
31	Sunday	100	81	62	68	42	11	29.92	10	10	10	9	4	-	0.00	SSW		
1		102	80	59	82	40	9	29.89	10	10	10	14	6	-	0.00	SSW		
2		96	78	59	67	40	12	29.87	10	10	10	9	6	-	0.00	SSW		
3		98	78	59	82	46	16	29.87	10	10	10	12	6	-	0.00	WSW		
4		100	80	60	77	45	18	29.93	10	10	10	9	7	-	0.00	SW		
5	Friday	102	83	64	68	40	15	29.93	10	10	10	12	5	-	0.00	SW		
6	Saturday	105	84	64	68	36	9	29.89	10	10	10	10	5	-	0.00	SSW		
7	Sunday	102	83	64	68	41	13	29.83	10	10	10	10	6	-	0.00	S		
8		96	79	62	72	44	22	29.83	10	10	10	9	5	-	0.00	SSW		
9		100	81	62	77	49	17	29.87	10	10	10	9	6	-	0.00	SSW		
10		96	78	60	77	50	22	29.9	10	10	10	9	3	-	0.00	SSW		
11		98	78	59	77	43	13	29.89	10	10	10	12	6	-	0.00	SSW		
12	Friday	100	81	62	68	43	18	29.79	10	10	10	15	5	-	0.00	SSW		
13	Saturday	86	70	53	94	63	33	29.8	10	10	10	12	5	-	0.00	S		
14	Sunday	87	71	55	94	66	35	29.81	20	11	10	12	6	-	0.00	S		
15		84	70	55	94	60	37	29.89	10	10	10	14	6	18	0.00	SSW		
16		95	80	66	73	48	23	29.94	10	10	10	10	3	-	0.00	W		
17		95	77	59	82	44	19	29.83	20	11	10	14	6	-	0.00	SSW		
18		84	68	53	100	67	27	29.83	10	10	8	14	8	20	0.00	SSW		
19	Friday	87	72	57	94	62	16	29.89	10	10	10	9	8	-	0.00	SSW		
	Saturday																	
	Sunday																	

Generally, the regional weather (Table 1, based on Mather airfield) showed wind direction roughly 160° at night, and roughly 270° during the day, with small variations. This pattern, confirmed by on-site meteorology, makes the Denio site downwind each night for about 8 hr every night from the Pool site direction.

Because of the orientation of the rail yard, daytime summer winds blew roughly parallel to the tracks, so that small variations could make either the Pool site or the Denio site downwind of the rail yard. However, wind velocities were generally higher and inversions weaker in daytime than at night, both of which would dilute rail yard influences. Further, yard operations are very different southwest of the Pool and Denio sites, and the distance from the yard operations to either of the potential receptor sites was greater than the cross yard transects at night.

Finally, there is a potentially large source at the Denio's Farmer's Market, southwest of the Denio site, with large parking lots, food preparation, and even a cattle auction yard and holding pens only a few hundred meters southwest of the Denio site. However, major operations at Denio's are confined to Fridays, Saturdays, and Sundays.

By fall, these patterns tend to weaken and a more complex meteorological regime ushers the site eventually to the storm and inversion dominated winter period.

Below we show the major data from the monitoring program for 2005. The pollutants were chosen to reflect a primarily diesel based emissions.

These data clearly shows the regular diurnal cycles, particularly in the summer, of the rail yard impacts on the Denio's site, and the breakdown of this pattern in fall. .

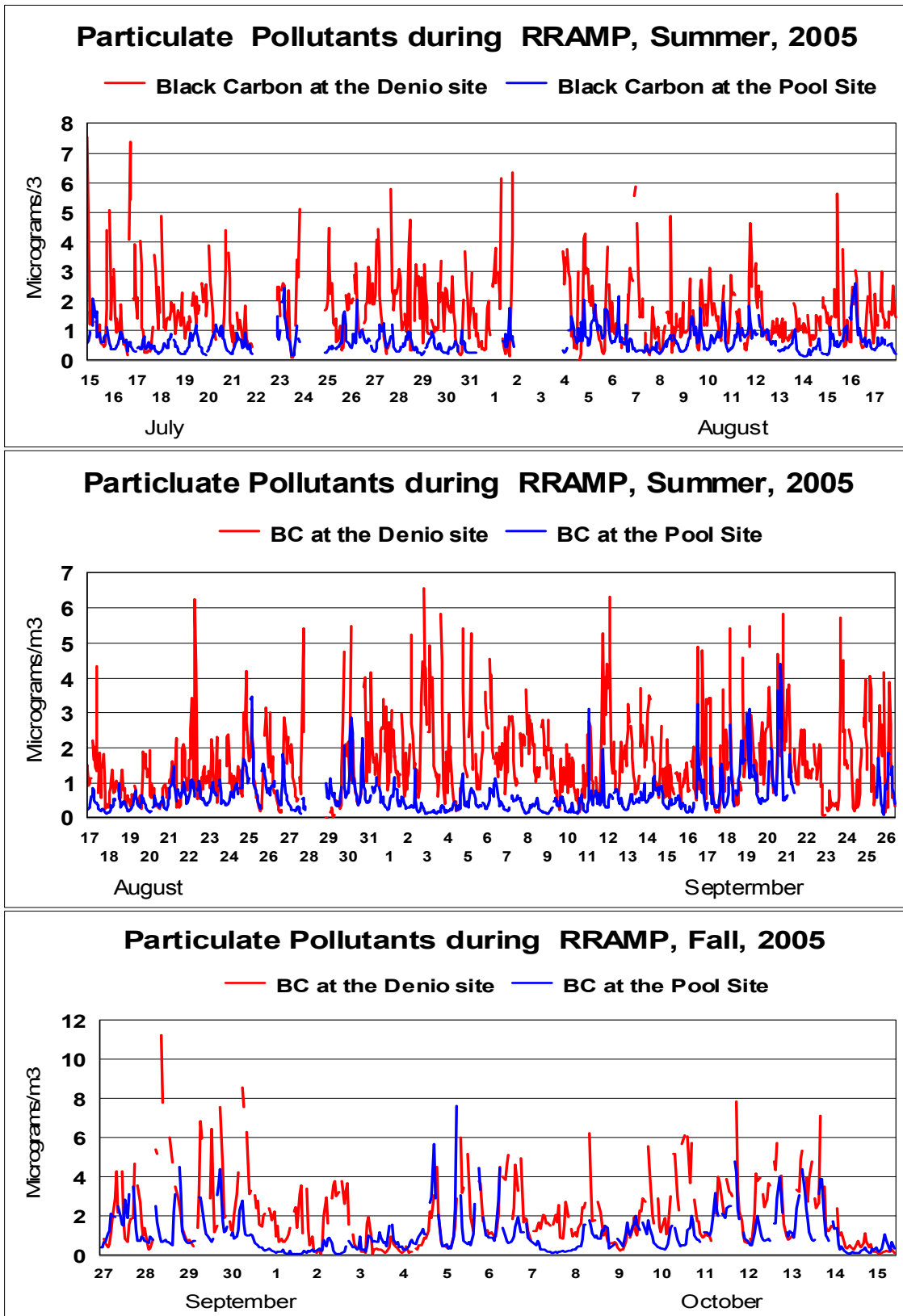


Figure 3 a, b, and c Data on “black carbon” (BC) for July - October, 2005

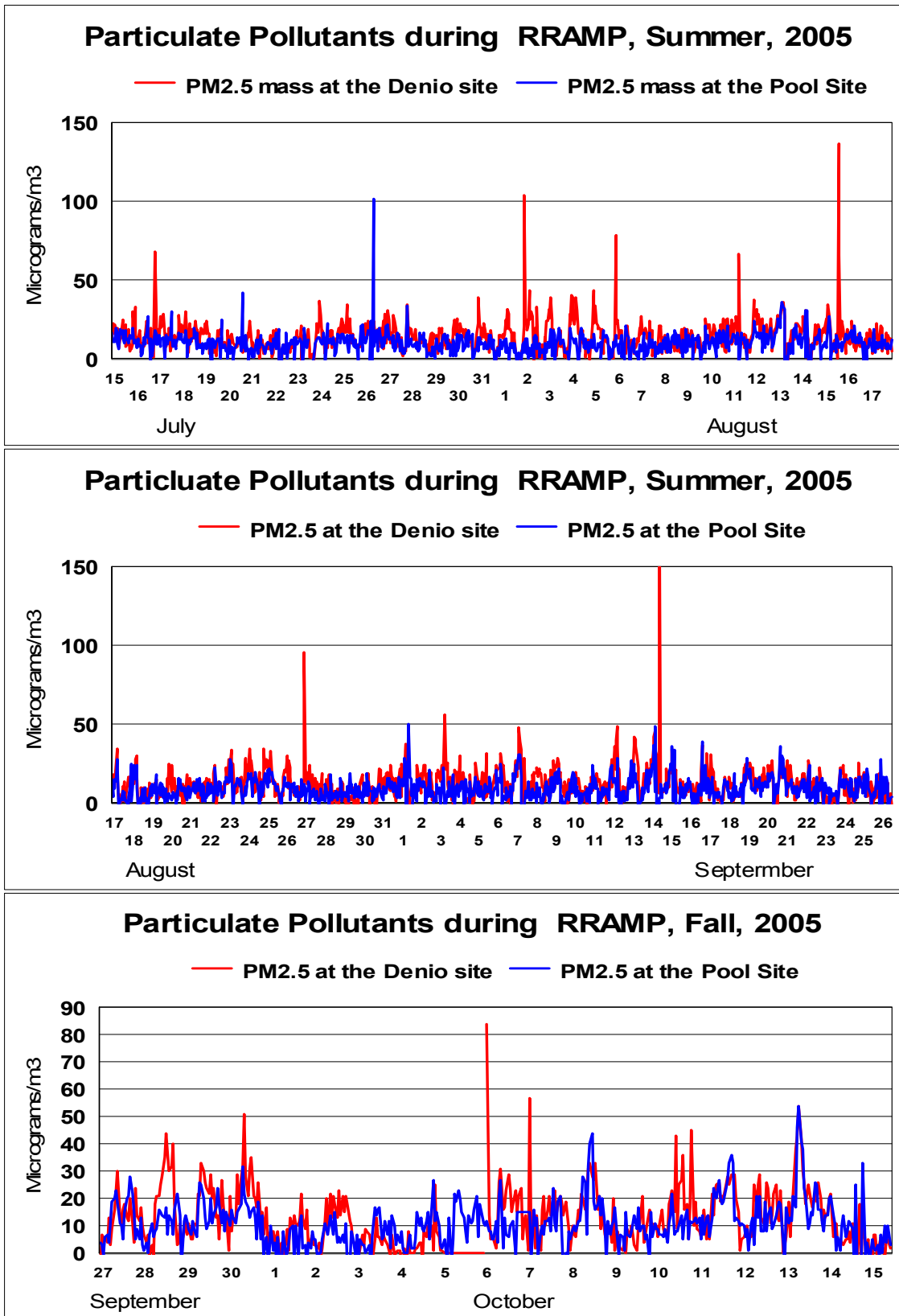


Figure 4 a, b, and c Data on PM_{2.5} mass, July – October, 2005

The role of trains, roughly 3/4 road haul, 1/4 switching, in generating NO_x for Placer County is shown in the 2005 Almanac summary, expressed as fraction of the total pollutant in each category. The table lists the top 8 contributors to NO_x, which amount to 96.9% of the total from all sources. Trains dominate NO_x, 24.2 % of the total, and SO_x, 63.3% of the total emissions.

Table 2 Placer County pollutant emissions for the 8 largest contributors to NO_x

Pollutant	TOG	ROG	CO	NO_x	SO _x	TSP	PM ₁₀	PM _{2.5}
Total (ordered by NO _x)	100.0	100.0	100.0	100.0	100.0	100.0	100.0	100.0
Trains	0.7	1.5	0.8	24.2	63.3	0.5	0.8	1.8
Off road vehicles (no trains)	8.4	19.6	25.1	21.1	4.1	1.5	2.4	5.1
Heavy duty trucks on road – diesels	0.3	0.6	0.5	13.4	4.1	0.2	0.4	0.9
Light duty trucks	5.0	11.8	18.4	10.7	2.0	0.3	0.5	0.8
Fuel combustion - commercial/utilities	1.4	1.5	1.1	10.1	4.1	0.5	0.9	2.0
Passenger cars	4.5	10.8	14.8	7.5	2.0	0.3	0.6	0.8
Medium and heavy Trucks - Gas	2.5	5.7	8.7	6.6	1.0	0.1	0.2	0.2
Residential fuel combustion	7.1	7.9	14.8	3.2	14.3	9.3	14.9	34.9
Fraction of total – 8 largest categories	29.9	59.4	84.2	96.9	94.9	12.9	20.7	46.5

B. Mass and elemental analysis of aerosols at the Denio and Pool sites

The UC Davis DELTA Group and Breathe California of Sacramento-Emigrant Trails (EC/SET) collaborated with the RRAMP project to assist its ongoing studies of aerosol sources and transport in general and diesel exhaust in particular. The RRAMP program was ideal for this purpose, with an upwind-downwind measurement protocol across the Roseville rail yard and numerous measurements. The regional meteorology was stable (above), with typical summer conditions and a persistent across-yard air transport almost every night.

1. Sampling

a. Duration and Sites

Aerosol sampling was initiated on July 8 at the Denio site, 3 hr resolution, with 2 DELTA 8 DRUM inertial impactors operated on a side by side mode for quality assurance validation until July 12 (Table 3). One 8 DRUM was then moved to the Pool site. Both samplers delivered data until August 15, but only the very fine (vf) size mode ($0.26 D_p > 0.09 \mu\text{m}$) for the Pool site sampler met all QA checks because of an internal leak.

Sampling for organic analysis commenced with another DELTA 8 DRUM at the Denio site on August 5, running to September 27. Finally, two sets of samples were collected with high flow Lundgren impactors, Sept. 27 – Oct. 7, the Oct. 7 to Oct. 17, the latter only operating for 12 hrs each night, 6 PM – 6 AM. In all three cases, samples were integrated over the sampling time.

Table 3 Sampling schedule and mean RRAMP monitoring data for the four time periods utilized.

Denio Site	Sampler	Analysis	NO	NO _x	Black Carbon	PM _{2.5} mass
Sampling Periods	Substrate		ppb	ppb	$\mu\text{g}/\text{m}^3$	$\mu\text{g}/\text{m}^3$
7/21 – 8/17, 3 hr	8 DRUM, 16 L/min, Mylar	Mass, elements	81.0	120.2	1.2	14.4
8/5 – 9/27 average	8 DRUM, 16 L/min, aluminum	Organics	62.8	94.2	1.4	12.9
9/27 – 10/7 nights	Lundgren, 150 L/min, aluminum	Organics	87.6	120.8	1.8	11.1
10/7 – 10/17 nights	Lundgren, 150 L/min aluminum	Organics	69.2	101.3	1.8	14.2
Pool Site						
7/21 – 8/17, 3 hr	8 DRUM, 16 L/min, Mylar	Mass, vf elements	3.7	17.0	0.5	9.7
8/5 – 9/27	None	None	8.3	26.2	0.6	9.3
9/27 – 10/7	None	None	30.8	59.5	1.0	9.6
10/7 – 10/17	None	None	17.7	45.9	1.0	12.2

Below we summarize the RRAMP air monitoring data averaged over the sampling periods of the DRUM samplers. Calculating differences and ratios, it become clear that nitric oxide (NO) has the best discrimination between Railyard and non-rail yard sources in summer, (x 22.1) with NO₂ close behind (x 7.2). Black carbon (BC) (x 2.3) is significantly worse, while PM_{2.5} is not very specific to the rail yard, as expected. (x 1.48). Note the breakdown of the clean summer Denio versus Pool downwind-upwind relationship as the program pushed into fall months.

Table 4a, 4b Denio site versus Pool site comparisons in parallel with DELTA Group sampling periods.

Site	Wind	Pool	Denio	Pool	Denio	Pool	Denio	Pool	Denio
Pollutant	Speed	NO	NO	NO ₂	NO₂	BC	BC	PM _{2.5}	PM_{2.5}
units	mph	Ppb	ppb	ppb	ppb	µg/m ³	µg/m³	µg/m ³	µg/m³
7/21 – 8/15	4.32	3.63	80.34	16.60	119.20	0.5	1.2	9.7	14.3
8/5 – 9/27	4.36	8.10	63.02	26.01	94.80	0.6	1.4	9.4	13.0
9/27 – 10/7	3.67	31.39	85.63	60.01	118.29	1.0	1.8	9.3	10.9
10/7 – 10/17	3.83	17.87	73.87	46.08	107.36	1.0	1.8	12.5	14.6
2/10 - 2/24									

Site	Denio - Pool	Denio/Pool	Denio - Pool	Denio/Pool	Denio - Pool	Denio/Pool	Denio - Pool	Denio/Pool
Pollutant	NO	NO	NO ₂	NO₂	BC	BC	PM _{2.5}	PM_{2.5}
Units	ppb	Ratio	ppb	Ratio	µg/m ³	Ratio	µg/m ³	ratio
7/21–8/15	76.7	22.1	102.6	7.2	0.7	2.3	1.5	1.48
8/5 – 9/27	54.9	7.8	68.8	3.6	0.8	2.5	1.4	1.38
9/27–10/7	54.2	2.7	58.3	2.0	0.8	1.8	1.2	1.17
10/7–10/17	56.0	4.1	61.3	2.3	0.8	1.8	1.2	1.17
2/10 - 2/24								

The excess black carbon, assigned to the rail yard, is remarkably constant at 0.7 µg/m³, or about ½ of the PM_{2.5} mass increment. It is also clear that the relationship, rail yard to non rail yard sources, is significantly poorer by the fall months, but the rail yard contribution is still about the same value. This may be, however, misleading as the Pool Site upwind values are rising sharply by fall, as much as a factor of 2 to 5 for the tracer species, so the difference and ratio are degraded while the concentrations are relatively stable. Thus, the monitoring data show that the Denio Site is the optimum site for measuring organic species at the Roseville rail yard even in the early fall periods.

b. Sampling Equipment

The sampling requirements for the study were set by the need to obtain data as a function of particle size, especially the important very fine ($< 0.25 \mu\text{m}$)/ultra fine ($< 0.1 \mu\text{m}$) modes, and composition, with adequate time resolution to resolve the dramatic diurnal patterns upon which the RRAMP study was based. The need for compositional data required selected substrates matched to the analytical needs. Finally, the presence of synoptic weather patterns demanded that the sampling extend for, at the minimum, a few weeks.

Inertial impactors have the capability to segregate particles as a function of size onto substrates that can be later analyzed by a variety of methods. The use of an inertial impactor with a slowly rotating deposition surface, a drum impactor, also allows samples to preserve time along the substrate. The subsequent analytical methods can then be matched to data needs, with the time resolution set by the overlap between the rotation rate, in mm/day, and the analytical probe, whose width is also expressed in mm. They also have the valuable characteristic that slotted and jetted drum impactors can have the particle sizing calculated analytically, so that calibration is really confirmation of well established aerodynamical calculations, not a means to ascertain the cut points. The last point to mention is that with the new methods of measuring elements, mass, and optical parameters from the drum substrates, the amount of information delivered per unit cost is vastly reduced, allowing continuous measurements of composition and size heretofore economically improbable. One of the efforts of the DELTA Group in the past decade is, in fact, cost reduction, as the number of valid, analyzable samples from a drum impactor can be daunting. For example, to measure an equivalent $\text{PM}_{2.5}$ 24 hr mass value with a drum sampler with 6 size cuts below $2.5 \mu\text{m}$ and 3 hr time resolution requires 48 separate mass measurements, versus one for the filter.

The samplers used were DELTA Group 8 DRUM inertial impactors (Cahill et al, 1985, Hering et al 1990, see DRUM publications in Appendix C). These slotted impactors are based on the Lundgren impactor (Cahill and Wakabayashi, 1993) with theoretical and experimental validation of sizing (Raabe et al, 1989). The DRUM collects aerosols continuously onto 8 slowly rotating drums in 8 size modes: 10 to 5.0, 2.5, 1.15, 0.75, 0.56, 0.34, 0.26, and $0.09 \mu\text{m}$ aerodynamic diameters. Each drum has a thin layer of Mylar, $480 \mu\text{g}/\text{cm}^2$ thick (roughly 1/8 mil) covered with about $5 \mu\text{g}/\text{cm}^2$ Apiezon-L grease (Wesolowski et al, 1979, Cahill 1980) as an anti-bounce measure. The flow was 16.7 L/min to match the standard PM_{10} heads.

In addition, in order to obtain enough mass for organic analysis in only 10 days of sampling, the original Lundgren 5 stage drum impactors were used, with a flow of 125 L/min. These samplers required an aluminum substrate for the organic analyses. The Lundgren impactors were keyed to nighttime-only winds on the basis of the well established rail yard nighttime impact at the Denio site.

One sampler, the Pool site, was an older model that had to be modified to meet equivalent upwind – downwind comparison. These samplers are shown below in figure 5.

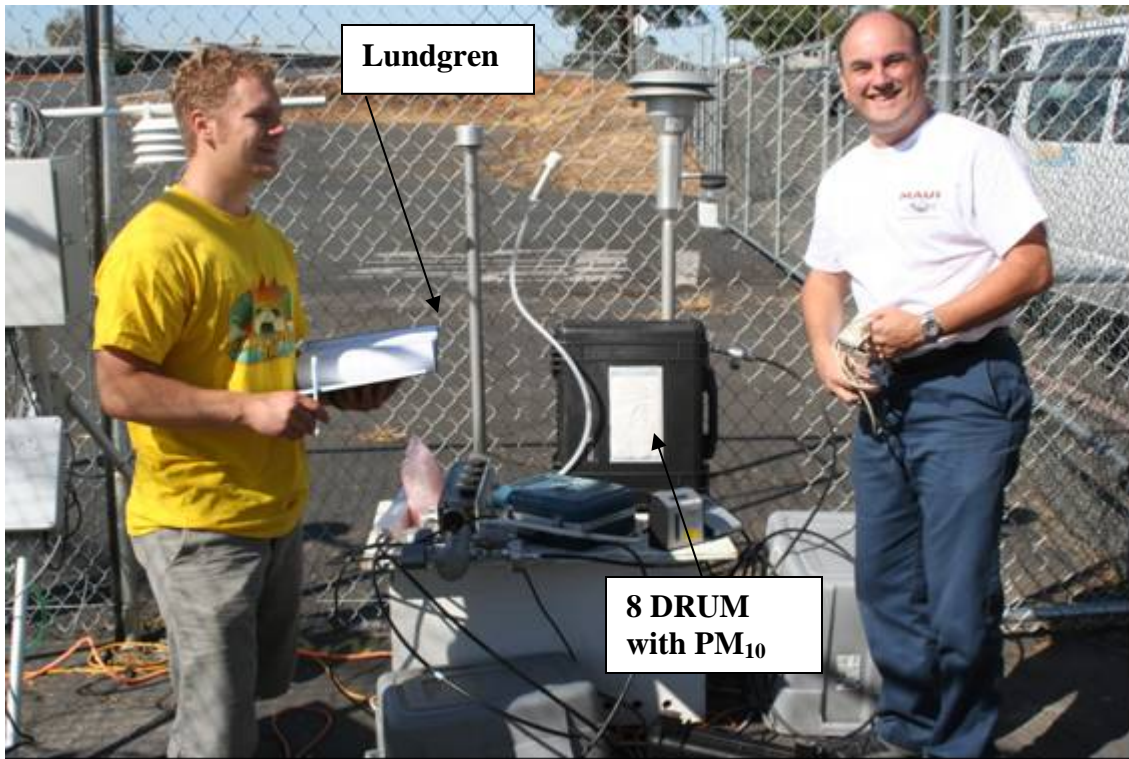


Figure 5 Nick Spada (left) and David Barnes at the Denio site, Sept. 27, 2005. The cattle auction buildings of the Denio's Farmer's Market are seen behind them, across a large parking lot.

In Appendix B, we include a selection of the publications describing the sampling and analysis with DRUM impactors.

c. Quality assurance

Full quality assurance documentation for DRUM samplers, and references on their use, are contained in the DRUM Quality Assurance Protocols version 1/05 (DQAP v 1/05) available on the DELTA web site <http://delta.ucdavis.edu>. A printed copy will be supplied with this Final Report, and a summary is included in Appendix QA.

As an example, we include below a precision test of soft beta ray mass analysis on a Denio site DRUM strip (Figure 6). Analysis was completed for mass values every 1 ½ hours in 8 size modes for the entire period. Each strip was analyzed at least 2 times, and the standard deviation of the data are included in the data file. Note that since the strip was remounted, the test also validates relative time precision. Any measurements where the analysis differs by more than $\pm 10\%$ is independently re-run until agreement is achieved.

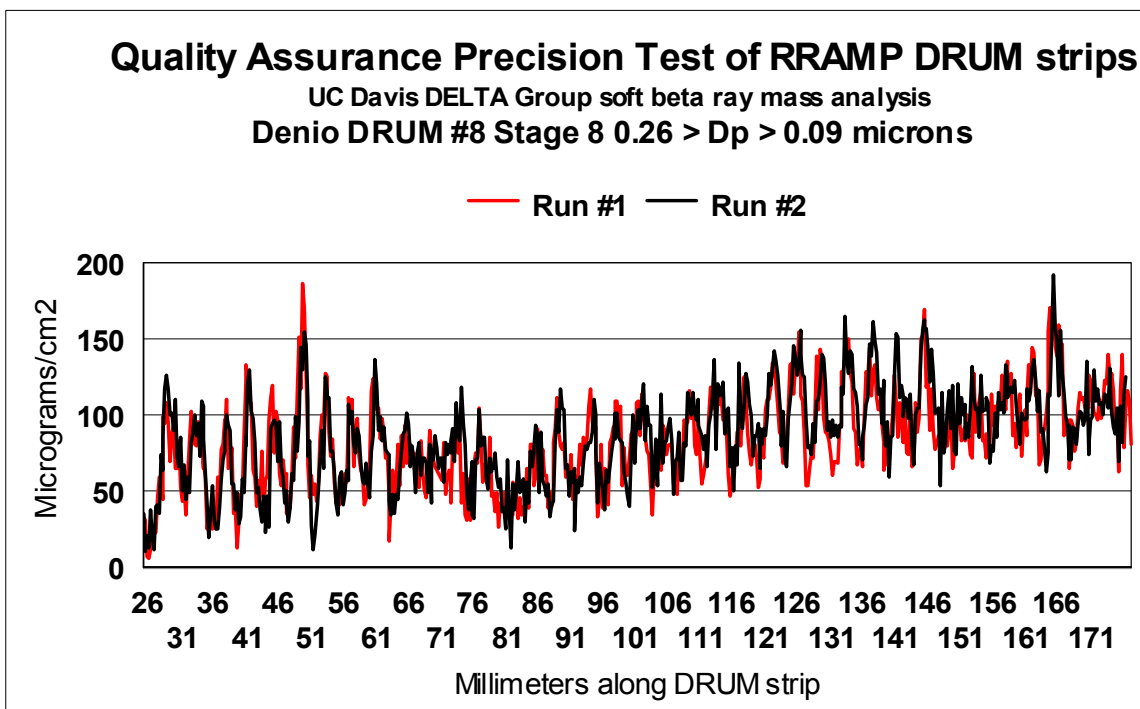


Figure 6 Precision test for mass

The samples collected by the DRUM sampler are designed to allow highly sensitive elemental analysis by the new DELTA Group designed aerosol analysis system of the x-ray micro beam of the Advanced Light Source, Lawrence Berkeley NL (Bench et al, 2002). The method, synchrotron-induced x-ray fluorescence (S-XRF) has been used by the DELTA Group since 1992, (Cahill et al, 1992) but in its present form since 1999.

The S-XRF system has been tested in blind inter-comparisons since 1999, and all of these are shown below (Table 5). Typically 32 elements are recorded for each analysis, all of which can be traced back to NIST primary (SRM # 1832, SRM # 1833) or secondary (Micromatter thin film) standards.

Table 5 S-XRF comparison, all blind tests since 1999

Study and date	Methods	Average ratio, Al to Fe	Std. dev.	Average ratio, Cu to Pb	Std. dev.
BRAVO, 1999	PIXE vs S-XRF	0.99	0.04		
BRAVO, 1999	CNL XRF vs S-XRF			1.24	0.14
FACES, 2001	ARB XRF vs S-XRF	0.93	0.21	1.02	0.08
FACES, 2001	ARB RAAS vs S-XRF	(0.98)	0.27	(0.74)	0.23
ARB LTAD 2005	DRI XRF vs S-XRF	1.037	0.085	0.907	0.009
All prior studies	Average	0.984	0.15	0.977	0.115

2. Results

All results are provided on a CD in the form of Excel spread sheets. The DRUM Quality Assurance Protocols (DQAP ver 1/05) are included by reference, but a hard copy (135 pages) can be downloaded if required.

Below we present the sub-2.5 μm soils (Figure 7) and the very fine soot like particles (Figure 8). The most striking results was the very highly correlated very fine particles (0.34 μm) at night anti-correlated with fine mass in the 2.5 to 1.15 μm mode, typically fine soil in the summer Central Valley conditions (Figure 9). The night mass peaks can confidently assigned to rail yard aerosols. Below we compare the very fine micron mass ($0.26 > D_p > 0.09 \mu\text{m}$) mass from the Pool site and the Denio site (Figure 10).

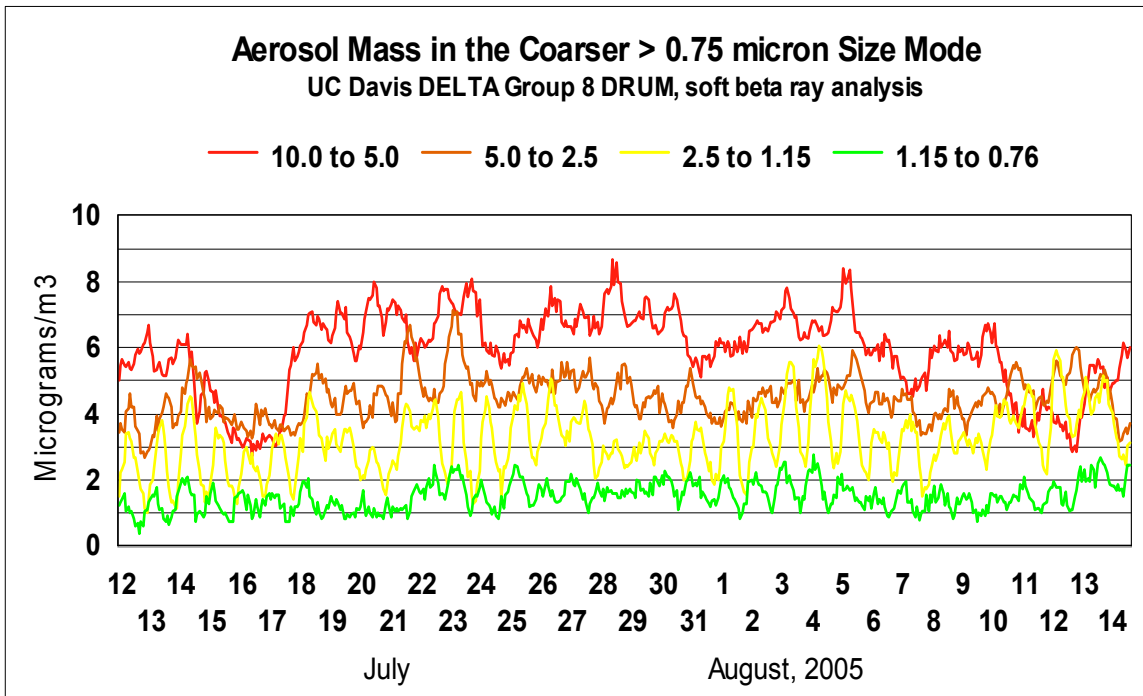


Figure 7 Mass from 10.0 to 0.75 μm

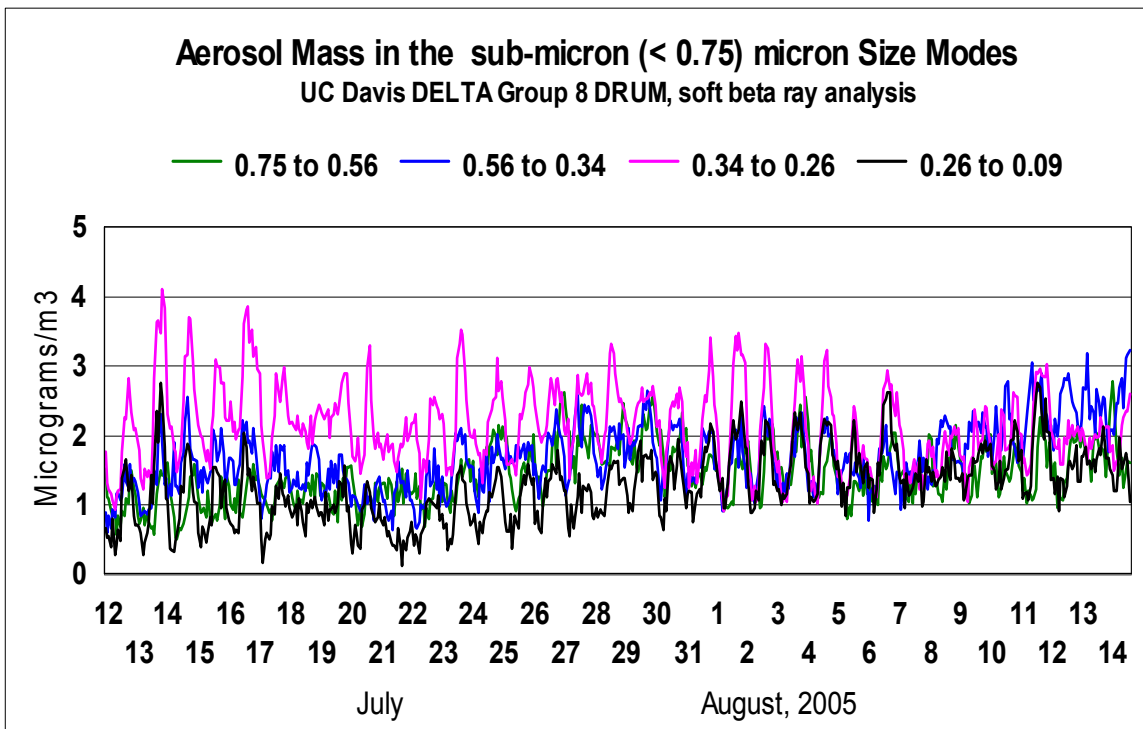


Figure 8 Mass from 0.75 to 0.09 μm

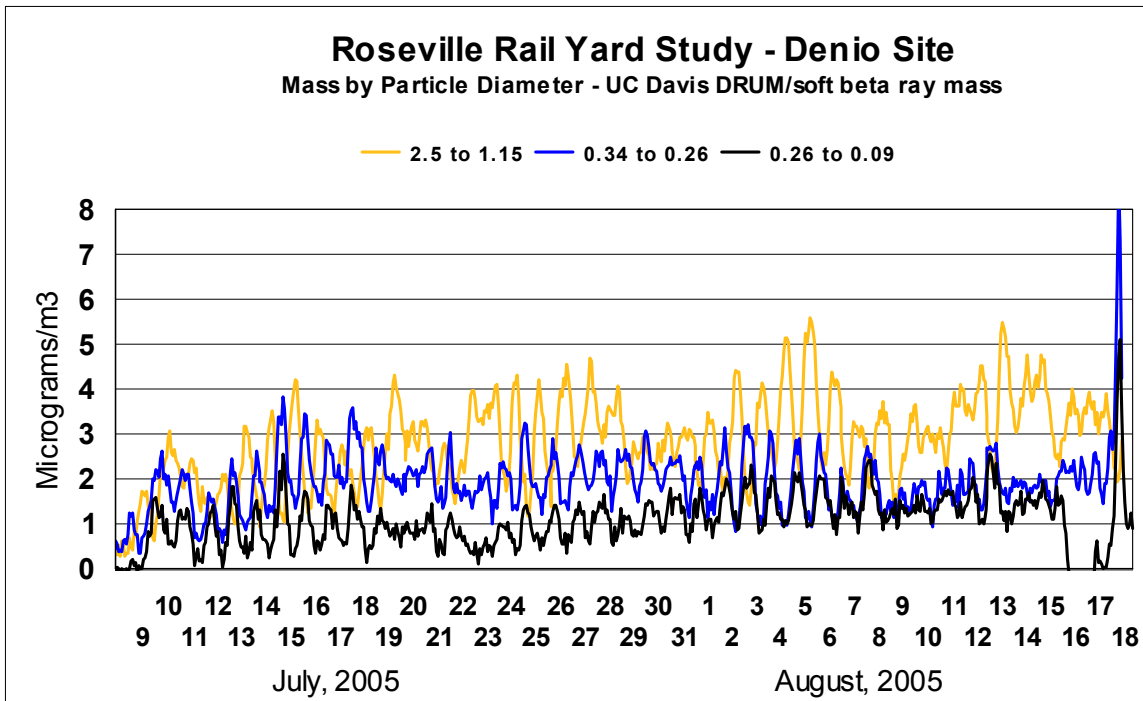


Figure 9 Three components of fine mass versus time

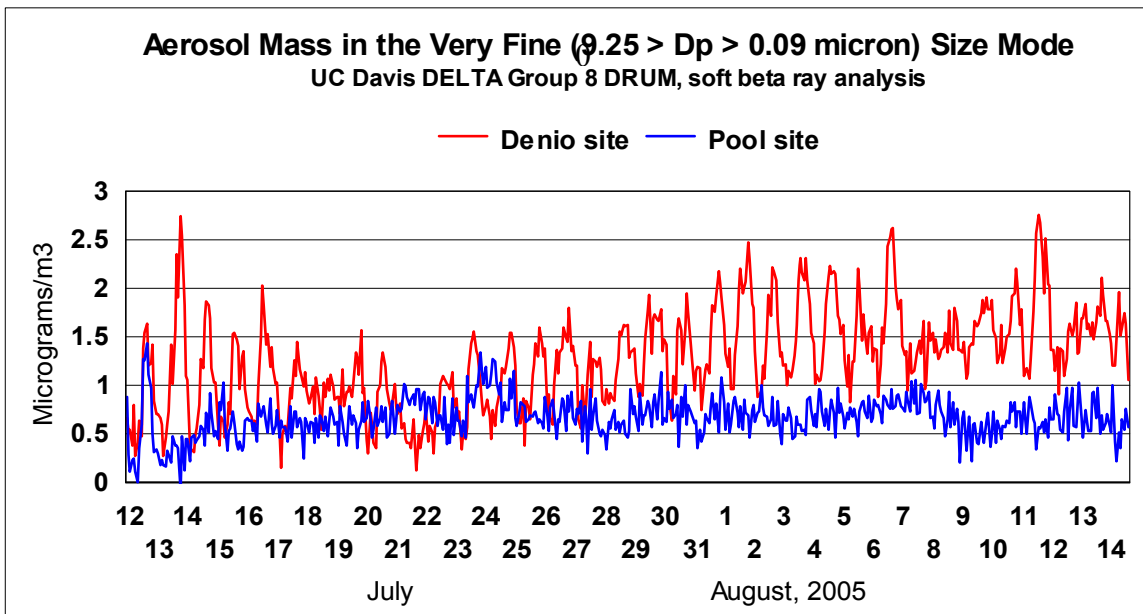


Figure 10 Comparison of the Pool and Denio sites for very fine mass

Detailed meteorological analysis is needed to interpret these data, augmented by high resolution data such as NO to properly assign DRUM time signatures. However, there are periods (July 14 – 16, July 29 – August 7) when daytime values at the Denio and Pool sites are similar and 6 hr average nighttime values at the Denio site are enhanced, with an approximate mean value of $1.35 \pm 0.27 \mu\text{g}/\text{m}^3$.

Average Denio/Pool difference for 9 hrs, 10:30 PM to 7:30 AM, for the July-August DRUM sampling period, was $0.83 \mu\text{g}/\text{m}^3$. The median (a better estimate) was $0.87 \mu\text{g}/\text{m}^3$, and maximum was $1.53 \mu\text{g}/\text{m}^3$. We can compare these data with the data for mass of black carbon (EC), since EC is known to be primarily in the very fine mode. The EC difference, Denio – Pool, was $0.7 \mu\text{g}/\text{m}^3$, while the average DRUM very fine mass difference was $0.83 \mu\text{g}/\text{m}^3$ (for $\text{PM}_{2.5}$, the value was $1.5 \mu\text{g}/\text{m}^3$). However, recall that this DRUM did not have an after filter for the $< 0.09 \mu\text{m}$ particles and thus would lose some mass.

There is an enormous amount of information on particle size, but interpretation of these data are hampered by lack of Pool site data and elemental analysis of the coarser modes. Nevertheless, below we plot 9 hr (9 PM- 6 AM, Figure 11) nighttime mass distributions at the Denio site for 5 days in early August when the very fine mode Pool site-Denio site comparisons indicate direct Railyard influence.

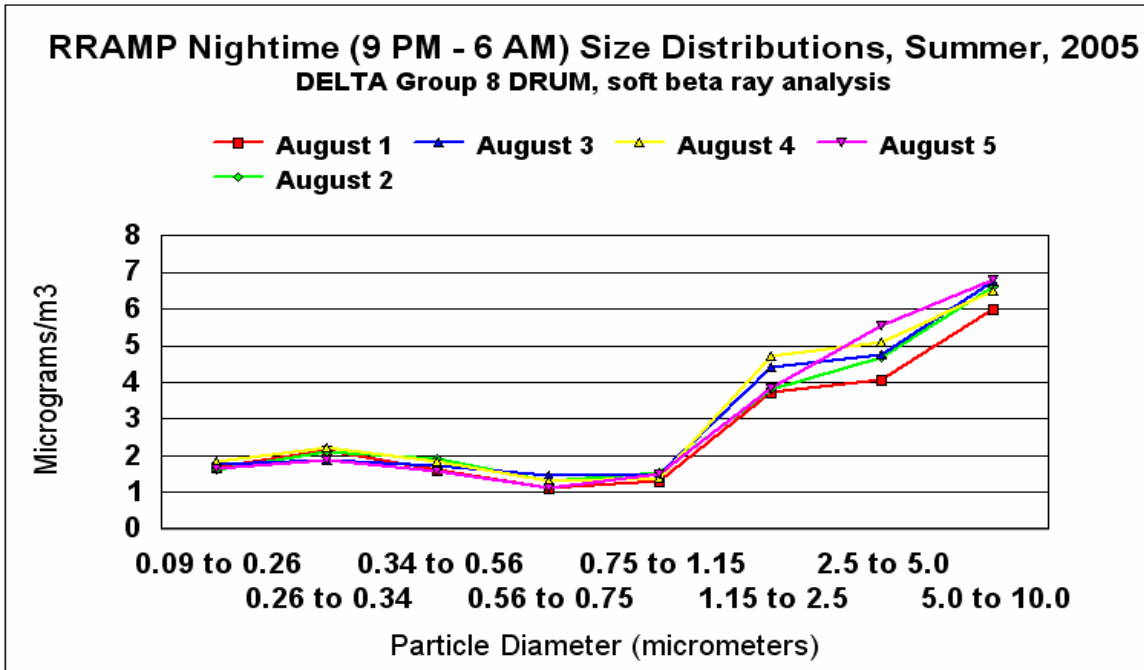


Figure 11 Nighttime (9 PM – 6 AM) mass size profiles for early August at the Denio site.

We can compare these data to other measurements of diesel exhaust in laboratory and field conditions (Figure 12). Below we plot these data for July 15 and compare them with a recent (2005) study we are doing with Johns Hopkins University on the Baltimore McHenry tunnels, one bore of which is all truck traffic and overwhelmingly diesel. These data are then compared to a 2002 study with the U. of Minnesota diesels in the laboratory, an average of 6 different runs, mostly with California fuel (Zielenska et al, 2004).

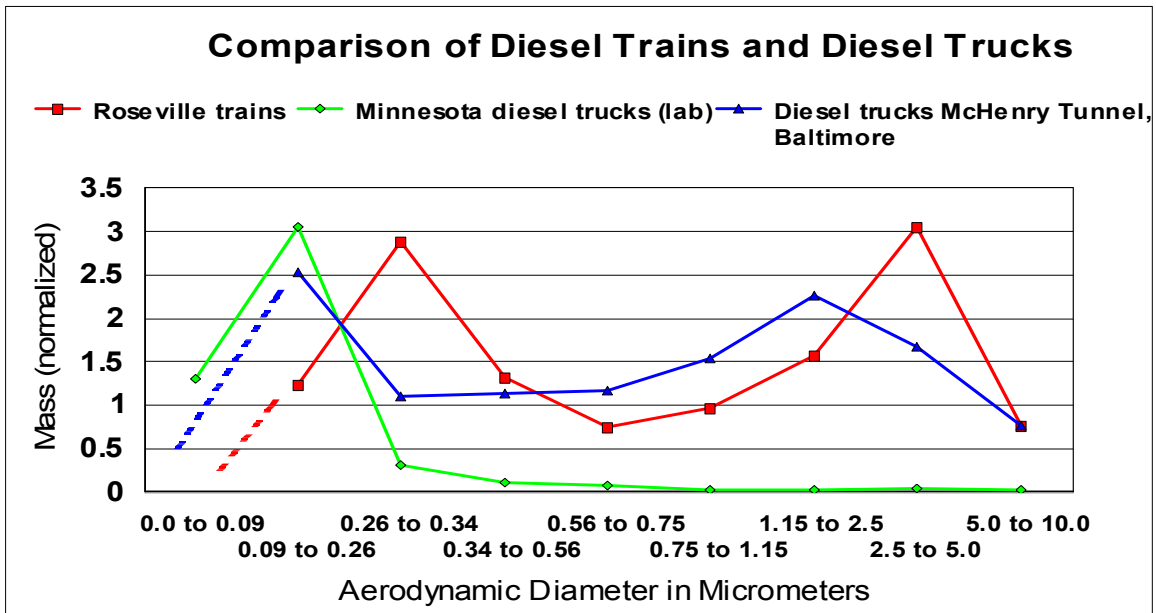


Figure 12 Size mode of aerosol mass, July 15, versus other recent diesel studies

From the plots, it is clear that the very fine and accumulation size modes of the diesel exhaust from the rail yard is considerable coarser in particle size than that in the laboratory or tunnel diesel trucks signature, while the coarse modes mimics the tunnel data.

The Stage 8 sample from the Denio site was first selected for elemental analysis by S-XRF as this stage is the size mode heavily represented in diesel exhaust (Zielenska et al, 2004). The strip was analyzed in 3 hr increments, resulting in 320 analyses with almost 9,000 data values and 9,000 individually calculated errors. The typical minimum detectable limits for this stage were 0.01 ng/m^3 or less, and are shown in Appendix QA.

An example of the almost 9,000 elemental data, each with an associated error, is shown below (Figure 13) for three elements previously identified with diesel exhaust from trucks (Zielenska et al, 2004), phosphorus and zinc from the zinc thiophosphate stabilizer in lubricating oils, sulfur from the fuel.

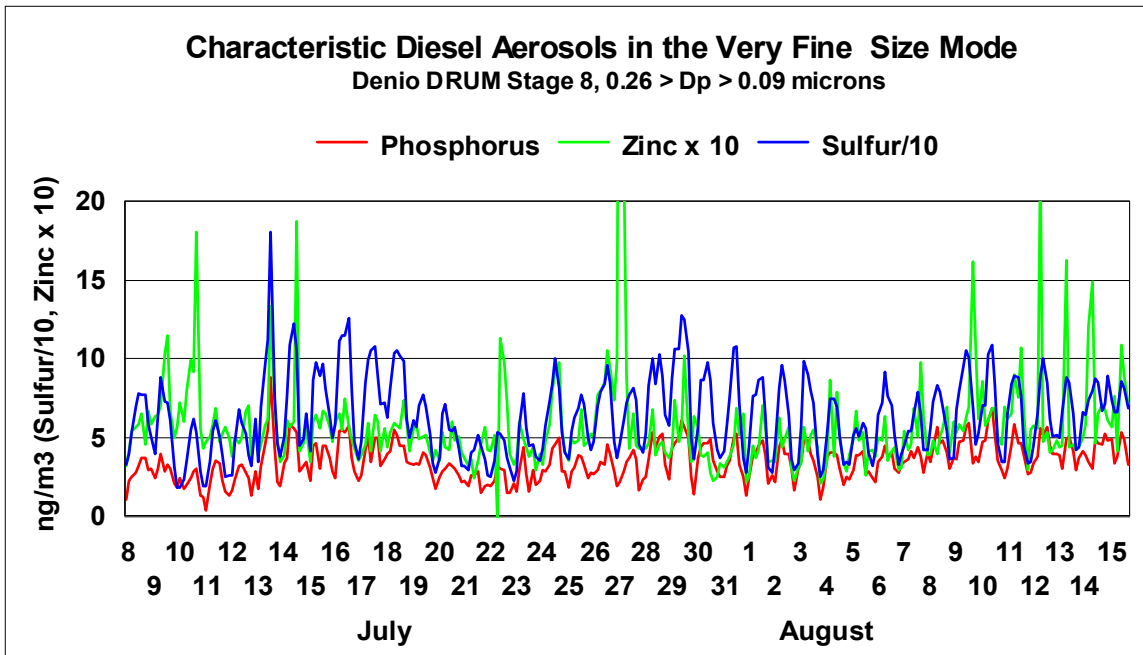


Figure 13 Typical elemental signatures of diesel, Denio site very fine mode

These elements had been seen earlier in this size mode in our work in Zielenska et al 2004, and tied to their sources in then fuel and lubricating oil (Figure 14).

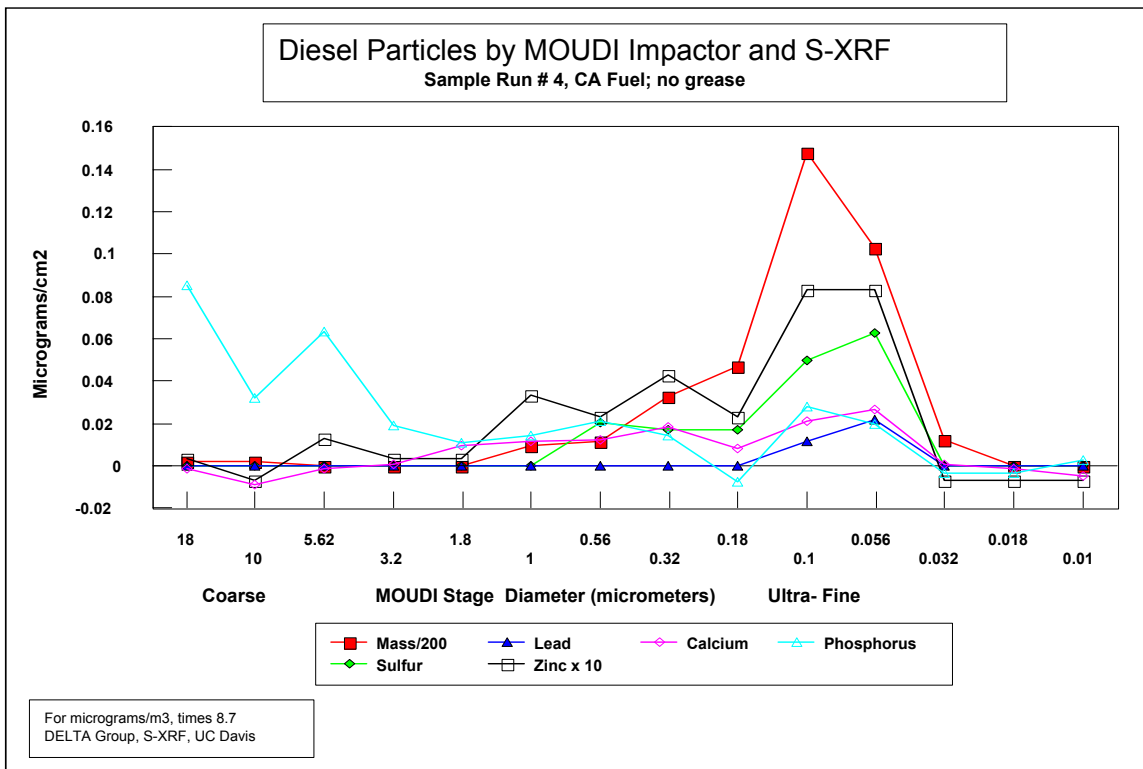


Figure 14. Zielenska et al diesel characterization results

There are additional very fine aerosols that have strong nighttime signatures (Figure 15).

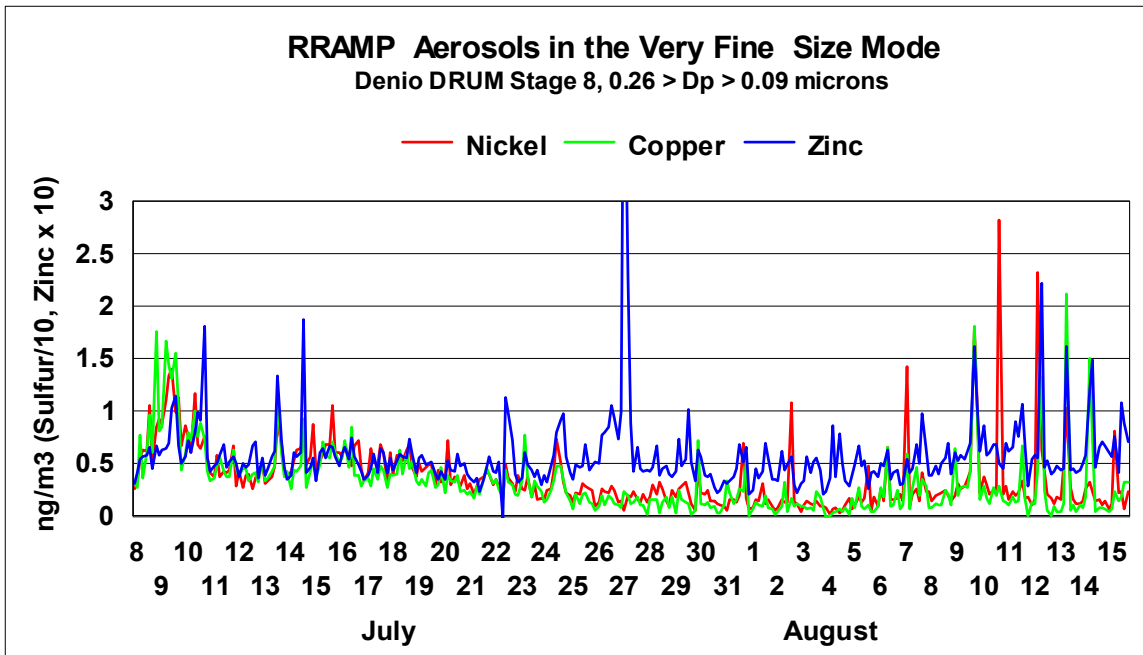


Figure 15 Transition mode elements nickel, copper, and zinc in the Denio site very fine mode.

Below we show some aerosols that would be, in coarser modes, derived from soil (Si, K, Ca, Fe) or in a finer mode, wood smoke (K) (Figure 16).

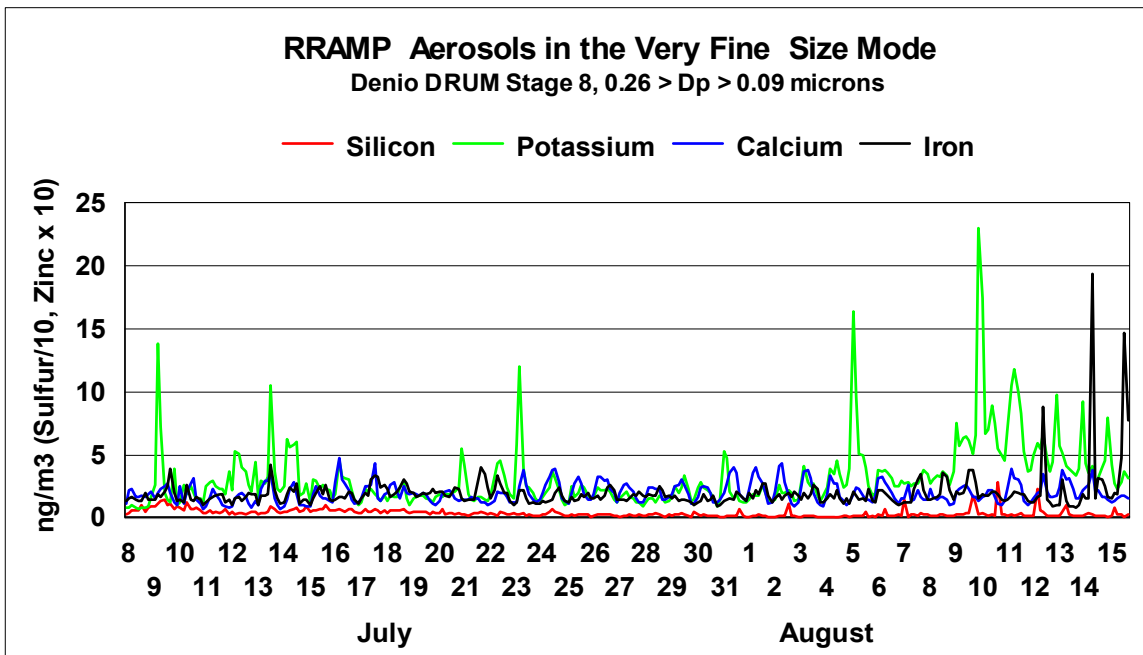


Figure 16 Crustal elements in the very fine mode, Denio site

Combining the mass and elemental data, we can identify sources for the observed mass. Below (Figure 17) we show a few days in early August, associating the nighttime mass

peaks with characteristic diesel effluents. Note the anti correlated mass near $PM_{2.5}$, associated with stronger daytime winds.

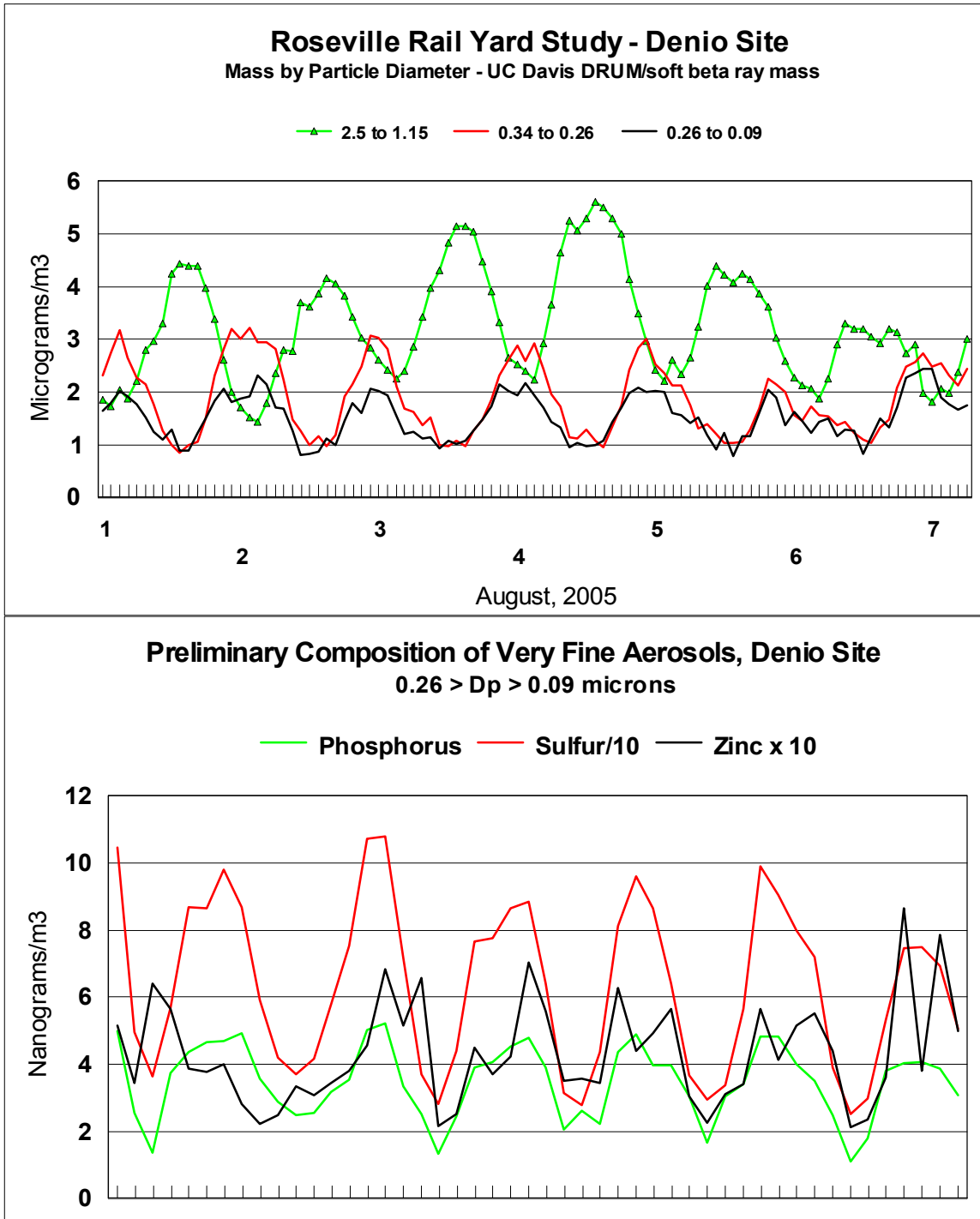


Figure 17 Mass versus typically diesel signature elements, Denio site

The mass data show that in the very finest mode of the Pool site DRUM sampler, the critical orifice Stage 8 from $0.26 > D_p > 0.09 \mu m$, had run properly. The mass delivered

was equivalent ($0.72 \mu\text{g}/\text{m}^3$ Denio, $0.68 \mu\text{g}/\text{m}^3$ Pool, each with an error of $\pm 0.2 \mu\text{g}/\text{m}^3$) when the Denio and Pool samplers were co-located at the Denio site from July 8 through July 12. Thus, the DELTA Group could safely compositionally analyze the samples by S-XRF. We report here the preliminary data pending the required S-XRF precision re-analysis protocol Level 1 of DQAP ver 1/06.

The results were again compared at the co-located site and were again equivalent. For the 5 major elements, which make up 87% of all S-XRF elemental mass, the ratio, Pool/Denio, was 0.97 ± 0.27 . On the other hand, two trace elements, Ni and Cu, did not agree, while there was also some excess soil seen in the first few hours of sampling, probably from contamination in handling. Since the amount of soil on this stages is \ll soil on coarser stages, we are hesitant to make conclusions on the small amount seen even though, because of the greased stages, the bounce-through is < 1 part in 5,000.

The largest element in the very fine particle mode was sulfur, which is most likely in the sulfate state (Figure 18). This will cause the values below to be increased by a factor of 3.0, making sulfate a major fraction of the observed very fine mass. The agreement during the co-located days is excellent. After moving the second DRUM sampler to the Pool site, the systematic nighttime enhancement disappears except for rare instances (August 1). Very fine sulfur is normally a signature of diesel fuel combustion.

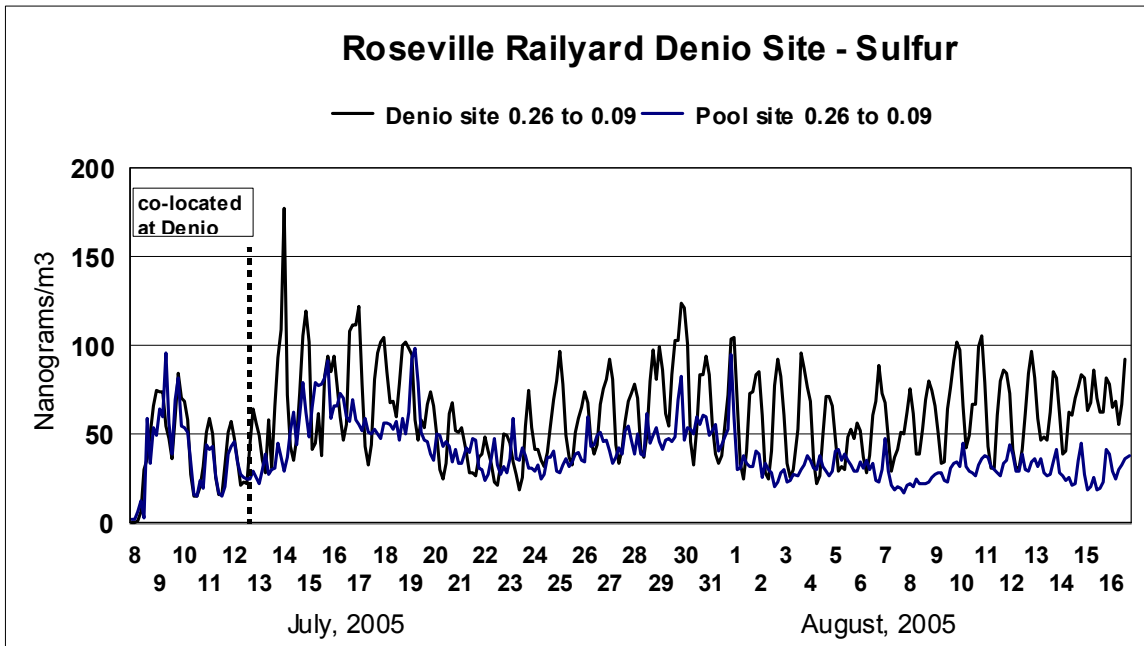


Figure 18 Comparison of very fine sulfur, Denio Site vs Pool Site

Phosphorus (Figure 19) is normally a signature of the combustion of lubricating oil from the zinc thiophosphate stabilizer. It, too, shows a nighttime enhancement synchronous with sulfur, but there are also other sources present at the upwind site, perhaps reflecting the heavy nighttime truck traffic on I-80. However, the phosphorus spike on July 18 is clearly some special situation that requires much more analysis.

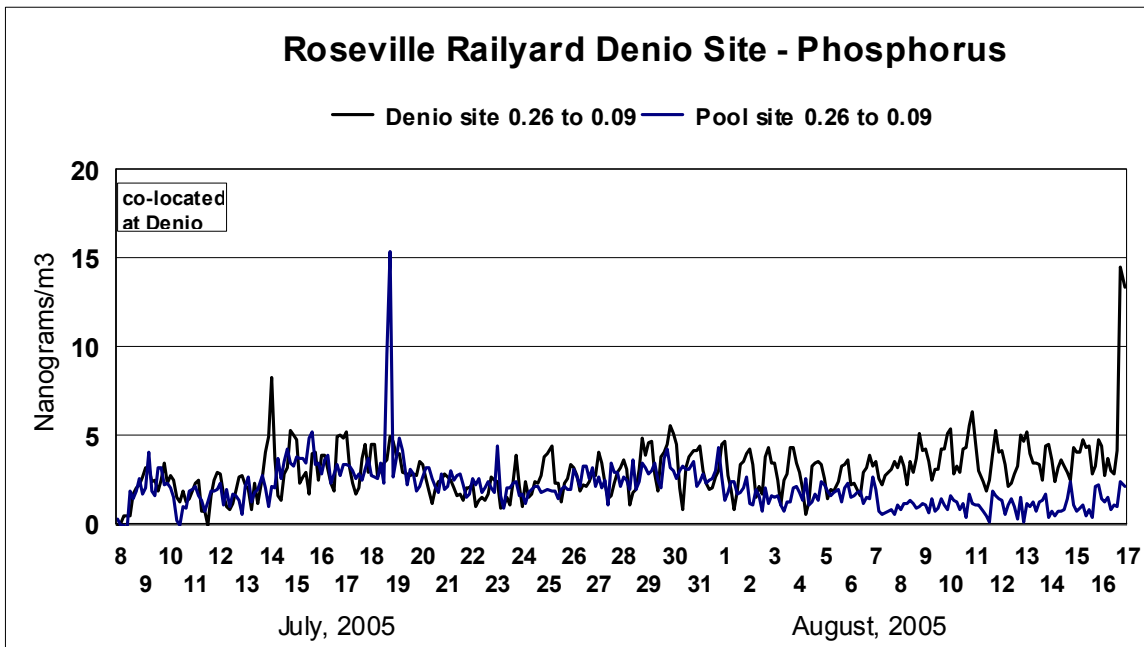


Figure 19 Comparison of very fine phosphorus, Denio Site vs Pool Site

Zinc (Figure 20), on the other hand, clearly has numerous sources in the area, although in August we do see a systematic nighttime enhancement.

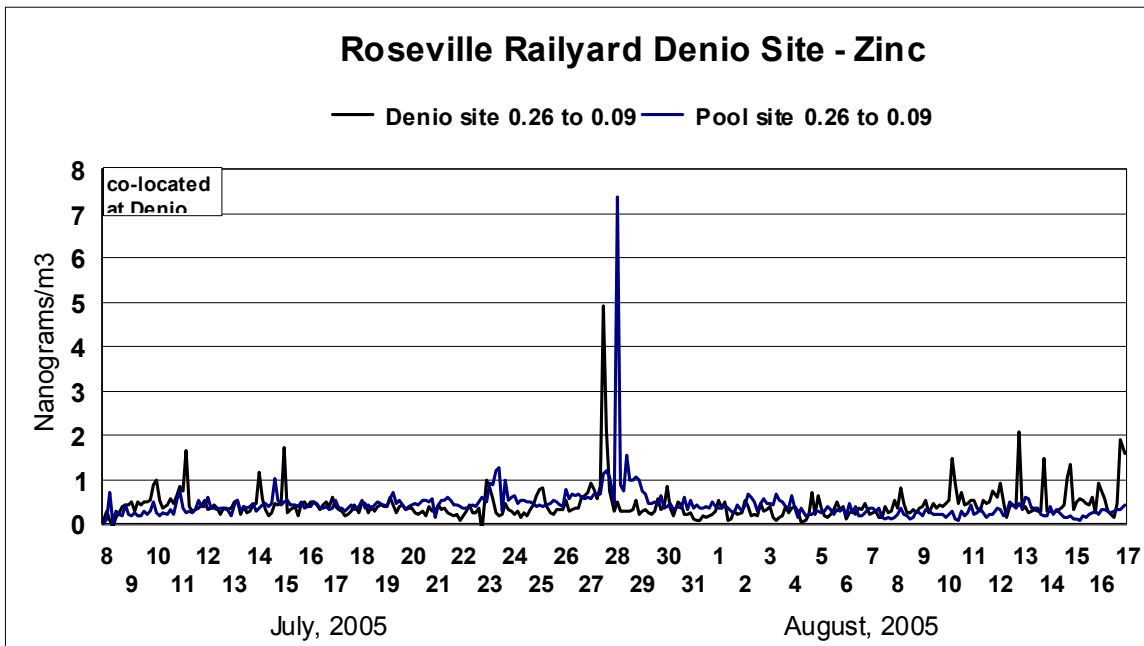


Figure 20 Comparison of very fine zinc, Denio Site vs Pool Site

The last element systematically associated with diesel combustion is calcium (Figure 21), which in this very fine size mode is a tracer of calcium carbonate, which is

an antacid in the lubricating oil. Sodium carbonate is also used in some oils, which may be the source of the relatively high sodium numbers.

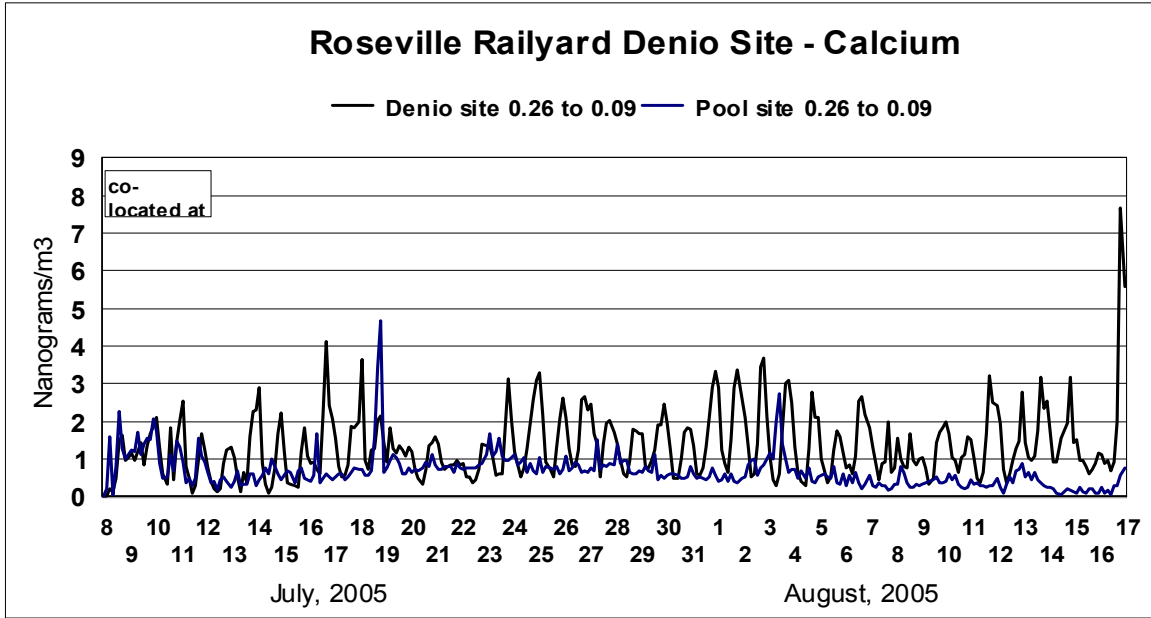


Figure 21 Comparison of very fine calcium, Denio Site vs Pool Site

In addition to the expected elements from the combustion of diesel fuel and lubricating oil, we observe other elements. Copper (Figure 22) and nickel (Figure 23) behave in a similar manner and have poor agreement at the co-located site for reasons that are not clear at this time, but based upon agreement in re-analysis, is probably accidental contamination of the first 8 cm (first 20 days of July).

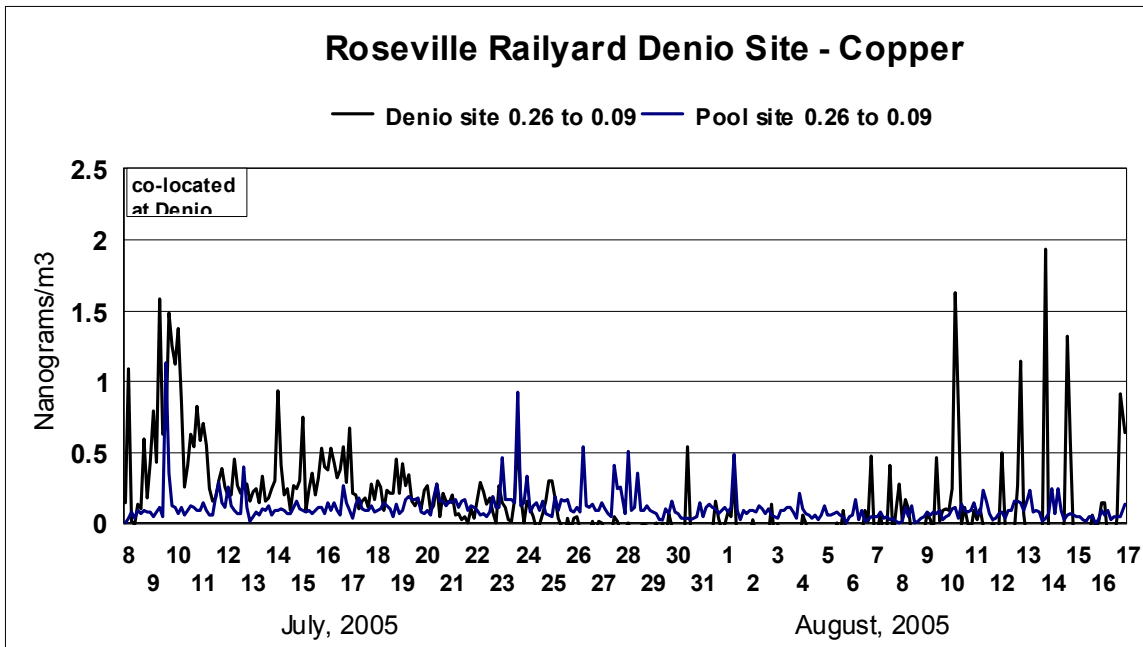


Figure 22 Comparison of very fine copper, Denio Site vs Pool Site

We must assign much of the Denio signal for these elements for the first 10 days to contamination, either on the drums or perhaps in the air, since it is well known that some motors give off a fine copper aerosols. Note that there was also an anomalous mass signature for the very coarsest particles for the first few days at Denio site, strengthening the argument for contamination.

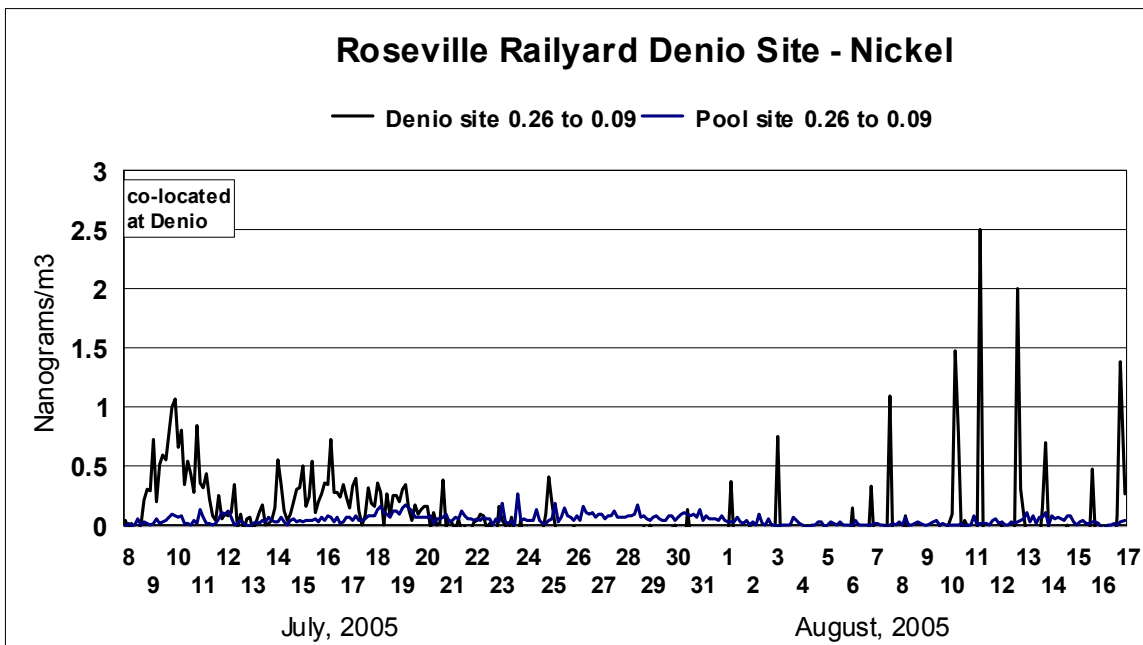


Figure 23 Comparison of very fine nickel, Denio Site vs Pool Site

Potassium (Figure 24), on the other hand, is usually dominated by internal combustion engines in this size mode. Potassium from wood smoke peaks in the 0.34 to 0.56 μm mode.

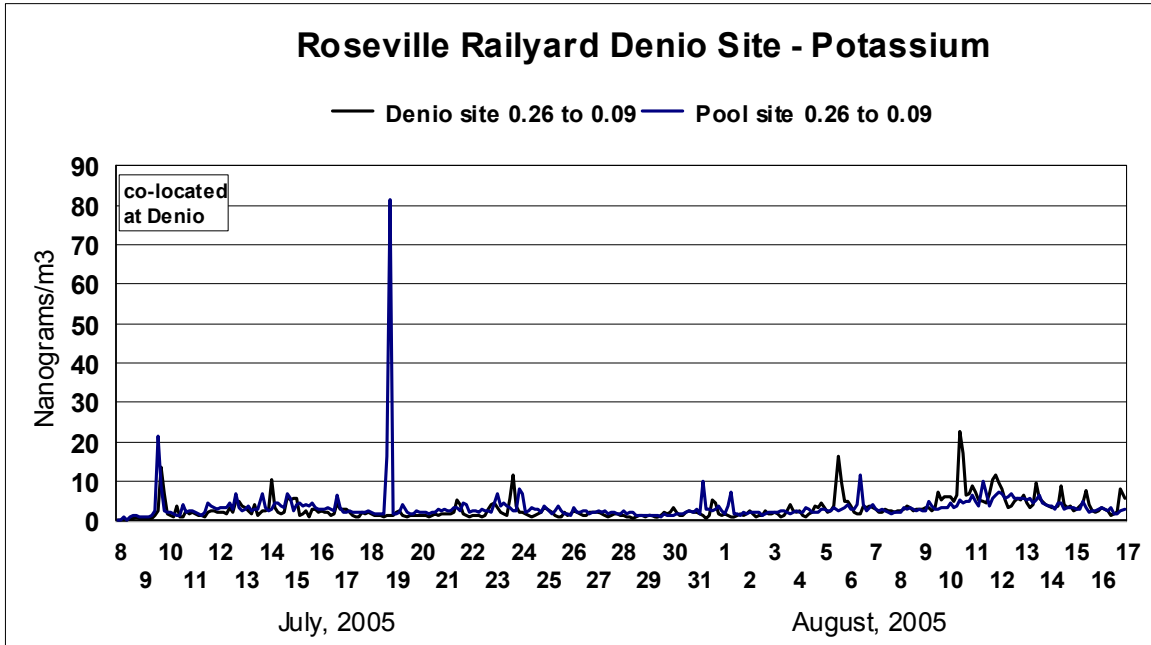


Figure 24 Comparison of very fine potassium, Denio Site vs Pool Site

Vanadium (Figure 25) is used in metallurgy and has a very high boiling point. It also occurs naturally in soil at a trace level. However, in this size mode, it is almost certainly from some high temperature process. The nighttime enhancement was unexpected.

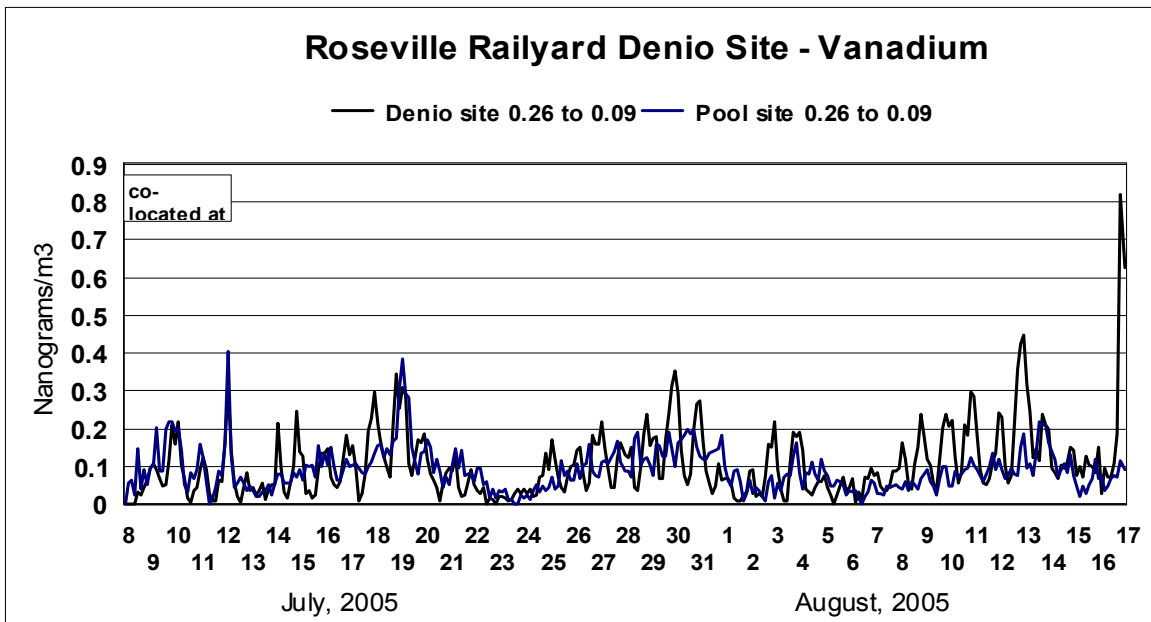


Figure 25 Comparison of very fine vanadium, Denio Site vs Pool Site

Chromium (Figure 26) has similar behavior to vanadium metallurgically, but has a very different behavior in RRAMP.

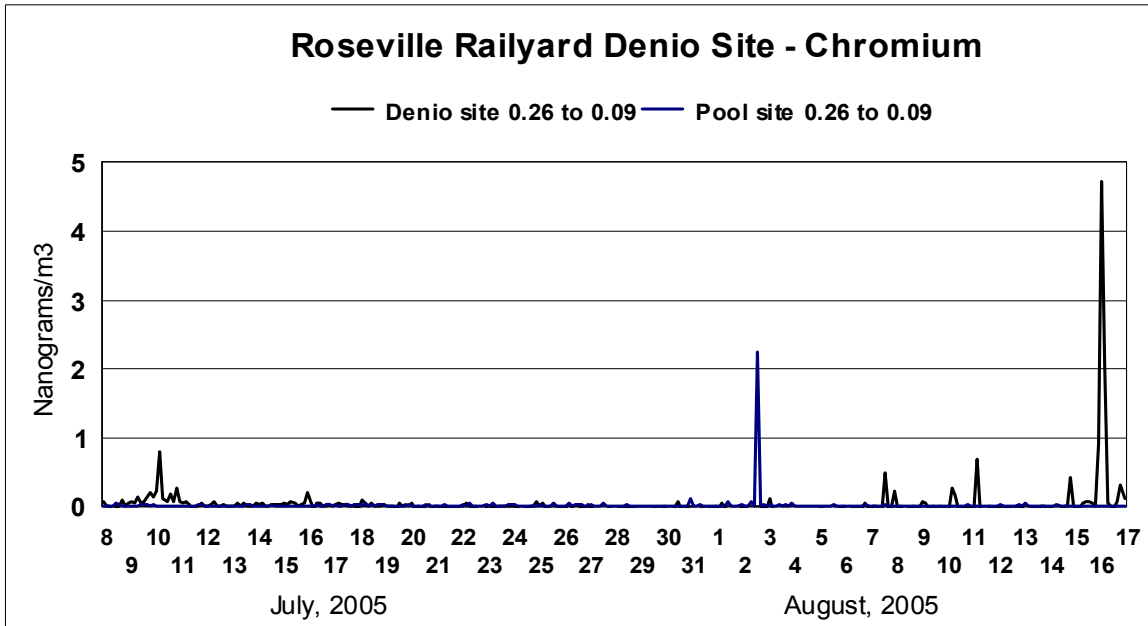


Figure 26 Comparison of very fine chromium, Denio Site vs Pool Site

In summary, the elemental data support and confirm the nighttime enhancement of aerosols expected from operations of the Roseville rail yard while identifying other components of unknown origin.

For this reason, with the completion of the EPA Region 9 grant, full elemental size distributions are now available at the Denio site, which greatly assists us in interpreting the data. We have also repeated S-XRF runs which are part of the Level 1 quality assurance protocols for S-XRF, similar to those shown earlier for mass.

The presence of a relatively large amount of mass (Figures 8 and 9) at sizes not typical of fresh diesel exhaust encourage DELTA to propose to measure these species to complete the picture of aerosols at the Denio site in summer. Thus, the un-analyzed DRUM Stages 1 through 7 (10.0 to 5.0, 5.0 to 2.5, 2.5 to 1.15, 1.15 to 0.75, 0.75 to 0.56, 0.56 to 0.34, 0.34 to 0.26 μm aerodynamic diameter) were analyzed by S-XRF in 3 hr increments.

The first result was the discovery of periodic oceanic influence in the form of sea salt (Figure 27).

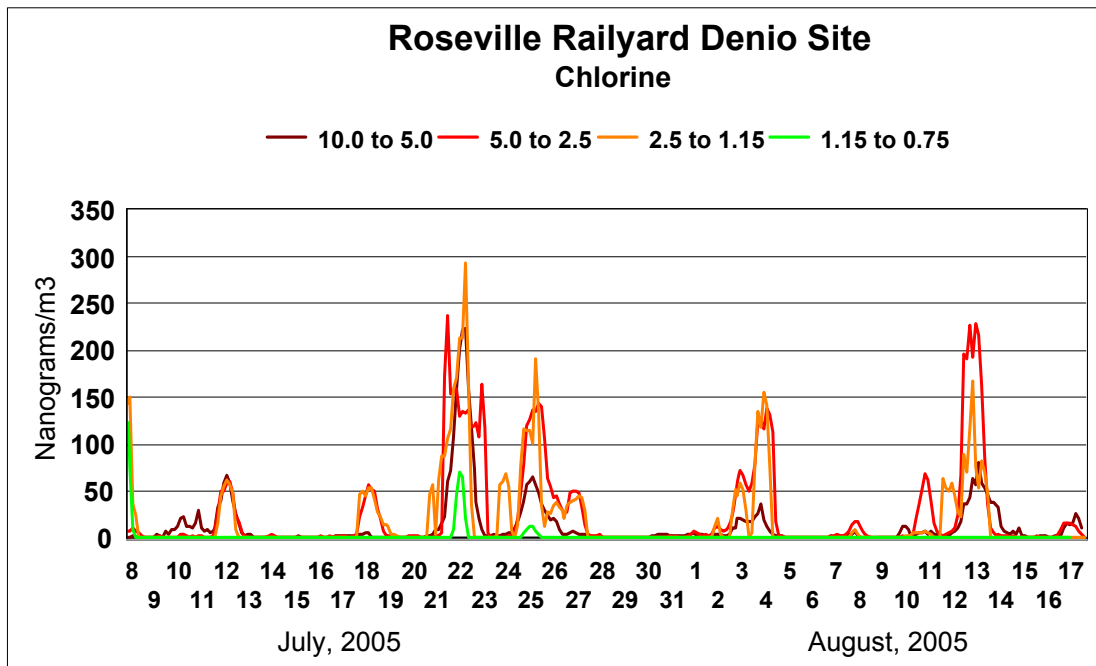


Figure 27 Sea salt signature in coarse particle chlorine.

This hypothesis was confirmed via trajectory analysis from the NOAA READY ARL HYSPLIT isentropic trajectory program, version 4. High speed transport trajectories for the chlorine peaks were associated with rapid transport of air from the ocean near Point Reyes to Roseville (Figure 28).

NOAA HYSPLIT MODEL
 Backward trajectories ending at 19 UTC 22 Jul 05
 FNL Meteorological Data

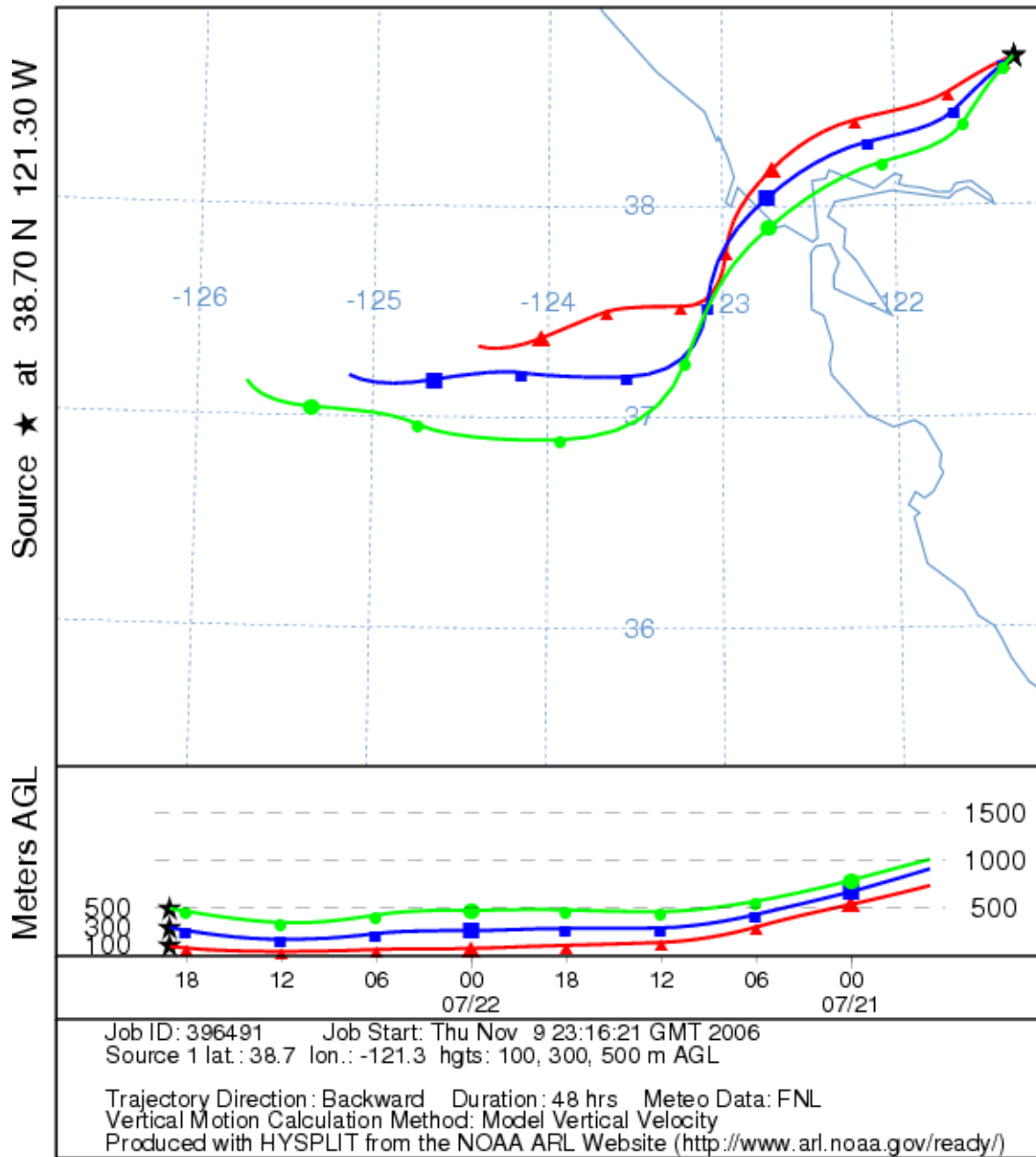


Figure 28 HYSPLIT trajectory showing Bay Area transport, July 22, 2005

The strongest correlation between nighttime transport across the rail yard was sulfur (Figure 29), a component of burned diesel fuel in the very fine particle mode (Figure 14). Examining the variation of sulfur with size and time, we can see that the pattern in the expected very fine ($0.26 > D_p > 0.09 \mu\text{m}$) mode extends into the accumulation mode.

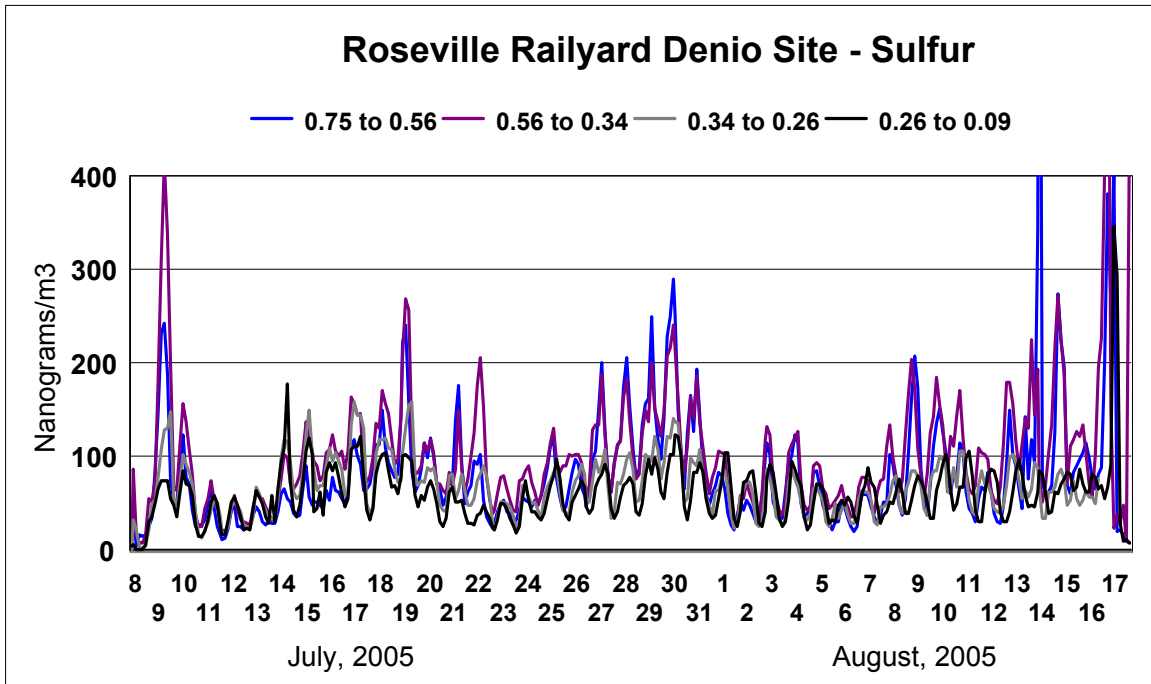


Figure 29 Sub-micron sulfur at the Denio site

While the strong day night pattern in very fine sulfur was expected, what was not expected was the continuation of this pattern into accumulation mode aerosols up to 0.75 μm diameter, and even larger (Figure 30), although mass measurements (Figures 8 and 9) had shown mass present in these sizes.

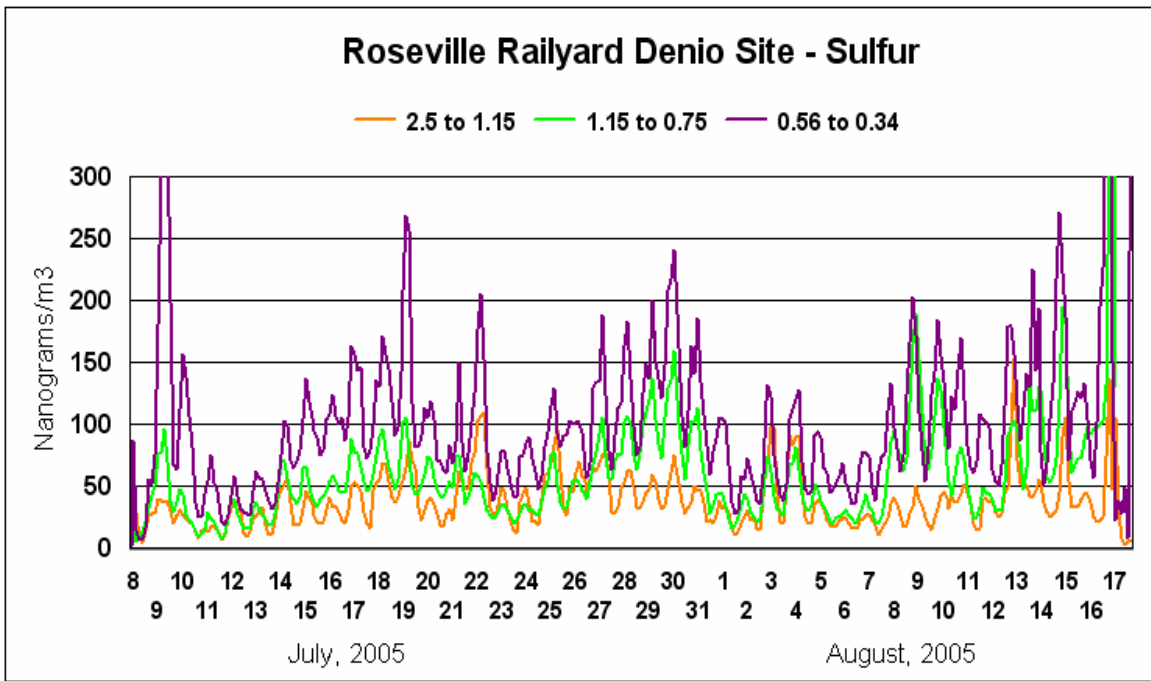


Figure 30 Components of fine sulfur at the Denio site

Then results from sulfur can be contrasted with that of soils, as shown by the iron tracer in the larger size modes (Figure 31, 32).

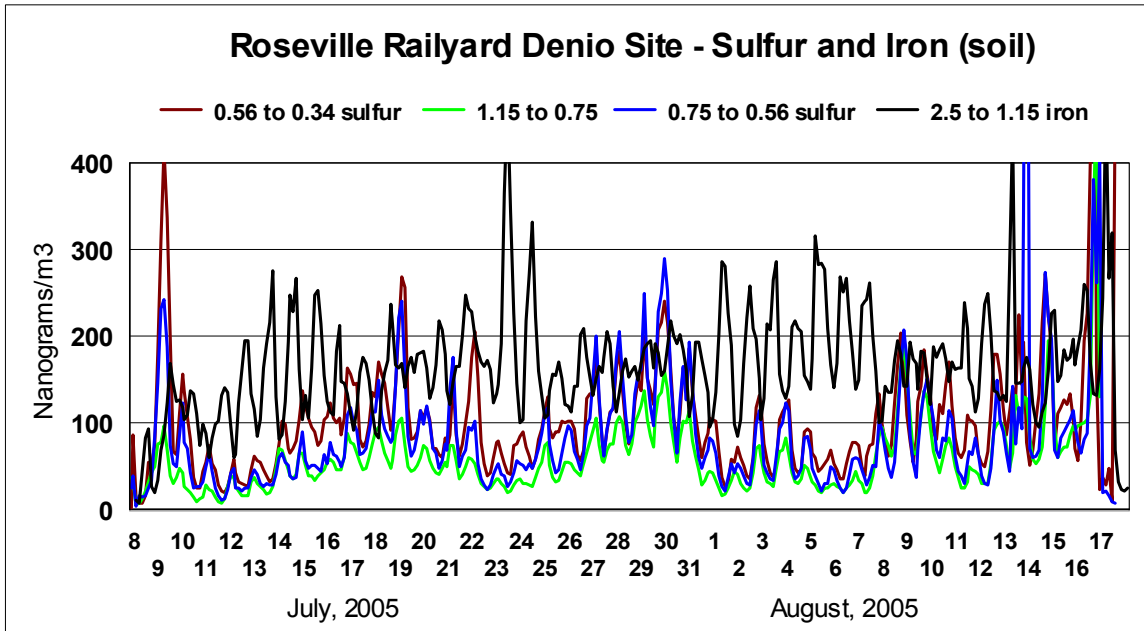


Figure 31 Sub-micron sulfur versus fine iron at the Denio site

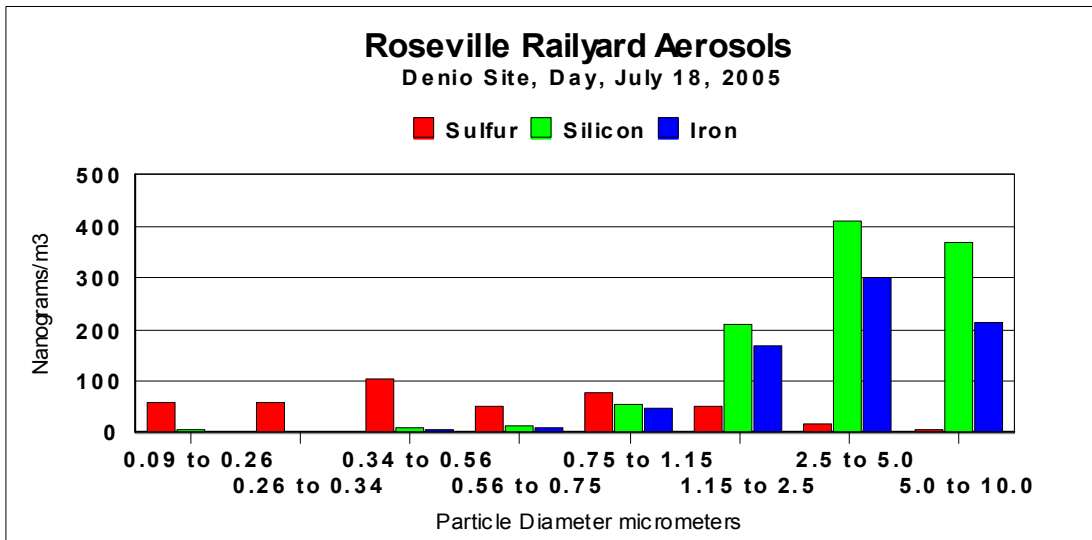


Figure 32 Size distribution of sulfur and soils, daytime, July 18, 2006

The almost perfect anti-correlation of fine sulfur to coarse soil is fully consistent with the meteorology of the site and the stronger daytime winds from the southwest. However, the situation becomes more complex than simply soil in day and diesels at night. Below we show the graph (Figure 33) for the major soil elements, silicon, for the summer period. The high levels on July 9 came on strong winds, gust to 18 mph, from the southwest, across the Denio’s Farmer’s Market, which was in operation that day. The size distribution is somewhat finer than typical wind blown dust.

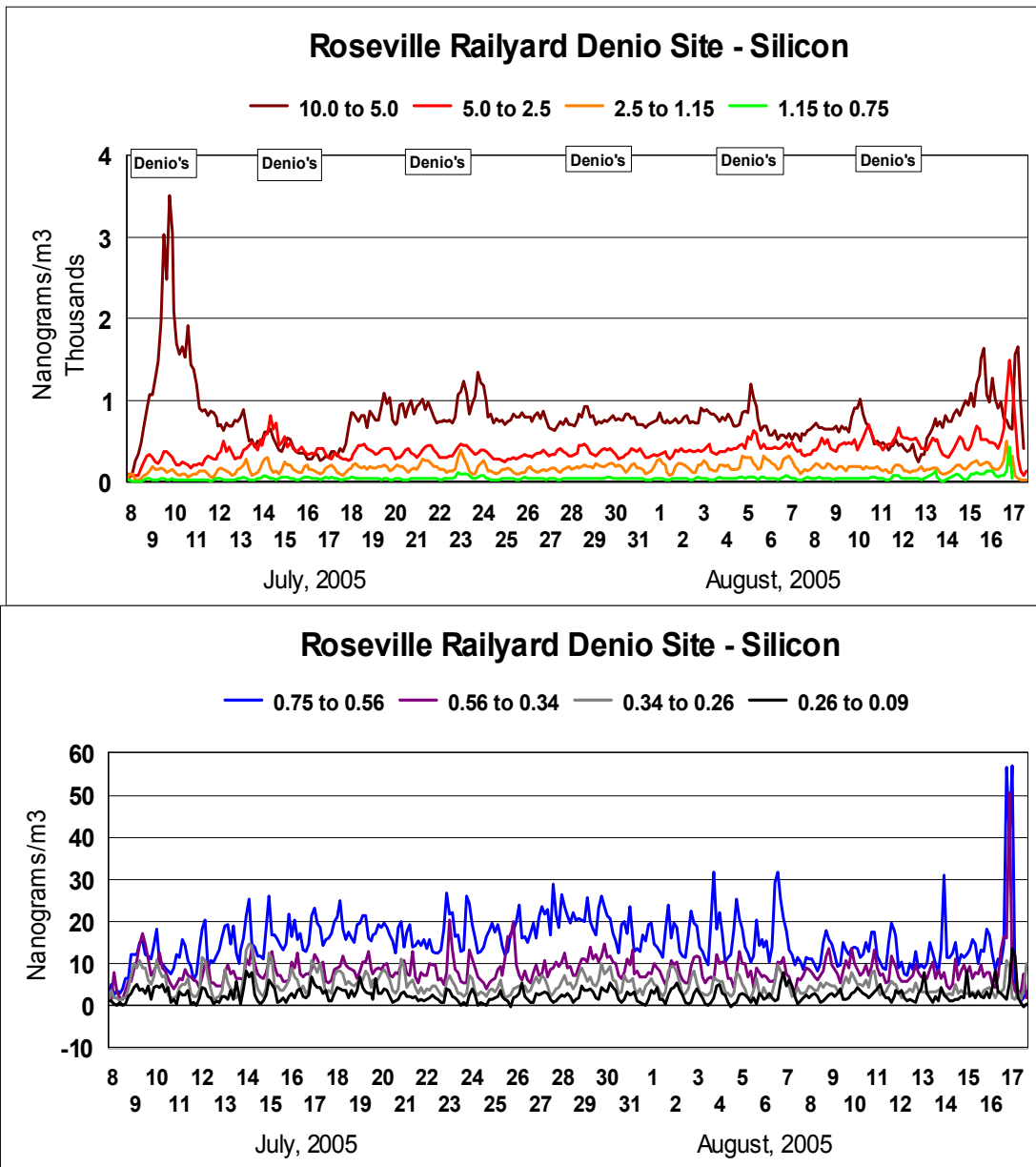


Figure 33 Time plots of coarse and fine silicon, Denio site

But there is also a small amount of silicon seen each night in very fine size modes, coming from the rail yard (Figure 34). The source of this material is unknown at this time.

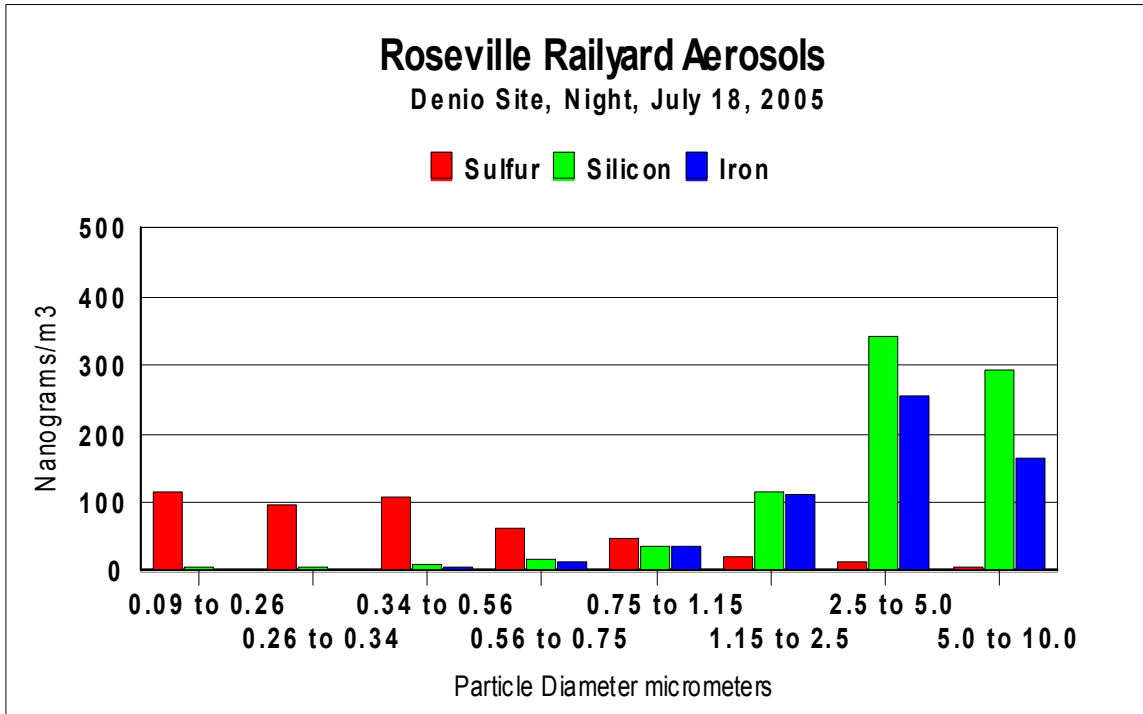


Figure 34 Size distribution of sulfur and soils, nighttime, July 18, 2006

Potassium also has anomalous behaviors, with the coarse potassium clearly of soil origin, but finer accumulation mode potassium, usually a signature of wood smoke, peaking typically when the Denio's Farmers Market was in operation (Figure 35).

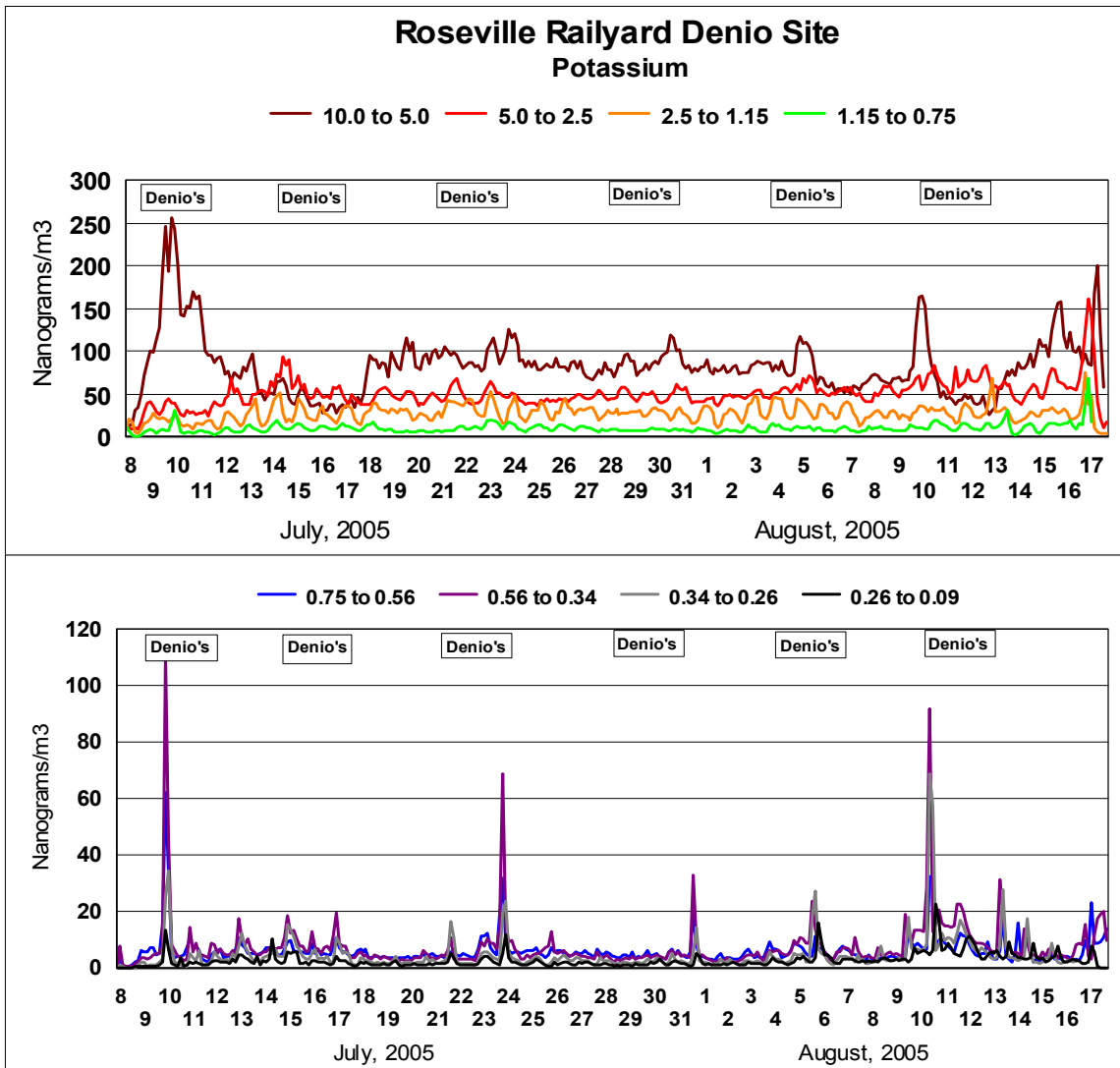


Figure 35 Time plots of coarse and fine potassium, Denio site

However, the coarser size modes also possess a number of anthropogenic metals. Below (Figure 36) we show an example of chromium and vanadium in the upper end of the fine size mode, 2.5 to 1.15 μm diameter, a region of particle size that has significant lung capture potential, circa 20%. Also shown is zinc in the fine particle and accumulation modes. The clear day-night patterns seen in some of the species like sulfur are much weaker in the metals, although at times there are strong enhancements at night. At other times, sources are clearly more complex.

NOAA HYSPLIT MODEL
 Backward trajectories ending at 17 UTC 27 Jul 05
 FNL Meteorological Data

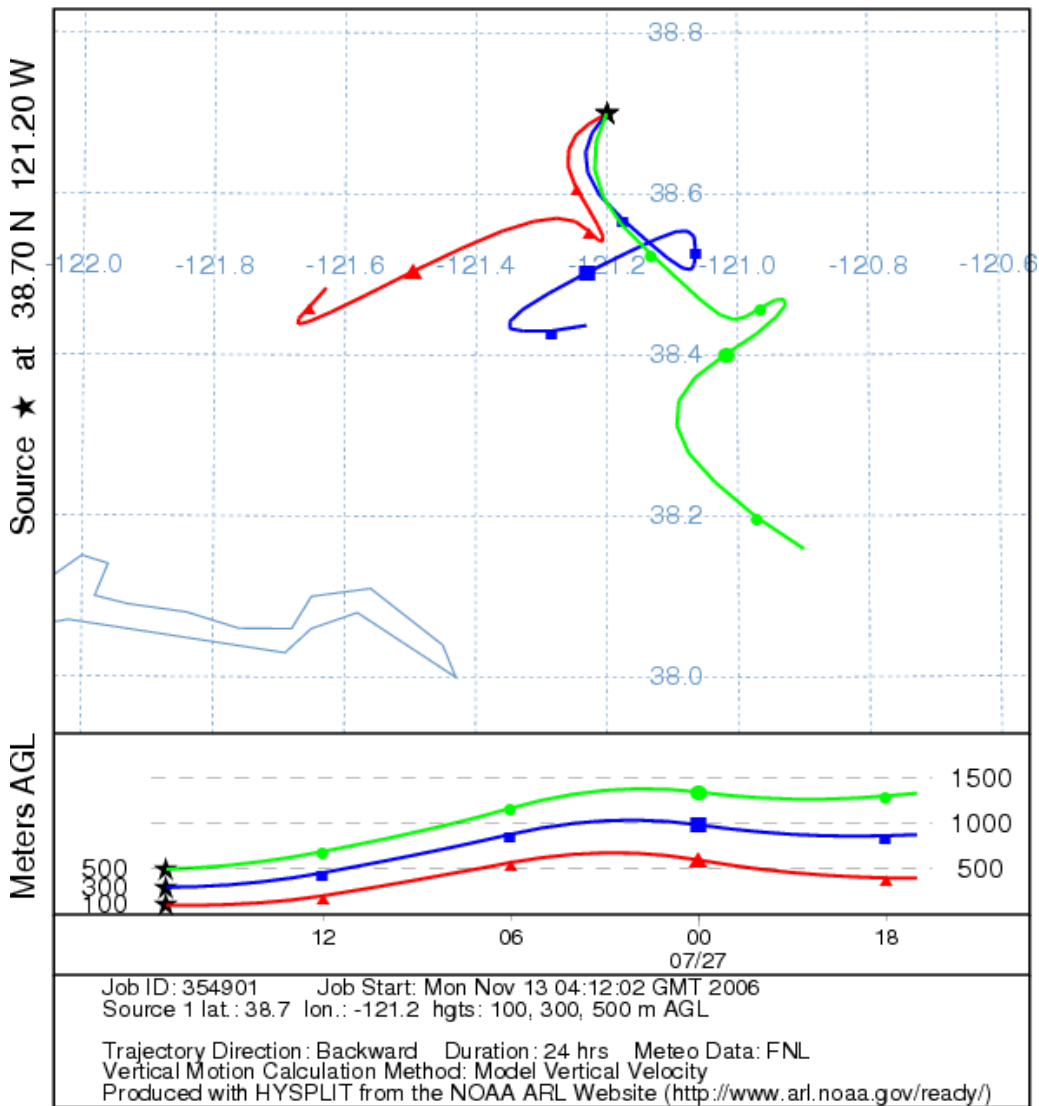


Figure 38 Wind trajectories at the beginning of the zinc episode, on the morning of July 27. The typical night time cross-rail yard winds were weak and of short duration. during this episode.

Other elements may or may not be involved in these episodic spikes of metals. For example, below we show the very fine data from both the Denio site and the pool site (Figure 39). Note that there is little copper in the zinc episode around July 27, and that the Pool site was also involved. All the evidence points to a source or sources southwest of and outside of the Roseville Rail yards.

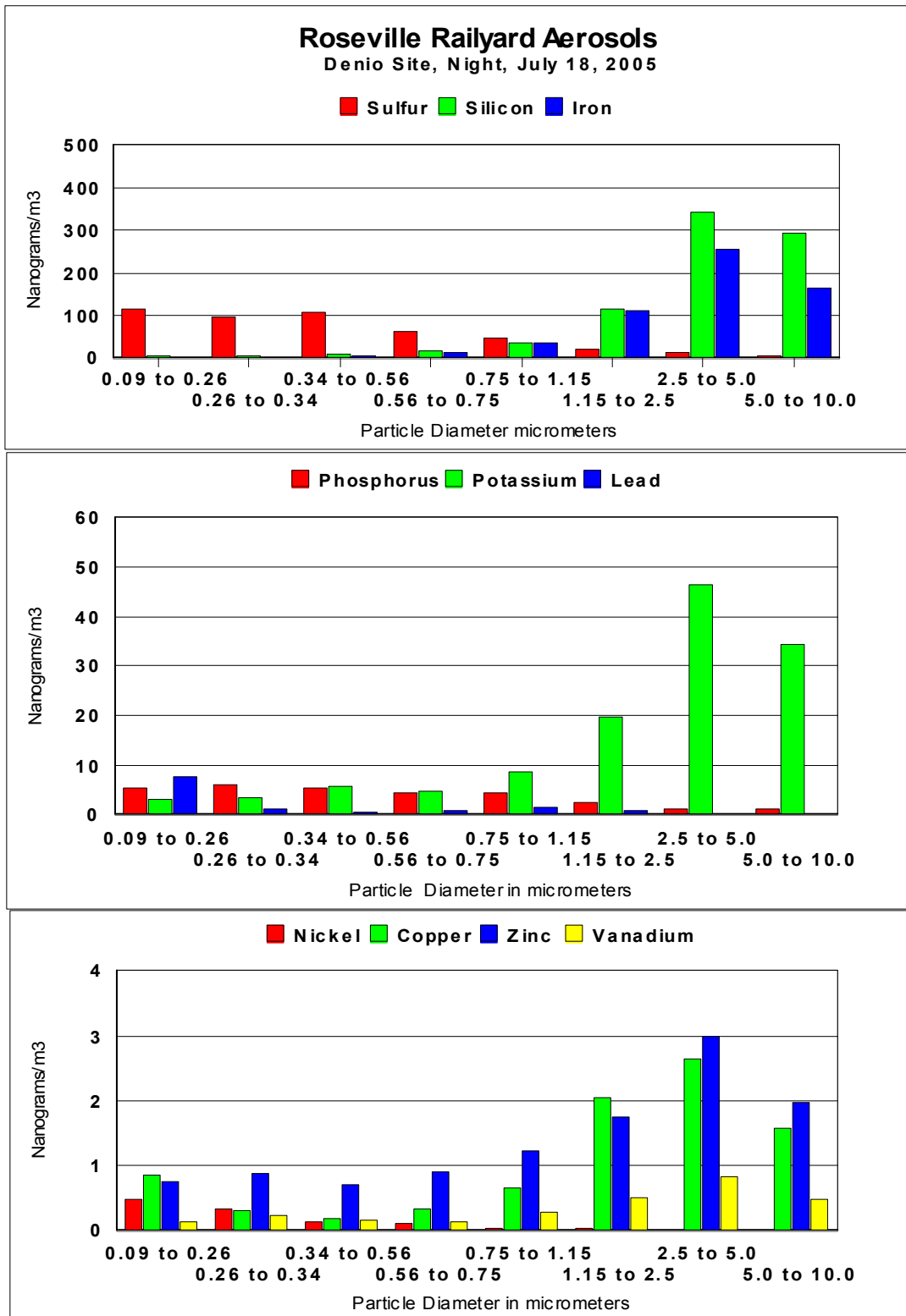


Figure 40 Size Distribution of elements on July 18, 2006, during night time cross rail yard winds.

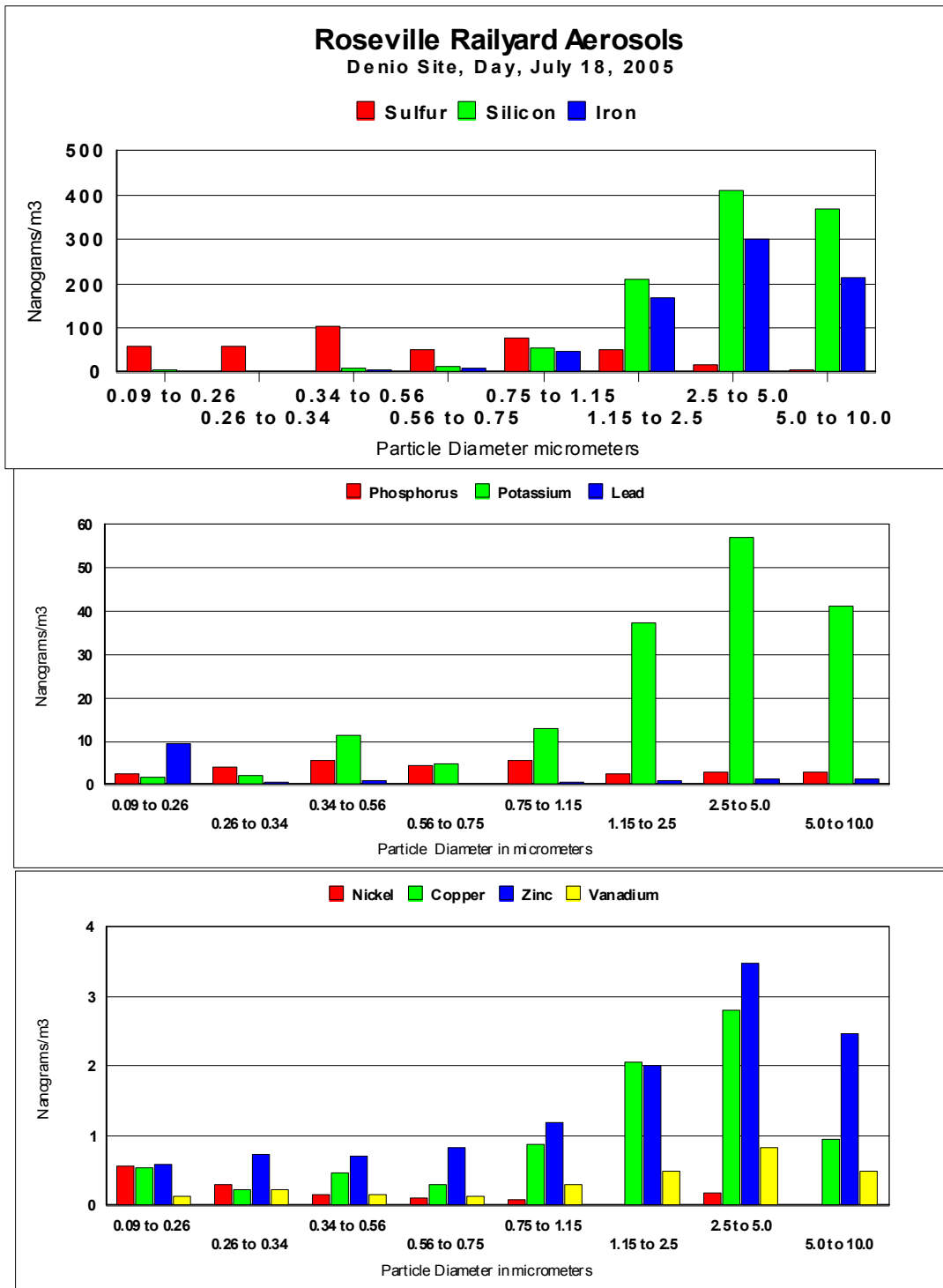


Figure 41 Size Distribution of elements on July 18, 2006, during day time winds from the southwest roughly parallel to the rail yard.

One of the most unexpected finding was that much of the same behavior occurred during daylight hours, when winds typically blew to the Denio site roughly parallel with to rail yard tracks and at a higher wind velocities.

C. Organic sampling and analysis of aerosols, Denio Site

The Roseville Rail Yard is a large source of diesel emissions. Most of the analysis done thus far in RRAMP have focused on monitoring gasses (NO, NO_x) and particulate matter, (Black Carbon (EC) mass, PM_{2.5} mass), enhanced by mass and elemental composition as a function of particle size from the DRUM samplers. However, these alone may not accurately assess the toxicity of the diesel emission from locomotives since the emissions of chemicals from locomotives have not been well characterized. If locomotives are assumed to have the same emission profiles as diesel trucks, then it would appear that they may have an impact. However, there are reasons to believe that the emission profiles from the locomotives may be different than the data from trucks.

The present mass measurements show that the size of the aerosols emitted by locomotives in RRAMP are different than diesel trucks, (Figure 9), so the amount of the emissions that are respirable and the toxic chemicals contained therein may also be different. Thus any accurate assessment of the rail yard will need to determine the toxicity, by measuring the PAH concentrations, of the locomotive emissions at the site. For this reason, we added sample collection suitable for organic analysis towards the end of the summer, 2005 campaign, in the hopes of eventually being able to conduct organic analysis of the aerosols downwind of the Roseville Rail Yard. The samples were collected and placed in freezers until funds could be obtained to do the analysis. This section of the Final Report contains the results of these analyses.

1. Methods

We collected particulate matter from August to October, 2005 at the Denio downwind site using an 8-stage DRUM sampler and a Lundgren impactor (see table 1, repeated below). The Lundgren impactor has a high flow rate (~130 L/min) that collects considerable mass, but the size cut points are rather coarse (50% cut points of 17µm, 5µm, 2µm and 0.5µm for the four stages) for diesel exhaust. However, the large amount of mass collected gives a high degree of sensitivity. A quartz filter was then be used to collect aerosols with a diameter of less than 0.5µm. The Lundgren impactor was deployed for a two – 10 days intervals to collect a single set of samples (4 stages, 1 filter and 2 blanks).

The other sampler utilized will be the 8-stage DRUM sampler with aluminum substrates, which is identical to the sampler used for elemental and mass analyses. Using identical samplers will ensure accurate comparisons between the elemental and organic results. This sampler has a much lower flow rate (~16 L/min), so less mass will be collected and the sensitivity of the analysis will be lower. However, this sampler has 8 fractions with most of them being smaller than the Lundgren impactor. This understanding in which size fractions the PAHs reside is particularly important since it will determine how much of the total PAH load is present in the respirable aerosol fraction. Since the flow rate of this sampler is much lower, it was run for 6 weeks to collect a set

of samples (8 stages, one filter and 3 blanks). For this study, we were able to modify the DRUM sampler to accept an after filter.

We obtained two sets of Lundgren impactor strips and filters, which will give a total of 10 samples (4 size fractions and a filter for each of 10 days of operation). The 8-stage DRUM will give a total of 9 samples during its six-week long operation (8 stages + a filter). Therefore, there will be a total of 19 samples that will be extracted and analyzed for PAHs and *n*-alkanes. In addition, there was approximately 8 blanks to ensure that the sample substrates were clean and that there was little/no contamination from sample handling. After sample collection, the samples were stored in sealed glass jars at -20°C until sample extraction.

2. Sample analysis

Each sample was tested for four classes of compounds, namely PAHs, alkanes, organic acids and sugars. The first two classes of chemicals are non-polar and are often the result of primary emission sources. The organic acids and the sugars/levoglucosan are polar chemicals that require derivatization prior to analysis. The organic acids arise from both combustion processes and from biological materials while the sugars are almost always biological in origin. Levoglucosan is a famous tracer of biomass combustion (“wood smoke”), so it was determined to assess the contribution of wood smoke to the aerosols that were collected. Considering that the sample collection period was in the summer, we did not anticipate significant wood smoke signatures in the samples.

Each of the field samples were enriched with 100 ng of a series of deuterated PAHs and *n*-alkanes to determine the extraction efficiency of the analytical method. The labeled PAHs were: phenanthrene-*d*₁₀, fluoranthene-*d*₁₀, pyrene-*d*₁₀, chrysene-*d*₁₂, and benzo[*k*]fluoranthene-*d*₁₂ (Cambridge Isotope Laboratories Inc. Andover, MA) while the *n*-alkanes were *n*-tetracosane-*d*₅₀ and hexatriacontane-*d*₇₄ (Cambridge Isotope Laboratories Inc.). The samples were also enriched with benzoic-*d*₆ acid and succinic-¹³C₂ acid to represent the organic acids that are in the samples.

Each sample was placed in a 10 ml centrifuge vial and extracted three times with 7 ml of toluene (HPLC grade, Burdick and Jackson, Muskegon, MI) to remove the non-polar fraction and then the samples were then extracted three times with 7ml of methanol (purge-and-trap grade, Fisher Scientific Company, Fair Lawn, NJ). For the first extraction with each solvent, the sample centrifuge tube was wrapped in aluminum foil to protect it from light and then placed on a test tube shaker (Labquake series 1104, Barnstead Thermolyne, Dubuque IW) for 20 hours. After the first solvent wash, the samples were centrifuged at 3000 RPM (IEC Clinical Centrifuge, International Equipment Co., Needham Heights, MA) for 5 minutes to settle any solids. The solution was removed and transferred to another centrifuge tube for concentration by nitrogen evaporation. The second and third washes with each solvent were conducted for 2 hours each, thus the total extraction time was 24 hours for each solvent. After each wash, the sample was centrifuged before the solution was removed. The non-polar (toluene) and

polar (methanol) extracts were stored separately. For each sample, the toluene and methanol fractions were reduced to 2 ml by nitrogen evaporation.

The analysis of PAHs and *n*-alkanes only utilized the toluene fraction since these compounds will only be found in this fraction. One milliliter (50% of the sample extract) was removed and passed through a pasture pipet clean-up column consisting of 1.5 g of silica gel (70-320 mesh, Fisher Scientific Co.) to remove polar chemicals that may interfere with the analysis. The silica gel column was eluted with 7 ml toluene. The extract was concentrated by nitrogen evaporation to 100 μ l and then it was transferred to a GC vial. Pyrene-*d*₁₀ was then added to the sample, giving a concentration of 100pg/ μ l, to serve as an internal standard. The samples were then ready for analysis by gas chromatography- ion trap mass spectrometry (GC-MS).

The analysis of sugars and acids required derivatization by BSTFA (Supelco, Bellefonte, PA), which is a silylation reagent. In this case, 100 μ l of the toluene extract and 100 μ l of the methanol extract, which represent 5% of the total sample mass, were added to a GC vial. The extract was evaporated to dryness by nitrogen evaporation in the GC vial. The samples were re-constituted in 100 μ l of a 50:50 BSTFA:pyridine derivatization solution (pyridine from Aldrich Chemical Co.). The samples were then placed on a drybath heater set to 40°C for 24 hours. After derivatization was complete, the samples were uncapped and pyrene-*d*₁₀ was added as an injection standard. The samples were then ready for analysis by GC-MS.

All samplers were quantified using a Varian 3400 GC coupled to a Saturn 2000 ion trap mass spectrometer (Varian Inc., Walnut Creek, CA). The analytical column was a Varian Factor Four High Temperature Column (30m length, 0.25mm ID, 0.1 μ m film thickness, and 5% phenyl substituted stationary phase). Helium was used as the carrier gas with a linear velocity of 37cm/sec. The oven program for the PAH and *n*-alkane analyses was: initial temperature of 64°C held for 5 minutes, then ramp 5°C/min to 375°C, and hold for 5 minutes. The sugar and acid analysis had a similar program except that it started at 35°C (hold 5 minutes), and then ramped 5°C to 330°C. Sample introduction consisted of 5 μ l injection of the sample extract onto a glass wool-packed injection port liner that was maintained at 5°C or more below the boiling temperature of the sample solvent. The injection port temperature was then increased to 375°C for the PAH and *n*-alkane analyses and 300°C for the sugar and acid analysis. This causes the analytes to volatilize from the injection port and move onto the column before the column temperature is increased. The PAH analysis were the only exception to this procedure since 20 μ l of the sample was injected rather than 5 μ l to achieve greater sensitivity.

The analysis of the sugars, acids and *n*-alkanes utilized a simple electron ionization (EI) mass spectrometer program with a scan range of 50 to 650 mass units. All instrumental conditions were Varian default settings except for the target ion count, which was reduced from 20,000 to 10,000. The ion trap temperature was set at 220°C for all analyses. The PAH analysis program was different in that it used MS-MS techniques to improve sensitivity and selectivity. In this case, the molecular ion of each PAH was isolated and then further fragmented by collision-induced disassociation where resonant

excitation was used to impart energy to the ions. The resonant excitation energy was optimized for each PAH to produce the maximum abundance of secondary ions. Identification and quantification was conducted using the product ions, which typically consisted of the loss of H₂ from the molecular ion.

Quantification was conducted by a six-point calibration curve for each class of chemicals. If a field sample had a concentration that exceeded the calibration curve, then the sample was diluted 10-fold and re-analyzed to bring the response within the calibration curve. For the *n*-alkanes, we only had authentic standards of C₁₆, C₂₄, C₃₀, and C₃₆ *n*-alkanes. The other alkanes between C₂₀ and C₃₅ are tentatively identified by their mass spectra and their retention time sequence. Quantification assumed the same relative response as the nearest authentic standard, which may create a minor bias in calibration. In the case of the acids and sugars, the calibration curve was derivatized alongside the samples to keep the derivatization time and conditions identical to the field samples. Pyrene-*d*₁₀ was used as the injection standard for all analyses. The other labeled compounds added to the sample before extraction were used to determine the extraction efficiency of the analytical method. The data are not corrected for extraction efficiencies of the analytes. All final concentration data are rounded to two significant digits of accuracy.

The results provide size-resolved PAH and alkane data from downwind of the Roseville Rail Yard. The important aspect of this research is determine the PAH concentrations in the aerosol size fractions that can penetrate into the deep lung, and thus represent the greatest exposure hazard. This is particularly important for the rail yard since the emissions from locomotive engines have not been well characterized in terms of the size of the particulate matter emitted, thus we need to determine the size distribution of the aerosols and the associated PAHs to assess the potential health effects.

3. Results for Organic Constituents

Recoveries of isotopically labeled compounds from samples

One of the best measures of the efficacy of an analytical method is the recovery of isotopically labeled surrogate compounds to the samples. Since the isotopically labeled compounds have a different mass from the “native” analytes, they do not interfere with the analytes in the samples. However, the isotopically labeled analytes have the same chemical properties and behavior as the native analytes. Therefore a good recovery of the labeled surrogate compounds from the samples gives a high degree of confidence that the native analytes were also effectively extracted.

A series of 9 labeled surrogate compounds were added to all samples and blanks. The recoveries of these labeled compounds were generally good to acceptable (Table 6). Phenanthrene had the lowest recovery of any of the PAHs at 54.6%, but this was expected since phenanthrene is a semi-volatile PAH and could easily evaporate from the samples during processing. The recoveries of all of the heavier PAHs and the two *n*-alkanes were good. Only two organic acids were utilized in this. Benzoic acid showed 118.5% recovery, which suggests that the spiking solution may have been inaccurately

measure. Succinic acid (AKA butanedioic acid) showed a poor recovery partly due to the low response of the instrument to this compound. In the future, long chain alkanolic acids (e.g. octadecanoic acid) should be added to the surrogate solution mixture since they were the most abundant organic acids detected and their chemistry is significantly different from the benzoic and succinic acid surrogates that were utilized.

Table 6. Average recovery (%) of isotopically labeled compounds to all the samples and blanks ($n = 27$) and MDLs for PAHs (for full list, see Appendix QA)

Compound	Recovery (%)	MDL pg/m ³	MDL pg/m ³
		8-stage DRUM	Lundgren Sampler
<u><i>n</i>-alkanes</u>			
<i>n</i> -tetracosane- <i>d</i> ₅₀ (C ₂₄)	71.0		
<i>n</i> -hexatriacontane- <i>d</i> ₇₄ (C ₃₆)	73.0		
<u>PAHs</u>			
phenanthrene- <i>d</i> ₁₀	54.6	2.8	1.4
chrysene- <i>d</i> ₁₂	76.9	8.9	4.4
benzo[<i>k</i>]fluoranthene- <i>d</i> ₁₂	74.1	3.5	1.7
benzo[<i>g,h,i</i>]perylene- <i>d</i> ₁₂	86.9	3.2	1.6
<u>acids</u>			
benzoic- <i>d</i> ₆ acid	118.5		
succinic- ¹³ C ₂ acid	50.5		

Based on the recovery data of the labeled surrogates from all the sample matrices (aluminum foil and quartz filters), it appears that the analytical method was effective for the heavier PAHs, *n*-alkanes and some of the organic acids. The data reported herein has not been corrected using the above recovery data, so we would anticipate that there is approximately a $\pm 30\%$ error for most of the chemicals.

a. Polycyclic aromatic hydrocarbons (PAHs)

The results from the PAH analysis clearly showed high concentrations of PAHs in the particulate matter (Table 7) with the majority of the PAH mass being collected in the ultra-fine stage (0.26 to 0.09 μm) and the afterfilter (Figure 43). The presence of PAHs in the ultra-fine size fraction corresponds well to previous observations of PAHs in diesel emissions (Zielenska et al, 2004; Gertler et al, 2002). The presence of a strong marker for fresh diesel emissions was expected.

Note that the Lundgren sampler was only operated at night when the air is coming from the rail yard, thus it has higher concentrations. For this reason, the 8 DRUM results are scaled by a factor 2.57 to account for PAHs only at night (from the NO ratios of Figure 2.a, x 2.0) and the ratio of EC, 1.4 (Table 3, x 1.29) to allow better comparison to the Lundgren data. This amounts essentially to an assumption that all PAHs come from the rail yard on night winds.

Table 7. Concentrations (pg/m³) of particulate PAHs observed at the Roseville Rail Yard in the summer of 2005 (MDLs in parentheses).

Compound and MDLs (in pg/m ³), (8 DRUM; Lundgren)	8-stage DRUM (8/5 - 9/27)	8-stage DRUM (scaled x 2.6) (8/5 - 9/27)	Early Lundgren (9/27 - 10/7)	Late Lundgren (10/7 - 10/17)
Phenanthrene (2.8; 1.4)	21	55	110	100
Anthracene (7.9; 3.9)	< 7.9	< 20	20	20
1-methylphenanthrene(0.61; 0.30)	< 0.61	< 1.6	32	28
Fluoranthene (1.3; 0.65)	57	147	160	160
Pyrene (1.5; 0.72)	74	190	310	300
Benz[<i>a</i>]anthracene	^a	^a	^a	^a
Chrysene+ triphenylene (8.9; 4.4)	24	62	130	130
Benzo [<i>b+k</i>]fluoranthene (3.5; 1.7)	68	175	350	330
Benzo[<i>e</i>]pyrene (0.69; 0.34)	90	231	360	350
Benzo{ <i>a</i> }pyrene (0.71; 0.35)	68	175	270	280
Perylene (4.4; 2.2)	< 4.4	< 11.4	35	36
Indo[1,2,3- <i>cd</i>]pyrene (4.0; 1.9)	84	216	240	230
Dibenz[<i>a,h</i>]anthracene (2.7;1.3)	100	257	270	270
Benzo[<i>g,h,i</i>]perylene (3.2; 1.6)	230	591	650	650
Coronene (5.5; 2.7)	175	450	380	370

^a Unable to quantify compound due to analytical problem, namely excessive enrichment of chrysene-*d*₁₂ that saturated the ion trap mass spectrometer.

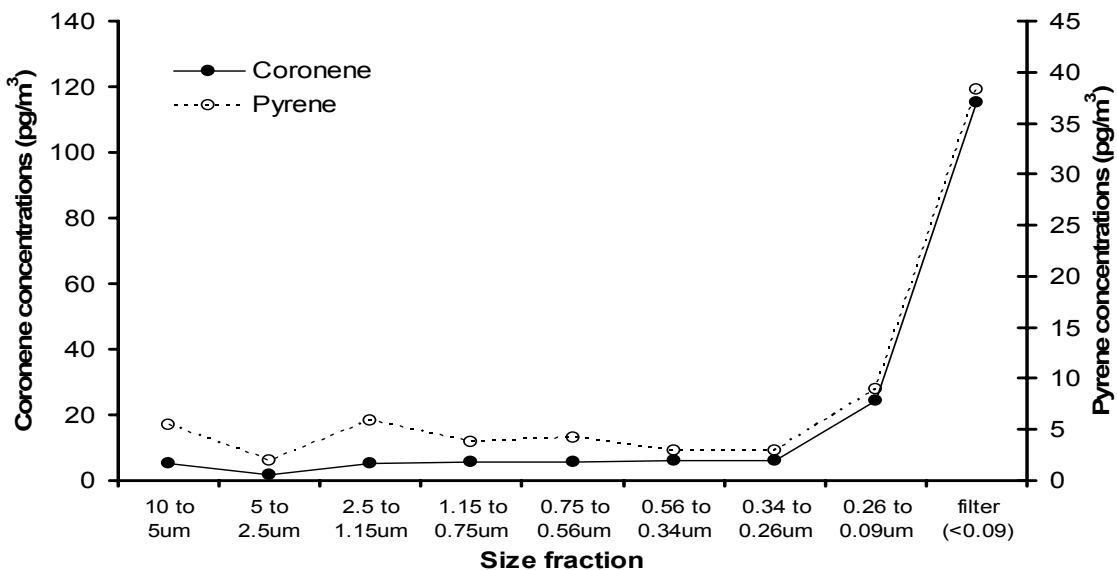


Figure 42. Coronene and pyrene concentrations (pg/m³) is the different size fractions of the 8-stage DRUM sampler and the afterfilter.

The presence of the PAHs in the ultra-fine stage indicates that the diesel source was close to the sampler since the particulates had not coagulated into larger particles, which also suggests that the source of the particulates was the rail yard.

The PAH results from the Lundgren sampler also support these observations. This sampler was only operated during the nighttime hours when the local meteorology brings a weak down-slope breeze across the rail yard and to the sampling site. Therefore, the higher concentrations observed by this sampler were expected and support the assertion that they are coming from the site. The air concentrations were approximately 4 times higher than the 8-stage DRUM, which appears to be the result of the 8-stage DRUM samples being “diluted” by the daytime sampling that lacked any rail yard influence (Figure 3 a, x 2) and the increasing mass in the fall periods (x 1.28). The combination of these factors give a multiplicative factor of 2.57, which is presented in the tables. Inversions become more common in fall and winter, raising the very fine mass from a value of $2.25 \mu\text{g}/\text{m}^3$ in summer (DRUM sages 7 + 8, 0.34 to $0.09 \mu\text{m}$) to $6.6 \mu\text{g}/\text{m}^3$ measured in February, 2006, using identical equipment. Thus, the Lundgren samplers were collecting in periods that would tend to have higher masses at the Denio site. In summary, the mass differences in organic matter from the summer 8 DRUM samplers and the fall night-only Lundgren samplers are consistent.

The PAHs from the locomotive diesel engines showed a very different trend in terms of the PAH profile compared to diesel engines used in trucks and other on-road applications. The PAH profile from the locomotives had considerably more of the heavy PAHs with molecular weights greater than 252 compared to the on-road diesel trucks and the NIST standard reference materials (Figure 43). This trend was observed with all three samples collected, namely the 8-stage DRUM and both of the Lundgren samples.

The higher proportion of the high molecular weight PAHs of locomotive emission may affect the overall toxicity of these emission compared to smaller diesel engines since the larger PAHs classes include some of the more toxic PAHs such as benzo{a}pyrene. Therefore, the standard cancer assessment based on diesel truck particulate mass may be biased on the low side. While it appears that the locomotive emissions have a higher proportion of heavier PAHs, it is unclear from these data whether the PAHs are arising from the large-bore engine technology, the locomotive fuel, which is different from the diesel fuel used in trucks, or the lubricating oils.

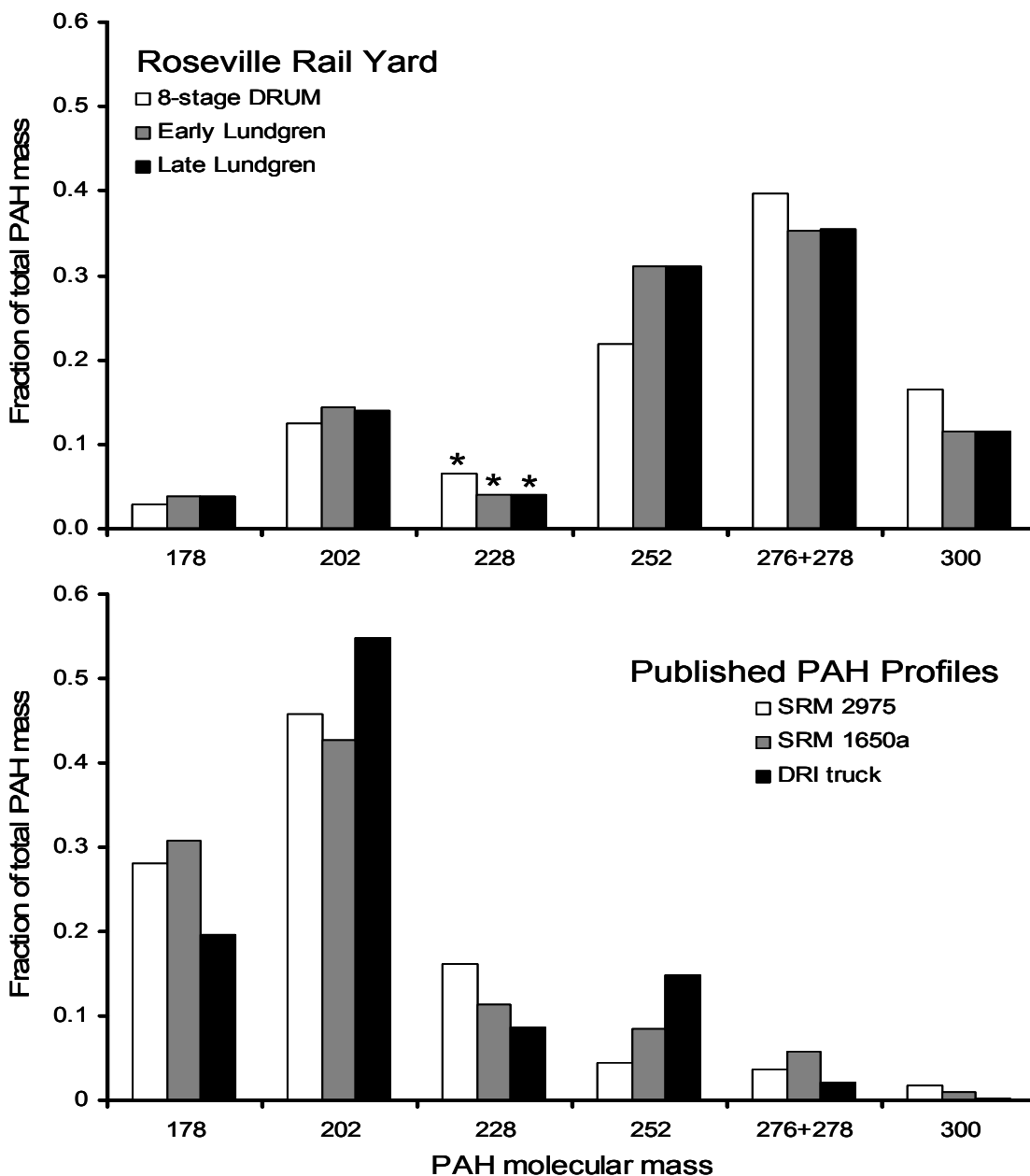


Figure 43. Profiles of PAHs as a function of molecular mass from the Roseville rail yard and the literature.

The molecular mass of benzo{a}pyrene is 252. Note that the molecular profile of the 8 DRUM (summer) and the Lundgren sampler (fall) are essentially identical. The “228” values in the Roseville samples are an underestimate since we could not quantify benz{a}anthracene due to an analytical problem.

One possible explanation for different PAH profiles is that the lighter PAHs could “blow-off” of the sample during the long sample collection periods. We do not believe this to be a significant effect since the “early” and “late” Lundgren samples had almost the identical profiles, yet the “early” sample were in the sampler for a week and a half

longer than the “late” samples. If blow-off was significant, then we would expect the samples exposed to the air stream for a longer period of time to have lower proportions of the lighter (178 and 202 amu) PAHs. This was not observed. Furthermore, the 8-stage DRUM sampler collected material for 6 weeks, and its profile is likewise very similar to the Lundgren samples that were only 1.5 weeks in duration and only operated at night. Therefore, the PAH profile does not appear to be the result of “blow-off” during sample collection.

b. Alkanes:

The second class of chemicals investigated was the alkanes and related hydrocarbons. Unlike the PAHs, there were appreciable alkanes in the field blanks, but the concentration of alkanes were generally low enough not to interfere with the quantification of the alkanes (Table 8).

Table 8. Concentrations (ng/m³) of particulate *n*-alkanes observed at the Roseville Rail Yard in the summer of 2005.

Compound	8-stage DRUM (8/5 to 9/27)	8-stage DRUM (8/5 to 9/27) (scaled x 2.6)	Early Lundgren (9/27 to 10/7)	Late Lundgren (10/7 to 10/17)
C ₂₀ <i>n</i> -alkane	0.25	0.64	1.1	1.0
C ₂₁ <i>n</i> -alkane	0.50	1.29	2.1	1.7
C ₂₂ <i>n</i> -alkane	0.42	1.08	3.6	2.8
C ₂₃ <i>n</i> -alkane	0.94	2.42	5.2	4.0
C ₂₄ <i>n</i> -alkane	1.3	3.34	2.8	1.5
C ₂₅ <i>n</i> -alkane	2.5	6.43	7.5	5.8
C ₂₆ <i>n</i> -alkane	2.8	7.11	7.6	5.7
C ₂₇ <i>n</i> -alkane	4.4	11.3	10	7.5
C ₂₈ <i>n</i> -alkane	4.5	11.6	9.4	4.2
C ₂₉ <i>n</i> -alkane	9.4	24.2	17	11
C ₃₀ <i>n</i> -alkane	5.7	14.7	11	3.8
C ₃₁ <i>n</i> -alkane	8.6	22.1	13	5.9
C ₃₂ <i>n</i> -alkane	4.2	10.6	7.0	0.5
C ₃₃ <i>n</i> -alkane	4.2	10.8	6.4	1.3
C ₃₄ <i>n</i> -alkane	1.4	3.6	2.7	< MQL
C ₃₅ <i>n</i> -alkane	0.76	1.95	1.9	< MQL
C ₃₆ <i>n</i> -alkane	0.94	2.42	1.3	< MQL
Total identified alkanes	53	140	110	55
Undifferentiated hydrocarbon	210	540	530	450

Note that the Lundgren sampler was only operated at night when the air is coming from the rail yard. The “undifferentiated hydrocarbon envelope” represents the

integration of m/z 57 (C_4H_9) between the C_{20} and C_{39} n -alkanes where the mass calibration was based on the n -alkane standards.

Both the 8-stage DRUM and the Lundgren samples showed that the C_{29} n -alkane was the most abundant chemical observed with concentrations in 9 to 17 ng/m^3 . Unlike the PAH data, the concentrations of alkanes were different between the early and the late Lundgren samples with the early sample having concentration that were almost twice as high as the late sample. The 8-stage and early Lundgren samples had no clear pattern of odd-even carbon number species. This would suggest a petroleum source of the hydrocarbons. However, the late Lundgren sample had a clear preference for odd-number hydrocarbons, particularly for the heavier alkanes. This pattern would suggest a biological source for the hydrocarbon rather than a petroleum source. The lower alkane concentrations and the odd-length chain bias suggests that there was a background biogenic source of hydrocarbons on which the rail yard emissions are superimposed.

In addition to the specific n -alkanes that were identified and quantified, there was a large “envelope” of undifferentiated hydrocarbons that approximately eluted between C_{23} and C_{39} n -alkanes (Figure 44). This undifferentiated hydrocarbon envelope was integrated by selecting only m/z ion 57, which corresponds to C_4H_9 fragment between the C_{20} and C_{39} n -alkanes where the mass calibration was based on the n -alkane standards. As a double-check, ion 85 (C_6H_{15}), which is another common ion from saturated alkane chains, was also selected and integrated. The results agreed between the two methods within 10%, thus giving a reasonable degree of confidence in the identification of the “envelope” as mostly alkanes. It should also be noted that this extract was the toluene extract from the samples, thus non-polar constituents would be removed from the aerosols but not the more polar chemicals. This further contributes to the confidence in the identification. The estimated mass of the undifferentiated alkane envelope was 210 ng/m^3 for the 8-stage DRUM sampler while it was 530 and 450 ng/m^3 in the early and late Lundgren sampler. The identified n -alkanes represented anywhere between 12 and 25% of the undifferentiated hydrocarbon envelope. The undifferentiated alkane envelope showed interesting trends as a function of particle size (Figure 45). The highest concentrations were found on the afterfilter followed by the 2.5 to 1.15 and the 1.15 to 0.75 μm size fraction. This differs from the PAH results since the PAHs lacked the relatively high concentrations in the accumulation mode. The presence of the alkanes in the accumulation mode in the absence of PAHs suggest that there is a separate source of these undifferentiated hydrocarbons in addition to diesel combustion emissions.

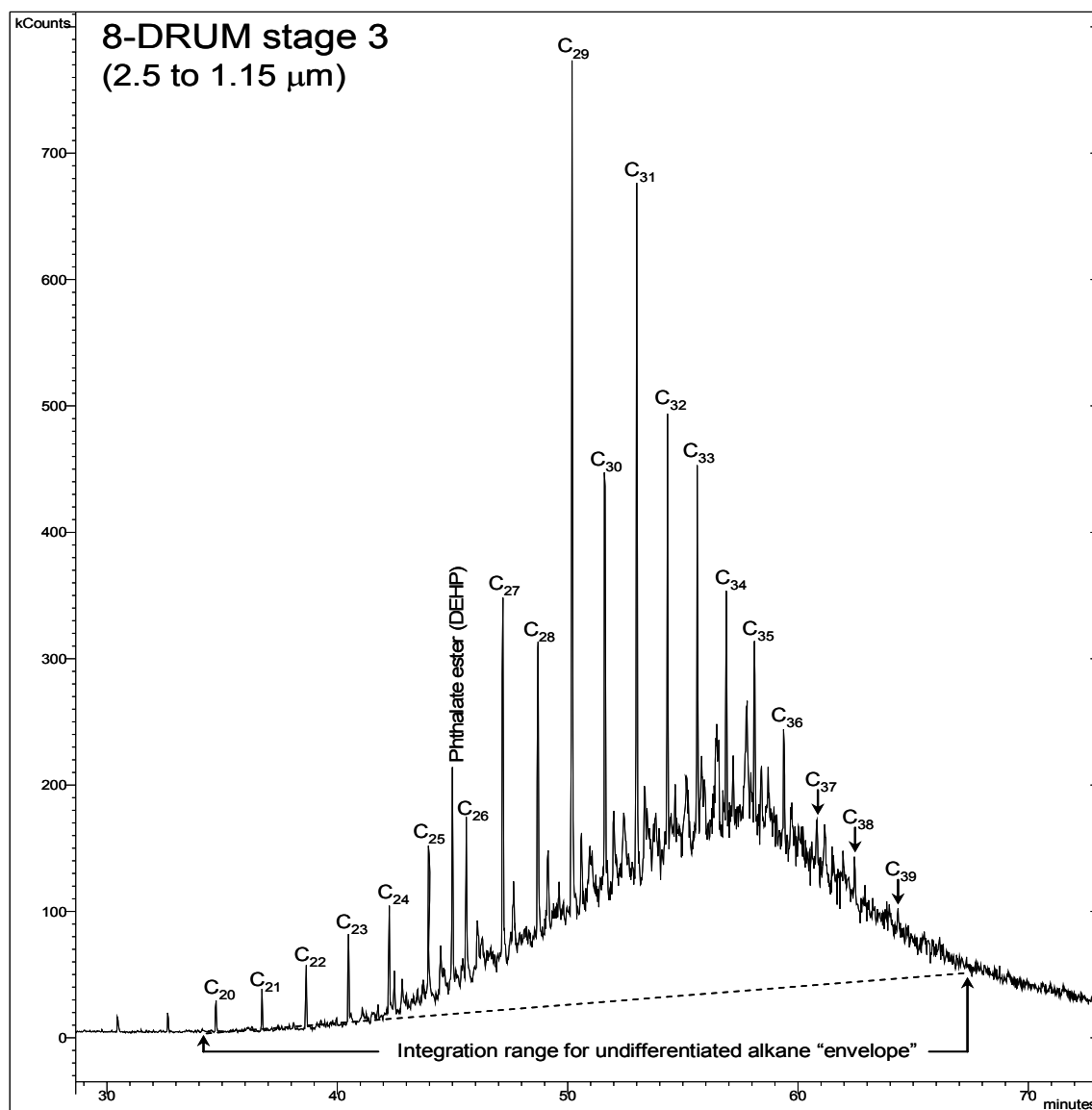


Figure 44. A selected ion chromatogram of m/z 57 showing the undifferentiated hydrocarbon “envelope”. The n -alkanes are labeled by their carbon number.

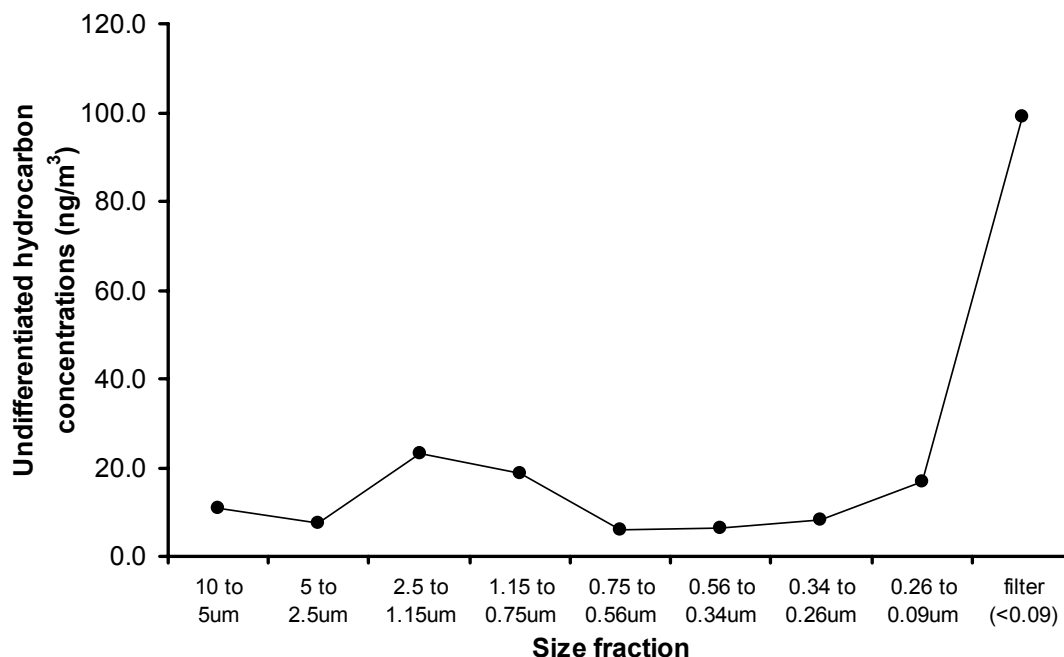


Figure 45 Concentrations of undifferentiated hydrocarbons in different size fractions of the 8-stage DRUM sampler.

Another interesting trend in the alkane results is the fraction of each alkane that was collected on the after filter differs with the size of the alkane (Figure 46). Quartz filters are famous for condensing organic vapors from the gas phase, so it is probable that alkanes in the gas phase were condensing on the filter. The results clearly show that increasing the carbon number of the alkane results in less of the alkane being collected on the after filter and more of the chemical being trapped on the aerosols that were impacted on the drums. The larger and heavier alkanes are simply not present in the gas phase of the atmosphere. Therefore, it appears that the lighter alkanes are passing through the impactor stages as a gas and then condensing on the filter. The implication of these results is that the *n*-alkanes may be volatilizing from the site in the gas phase as well as some particulate re-suspension.

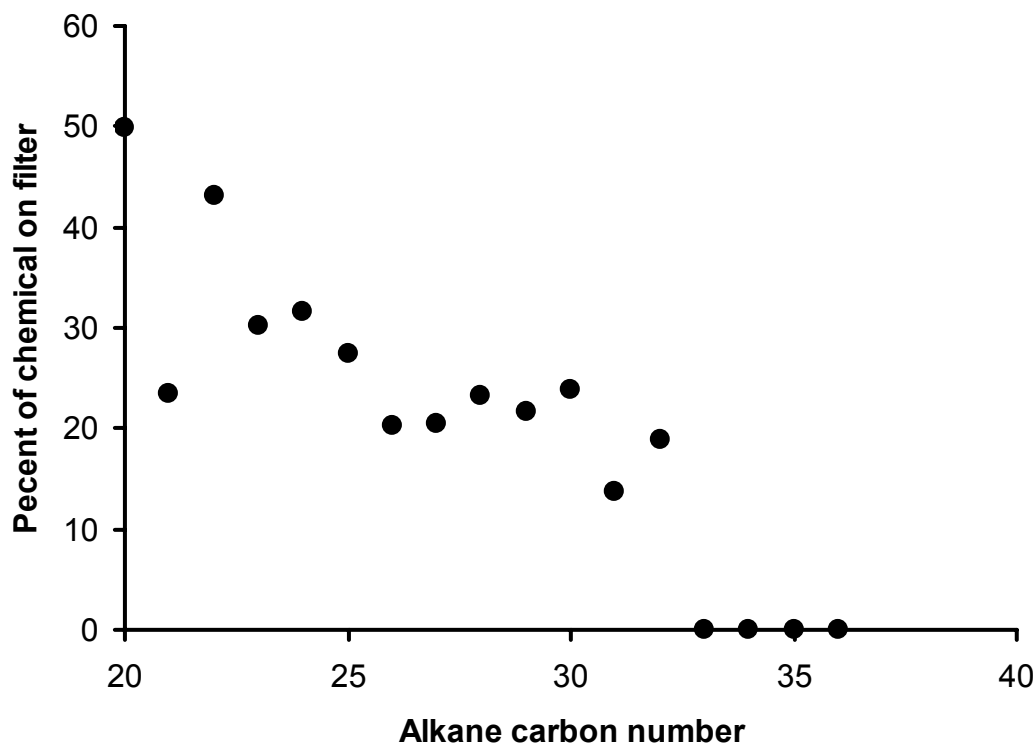


Figure 46. The fraction of *n*-alkanes collected on the after filter of the 8-stage DRUM. The C₃₃ to C₃₆ alkanes were not detected on the filter.

b. Organic acids

The particulate-associated organic acids were dominated by the long-chain alkanolic acids (Table 9) and hexadecanoic and octadecanoic acids in particular. The high abundance of these two acids strongly suggests a biological source for this particulate matter. This biological source can be either suspended bio-aerosols (pollen, microbes, spores, etc.) or biomass combustions (e.g. wood smoke). Another potential source would be cooking oil that may have been used at the nearby farmer's market. However, the presence of these acids combined with the effective absence of adjacent odd-number chain-length acids implies a non-petroleum source of this organic matter that is not associated with the rail yard.

Table 9. Concentrations (ng/m³) of particulate organic acids observed at the Roseville Rail Yard in the summer of 2005. Note that the Lundgren sampler was only operated at night when the air is coming from the rail yard.

Compound	8-stage DRUM (8/5 to 9/27)	8-stage DRUM (8/5 to 9/27) (scaled x 2.6)	Early Lundgren (9/27 to 10/7)	Late Lundgren (10/7 to 10/17)
Decanoic acid	< MQL	< <i>MQL</i>	< MQL	< MQL
Undecanoic acid	2.2	5.7	< MQL	< MQL
Dodecanoic acid	0.09	0.23	< MQL	< MQL
Tridecanoic acid	0.63	1.62	< MQL	< MQL
Tetradecanoic acid	0.43	1.11	< MQL	< MQL
Pentadecanoic acid	0.72	1.85	< MQL	< MQL
Hexadecanoic acid	4.6	11.8	7.7	8.4
Heptadecanoic acid	0.30	0.66	0.51	0.46
Octadecanoic acid	4.6	10.1	7.6	7.7
Nonadecanoic acid	0.05	0.13	0.08	< MQL
9-octadecenoic acid; (oleic acid)	0.70	1.80	0.79	< MQL
Butanedioic acid	1.6	4.1	5.1	5.5
Pentanedioic acid	0.65	1.67	1.4	1.5
Hexanedioic acid	1.3	3.34	0.41	0.41
Heptanedioic acid	0.23	0.59	0.74	0.77
Octanedioic acid	0.53	1.36	3.8	4.8
Nonanedioic acid	0.98	2.52	3.0	3.3
Decanedioic acid	0.05	0.13	0.61	0.63
2,3-hydroxybutanedioic 2-methyl-2-butenedioic acid	0.61	1.57	3.3	3.4
	< MQL	< <i>MQL</i>	0.21	< MQL
<i>Cis</i> -pinonic acid	< MQL	< <i>MQL</i>	< MQL	< MQL
Pinic acid	0.10	0.26	4.0	3.6
<i>Trans</i> -norpinic acid	< MQL	< <i>MQL</i>	< MQL	< MQL
Sum of acids	20	51	40	42

The scaling factor for night-time only emissions for RRAMP sources is not necessarily true for these acids. Thus, the agreement (or lack thereof) between the scaled data and the night only Lundgren data is just another tool to identify sources. However, there are a number of case for which the scaling makes the (DRUM 24 hour data agree better with the nighttime only Lundgren data, hinting at a mixture of biogenic and anthropogenic sources.

The concentrations of the predominant organic acids as a function of aerosol size further supports the identification of these chemicals as having a biological source (Figure 47). Octadecanoic acid was only found in the larger size fractions greater than 0.75µm and the afterfilter. Additionally, there was appreciable mass in the largest size

fraction between 5 and 10 μm , which is typically the domain of suspended dust. Therefore, these largest particles simply contain biological materials as part of the ambient dust. The hexadecanoic and octadecanoic acids were effectively absent from the fine particulate sizes, except for the afterfilter, thus implying that combustion probably was not a significant source of these acids.

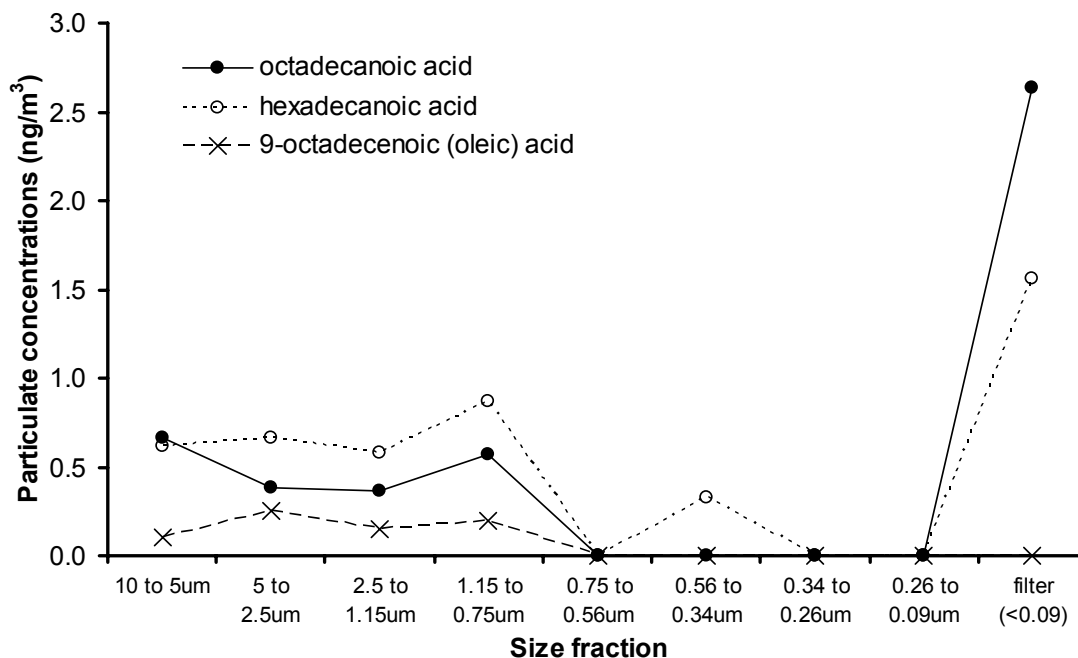


Figure 47. Concentration of octadecanoic, hexadecanoic and 9-octadecenoic (oleic) acid as a function of particle size.

d. Sugars and other polyols

The last group of chemicals investigated were the sugars and other polyhydroxylated compounds (Table 10). The sugars are clearly of biological origin and therefore do not come from the rail yard. However, the sugars, including levoglucosan, can add a considerable amount of organic matter in the particulate phase. Therefore, the sugars need to be accounted for if simple EC/OC measurements are conducted in the future to assess the emissions of organics from the rail yard.

Table 10. Concentrations (ng/m³) of particulate sugars observed at the Roseville Rail Yard in the summer of 2005.

Compound	8-stage DRUM (8/5 to 9/27)	Early Lundgren (9/27 to 10/7)	Late Lundgren (10/7 to 10/17)
Methyl-B-L-arabinopyranoside	< MQL	< MQL	< MQL
D-arabitol	1.5	3.2	2.9
Levoglucozan	2.2	9.7	12
Fructose	2.6	3.2	3.4
Glucose	3.7	5.2	4.8
Mannitol	2.0	3.3	3.2
Inositol	0.32	0.50	0.52
Sucrose	7.3	5.2	5.7
2-methylthreitol	0.60	0.60	0.73
2-methylerythritol	1.9	1.8	2.2

Seven of the eight sugars for which we had standards were detected in the 8-stage DRUM sampler. Sucrose was the most abundant sugar (7.3 ng/m³) followed by glucose (3.7 ng/m³). The high concentrations of refined table sugar (sucrose) implies that some of the aerosols were generated from cooking at the “farmer’s market” nearby. The mass of sucrose was greater than either of the most abundant organic acids and comparable to the single most abundant *n*-alkane, which emphasizes the importance of a thorough organic chemical assessment including species that were not anticipated to be important emissions from the rail depot. While the presence of sucrose suggests a source of the aerosols, the notable absence of levoglucozan effectively eliminates biomass burning as an appreciable source of the aerosol. These samples were collected in the late summer when home heating by fireplaces is non-existent and agricultural burning had not yet commenced, so these results, which are very low relative to other published values, make intuitive sense. It also suggests that the high concentrations of the hexadecanoic and octadecanoic acids are the result of primary biogenic origin rather than biomass combustion.

The size distribution for the sugars showed the highest mass loading in the largest size fraction (Figure 48). This size distribution suggests that the sugars are present in larger aerosols that may have been mechanically generated. Once again, this indicates that they had been formed at the “farmer’s market” and the associated cooking activities at that site. The high concentration of the sugars may also be indicative of soil microbes since many of the sugars are used in metabolic processes. Thus, the profile of the sugars could also indicate that the re-suspended dust from a biological origin. There is a livestock auction building very close to the Denio’s site that would be a potential candidate for this type of biologically-rich dust.

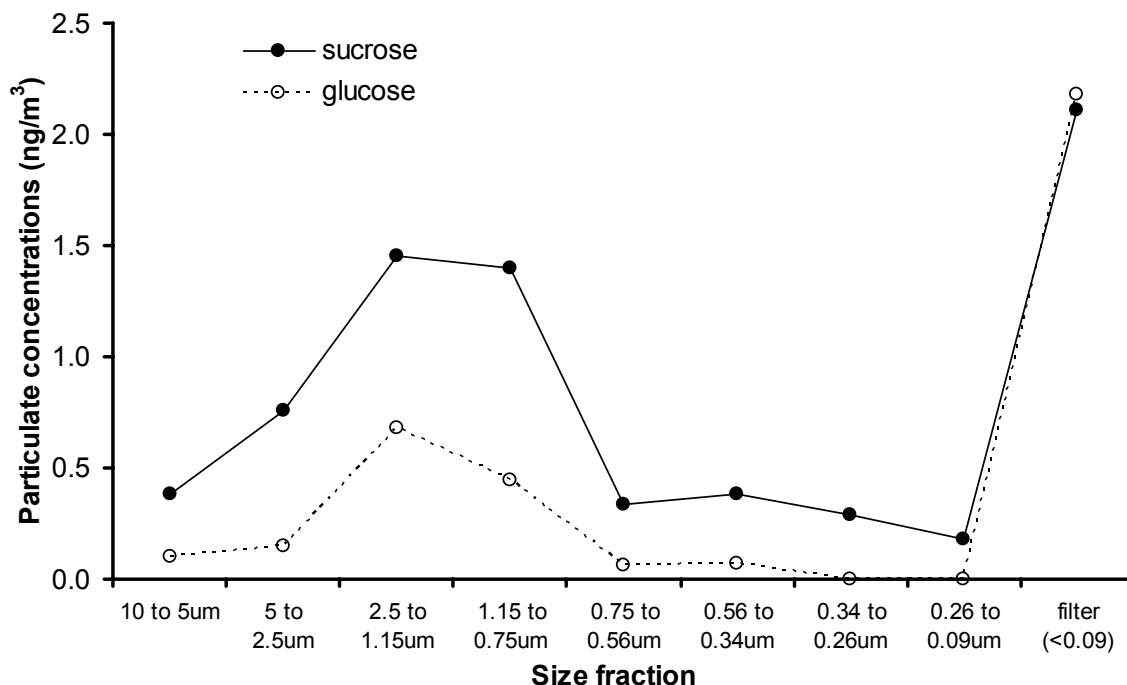


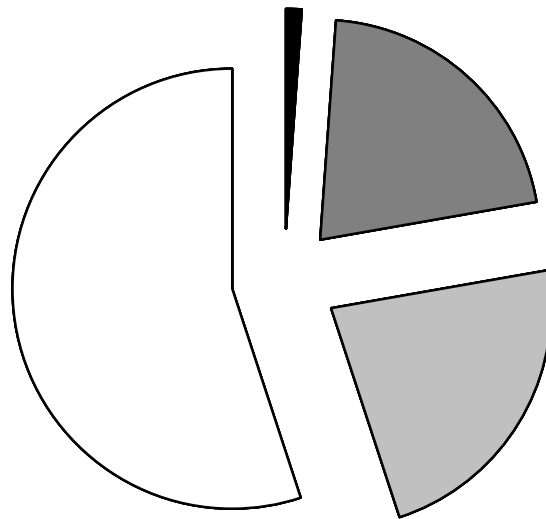
Figure 48. Sucrose and glucose concentrations (ng/m³) as a function of aerosol size.

The last two chemicals quantified were the 2-methyltetrols which have been recently shown to be a major contributor to biogenic secondary aerosols. These compounds are believed to originate from the atmospheric oxidation of isoprene and other volatile biogenic gases.

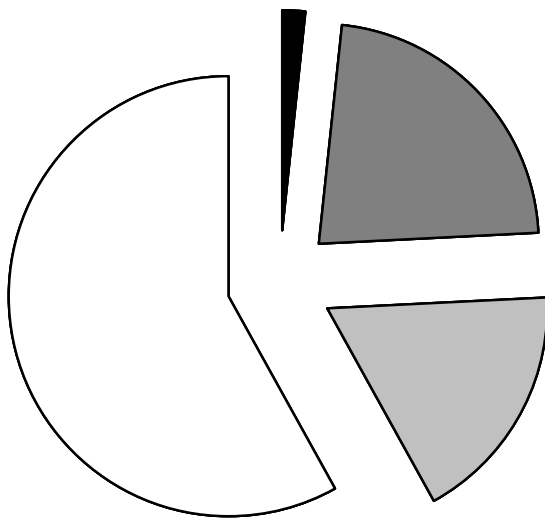
Aerosol Composition Profiles

The relative fraction of the different identified organic constituents (Figure 49) shows that the identified alkanes represent the greatest proportion of the identified mass while sugars represented 18 to 25% of the identified mass and organic acids were 21 to 31% of the mass. The PAHs, which are considered one of the more toxic components of the aerosols, were 1.1 to 2.0% of the identified organic matter. These chemical profiles show that a considerable fraction of the organic matter probably originated from sites other than the Roseville rail yard. In particular, the sugars and the long-chain alkanolic acids are likely biological and/or cooking in origin. Therefore, it is important to conduct chemical speciation at the site since simple EC/OC analysis may over-estimate the contribution of organic matter from the rail yard since it cannot speciate the different sources of the organic matter.

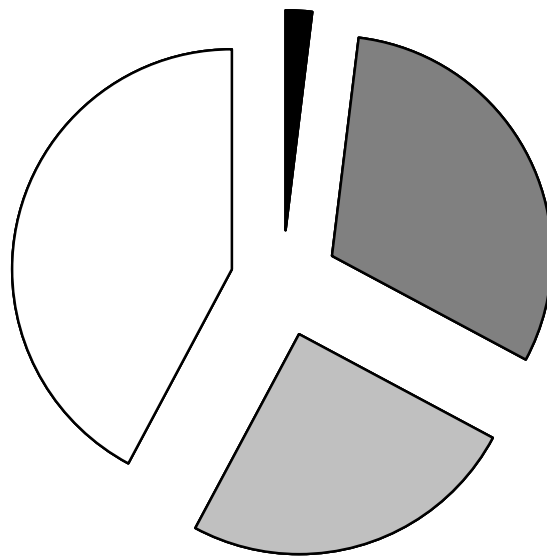
■ PAHs □ Sugars and polyols
 ■ Organic acids □ Identified alkanes



8-stage DRUM



Early Lundgren



Late Lundgren

Figure 49 Fraction of the identified organic mass belonging to the four different classes of chemicals identified.

The next aerosol composition calculation attempts to reconstruct the total aerosol mass, as measured by beta-gauge, from the known elemental and organic constituents (Figure 50). For this calculation, the elements of Al, Si, Ca, Ti, Mn, and Fe are assumed to be in their oxide states that are common of the crustal materials. This roughly doubles the weight of each of these elements. Sulfur is assumed to be in the sulfate form, which results in the sulfur contribution to aerosol mass to be 4.125 times sulfur. (Malm et al, 1994) The elements (and assumed elemental oxides) are summed for each size fraction of the 8-stage DRUM sampler.

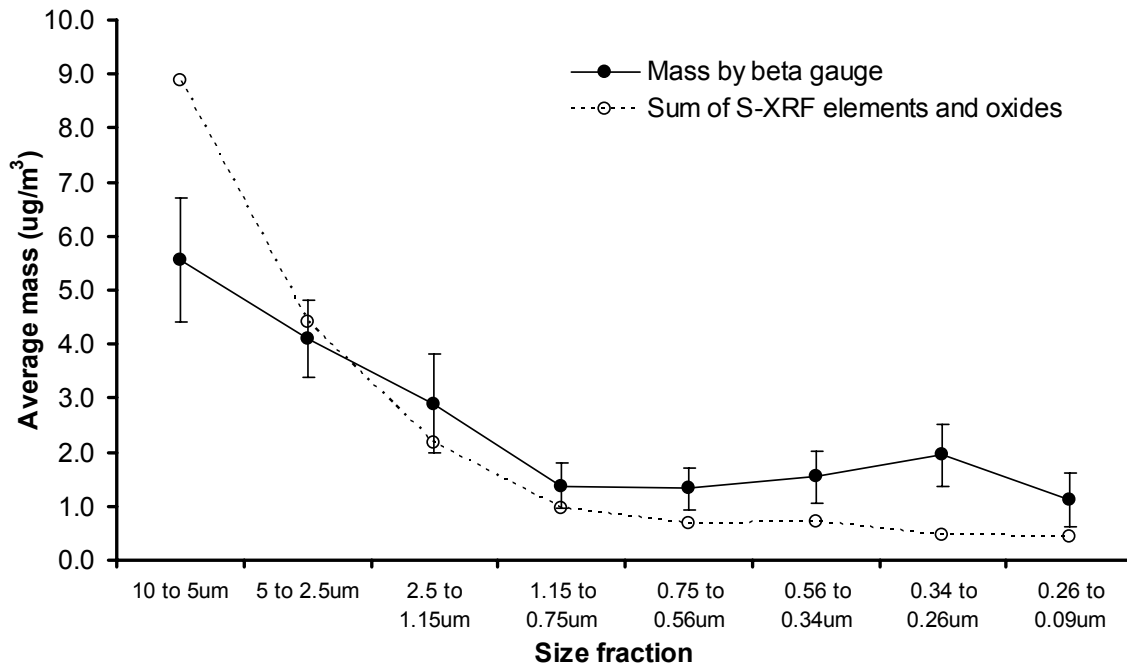


Figure 50. Mass of aerosols as determined by beta gauge and by the sum of the elements and oxides as determined by S-XRF.

The results (Figure 49) showed that the elemental mass was the largest fraction of the aerosol mass in the coarse stages and then the importance of elemental mass declines with the smaller size fractions. In the largest size fraction, the estimated elemental contribution to total aerosol mass exceeded the beta-gauge measured mass, but this is probably the result of the addition of many separate elemental measurements to determine the S-XRF elements and oxides. In all cases, the contribution of organic chemicals to the total mass measured by beta-gauge was relatively minor. Stage 4 (1.8%) and stage 8 (1.6%) had the greatest contributions, mostly due to the “undifferentiated alkane envelope” (Figure 51). The remaining mass was attributed as “unknown”. Although it was not measured, we would expect elemental carbon to make up a considerable fraction of the unknown mass since the samples were a dark black color that is typical of elemental carbon. Also, the fraction of the unknown mass was larger in the finer size fractions that would be combustion processes and diesel.

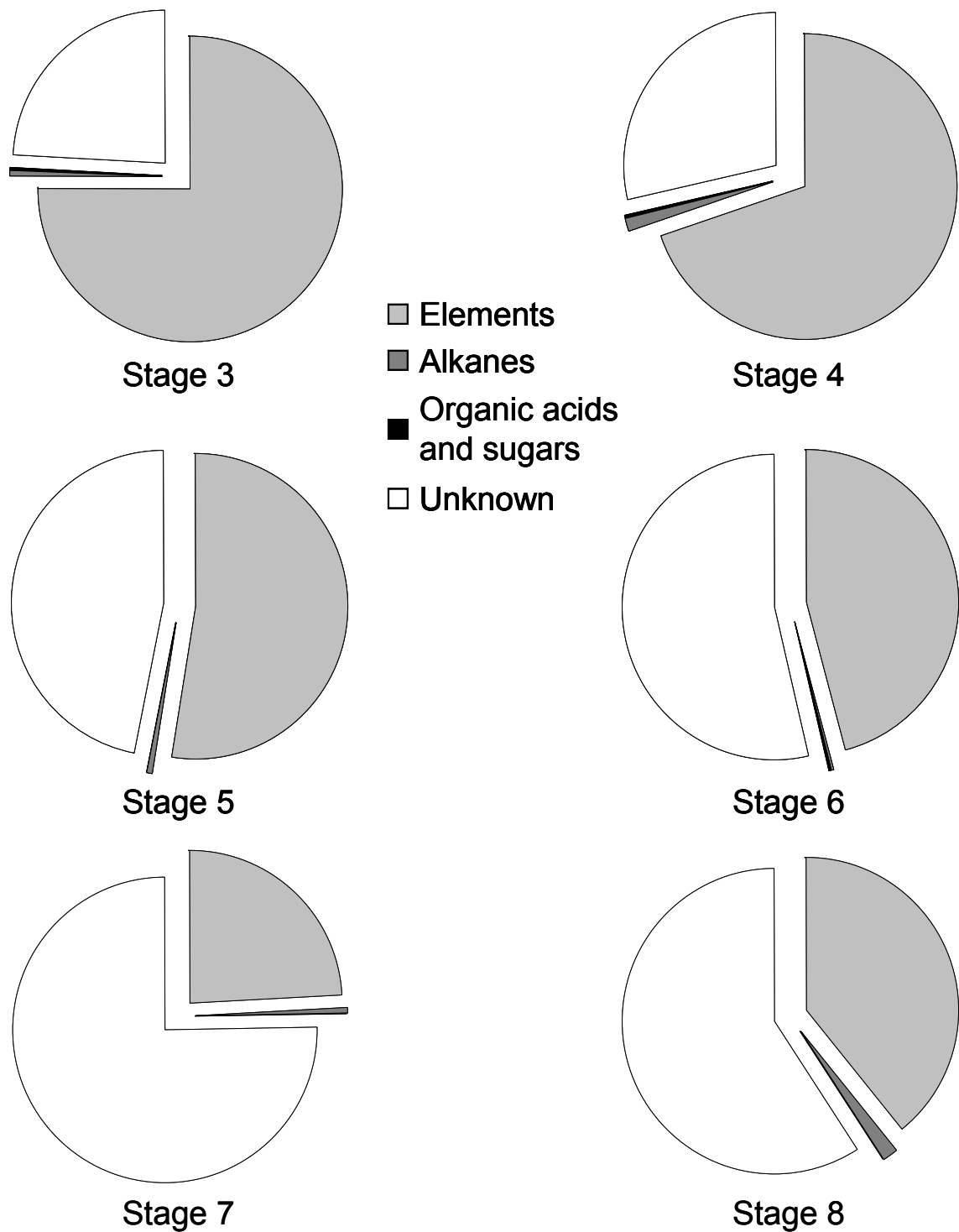


Figure 51. Composition of aerosol mass as determined by beta-gauge.

D. Comparison of Rail Yard data to On-road Vehicles

1. Diesel trucks

The relative distribution of PAHs into heavier and more toxic modes, as shown in Figure 43 (repeated below), is not by itself adequate to determine impacts from Roseville rail yard aerosols.

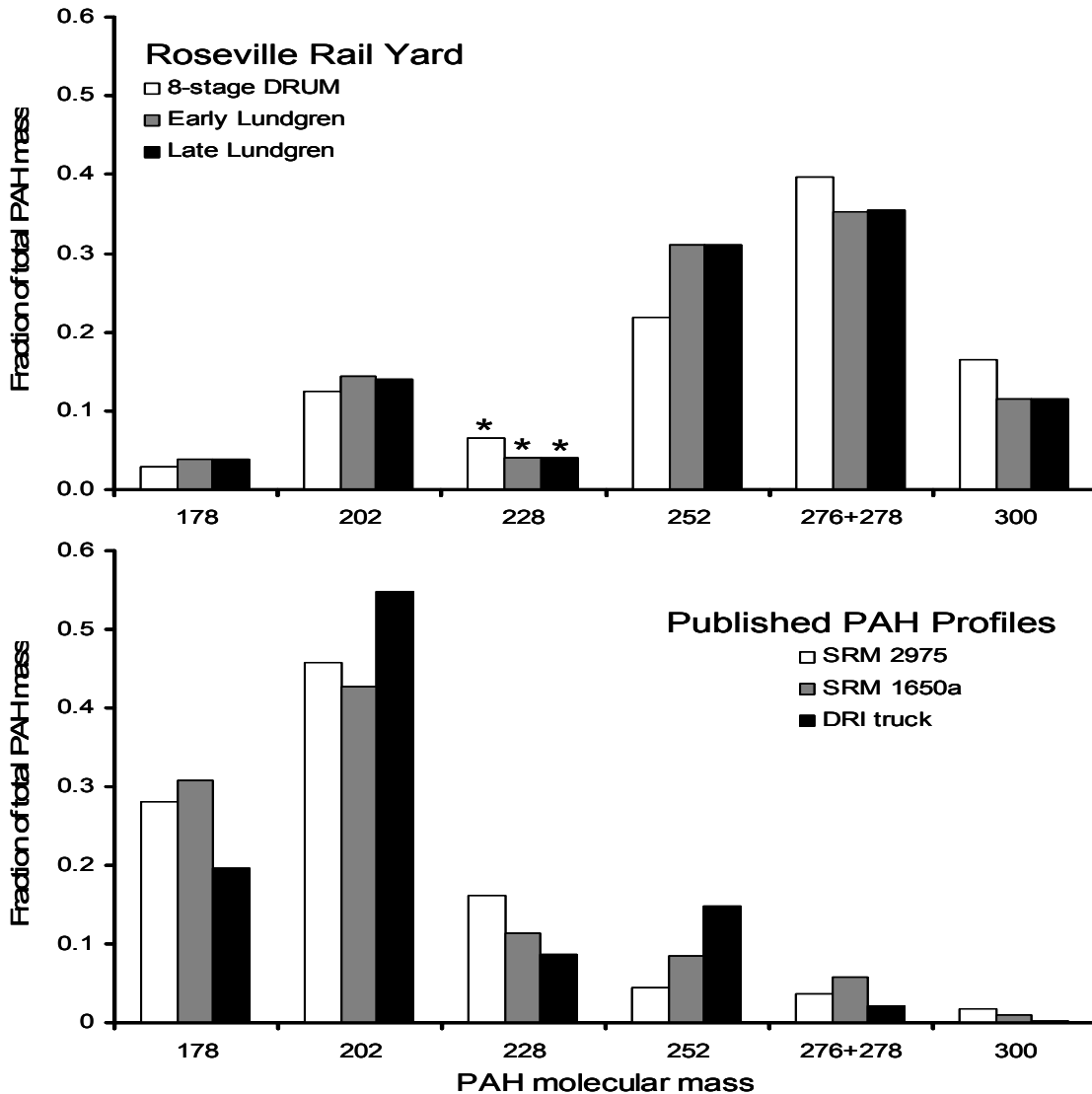


Figure 43. Profiles of PAHs as a function of molecular mass from the Roseville rail yard and the literature.

It is also necessary to determine the mass of PAHs in the aerosols, and/or the ratio as a fraction of total aerosol mass, fine mass, and/or elemental carbon, to allow estimates of aerosols impacts. The most direct way is to form the ratio of PAHs to the major diesel aerosol component, elemental carbon. This is not available from the NIST diesel SRM

1650a and SRM 2975, but these data are available from the Desert Research Institute Report to the National Renewable Energy Laboratory, 2004. (Zielenska et al, 2004). An additional source is from the work of Gertler et al (2004) in a report to the Health Effects Institute and publications (Gertler et al, 2002, Gertler et al, 2004). For the Roseville data, elemental carbon was measured at the Denio and Pool sites through October, 2005.

In addition, during the summer, very fine mass was also measured at the Denio and Pool sites, allowing a comparison to size resolved data in Zielenska et al 2004. These data can be further sorted by total material at the Denio site, and the difference between the Pool and Denio sites. These estimates are necessary because no upwind-downwind organic measurements were taken. Combining the data on Table 1 for elemental carbon (EC) and Table 8 for benzo{a}pyrene, we can form ratios that can be compared to literature values, rail yard data to trucks.

These calculations have been done in Table 11.

There are three columns of results, the first being for very fine/ultra fine mass, and the second and third for elemental carbon (EC).

Using only mass data to form the ratio, we suffer from the uncertainty as to how one accounts for the $< 0.09 \mu\text{m}$ components not measured by the DELTA 8 DRUM. The first mass values in Table 11 assume that there is negligible mass below $0.09 \mu\text{m}$ diameter, which is unrealistic and gives a high ratio, 12.7

The next two measures use estimates of the missing sub- $0.09 \mu\text{m}$ estimated from the difference of the RRAMP $\text{PM}_{2.5}$ and the measured DRUM masses, and an estimate using the ratio observed for diesel trucks in Zielenska et al 2004. Using only the mass data, we obtain a mean RRAMP/truck ratio 7.5 ± 4.0 .

However, in the final analysis, we drop the unrealistic highest ratio, 12.7, and arrive at a mean mass ratio of 4.8 ± 2.7 .

Considerably more data exist that allow us to form a ratio to elemental carbon (EC) the largest single component of diesel exhaust by mass. These data were compared with literature emission rates of benzo-a-pyrene derived from both laboratory studies (Zielenska et al, 2004) and on-roadway tunnel studies (Gertler et al, 2002). Ratios were derived elemental carbon (EC), for the DELTA 8 DRUM in summer, and two Lungdren impactors in fall. Finally, we used both total EC at the Denio site and the EC difference, Denio to Pool site. This generated 15 different ratios based on the method used.

Table 11 Comparison of RRAMP Benzo{a}pyrene results to literature values for diesel trucks, in a highway tunnel (Gertler et al, 2002) and in the laboratory (Zielenska et al, 2004). The most precise values for the rail yard/truck ratios are in bold type.

RRAMP – Denio site	Period	Ratio – vf/uf mass laboratory	Ratio - EC/DRI laboratory	Ratio – EC/highway tunnel
8 DRUM – very fine mass	7/21 – 8/17	12.7		
8 DRUM – vf mass corr. by PM _{2.5} diff.	7/21 – 8/17	3.0		
8 DRUM – vf mass corr. by DRI ratio	7/21 – 8/17	6.8		
Mass average - corrected		4.8 ± 2.7		
8 DRUM – all EC	8/5 – 9/27		5.15	3.7
8 DRUM – corr. by EC diff.	8/5 – 9/27		9.02	6.7
Lundgren 5 drum – all EC	9/27 – 10/7		6.18	4.5
Lundgren 5 drum – corr. by EC diff.	9/27 – 10/7		13.9	10.1
Lundgren 5 drum – all EC	10/7 – 10/17		6.41	4.7
Lundgren 5 drum – corr. by EC diff.	10/7 – 10/17		14.4	10.5
Average values (all)	7/21 – 10/17	7.5 ± 4.0	9.2 ± 3.7	6.7 ± 2.7
Average values (Denio EC only)	7/21 – 10/17		5.9 ± 0.6	4.3 ± 4.0
Grand weighted average (EC + mass, Denio only)	7/21 – 10/17		5.5 ± 0.7	

A raw average of the 15 values gives a ratio of the RRAMP benzo{a}pyrene to diesel trucks of 7.7 ± 3.5 . However, we conclude that the Denio – Pool difference in EC is not a good match to the Denio-only PAHs. Removing these data, and weighting the averages by errors, we derive 5.5 ± 0.7 . This means that there was about 5.5 times more benzo{a}pyrene from the RRAMP aerosols than from diesel truck aerosols, per unit very fine/ultra fine mass and per unit elemental carbon.

Combining this with the PAH ratio data above, we find that the factor of 6 is made up equally from the shift in mass of the PAHs to heavier masses in RRAMP and an increase in the gross emission rate of PAHs.

While we used EC to scale from summer to fall conditions we could easily have used mass if we had had it. This is important since inversions become more common in fall and winter, raising the very fine mass from a value of $2.25 \mu\text{g}/\text{m}^3$ in summer (DRUM sages 7 + 8, 0.34 to $0.09 \mu\text{m}$) to $6.6 \mu\text{g}/\text{m}^3$ measured in February, 2006, using identical equipment. Thus, the Lundgren samplers were collecting in periods that would tend to have higher masses at the Denio site, and the factor may be greater than the 1.25 used from the EC data. This would improve the 8 DRUM to Lundgren agreement.

4. Automobile-dominated Secondary Streets

Aerosol concentrations in the Sacramento region typically maximize in winter months when stagnation and inversions are common. For this reason, even though the clan upwind-downwind Pool site to Denio Site relationship of summer was degraded, it was decided to obtain at least 2 weeks of winter data to complete the 6 month period and gain an annual perspective. In addition, in order to aid in comparison of the rail yard data to other local pollution sources, the same protocol was applied to the Arden iddel School site, 25 m downwind of heavily traveled (65,0000 v/day) Watt Avenue, a road that typically has about 1.5% truck traffic. This work is not part of the grant but a contribution from Breathe California of Sacramento-Emigrant Trails Health Effects Task Force and the UC Davis DELTA Group. Two DELTA 8 DRUM samplers with ultra-fine after filters were placed at Arden Middle School, Jan. 27. On February 10, they were both moved to the Denio site downwind of the Roseville Rail yard. As shown below (Figure 52), the weather during each two week period was roughly comparable, with Arden having slightly better ventilation.

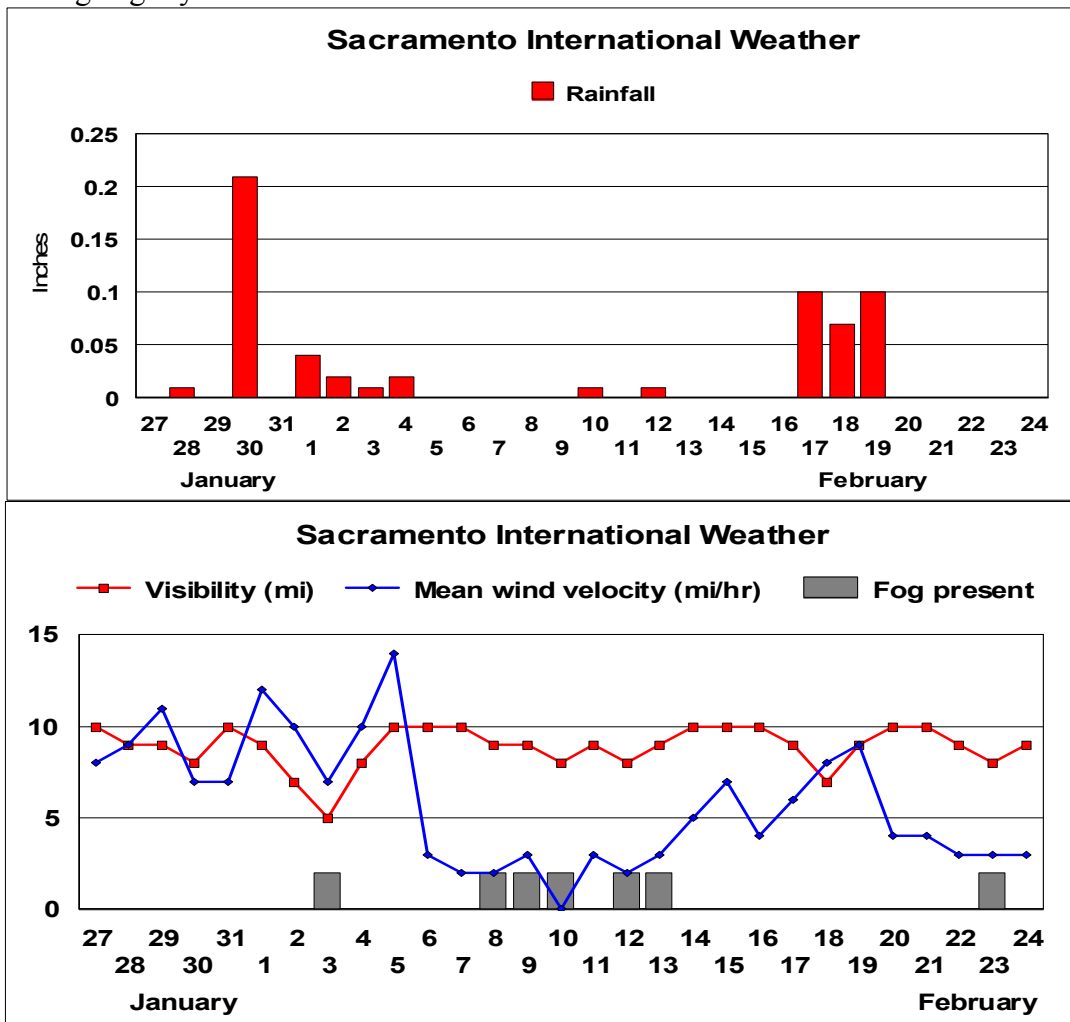


Figure 52 Meteorology during the winter sampling, 2006

The Arden outdoor site was on the roof of the teacher ready room, about 25 m from the edge of the nearest traffic lane and above a small (6 car) parking lot. It was at the same elevation but about at ½ the distance to Watt Avenue that we used in 2003 and 2005. The roof (painted white) was filthy with black soot.

Below (Figure 53) we show the actual particles photographed in natural light (hence the bluish tinge to the clean Mylar). There is an obvious soil like component at the Denio site absent at the Arden site, but other than that, the traces seen roughly comparable.

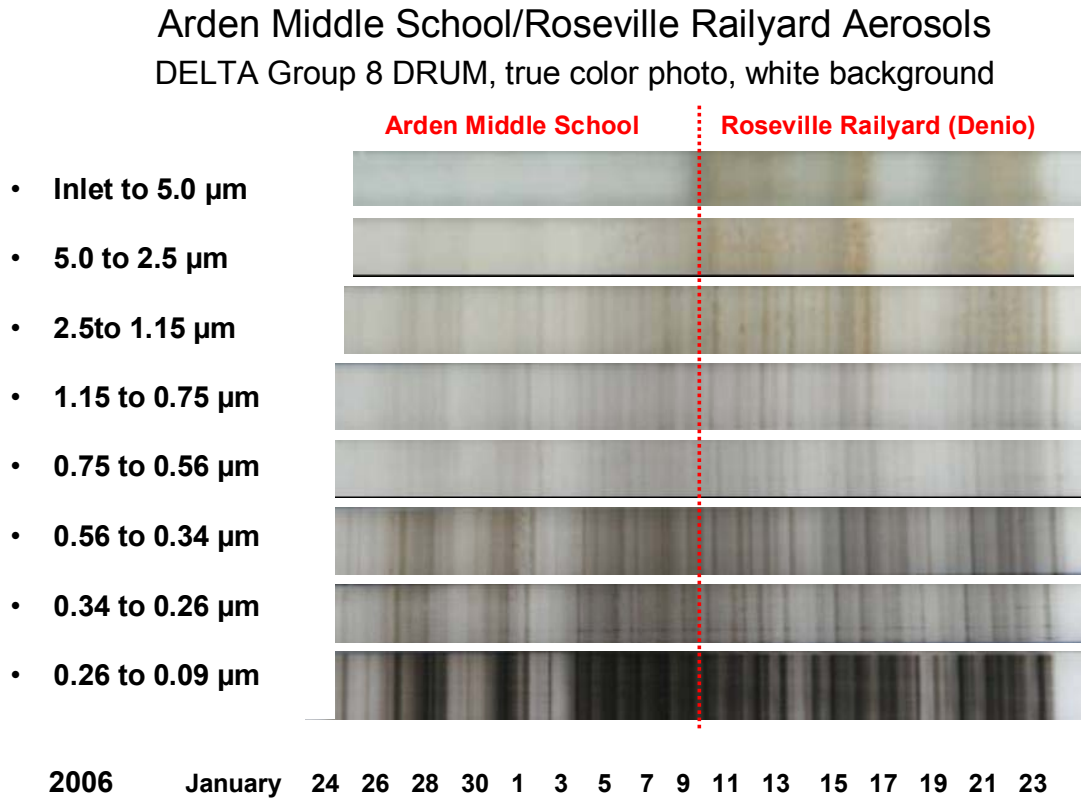


Figure 53 Photograph of winter drum strips, Watt Ave at Florin versus Denio site

Based on the compositional information, the finest 2 stages (< 0.34 µm) are dominated by automobile and diesel exhaust, while there is clearly additional smoke impact on the 0.56 to 0.34 µm stage.

Mass measurements were made by soft beta ray transmission by the DELTA Group, and these are shown below (Figure 54).

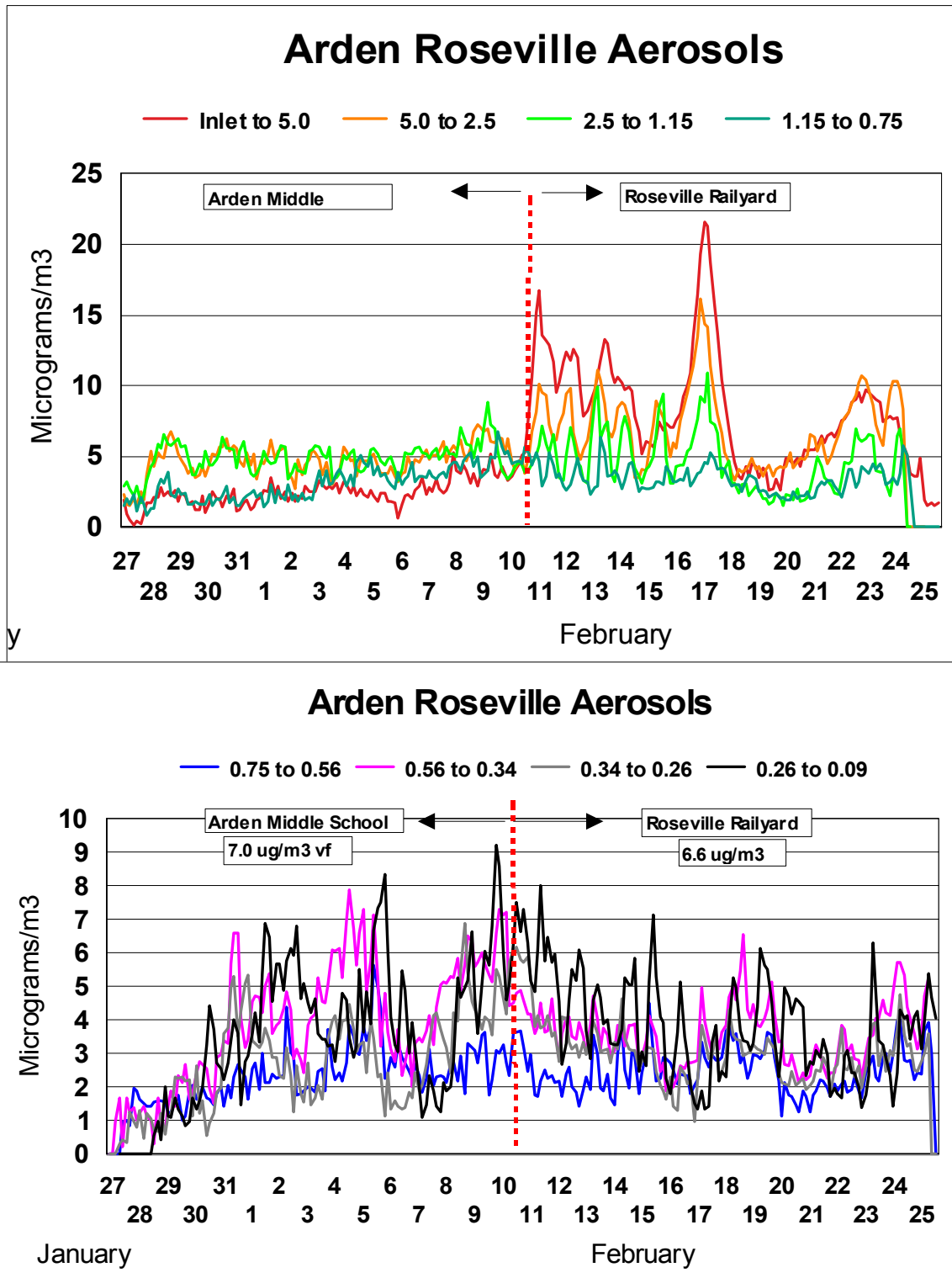


Figure 54 Coarse and fine mass at Watt and Arden versus the Denio site, winter, 2006

Qualitative comparison to winter, 2004 study

Arden Middle School Very Fine Aerosols

DELTA 8 DRUM, $0.26 > D_p > 0.09 \mu\text{m}$

January 16 – February 4, 2004



January 24 – February 10, Arden roof:
February 10 - 24 – Denio site – Roseville rail yard



Figure 55 Photographs of winter DRUM strips, Watt/Arden, 2004, vs Watt/Arden and Denio, 2006

Compositional analyses were made of the winter samples. First, chlorine in coarse modes is plotted, generally an indicator of sea salt and strong marine winds (Figure 56).

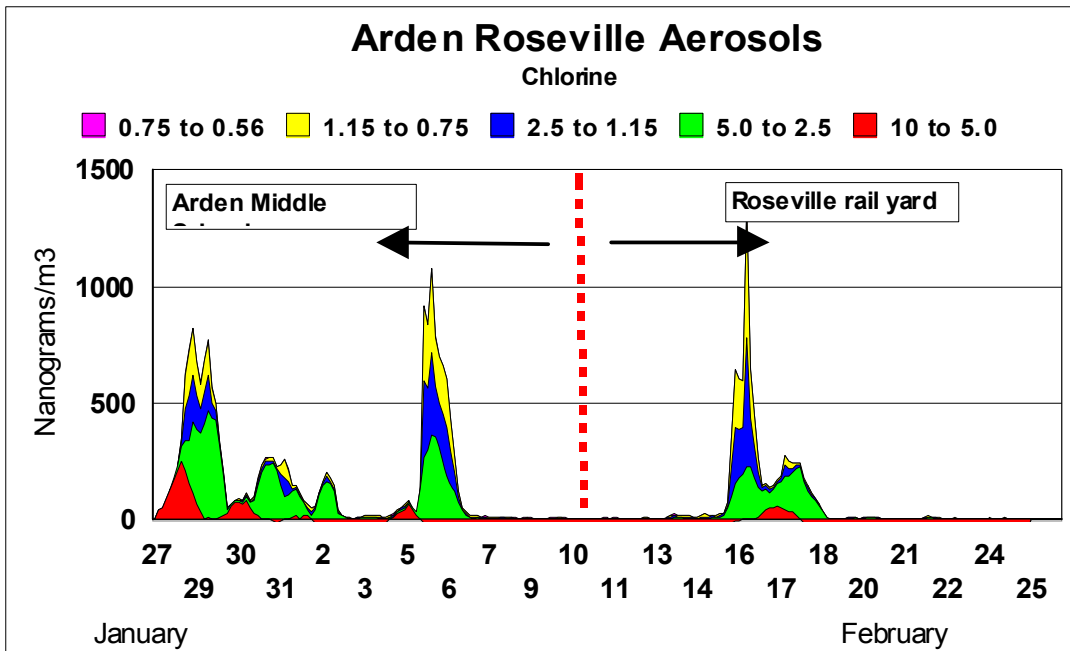


Figure 56 Chlorine aerosols (sea salt) at Watt/Arden and Denio, winter, 2006

The second element is iron, a tracer of soil. This can be matched to the coarse mass fraction seen only at the Denio site in mass (Figure 57).

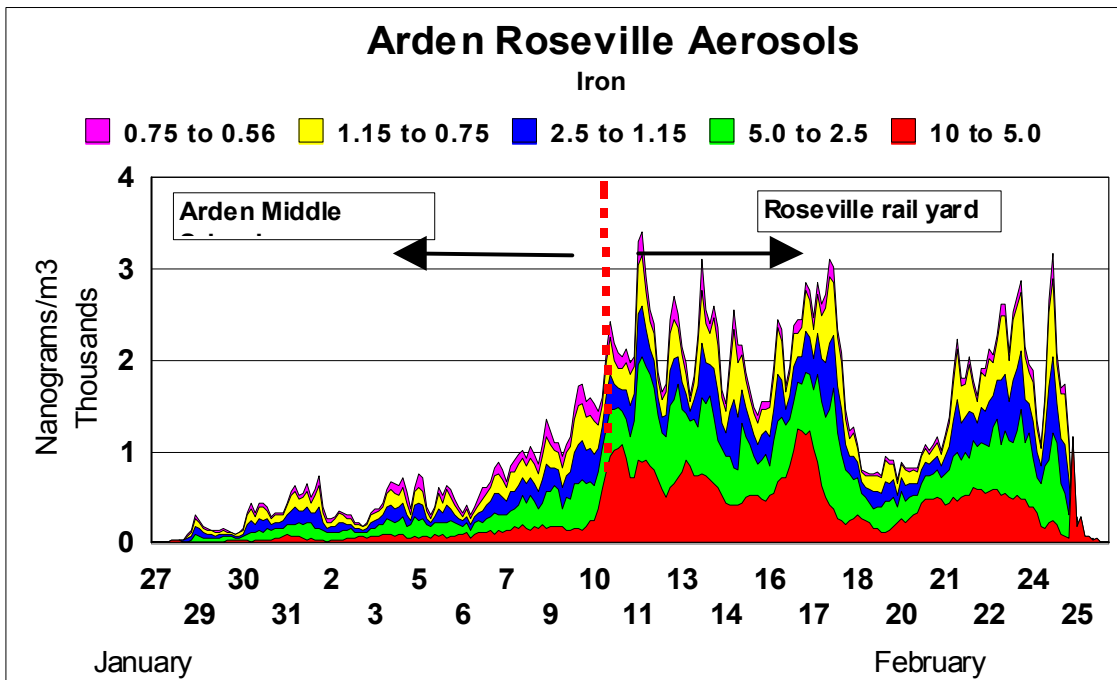


Figure 57 Iron aerosols (soil) at Watt/Arden vs Denio, winter, 2006

Finally, we plot sulfur (Figure 58). The peaks from January 29 through February 6 are associated with Bay Area sources as shown by both the chlorine and the vanadium (Figure 59), generally a tracer of heavy fuel oil. Note that the sulfur at the Denio site shows the characteristic diurnal maxima and minima pattern only weakly present at Arden Middle School.

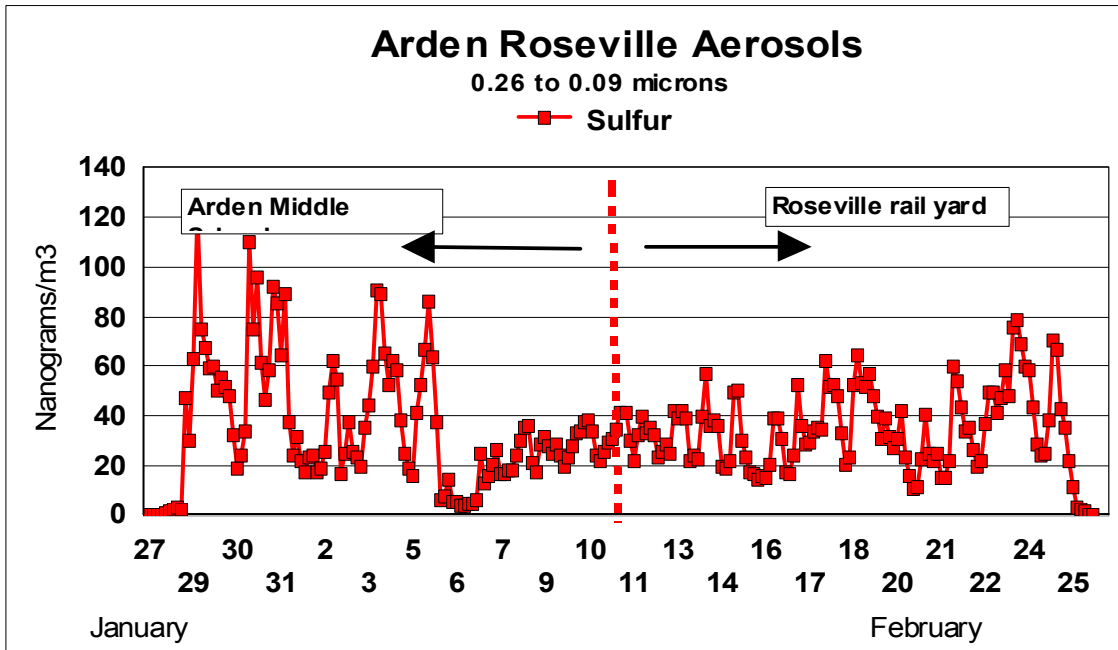


Figure 58 Iron aerosols (soil) at Watt/Arden vs Denio, winter, 2006

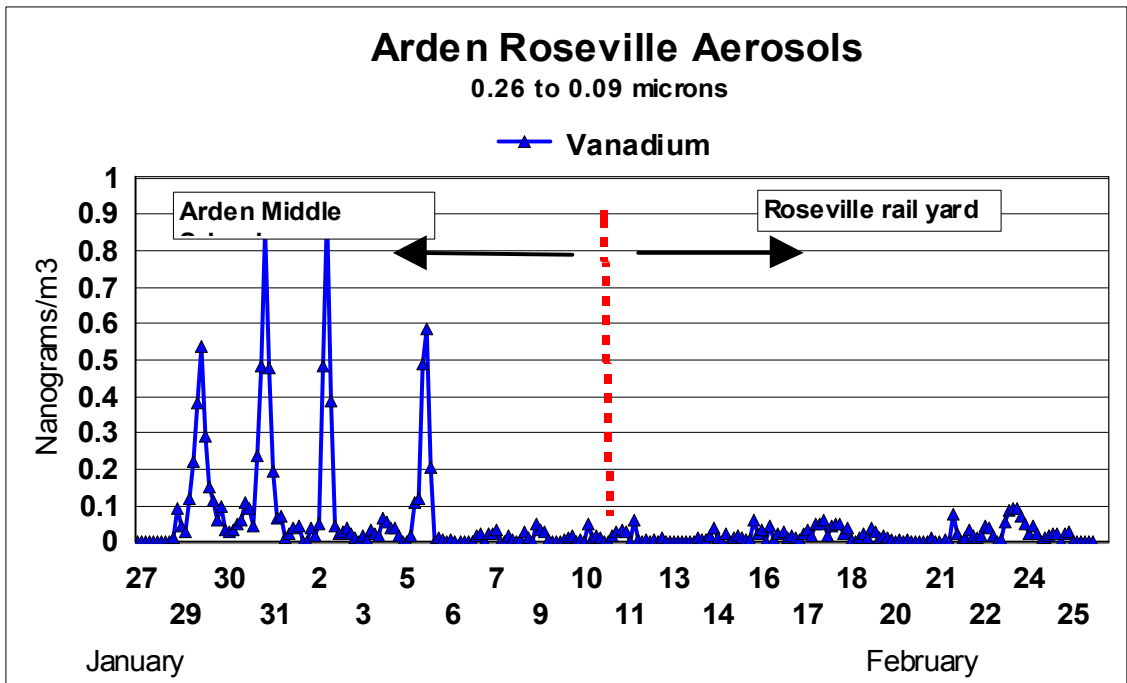


Figure 59 Vanadium aerosols (heavy fuel oil) at Watt/Arden vs Denio, winter, 2006

Potassium in the coarser modes is a component of soil. Compare this (Figure 60) plot to iron.

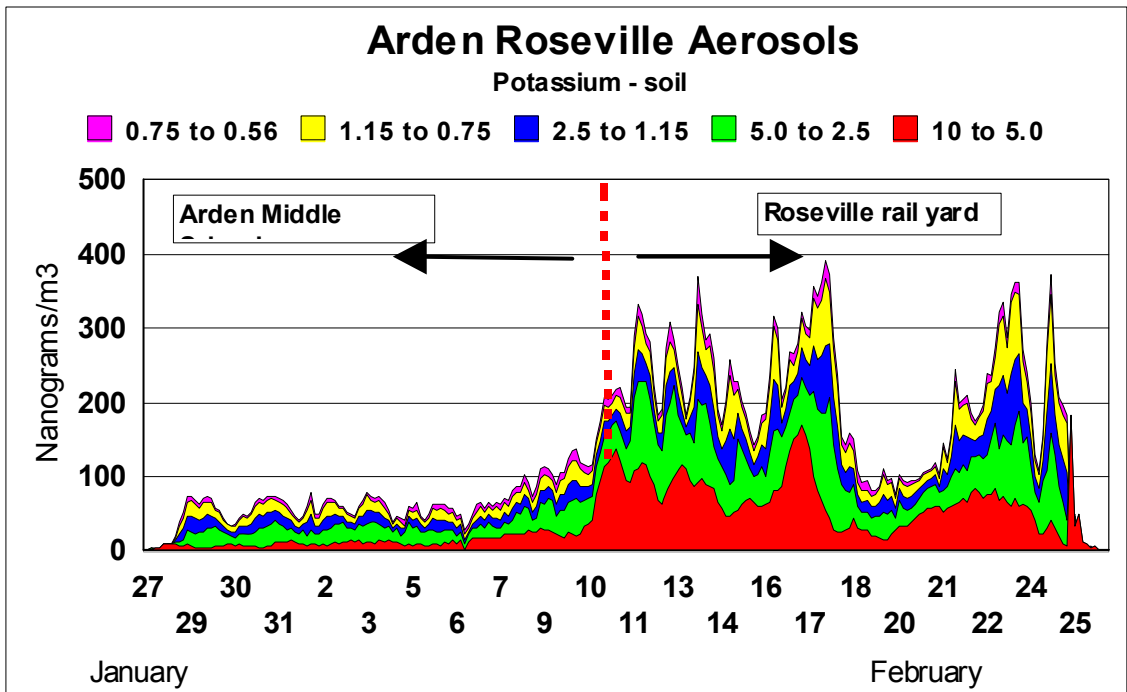


Figure 60 Coarse potassium aerosols (soil) at Watt/Arden vs Denio, winter, 2006

Potassium in the finer modes has both a biomass combustion component (0.35 to 0.75 μm) and an internal engine combustion component ($< 0.34 \mu\text{m}$) (Figure 61).

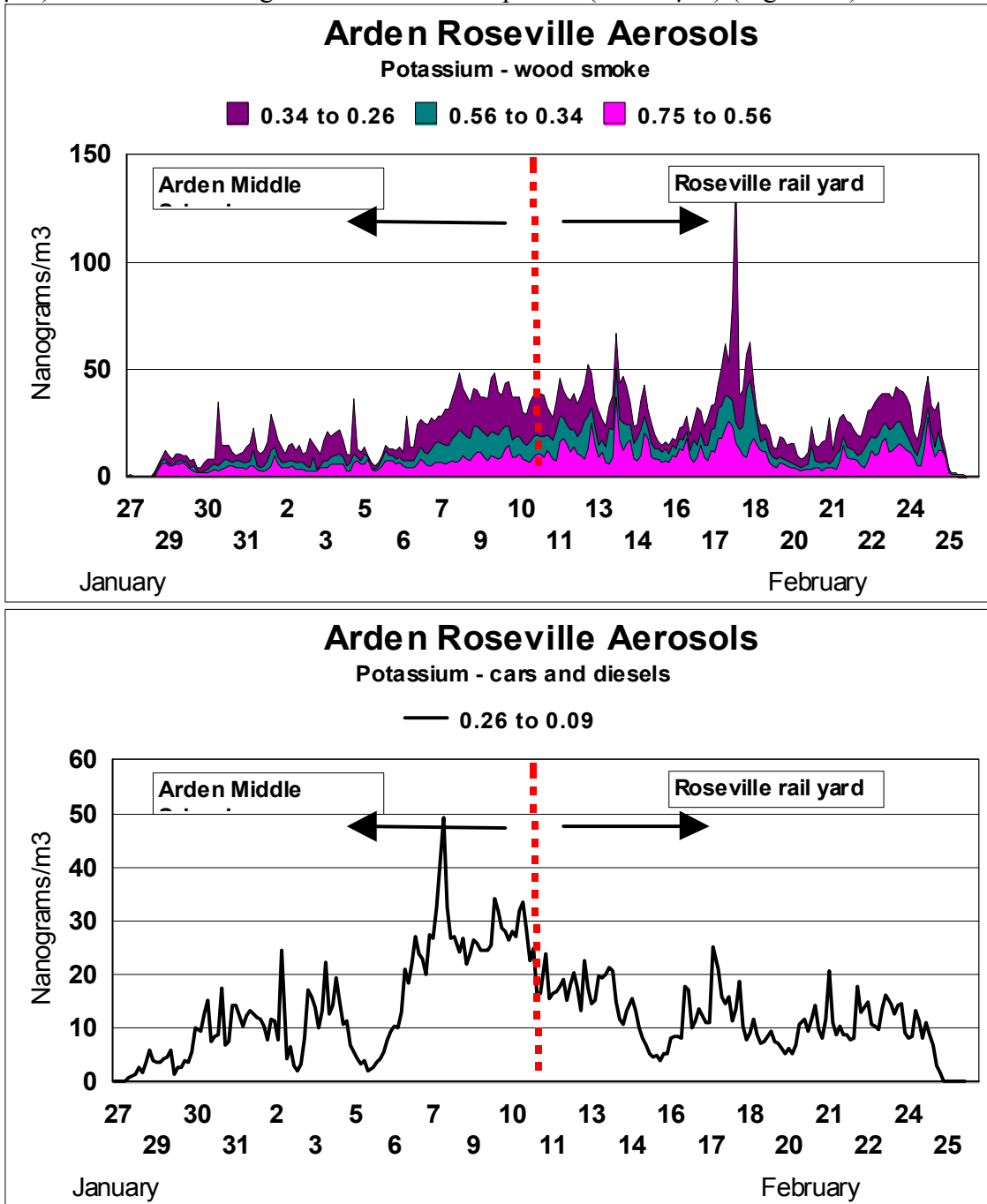


Figure 61 a, b Accumulation mode potassium aerosols (wood smoke) and very fine potassium aerosols (vehicular) at Watt/Arden vs Denio, winter 2006

Examining the very fine zinc signature (Figure 62), we can add the phosphorus component from the zinc thiophosphate stabilizer in lubricating oils. Ignoring the period of high Bay Area transport, we can see that the Zn/P ratio is smaller at the rail yard than

at Watt Ave, most likely a reflection of the differences between the spark emission dominated Watt Ave. and the diesel dominated Roseville Rail Yard.

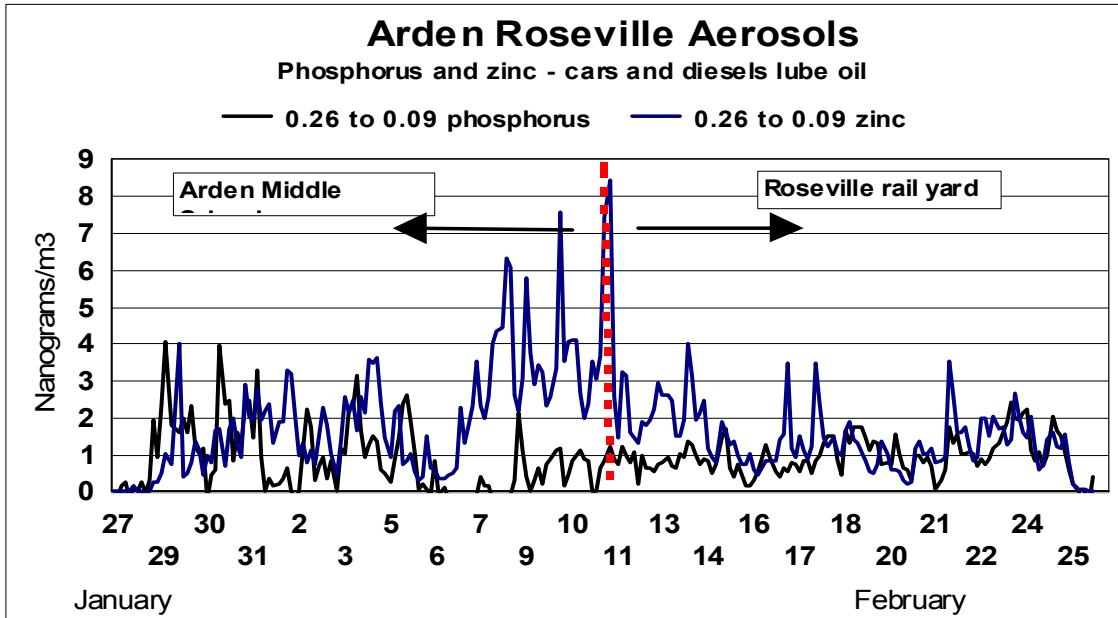


Figure 62 Very fine mode phosphorus and zinc aerosols (vehicular) at Watt/Arden vs Denio, winter 2006

Finally, for completeness sake, we include some typically anthropogenic metals (Figure 63). The high nickel levels from the Bay Area are the match to the vanadium values, above, as both are in heavy oils. The high copper levels at Arden at the moment lack any rationale.

Conclusions:

The objective of this project was to assess the aerosols emitted from the Roseville Rail Yard. While there is considerable data on the emissions from diesel trucks, there is effectively no data on the emissions of elements and chemicals from diesel locomotives. The diesel locomotive engines are significantly different from the truck diesel engines, so there is reason to believe that the emissions may be different.

The results from the summer showed that the diurnal meteorology was stable and predictable. Typically the wind blows from the rail yard to the Denio site each night, thus giving a good signature of fresh diesel locomotive emissions. The gas and very fine particulate results showed the characteristic signatures of diesel emissions, namely high concentrations of NO, sulfur, zinc, phosphorus and PAHs. The time-resolved elemental data showed a very good diurnal cycle with high concentrations occurring at the Denio site every night. The diesel emissions were in the very fine to ultra-fine size fraction which is similar to diesel truck emissions, although the sulfur results appeared in the 0.3 μm size fraction that is larger than the typical diesel results presented in the literature. The most significant difference between the locomotive emissions and truck emissions is that the emissions from the locomotives had a higher concentration of the larger and more toxic PAHs. This indicates that the diesel emissions from the rail yard are probably more toxic than diesel truck emissions that are the basis of many risk assessments.

While the diesel emissions aerosols were expected, there were also other particulate emissions from the rail yard. There was coarse particulate matter that was being blown off of the site. These aerosols were characterized by very high concentrations of certain metals such as copper and zinc that are common in metallurgy. These coarse particles also had high concentration of petroleum hydrocarbons, which are probably the result of oils and tars used on the site. Some of these alkane hydrocarbons may be volatilizing from the site as vapors.

The last group of chemicals gave a signature of biological materials since they contained high concentrations of sugars and organic acids. These chemicals are unlikely to come from the rail yard, but rather the nearby farmer's market that conducts considerable cooking and livestock auction activities. Both of these activities could supply the biological chemicals that were observed in the samples. The reason for quantifying these chemicals is that they contribute a large fraction to the organic carbon of the samples, thus simple EC/OC measurements may over-estimate the influence of the rail yard.

References:

- Bench, G., P.G. Grant, D. Ueda, S.S. Cliff, K.D. Perry, and T. A. Cahill. The use of STIM and PESA to respectively measure profiles of aerosol mass and hydrogen content across Mylar rotating drum impactor samples. 2001 *Aerosol Science and Technology* 36:642-651.
- Cahill, Thomas A. and Paul Wakabayashi. Compositional analysis of size-segregated aerosol samples. Chapter in the ACS book *Measurement Challenges in Atmospheric Chemistry*. Leonard Newman, Editor. Chapter 7, Pp. 211-228 (1993).
- Cahill, T.A., P. Wakabayashi, T. James. Chemical State of Sulfate at Shenandoah National Park During Summer 1991 *Nuclear Instruments and Methods in Physics Research B: Beam Interactions with Materials and Atoms*, 109/110 542-547, (1996)
- Cahill, Thomas A., Kent Wilkinson, and Russ Schnell. Composition analyses of size-resolved aerosol samples taken from aircraft downwind of Kuwait, Spring, 1991. *Journal of Geophysical Research*. Vol. 97, No. D13, Paper no. 92JD01373, Pp. 14513-14520, September 20 (1992).
- Cahill, T.A., C. Goodart, J.W. Nelson, R.A. Eldred, J.S. Nasstrom, and P.J. Feeney. Design and evaluation of the drum impactor. *Proceedings of International Symposium on Particulate and Multi-phase Processes*. Teoman Ariman and T. Nejat Veziroglu, Editors. Hemisphere Publishing Corporation, Washington, D.C. 2:319-325. (1985).
- Cahill, T. A. Comments on surface coatings for Lundgren-type impactors. *Aerosol Measurement*. Dale A. Lundgren, Editor. University Presses of Florida, Pp. 131-134 (1979).
- Draxler, R.R. and Rolph, G.D., 2003. HYSPLIT (HYbrid Single-Particle Lagrangian Integrated Trajectory) Model access via NOAA ARL READY Website (<http://www.arl.noaa.gov/ready/hysplit4.html>). NOAA Air Resources Laboratory, Silver Spring, MD.
- Raabe, Otto G., David A. Braaten, Richard L. Axelbaum, Stephen V. Teague, and Thomas A. Cahill. Calibration Studies of the DRUM Impactor. *Journal of Aerosol Science*. 19.2:183-195 (1988).
- Rolph, G.D., 2003. Real-time Environmental Applications and Display sYstem (READY) Website (<http://www.arl.noaa.gov/ready/hysplit4.html>). NOAA Air Resources Laboratory, Silver Spring, MD.
- Wesolowski, J.J., W. John, W. Devor, T.A. Cahill, P.J. Feeney, G. Wolfe, R. Flocchini. Collection surfaces of cascade impactors. In *X-ray fluorescence analysis of environmental samples*. Dzubay, T., Editor. Ann Arbor Science, Pp. 121-130 (1978).
- Zielenska, B., Cahill, T.A., Steve Cliff, Michael Jimenez-Cruz, and Kevin Perry, Elemental analysis of diesel particles from MOUDI samplers, Final Report to Doug Lawson, the National Renewable Energy Laboratory, Golden, CO (2004)

Acknowledgments:

The authors wish to acknowledge the continual support and encouragement of the Health Effects Task Force of Breathe California of Sacramento-Emigrant Trails, its Chair, Jan Sharpless, and its Consultant, Betty Turner.

The staff of the Placer County APCD were exemplary in their support of our field analyses and their provision of meteorology and data from RRAMP.

The authors also gratefully acknowledge the NOAA Air Resources Laboratory (ARL) for the provision of the HYSPLIT transport and dispersion model and/or READY website (<http://www.arl.noaa.gov/ready.html>) used in this publication.

This report has benefited greatly from the comments and suggestions of the RRAMP Technical Advisory Committee, but the opinions expressed herein are solely those of the authors.

Appendix QA:

The DRUM cuts are sharp and fully predictable by standard aerodynamic principles, and mis-sizing by bounce-off is reduced to less than 1 part in 5,000 by mass by a light grease coating (Wesolowski et al, 1979, Cahill 1979, Cahill et al, 1985).

A side by side comparison study of DRUM and other samplers was done on October 2 – 14, 2005, at Davis as part of the Quality Assurance component of the new EPA Particulate Matter Research Center grant to UC Davis which will be using DELTA Group DRUM samplers and analysis, 2005-2010.

However, an error in the modification in old DRUM #4, (1987) the Pool site sampler, resulted in an internal leak in that could not be detected during field sampling at RRAMP using standard vacuum and flow audit devices. It was discovered after analyses of the co-located sampling for quality assurance purposes at the Denio site and confirmed by disassembly of the unit. This invalidated all size modes from the Pool sampler except the finest, $0.26 > D_p > 0.09 \mu\text{m}$, which as a critical orifice has separate quality assurance checks. The side by side comparison yielded an average of $0.72 \mu\text{g}/\text{m}^3$ for the Denio sampler, $0.68 \mu\text{g}/\text{m}^3$ for the Pool site.

Comparison between data on DRUM samplers to standard PM is difficult due to:

1. Sharper size cut profiles, DRUM vs filters, especially important near the PM_{10} and $\text{PM}_{2.5}$ cut points,
2. Differences in the way impactors handle aerosols, since air is not drawn through the deposit, preserving chemical information sometimes lost in filters (i.e., sulfuric acid, Cahill et al, 1996)
3. Lack of ultra fine data below $0.09 \mu\text{m}$. This latter problem is especially important near strong combustion sources.
4. Time registration. DRUM samplers have errors in timing inherent to continuous sampling. The finite width of the impaction slot introduces an irreducible averaging over $1 \frac{1}{2}$ to 3 hr, the stretching of the Mylar onto the analysis frame adds typically 6 ± 3 hr of uncertainty. The relative time uncertainty is very small, 10 min/day, so that alignment of DRUM data with high precision gas and particulate data (such as NO) is an essential next step in data reduction.
5. Propagation of error problems. To match a single 24 hr $\text{PM}_{2.5}$ RRAMP filter, one has to sum 96 individual $1 \frac{1}{2}$ hr mass measurements or 48 3 hr elemental values from the DRUM samplers.
6. Dilution of the mass signal. The aerosols are spread over 8 size modes, resulting in almost a reduction of 10 in the amount of mass available to analyze on each stage.

5. Analysis

The UC Davis DELTA Group performs analyses by 7 different non-destructive methods, also described in publications and the 135 page DRUM Quality Assurance

Document, latest version 1/2005 (DQAP ver. 1/05), posted on the DELTA web site <http://delta.ucdavis.edu>.

c. Mass

Analysis was completed for mass values every 1 ½ hours in 8 size modes for the entire period. Each strip was analyzed at least 2 times, and the standard deviation of the data are included in the data file. An example of the precision repeated measurements of DRUM strip is shown below.

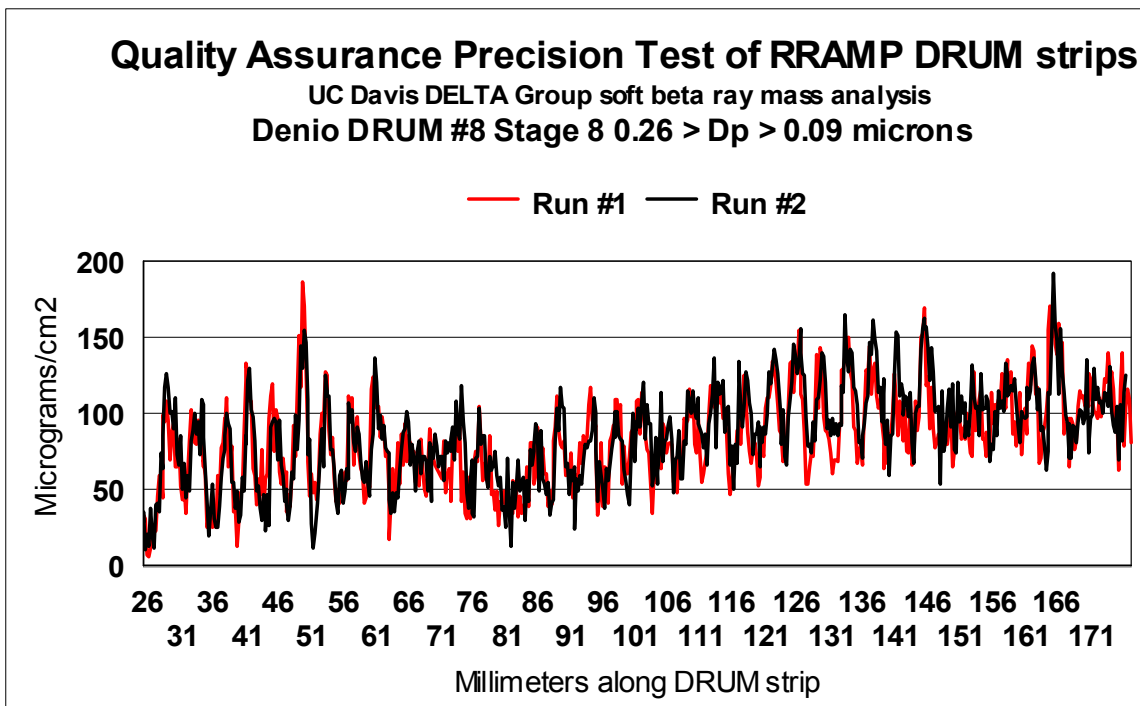


Figure 1 Precision test for mass

Note that since the strip was remounted, the test also validates relative time precision. Any measurements where the analysis differs by more than $\pm 10\%$ is independently re-run until agreement is achieved.

As mentioned above, comparisons with 24 hr filters are difficult. There have been 2 recent comparisons completed and one in progress (the US EPA PMRC Center tests at Davis) in rural conditions where the lack of ultra fine particulate mass should not be a major effect. The first was with IMPROVE and the National Park Service at Yosemite NP, 2002. (Final Report, 2004) Despite having to average 144 soft beta mass measurements (data taken every hour in 6 size modes), there is good overall agreement ($r^2 = 0.74$, slope = 1.14). However, the worst agreement occurred on 4 successive days with the arrival of fresh forest fire smoke from massive fires in Oregon.

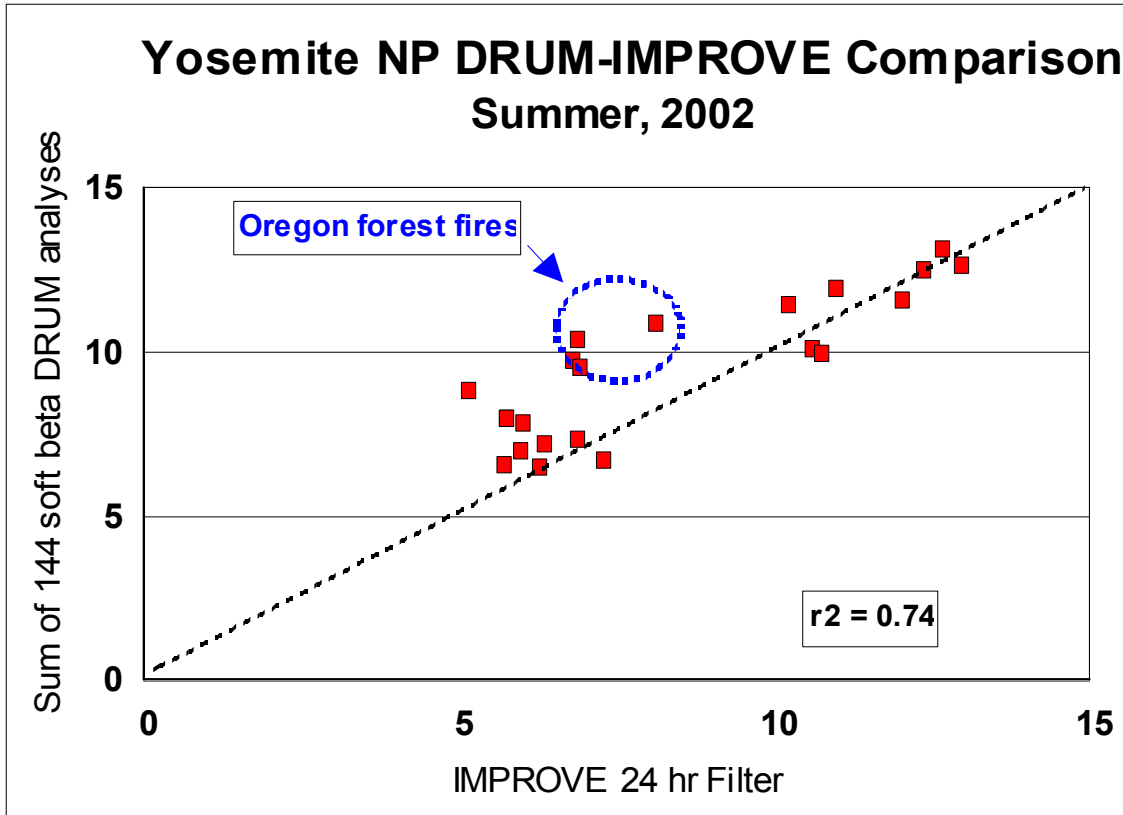


Figure 2 DRUM mass versus filters at Yosemite NP

The second test involved a comparison of DRUM mass at Davis to the district PM_{2.5} data at Woodland, roughly 10 miles away.

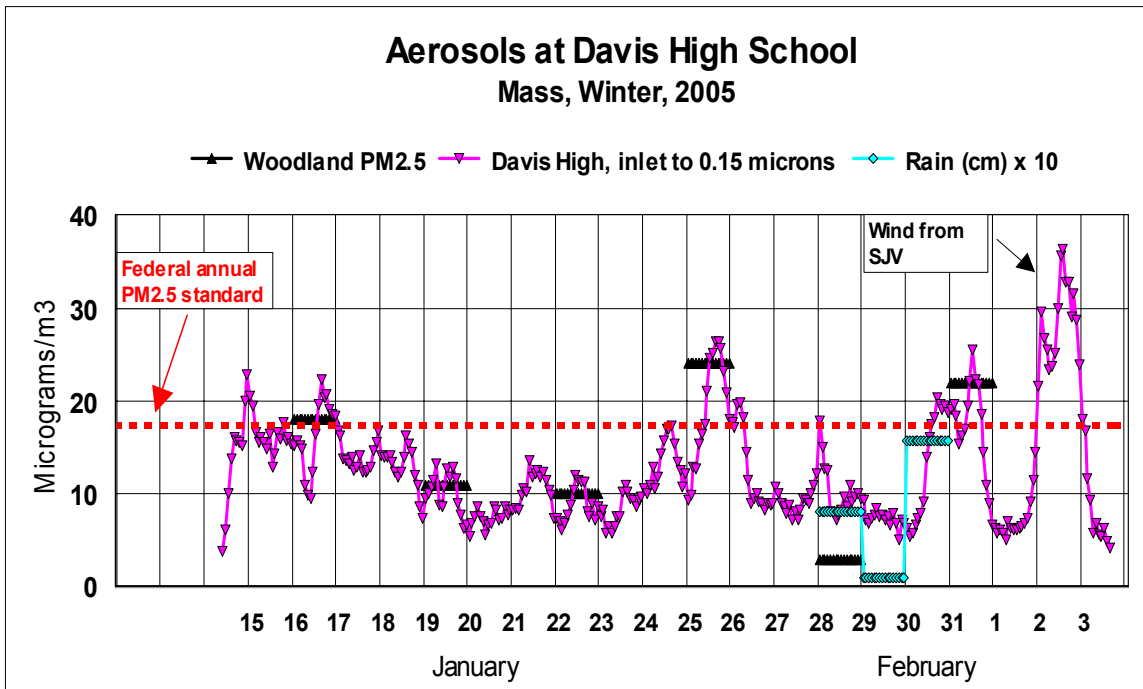


Figure 3 DRUM versus district filter sampler, Yolo County

In summary, DRUM mass data are vital for elucidating temporal and size behavior of aerosols while suffering some loss of accuracy and precision when compared to standard filter methods.

c. Compositional Analysis of Elements

The samples collected by the DRUM sampler are designed to allow highly sensitive elemental analysis by the new DELTA Group designed aerosol analysis system of the x-ray micro beam of the Advanced Light Source, Lawrence Berkeley NL (Bench et al, 2002). The method, synchrotron-induced x-ray fluorescence (S-XRF) has been used by the DELTA Group since 1992, (Cahill et al, 1992) but in its present form since 1999.

Table 2 S-XRF comparison, all blind tests since 1999

Study and date	Methods	Average ratio, Al to Fe	Std. dev.	Average ratio, Cu to Pb	Std. dev.
BRAVO, 1999	PIXE vs S-XRF	0.99	0.04		
BRAVO, 1999	CNL XRF vs S-XRF			1.24	0.14
FACES, 2001	ARB XRF vs S-XRF	0.93	0.21	1.02	0.08
FACES, 2001	ARB RAAS vs S-XRF	(0.98)	0.27	(0.74)	0.23
ARB LTAD 2005	DRI XRF vs S-XRF	1.037	0.085	0.907	0.009
All prior studies	Average	0.984	0.15	0.977	0.115

The S-XRF system has been tested in blind inter-comparisons since 1999, and all of these are shown above. Typically 32 elements are recorded for each analysis, all of which can be traced back to NIST primary (SRM # 1832, SRM # 1833) or secondary (Micromatter thin film) standards. Over 250,000 S-XRF analyses have been done by the DELTA Group since completion of the system in 1999.

The sensitivity of S-XRF is typically about 10 x better than standard XRF since the polarized x-rays eliminate over 90% of the x-ray background and the beam intensity is almost unlimited. This allows the standard analysis duration of 30 seconds to achieve a sensitivity for a DRUM sampler of about 0.01 ng/m³ for elements between titanium and bromine, and roughly 0.03 ng/m³ for most other elements reported. Below we show the MDLs for the RRAMP program, Stage 8 (0.26 to 0.09 µm diameter) of the 8 DRUM impactor.

S-XRF analysis of RRAMP			
Elements	MDLs (ng/m ³)	Elements	MDLs (ng/m ³)
Sodium	2.0	Cobalt	0.02
Magnesium	0.14	Nickel	0.02
Aluminum	0.09	Copper	0.03
Silicon	0.15	Zinc	0.05
Phosphorus	0.20	Gallium	0.001
Sulfur	0.20	Arsenic	0.001
Chlorine	0.02	Selenium	0.002
Potassium	0.02	Bromine	0.005
Calcium	0.05	Rubidium	0.01
Titanium	0.015	Strontium	0.02
Vanadium	0.003	Yttrium	0.15
Chromium	0.003	Zirconium	0.15
Manganese	0.005	Molybdenum	0.25
Iron	0.05	Lead	0.15

Minimum detected limits for organic analyses are a much more complex problem for organics than for elements due to the need for complex particle analysis protocols and presence of interferences. However, with the use of isotopically labeled organic compounds introduced at the very beginning of the analytical process, robust values have been achieved for RRAMP.

Minimum detectable limits (pg/m³) of particulate PAHs observed at the Roseville Rail Yard in the Summer of 2005. The MDL is for a single stage (or filter) since the chemical needs to be detected on only one stage to be detected for the whole sampling period.

Compound	8-stage DRUM Sampler	Lundgren Sampler
Phenanthrene	2.8	1.4
Anthracene	7.9	3.9
1-methylphenanthrene	0.61	0.30
Fluoranthene	1.3	0.65
Pyrene	1.5	0.72
Benz[<i>a</i>]anthracene	^a	^a
Chrysene + triphenylene	8.9	4.4
Benzo [<i>b+k</i>]fluoranthene	3.5	1.7
Benzo[<i>e</i>]pyrene	0.69	0.34
Benzo[<i>a</i>]pyrene	0.71	0.35
Perylene	4.4	2.2
Indo[1,2,3- <i>cd</i>]pyrene	4.0	1.9
Dibenz[<i>a,h</i>]anthracene	2.7	1.3
Benzo[<i>g,h,i</i>]perylene	3.2	1.6
Coronene	5.5	2.7

^a Compound not reported due to an interference.

Appendix B Delta Group DRUM Publications

History: The Air Quality Group (AQG, 1971 – 1997) and the Detection and Evaluation in Long-range Transport of Aerosols (DELTA Group, 1997 – present) have always preferred on fundamental and scientific grounds to perform experiments with continuous sampling of size and compositionally resolved aerosols. The samplers used have varied in time (typical time resolutions have and can be varied at will):

1. Lundgren sampler 1972-1974 , thereafter 5 stages, slots, 4 hr resolution, 160 L/min
2. Multiday sampler 1973 – 1981 3 stages, slots, 24 hr resolution 35 L/min
3. DRUM samplers
 - a. Jetted 8 DRUM 1985 – 1995 8 stages, jets, 3 hr resolution, 1.0 L/min
 - b. DELTA 8 DRUM 1996 – 8 stages, slots, 3 hr resolution 10.0 L/min
 - c. DELTA 8 DRUM, 2001 – 8 stages, slots, 3 hr resolution 16.7 L/min
 - d. DELTA 3 DRUM, 2001 – 3 stages, slots, 3 hr resolution 22.5 L/min
 - e. 8 DRUM upgrade, 2005 – 8 stages, slots, 3 hr resolution 16.7 L/min

The publications below are roughly separated by instrument in inverse chronological order. The numbers are the identifiers in the Master AQG/DELTA master publication list

Publications from DRUM samplers (slotted, 3 and 8 stage, types b through e)

- 04-4 Cahill, T. A., Cliff, S.S., Shackelford, J.F., Meier, M., Dunlap, M., Perry, K.D., Bench, G., and Leifer, R. Very fine aerosols from the World Trace Center collapse piles: Anaerobic incineration? ACS Symposium Series 919, 152-163 (2005)
- 04-3 Seinfeld, J.H., Carmichael, G.R., Arimoto, R, Conant, W. C., Brechtel, F. J., Bates, T. S., Cahill, T. A., Clarke, A.D., Flatau, B.J., Huebert, B.J., Kim, J., Markowicz, K.M., Masonis, S.J., Quinn, P.K., Russell, L.M., Russell, P.B., Shimizu, A., Shinzuka, Y., Song, C.H., Tang, Y., Uno, I., Vogelmann, A.M., Weber, R.J., Woo, J-H., Zhang, Y. ACE-Asia: Regional Climatic and Atmospheric Chemical Effects of Asian Dust and Pollution, *Bulletin American Meteorological Society* 85 (3): 367+ MARCH 2004
- 04-2 Han, J.S, K.J. Moon, J.Y. Ahn, Y.D. Hong, Y.J Kim, S. Y. Rhu, Steven S. Cliff, and Thomas A. Cahill, Characteristics of Ion Components and Trace Elements of Fine Particles at Gosan, Korea in Spring Time from 2001 to 2002, *Environmental Monitoring and Assessment* 00: 1-21, 2003

- 04-1 Thomas A. Cahill, Steven S. Cliff, Michael Jimenez-Cruz, James F. Shackelford, Michael Dunlap, Michael Meier, Peter B. Kelly, Sarah Riddle, Jodye Selco, Graham Bench, Patrick Grant, Dawn Ueda, Kevin D. Perry, and Robert Leifer, Analysis of Aerosols from the World Trade Center Collapse Site, New York, October 2 to October 30, 2001. *Aerosol Science and Technology* 38; 165–183 (2004)
- 03-1 Cahill, C.F. Asian Aerosol Transport to Alaska during ACE-Asia. *J. Geophys. Res.* 108 (D23), 8664 (2003)
- 03-4 Reuter, John E., Cahill, Thomas A., Cliff, Steven S., Goldman, Charles R., Heyvaert, Alan C., Jassby, Alan D., Lindstrom, Susan, and Rizzo, Davis M., An Integrated Watershed Approach to Studying Ecosystem health at Lake Tahoe, CA-NV, in *Managing for Healthy Ecosystems* Rapport et al, ed., CRC Press, New York, 1283-1298 (2003)
- 01-1 V. Shutthanandan, S. Thevuthasan, R. Disselkamp, A. Stroud, A. Cavanaugh, E.M. Adams, D.R. Baer, L. Barrie, S.S. Cliff, T.A. Cahill. Development of PIXE, PESA and transmission ion microscopy capability to measure aerosols by size and time. 2001 *Nuclear Instruments and Methods in Physics Research B: Beam Interactions with Materials and Atoms*.
- 01-4 Graham Bench, P.G. Grant, D. Ueda, S.S. Cliff, K.D. Perry, and T. A. Cahill. The use of STIM and PESA to respectively measure profiles of aerosol mass and hydrogen content across Mylar rotating drum impactor samples. 2001 *Aerosol Science and Technology* 36:642-651.
- 00-1 Miller, Alan E. and Thomas A. Cahill. Size and compositional analyses of biologically active aerosols from a CO₂ and diode laser plume. 2000 *International Journal of PIXE*. Vol. 9, Nos. 3 & 4.
- 99-3 Perry, Kevin D., Thomas A. Cahill, Russell C. Schnell, and Joyce M. Harris. Long-range transport of anthropogenic aerosols to the NOAA Baseline Station at Mauna Loa Observatory, Hawaii. 1999 *Journal of Geophysical Research Atmospheres*. Vol. 104, No. D15, Pages 18,521-18,533.
- 98-2 Pryor, S.C., R. J. Barthelmie, L. L. S. Geernaert, T. Ellerman, and K. Perry. Aerosols in the Western Baltic: Results from ASEPS '97. *Submitted to the 5th International Aerosol Conference, Edinburgh, 12-18th September, 1998*.
- 97-1 Cahill, Thomas A., and Kevin D. Perry. Asian Transport of Aerosols to Mauna Loa Observatory, Spring. 1994 *Climate Monitoring and Diagnostics Laboratory, No. 23, Summary Report 1994-1995, U.S. Department of Commerce National Oceanic and Atmospheric Administration Environmental Research Laboratories/CMDL 94-95, pp 114-116*.

Publications from DRUM samplers (jetted 8 drum, type a)

- 97-8 Perry, Kevin, Cahill, T.A., Eldred, R. A., Dutcher, D.D, Gill, T.E. Long-range transport of North African dust to the eastern United States. 1996 *Journal of Geophysical Research-Atmospheres*, 102, D10, 11,225-11,238.
- 97-10 Cahill, Catherine F., D.D Dutcher, P.H. Wakabayashi, M. Geever, and S.G. Jennings. 1997 The size-resolved chemical composition of natural and anthropogenic aerosols at Mace Head, Ireland. *Proceedings of a Specialty*

- Conference sponsored by Air & Waste Management Association and the American Geophysical Union. *Visual Air Quality: Aerosol and Global Radiation Balance*, Vol. I, pp. 487-497.
- 97-11 Perry, Kevin D., T.A. Cahill, R.C. Schnell, J.M. Harris. 1997 Long-range transport of anthropogenic aerosols to the NOAA Baseline Station at Mauna Loa Observatory, Hawaii. Proceedings of a Specialty Conference sponsored by Air & Waste Management Association and the American Geophysical Union. *Visual Air Quality: Aerosol and Global Radiation Balance*, Vol. I, pp. 130-139.
- 97-16 Cahill, Thomas A., K.D. Perry, Dutcher, D.D, R.A. Eldred, D.E. Day. 1997 Size/compositional profiles of aerosols at Great Smoky Mountains National Park during SEAVS. Proceedings of a Specialty Conference sponsored by Air & Waste Management Association and the American Geophysical Union. *Visual Air Quality: Aerosol and Global Radiation Balance*, Vol. II, pp. 1049-1056.
- 96-6 T.A. Cahill, P. Wakabayashi, T. James. Chemical State of Sulfate at Shenandoah National Park During Summer 1991 *Nuclear Instruments and Methods in Physics Research B: Beam Interactions with Materials and Atoms*, 109/110 (1996) 542-547.
- 95-4 Cahill, Thomas A. Compositional Analysis of Atmospheric Aerosols. 1995 *Particle-Induced X-Ray Emission Spectrometry*, Edited by Sven A. E. Johansson, John L. Campbell, and Klas G. Malmqvist. *Chemical Analysis Series*, Vol. 133, pp. 237-311. John Wiley & Sons, Inc.
- 94-5 Reid, Jeffrey S., Thomas A. Cahill, and Micheal R. Dunlap. Geometric/aerodynamic equivalent diameter ratios of ash aggregate aerosols collected in burning Kuwaiti well fields. 1994 *Atmospheric Environment*, Vol.28, No. 13, pp. 2227-2234.
- 93-1 Cahill, Thomas A. and Paul Wakabayashi. Compositional analysis of size-segregated aerosol samples. Chapter in the ACS book *Measurement Challenges in Atmospheric Chemistry*. Leonard Newman, Editor. Chapter 7, Pp. 211-228 (1993).
- 90-1 Hering, Susanne V., Bruce R. Appel, W. Cheng, F. Salaymeh, Steven H. Cadle, Patricia A. Mulawa, Thomas A. Cahill, Robert A. Eldred, Marcelle Surovik, Dennis Fitz, James E. Howes, Kenneth T. Knapp, Leonard Stockburger, Barbara J. Turpin, James J. Huntzicker, Xin-Qui Zhang, and Peter H. McMurry. Comparison of sampling methods for carbonaceous aerosols in ambient air. *Aerosol Science and Technology*. 12:200-213 (1990).
- 90-2 Cahill, Thomas A., Marcelle Surovik, and Ian Wittmeyer. Visibility and aerosols during the 1986 carbonaceous species methods comparison study. *Aerosol Science and Technology*. 12:149-160 (1990).
- 90-5 Cahill, Thomas A. Analysis of air pollutants by PIXE: The second decade. *Nuclear Instruments and Methods in Physics Research*, North-Holland. B49:345-350 (1990).
- 88-1 Raabe, Otto G., David A. Braaten, Richard L. Axelbaum, Stephen V. Teague, and Thomas A. Cahill. Calibration Studies of the DRUM Impactor. *Journal of Aerosol Science*. 19.2:183-195 (1988).

- 88-2 Cahill, Thomas A. Investigation of particulate matter by size and composition during WATOX, January 1986. *Global Biogeochemical Cycles*. 2.1:47-55, Paper No. 8J0052, March (1988).
- 88-4 Cahill, Thomas A., Marcelle Surovik, Robert A. Eldred, Patrick J. Feeney, and Nehzat Motallebi. Visibility and particulate size at the 1986 "Carbon Shoot-out" and 1987 "WHITEX" programs. *Proceedings of the Air Pollution Control Association 81st Annual Meeting*. Dallas, TX, June 19-24. Paper No. 88-54.2:1-20 (1988).
- 88-7 Annegarn, H.J., T.A. Cahill, JPF Sellschop, and A. Zucchiatti. Time sequence particulate sampling and nuclear analysis. Adriatico Research Conference on Aerosols. Trieste, Italy, July 22-25, 1986. *Physica Scripta*. 37:282-290 (1988).
- 87-4 Annegarn, H., Zucchiatti, A., Sellschop, J., Booth-Jones, P. PIXE characterization of airborne dust in the mining environment. Fourth International PIXE Conference, Tallahassee, FL, June 9-13, 1986. *Nuclear Instruments and Methods in Physics Research*. B22:289-295 (1987).
- 87-7 Cahill, Thomas A., Patrick J. Feeney, and Robert A. Eldred. Size-time composition profile of aerosols using the drum sampler. Fourth International PIXE Conference. Tallahassee, FL, June 9-13, 1986. *Nuclear Instruments and Methods in Physics Research*. B22:344-348 (1987).
- 87-9 Feeney, P.J., T.A. Cahill, H.J. Annegarn, R. Dixon, and P. Beveridge. Solar-powered aerosol samplers for use with PIXE analysis. Fourth International PIXE Conference. Tallahassee, FL, June 9-13, 1986. *Nuclear Instruments and Methods in Physics Research*. B22:349-352 (1987).
- 87-13 Eldred, Robert A., Thomas A. Cahill, Patrick J. Feeney, and William C. Malm. Regional patterns in particulate matter from the National Park Service network, June 1982 to May 1986. In *Transactions TR-10; Visibility Protection: Research and Policy Aspects*. P. Bhardwaja, Editor. Pittsburgh, PA: APCA, Pp. 386-396 (1987).
- 87-14 Cahill, Thomas A., Patrick J. Feeney, Robert A. Eldred, and William C. Malm. Size/time/composition data at Grand Canyon National Park and the role of ultrafine sulfur particles. In *Transactions TR-10; Visibility Protection: Research and Policy Aspects*. P. Bhardwaja, Editor. Pittsburgh, PA: APCA, Pp. 657-667 (1987).
- 86-1 Braaten, D.A. and T.A. Cahill. Size and composition of Asian dust transported to Hawaii. *Atmospheric Environment* (Great Britain). 20:1105-1109 (1986).
- 86-7 Cahill, T.A. Physical methods in air pollution research: The second decade. *Physics in Environmental and Biomedical Research*. S. Onori and E. Tabet, Editors. World Scientific Pub. Co., Pp. 55-61 (1986).
- 85-3 Cahill, T.A., C. Goodart, J.W. Nelson, R.A. Eldred, J.S. Nasstrom, and P.J. Feeney. Design and evaluation of the drum impactor. *Proceedings of International Symposium on Particulate and Multi-phase Processes*. Teoman Ariman and T. Nejat Veziroglu, Editors. Hemisphere Publishing Corporation, Washington, D.C. 2:319-325. (1985).

Publications from the Multiday 2 drum sampler (plus afterfilter)

- 90-11 Motallebi, Nehzat, Thomas A. Cahill, and Robert G. Flocchini. Influence of particulate size on statistical studies of visibility at California regions. *Atmosfera*. Pp. 111-126 (1990).
- 90-12 Motallebi, Nehzat, Robert G. Flocchini, Leonard O. Myrup, and Thomas A. Cahill. A principal component analysis of visibility and air pollution in six California cities. *Atmosfera*. Pp. 127-141 (1990).
- 82-3 Cahill, T.A. and D.A. Braaten. Size characteristics of Asian dust sampled at Mauna Loa Observatory. *Geophysical Monitoring for Climatic Change*. J. Harris and B. Bodhaine, Editors. Summary Report No. 11 (1982).
- 81-1 Flocchini, R.G., T.A. Cahill, Marc L. Pitchford, R.A. Eldred, P.J. Feeney, and L.L. Ashbaugh. Characterization of particles in the arid West. *Atmospheric Environment*. 15:2017-2030 (1981).
- 81-3 Cahill, Thomas A. Innovative aerosol sampling devices based upon PIXE capabilities. *Nuclear Instruments and Methods*. 181:473-480 (1981).
- 81-4 Cahill, Thomas A. Ion beam analysis of environmental samples. Symposium on Recent Developments in Biological and Chemical Research with Short Lived Radioisotopes. American Chemical Society Meeting. Honolulu, Hawaii, 1979. *Short-Lived Radionuclides in Chemistry and Biology*. John W. Root and Kenneth A. Krahn, Editors. No. 27:511-522. Advances in Chemistry Series, No. 197 (1981).
- 81-6 Leifer, R., L. Hinchliffe, I. Fisenne, H. Franklin, E. Knutson, M. Olden, W. Sedlacek, E. Mroz, T. Cahill. Measurements of the stratospheric plume from the Mount St. Helens eruption: Radioactivity and chemical composition. *Science*. 214:904-907 (1981).
- 81-7 Cahill, T.A., B.H. Kusko, L.L. Ashbaugh, J.B. Barone, R.A. Eldred, and E.G. Walther. Regional and local determinations of particulate matter and visibility in the southwestern United States during June and July, 1979. Symposium on Plumes and Visibility. Grand Canyon, AZ, 1980. *Atmospheric Environment*. 15:2011-2016 (1981).
- 81-8 Pitchford, A., Pitchford, M., Malm, W., Flocchini, R., Cahill, T., Walther, E. Regional analysis of factors affecting visual air quality. Symposium on Plumes and Visibility. Grand Canyon, AZ, 1980. *Atmospheric Environment*. 15:2043-2054 (1981).
- 81-9 Macias, E.S., J.O. Zwicker, J.R. Ouimette, S.V. Hering, S.K. Friedlander, T.A. Cahill, G.A. Kuhlmeier, and L.W. Richards. Regional haze in the southwestern US, II: Source Composition. Symposium on Plumes and Visibility. Grand Canyon, AZ, 1980. *Atmospheric Environment*. 15:1971-1986 (1981).
- 81-10 Flocchini, R., Cahill, T., Ashbaugh, L., Eldred, R., Feeney, P., Shadoan, D. Regional scale synoptic air monitoring for visibility evaluation based on PIXE analyses. *Nuclear Instruments and Methods*. 181:407-410 (1981).
- 81-11 Flocchini, Robert G., Thomas A. Cahill, Lowell L. Ashbaugh, Robert A. Eldred, and Marc Pitchford. Seasonal behavior of particulate matter at three rural Utah sites. *Atmospheric Environment*. 15:315-320 (1981).

- 81-12 Pitchford, Marc, Robert G. Flocchini, Ronald G. Draftz, Thomas A. Cahill, Lowell L. Ashbaugh, and Robert A. Eldred. Silicon in submicron particles in the Southwest. *Atmospheric Environment*. 15:321-333 (1981).
- 81-13 Cahill, T.A. Size-chemical profiles of environmental samples by PIXE. *Proceedings of the American Nuclear Society Meeting*. San Francisco, CA. IEEE Series: Terrestrial and Extraterrestrial Radiation II. Pp. 71-73 (1981).
- 81-15 Barone, J.B., L.L. Ashbaugh, B.H. Kusko, and T.A. Cahill. The effect of Owens Dry Lake on air quality in the Owens Valley with implications for the Mono Lake area. *Atmospheric Aerosol: Source/Air Quality Relationships*. P. Radke, Editor. No. 18:327-346. ACS Symposium Series, No. 167 (1981).
- 81-16 Cahill, Thomas A., Lowell L. Ashbaugh, and Bruce Kusko. Size-elemental profiles of fine particulate matter at Mauna Loa and Hilo, Hawaii. *Geophysical Monitoring for Climatic Change*. J.J. DeLuisi, Editor. Summary Report No. 9, December, P. 103 (1981).
- 80-3 Cahill, T.A., J. Barone, R.A. Eldred, R.G. Flocchini, D.J. Shadoan, and T.M. Dietz. Influence of sulfur size distribution on optical extinction. *Environmental and Climatic Impact of Coal Utilization*. J.J. Singh and A. Deepak, Editors. Academic Press, Pp. 213-244 (1980).
- 80-4 Cahill, T.A. Proton microprobes and particle-induced x-ray analytical systems. *Annual Reviews Nuclear and Particle Science*. 30:211-252 (1980).
- 79-2 Cahill, Thomas A. Comments on surface coatings for lundgren-type impactors. *Aerosol Measurement*. Dale A. Lundgren, Editor. University Presses of Florida, Pp. 131-134 (1979).
- 78-2 Eldred, Robert A., Thomas A. Cahill, and Robert G. Flocchini. Bromine loss from automotive particulates at California sites. *Proceedings of the 71st Annual Meeting of the Air Pollution Control Association*. June 25-30. Paper No. 78-69.6:2-15 (1978).
- 78-3 Wesolowski, J.J., W. John, W. Devor, T.A. Cahill, P.J. Feeney, G. Wolfe, R. Flocchini. Collection surfaces of cascade impactors. In *X-ray fluorescence analysis of environmental samples*. Dzubay, T., Editor. Ann Arbor Science, Pp. 121-130 (1978).
- 78-8 Flocchini, Robert G., Thomas A. Cahill, Robert A. Eldred, Lowell L. Ashbaugh, and John B. Barone. Sulfur size distribution by season and site in California. *Proceedings of the 71st Annual Meeting of the Air Pollution Control Association*. Houston, TX, June 25-30. Paper No. 78-39.6:3-15 (1978).
- 77-4 Cahill, Thomas A. X-ray analysis of environmental pollutants. *Environmental Pollutants*. T.Y. Toribara et al., Editors. Plenum Press, Pp. 457-463 (1977).
- 76-3 Flocchini, Robert G., Thomas A. Cahill, Danny J. Shadoan, Sandra J. Lange, Robert A. Eldred, Patrick J. Feeney, Gordon W. Wolfe, Dean C. Simmeroth, and Jack K. Suder. Monitoring California's aerosols by size and elemental composition. *Environmental Science and Technology*. 10:76-82 (1976).
- 76-4 Cahill, T.A., R.G. Flocchini, R.A. Eldred, P.J. Feeney, S. Lange, D. Shadoan, and G. Wolfe. Monitoring of smog aerosols with elemental analysis by accelerator beams. *Proceedings of the 17th Materials Research Symposium*. Gaithersburg, MD, October 7-11, 1974. National Bureau of Standards Special Publication, 422:1119-1136 (1976).

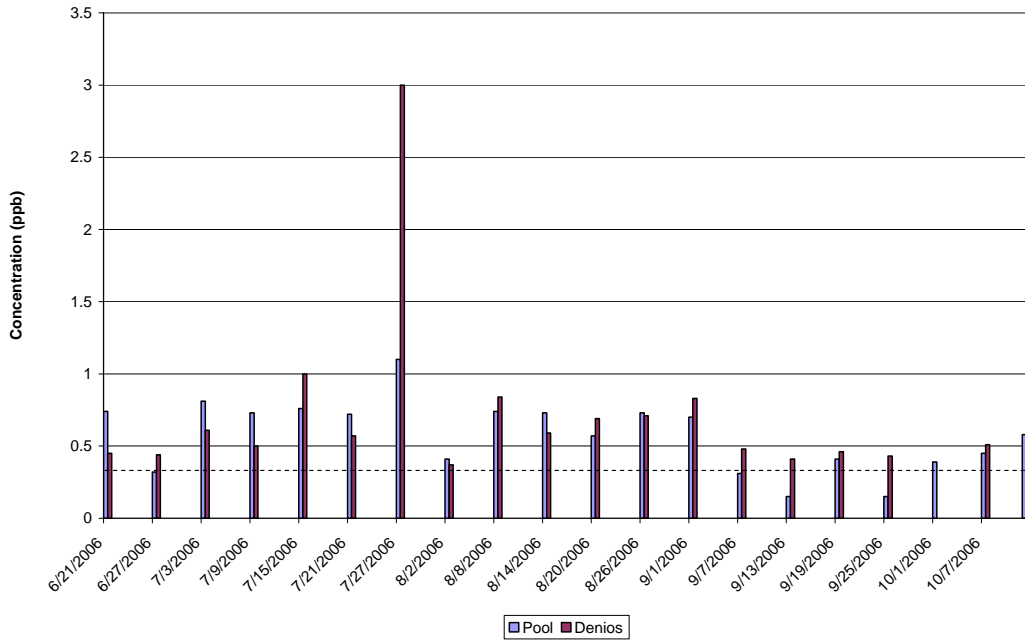
Publications from Lundgren 4 drum sampler (plus afterfilter)

- 80-5 Cahill, T.A. and L.L. Ashbaugh. Size/composition profiles of resuspended fly ash. *Environmental and Climatic Impact of Coal Utilization*. J.J. Singh and A. Deepak, Editors. Academic Press, Pp. 569-573 (1980).
- 78-5 Cahill, Thomas A. Results of highway particulate investigations in California. *Proceedings Federal Highway Administration Symposium on Environmental Impacts of Highway Transportation*. Charlottesville, VA. (1978).
- 75-2 Feeney, P.J., T.A. Cahill, R.G. Flocchini, R.A. Eldred, D.J. Shadoan, and T. Dunn. Effect of roadbed configuration on traffic derived aerosols. *Journal of the Air Pollution Control Association*. 25:1145-1147 (1975).
- 75-3 Ensor, D.S, T.A. Cahill, and L.E. Sparks. Elemental analysis of fly ash from combustion of a low sulfur coal. *Proceedings of the 68th Annual Meeting-Air Pollution Control Association*. Boston, MA. Paper No. 75-33.7:1-18 (1975).
- 75-5 Cahill, Thomas A. Ion-excited x-ray analysis of environmental samples. Chapter 1 of *New uses for ion accelerators*. James Ziegler, Editor. Plenum Press, Pp. 1-72 (1975).
- 74-4 Azevedo, J., R.G. Flocchini, T.A. Cahill, and P.R. Stout. Elemental composition of particulates near a beef cattle feedlot. *Journal of Environmental Quality*. 3:171-174 (1974).
- 74-5 Cahill, T.A., R.G. Flocchini, R.A. Eldred, P.J. Feeney, S. Lange, D. Shadoan, and G. Wolfe. Use of ion beams for monitoring California's aerosols. *Proceedings of the 2nd Annual NSF-RANN Trace Contaminants Conference*. Asilomar, Pacific Grove, CA. Paper No. LBL-3217:133-134 (1974).

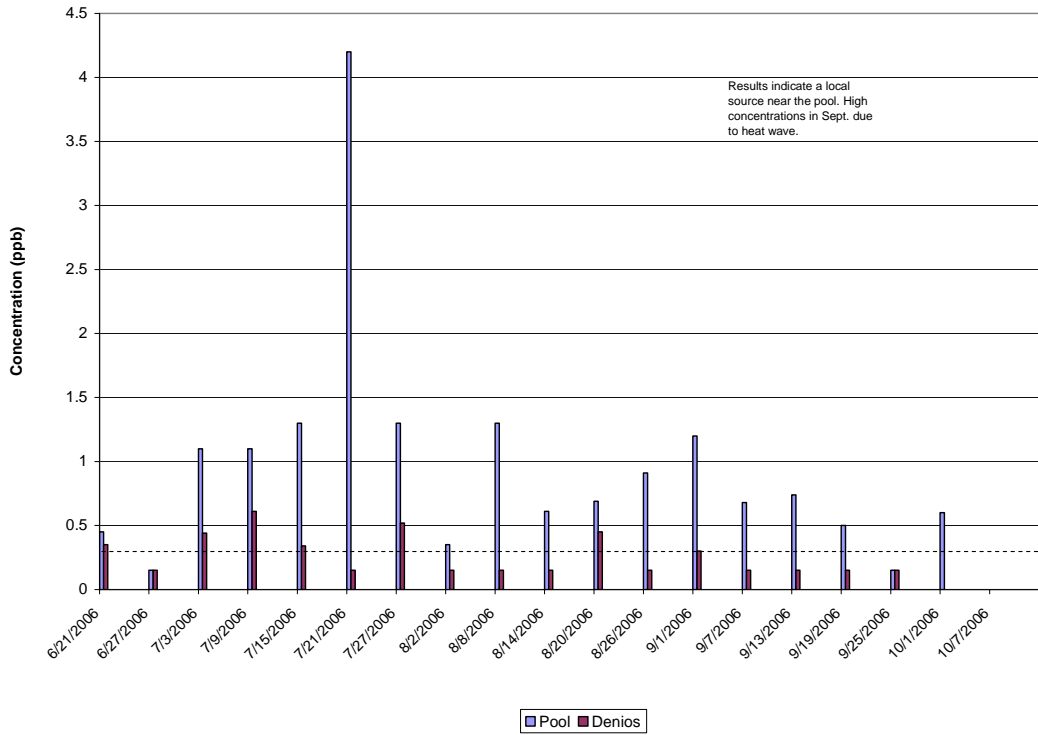
Attachment 3

Partial List of VOC & Carbonyl Compounds Measured at the Roseville Rail Yard in Summer 2006

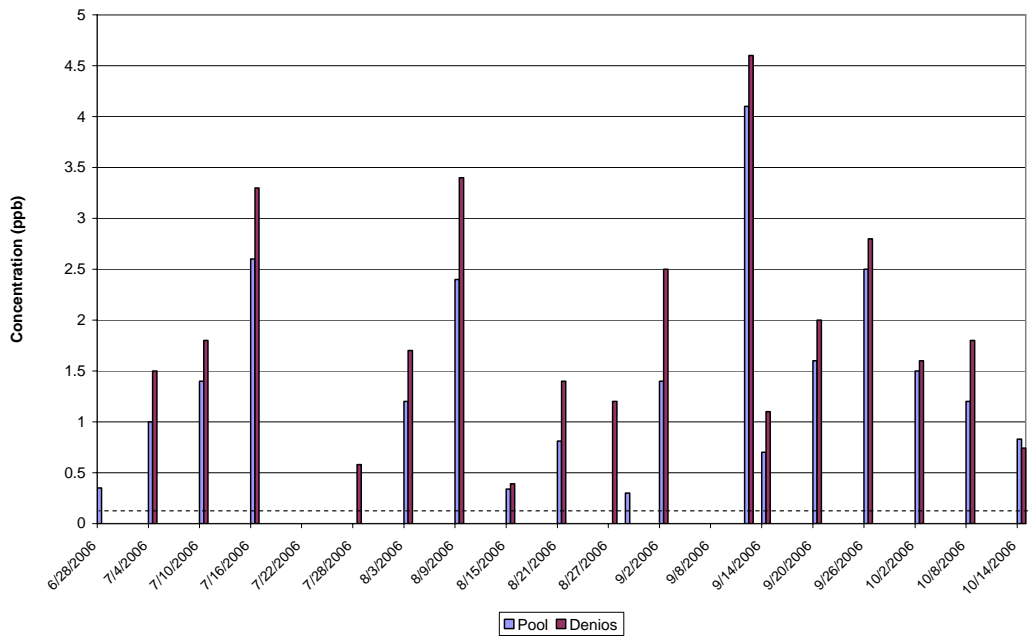
Acrolein



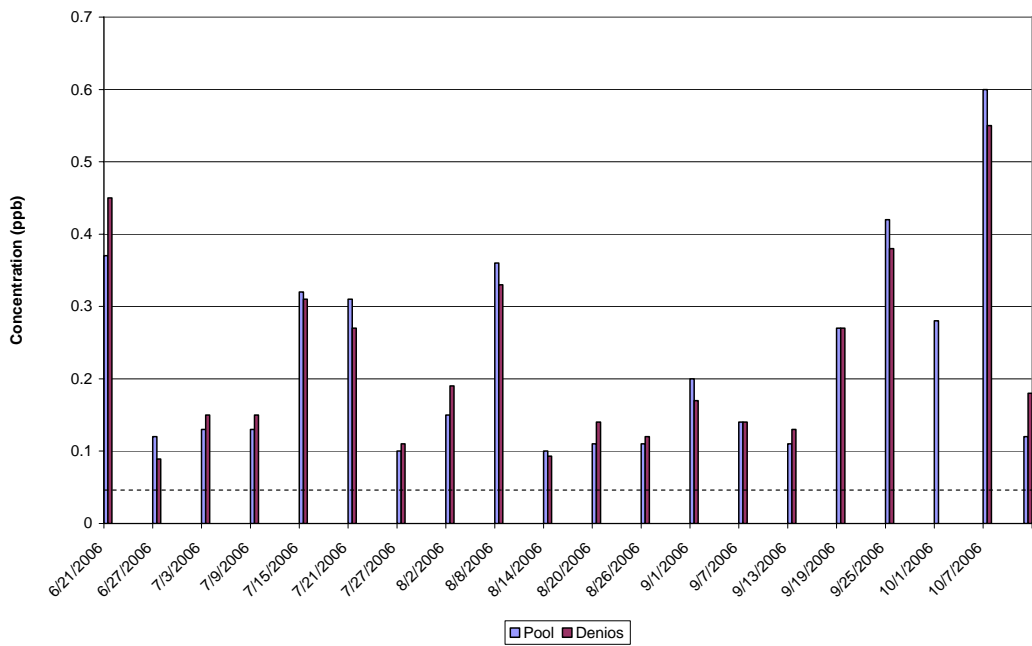
Acrylonitrile



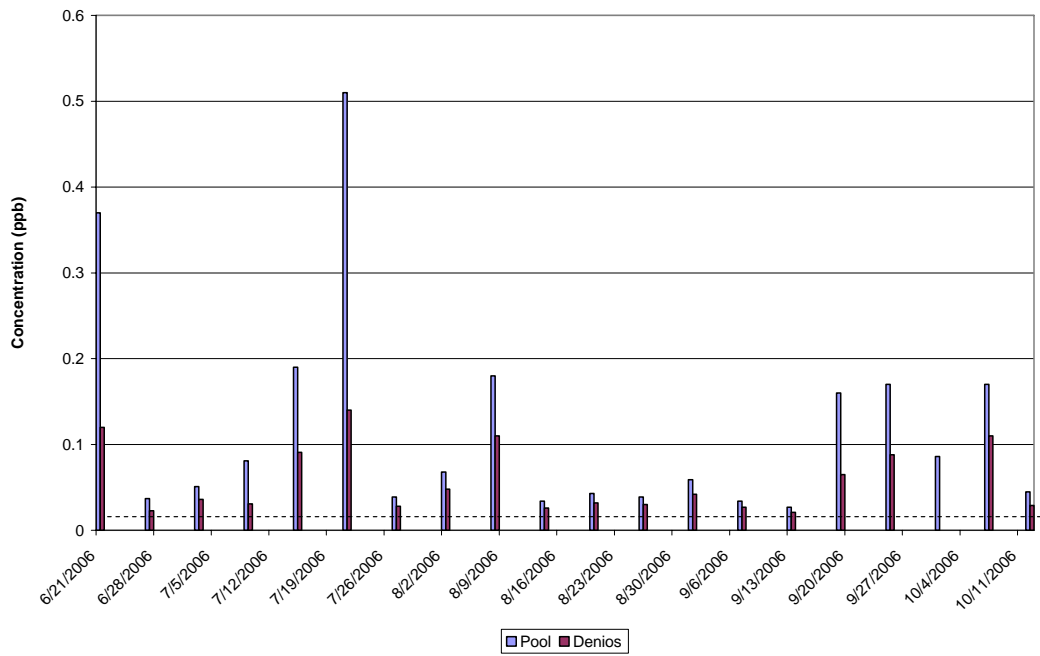
Acetaldehyde



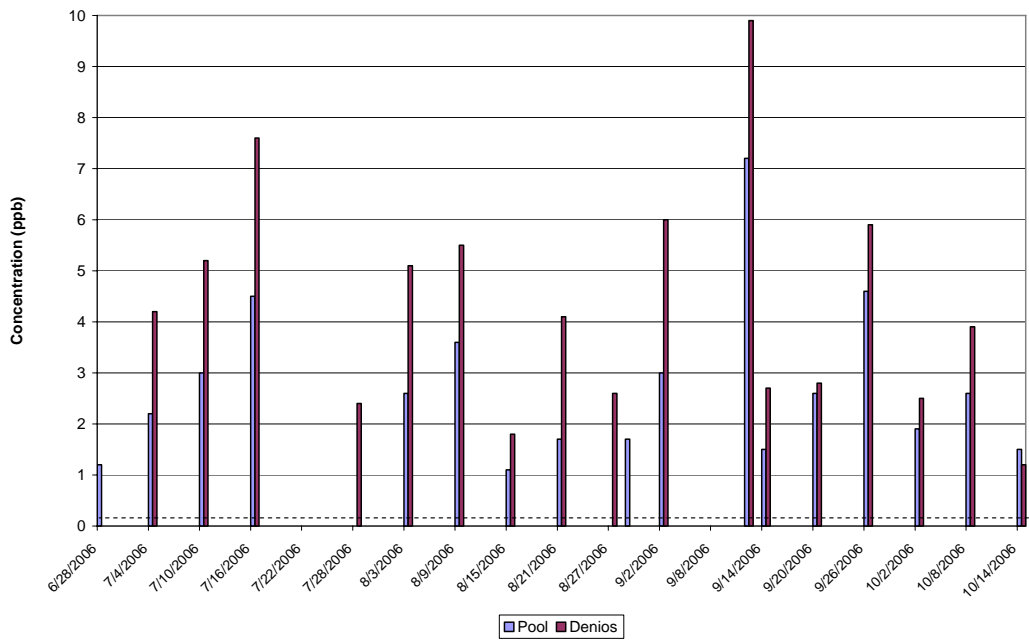
Benzene



Chloroform



Formaldehyde



Toluene

